LEABHARLANN CHOLÁISTE NA TRÍONÓIDE, BAILE ÁTHA CLIATH | TRINITY COLLEGE LIBRARY DUBLIN
Ollscoil Átha Cliath | The University of Dublin

Terms and Conditions of Use of Digitised Theses from Trinity College Library Dublin

Copyright statement

All material supplied by Trinity College Library is protected by copyright (under the Copyright and Related Rights Act, 2000 as amended) and other relevant Intellectual Property Rights. By accessing and using a Digitised Thesis from Trinity College Library you acknowledge that all Intellectual Property Rights in any Works supplied are the sole and exclusive property of the copyright and/or other IPR holder. Specific copyright holders may not be explicitly identified. Use of materials from other sources within a thesis should not be construed as a claim over them.

A non-exclusive, non-transferable licence is hereby granted to those using or reproducing, in whole or in part, the material for valid purposes, providing the copyright owners are acknowledged using the normal conventions. Where specific permission to use material is required, this is identified and such permission must be sought from the copyright holder or agency cited.

Liability statement

By using a Digitised Thesis, I accept that Trinity College Dublin bears no legal responsibility for the accuracy, legality or comprehensiveness of materials contained within the thesis, and that Trinity College Dublin accepts no liability for indirect, consequential, or incidental, damages or losses arising from use of the thesis for whatever reason. Information located in a thesis may be subject to specific use constraints, details of which may not be explicitly described. It is the responsibility of potential and actual users to be aware of such constraints and to abide by them. By making use of material from a digitised thesis, you accept these copyright and disclaimer provisions. Where it is brought to the attention of Trinity College Library that there may be a breach of copyright or other restraint, it is the policy to withdraw or take down access to a thesis while the issue is being resolved.

Access Agreement

By using a Digitised Thesis from Trinity College Library you are bound by the following Terms & Conditions. Please read them carefully.

I have read and I understand the following statement: All material supplied via a Digitised Thesis from Trinity College Library is protected by copyright and other intellectual property rights, and duplication or sale of all or part of any of a thesis is not permitted, except that material may be duplicated by you for your research use or for educational purposes in electronic or print form providing the copyright owners are acknowledged using the normal conventions. You must obtain permission for any other use. Electronic or print copies may not be offered, whether for sale or otherwise to anyone. This copy has been supplied on the understanding that it is copyright material and that no quotation from the thesis may be published without proper acknowledgement.



TRINITY COLLEGE DUBLIN
COLÁISTE NA TRÍONÓIDE
THE UNIVERSITY OF DUBLIN

School of Pharmacy and Pharmaceutical Sciences,
Trinity College Dublin

ENGINEERING A NOVEL INSULIN DELIVERY SYSTEM

by

Maria Dul, M.Sc.

being a thesis submitted for the degree of
Doctor of Philosophy in Pharmacy and Pharmaceutical Sciences

at
University of Dublin Trinity College

under the supervision and direction of

Lidia Tajber, MPharm, PhD

and

Dr. rer. nat. Astrid Sasse, MA, MPSI

October 2013

TRINITY COLLEGE
0 9 JUN 2014
LIBRARY DUBLIN
Thesis 10389

DECLARATION

I declare that this thesis has not been submitted as an exercise for a degree at this or any other university. I have carried out all the practical work except where duly acknowledged.

I agree to deposit this thesis in the University's open access institutional repository or allow the library to do so on my behalf, subject to Irish Copyright Legislation and Trinity College Library conditions of use and acknowledgment.

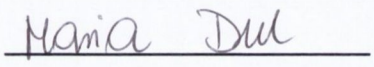

Maria Dul

To my beloved parents

Zofia and Bronisław

Table of Contents

ACKNOWLEDGEMENTS xv
PRESENTATIONS ASSOCIATED WITH THIS THESIS xvi
ABBREVIATIONS AND SYMBOLS xvii
SUMMARY xxii
ORIGIN AND SCOPE 1
CHAPTER 1 4
INTRODUCTION 4
1.1 Diabetes mellitus 5
1.2. Insulin market 6
1.3 Insulin structure – biosynthesis and metabolism 7
1.4 Recombinant DNA technology – methods of insulin production 9
1.4.1 Recombinant human insulin production in bacteria 10
1.4.1.1 Two-chain method 10
1.4.1.2 Proinsulin method (intracellular) 10
1.4.2 Recombinant human insulin production in yeast 12
1.5 Expression of proteins in *Escherichia coli* as a host organism 15
1.6 Recombinant protein production in *Escherichia coli* 18
1.6.1 Expression of proteins in form of inclusion bodies 18
1.6.2 Periplasmic production of proteins 20
1.7 Insulin delivery 22
1.7.1 Subcutaneous delivery of insulin 22
1.7.2 Non-invasive delivery of insulin 23
1.8 Oral insulin 24
1.8.1 Oral insulin delivery – main barriers 25
1.8.1.1 The physical barrier to oral protein delivery 25
1.8.1.2 The enzymatic barrier to oral protein delivery 25
1.8.1.3 Barriers due to manufacturing of formulation 26
1.8.2 Strategies for oral insulin delivery 27
1.8.2.1 Chemical modification or conjugation 27
1.8.2.2 Protease inhibitors 27
1.8.2.3 Permeation enhancers 28
1.8.2.4 Carrier systems 29
1.9 Formulation vehicles used for an oral delivery of insulin 30
1.9.1 Enteric-coated capsules 30
1.9.2 Intestinal Patches 30
1.9.3 Hydrogels 31

1.9.4 Microemulsions 31
1.9.5 Hydrogel Microparticles 31
1.9.6 Liposomal Formulations 32
1.9.7 Niosomes 33
1.9.8 Nanoparticle delivery systems 33
1.10 Characterisation of polymers: alginic acid and carrageenan 35
1.10.1 Alginic acid 36
1.10.2 Carrageenan 38
1.11 Cell penetrating peptides in drug delivery 40
1.11.1 Approaches to use cell penetrating peptides in drug delivery 41
1.11.1.1 Recombinant fusion protein 41
1.11.1.2 Covalent chemical linkage 41
1.11.1.3 Non-covalent method 42
1.11.1.4 Surface modifications of nanoparticle-based drug carriers 42
1.11.2 Application of cell penetrating peptides for insulin delivery 43
1.11.3 Characterisation of protamine sulfate 44
CHAPTER 2 45
MATERIALS AND METHODS 45
2.1 Materials 46
2.2 Bacterial strains and plasmids 49
2.3 Equipment 50
2.4 Methods 51
2.4.1 Methods - preparation, expression and purification of insulin plasmids 51
2.4.1.1 Preparation of solutions 51
2.4.1.2 Transformation 53
2.4.1.3 Inoculation and bacterial culture 53
2.4.1.4 Plasmid amplification – Maxi Prep Kit 53
2.4.1.5 Enzymatic digestion of DNA 53
2.4.1.6 Agarose gel electrophoresis 53
2.4.1.7 Gel extraction 54
2.4.1.8 PCR – Polymerase Chain Reaction 54
2.4.1.9 Ligation 55
2.4.1.10 Clone isolation 55
2.4.1.11 DNA concentrations UV analysis 55
2.4.1.12 Preparation of pMD2 plasmid 55
2.4.1.12.1 Vector preparation 56
2.4.1.12.2 Insert preparation 56

2.4.1.12.3 Ligation 57
2.4.1.12.4 Mutation 57
2.4.1.13 Preparation of pMD3 plasmid 59
2.4.1.13.1 Vector preparation 59
2.4.1.13.2 Insert preparation 60
2.4.1.13.3 Insert preparation 60
2.4.1.14 Glycine SDS-PAGE protein electrophoresis 61
2.4.1.14.1 Gel preparation 61
2.4.1.14.2 Sample loading 61
2.4.1.14.3 Staining with Coomassie 62
2.4.1.15 Western blot 62
2.4.1.16 Preparation of samples for expression test 63
2.4.1.16.1 Expression induced by IPTG 63
2.4.1.16.2 Expression in the auto-induction system 63
2.4.1.17 Preparation of samples for periplasmic localisation test 64
2.4.1.18 Preparation of samples for solubility test 64
2.4.1.19 Purification of proteins with His tag column 65
2.4.1.20 Bio-Rad Protein Assay 65
2.4.1.21 Dialysis 66
2.4.1.22 Digestion by ALP protease 66
2.4.1.23 Optimisation of refolding reaction 67
2.4.1.23.1 Denaturation of proinsulin 67
2.4.1.23.2 Oxidative sulfitolysis reaction 67
2.4.1.23.3 Refolding reaction 67
2.4.1.24 Purification of pHB1 inclusion bodies – optimised protocol 68
2.4.1.24.1 Cells harvesting, disruption and washing 68
2.4.1.24.2 Solubilisation and oxidative sulfitolysis 68
2.4.1.24.3 CNBr cleavage 68
2.4.1.24.4 Cation exchange purification 68
2.4.1.24.5 Dialysis and refolding reaction 69
2.4.1.24.6 Proteolytic cleavage of proinsulin 69
2.4.2 Methods – nanoparticle (NP) preparation and characterisation 69
2.4.2.1 Preparation and characterisation of protamine sulphate and polymer solutions 69
2.4.2.1.1 Alginic acid (as sodium alginate) solutions 69
2.4.2.1.2 Carrageenan solutions 69
2.4.2.1.3 Protamine (as protamine sulphate) solutions 69

2.4.2.2 Synthesis of empty nanoparticles (NPs) 70
2.4.2.2.1 Synthesis and characterisation NPs composed of alginic acid and protamine 70
2.4.2.2.2 Synthesis and characterisation NPs composed of carrageenan and protamine 70
2.4.2.3 Methods of NPs formation 70
2.4.2.4 Synthesis of insulin loaded NPs 71
2.4.2.5 Size, polydispersity and zeta potential analyses 71
2.4.2.6 pH measurements 71
2.4.2.7 Viscosity measurements 71
2.4.2.8 Influence of different cations on the formation of empty carrageenan-based NPs 72
2.4.2.9 Physical stability of empty NPs 72
2.4.2.10 Physical stability of NPs in different liquid media 72
2.4.2.11 Separation of non-associated insulin 72
2.4.2.12 Release studies 73
2.4.2.13 RP-HPLC method for insulin quantification 74
2.4.2.14 Cell culture studies 74
2.4.2.15 Cytotoxicity MTS assay 75
2.4.2.16 Transport of insulin through Caco-2 monolayer 75
2.4.2.16.1 Seeding and growing Caco-2 cells on Transwell® plates 75
2.4.2.16.2 Sample preparation 76
2.4.2.16.3 Transport study – procedure 76
2.4.2.16.4 Integrity of Caco-2 monolayers 76
2.4.2.16.5 Permeability coefficient (P_{app}) caluclation 77
2.4.2.17 Statistical analysis 77
CHAPTER 3 78
OPTIMISATION OF PROINSULIN EXPRESSION AND PURIFICATION FROM NEWLY DESIGNED PLASMIDS 78
3.1 Introduction 79
3.2 Design and preparation of proinsulin plasmids 80
3.2.1 Composition of plasmids pHB1-3 80
3.2.2 pMD2 insulin construct preparation 81
3.2.3 pMD3 insulin construct preparation 82
3.3 Expression/ auto-induction of proinsulin from prepared plasmids 82
3.3.1 Expression and cellular localisation of proteins expressed by IPTG induction 82

3.3.2 Development of an auto-induction system for high level expression of proinsulin 87
3.3.2.1 pHB1 plasmid expression by using auto-induction 87
3.3.2.2 pHB3 plasmid expression by using auto-induction 90
3.3.3 Impact of temperature on proinsulin expression by pHB1 and pHB3 plasmid using auto-induction system 95
3.4 Establishing protocols for purification of expressed proinsulin 98
3.4.1 Purification and ALP protease cleavage of proinsulin expressed by pMD2 plasmid 98
3.4.1.1 His tag column purification of periplasmic fraction of pMD2 plasmid 98
3.4.1.2 ALP protease digestion 100
3.4.2 Purification of pHB1 plasmid expressed in the form of insoluble inclusion bodies 103
3.4.2.1 Establishment of an optimised method for proinsulin refolding reaction 103
3.4.2.2 Establishement of final protocol for pHB1 inclusion bodies purification 105
3.5 Conclusions 109
CHAPTER 4 112
CHARACTERISATION AND STABILITY OF ALGINATE/PROTAMINE CARRIERS 112
4.1 Introduction 113
4.2 Formulation of empty alginic acid/ protamine NPs 114
4.2.1 Physicochemical properties of NP components: alginic acid and protamine 114
4.2.2 Preliminary studies on the formation of alginic acid/protamine nanoparticles 115
4.2.3 Influence of formulation process on the properties of NPs 118
4.2.3.1 Sequence of alginic acid/protamine solution addition on NPs characteristics 118
4.2.3.2 Slow/fast protamine solution addition to alginic acid 119
4.2.4 Impact of changing solution pH on properties of NPs 119
4.2.4.1 Properties of NPs using alginic acid solution at pH 2 119
4.2.4.2 Properties of NPs using protamine solution at pH 2 120
4.2.5 Formation of NPs using protamine solution at pH3 and alginic acid 124
4.2.6 Evaluation of nanoparticles composed of AAM and P 129
4.2.7 Formation of NPs using protamine solution at pH 3 and AAM 134
4.3 Physical stability of AAL/P_pH3 NPs 138
4.3.1 Stability of AAL/P_pH3 NPs up to 72 h storage at RT 139
4.3.2 Stability of AAL/P_pH3 NPs in 0.1 M and 0.01 M HCl 141
4.3.3 Stability of AAL/P_pH3 NPs in 0.1 M acetate buffer at pH 4.5 143

4.3.4 Stability of AAL/P_pH3 NPs in 0.1 M HEPES at pH 6.5 145
4.3.5 Stability of AAL/P_pH3 NPs in 0.01 M PBS at pH 7.4 147
4.3.6 Stability of AAL/P_pH3 NPs in 0.1 M and 0.01 M NaCl 148
4.3.7 Stability of AAL/P_pH3 NPs in cell culture medium 151
4.4 Conclusions 155
CHAPTER 5 157
CHARACTERISATION AND STABILITY OF CARRAGEENAN/PROTAMINE CARRIERS 157
5.1 Introduction 158
5.2 Formulation of empty carrageenan/ protamine NPs 159
5.2.1 Solubility and physicochemical properties of carrageenans 159
5.2.2 Preliminary studies on the formation of carrageenan/protamine nanoparticles 160
5.2.3 Influence of carrageenan/protamine concentration on NPs formation ... 163
5.2.4 Influence of formulation method on the properties of NPs 165
5.2.5 Formation of NPs using protamine solution at pH 3 and iota carrageenan 170
5.2.6 Influence of Ca^{2+} and Zn^{2+} cations on carrageenan/ protamine NPs formation 175
5.3 Physical stability of IC/P_pH3 NPs 178
5.3.1 Stability of IC/P_pH3 NPs up to 72 h storage at RT 178
5.3.2 Stability of IC/P_pH3 NPs in 0.1 M and 0.01 M HCl 180
5.3.3 Stability of IC/P_pH3 NPs in 0.1 M acetate buffer at pH 4.5 184
5.3.4 Stability of AAL/P_pH3 NPs in 0.1 M HEPES at pH 6.5 186
5.3.5 Stability of IC/P_pH3 NPs in 0.1 M and 0.01 M PBS at pH 7.4 187
5.3.6 Stability of IC/P_pH3 NPs in 0.1 M and 0.01 M NaCl 190
5.3.7 Stability of IC/P_pH3 NPs in cell culture medium 193
5.4 Conclusions 197
CHAPTER 6 199
PHYSICOCHEMICAL CHARACTERISATION, *IN VITRO* TOXICITY AND PEPTIDE TRANSPORT CHARACTERISTICS OF INSULIN LOADED NANOPARTICLES .. 199
6.1 Introduction 200
6.2 Formulation and *in vitro* characterisation of AAL/P_pH3 NPs loaded with insulin 200
6.2.1 Insulin association efficiency of AAL/P_pH3 NPs 200
6.2.2 Characterisation of AAL/P_pH3 NPs loaded with insulin 201
6.2.3 Stability of AAL/P_pH3 NPs loaded with insulin 203
6.2.4 Release of insulin from AAL/P_pH3 205

6.2.4.1 Release from AAL/P_pH3 NPs loaded with 100 µg/ml of insulin 205
6.2.4.1.1 Release in HCl buffer (pH 2) 205
6.2.4.1.2 Release in the acetate buffer (pH 4.5) 207
6.2.4.1.3 Release in PBS (pH 7.4) 208
6.2.4.1.4 Comparison of release profiles from AAL/P_pH3 NPs loaded with 100 µg/ml of insulin 209
6.2.4.1.5 Release in FaSSIF 210
6.2.4.2 Release from AAL/P_pH3 NPs loaded with 500 µg/ml of insulin 211
6.2.4.2.1 Release in HCl buffer (pH 2) 211
6.2.4.2.2 Release in the acetate buffer (pH 4.5) 212
6.2.4.2.3 Release in PBS (pH 7.4) 213
6.2.4.2.4 Comparison of release profiles from AAL/P_pH3 NPs loaded with 500 µg/ml of insulin 214
6.2.4.3 Comparison of release profiles from AAL/P_pH3 NPs loaded with 100 and 500 µg/ml of insulin 215
6.2.5 Cytotoxicity of AAL/P_pH3 NPs 216
6.2.6 Transport of insulin from AAL/P_pH3 NPs through Caco-2 monolayers 216
6.3 Formulation and *in vitro* characterisation of IC/P_pH3 NPs loaded with insulin 222
6.3.1 Characterisation of IC/P_pH3 NPs loaded with insulin 222
6.3.2 Stability of IC/P_pH3 NPs loaded with insulin 223
6.3.3 Insulin association efficiency of IC/P_pH3 NPs composed 226
6.3.4 Release of insulin from IC/P_pH3 226
6.3.4.1 Release from IC/P_pH3 NPs loaded with 100 µg/ml of insulin 226
6.3.4.1.1 Release in HCl buffer (pH 2) 227
6.3.4.1.2 Release in the acetate buffer (pH 4.5) 229
6.3.4.1.3 Release in PBS buffer (pH 4.5) 230
6.3.4.1.4 Comparison of release profiles from IC/P_pH3 NPs loaded with 100 µg/ml of insulin 231
6.3.4.1.5 Release in FaSSIF 232
6.3.4.2 Release from IC/P_pH3 NPs loaded with 500 µg/ml of insulin 233
6.3.4.2.1 Release in HCl buffer (pH 2) 234
6.3.4.2.2 Release in the acetate buffer (pH 4.5) 235
6.3.4.2.3 Release in PBS (pH 7.4) 236
6.3.4.2.4 Comparison of release profiles from IC/P_pH3 NPs loaded with 500 µg/ml of insulin 237
6.3.5 Cytotoxicity of IC/P_pH3 NPs 240
6.3.6 Transport of insulin from ICP_pH3 NPs through Caco-2 monolayer 241
6.4 Conclusions 245

CHAPTER 7 247
GENERAL DISCUSSION 247
7.1 Preparation of a novel insulin plasmids 250
7.2 Carrier system for insulin approach 253
7.2.1 Preparation of polyelectrolyte complex nanoparticles 253
7.2.2 Design of new polyelectrolyte complex-based nanocarriers 255
7.2.2.1 Polyelectrolyte components of investigated NPs 255
7.2.2.2 Physicochemical characteristics of investigated NPs 256
7.2.2.3 Stability studies of NPs 258
7.2.2.4 Incorporation of insulin into developed NPs and in vitro characterisation of formed NPs 261
7.2.2.4.1 Association efficiency of insulin into investigated NPs 261
7.2.2.4.2 *In vitro* release of insulin in media at various pH 262
7.2.2.4.3 Cytotoxicity of NPs and transport of insulin *in vitro* 266
7.3 Main findings 267
7.4 Future work: 268
CHAPTER 8 270
REFERENCES 270
APPENDICES 292
APPENDIX A Characterisation of alginate/ protamine carriers 293
APPENDIX B Characterisation of carrageenan/ protamine carriers 301
APPENDIX C *In vitro* characterisation of AAL/P_pH3 and IC/P_pH3 NPs loaded with insulin 303

ACKNOWLEDGEMENTS

It would not have been possible to write this doctoral thesis without the help and support of the kind people around me, to only some of whom it is possible to give particular mention here.

In particular I am most grateful to my supervisor Dr Mariusz Kamionka for giving me the opportunity to do a Ph.D. at Trinity College Dublin. I would like to express my deepest gratitude to my supervisors, Dr Lidia Tajber and Dr Astrid Sasse for excellent guidance, caring, patience, and providing me with an excellent atmosphere for doing research.

I would like to say thank you to Georgios-Charalompos Boutsikaris, whose project I had a chance to continue.

Special thanks to all of the students that I had a chance to supervise. It was a pleasure to introduce you to my research and to work with you. Thank you for contribution that you made for this thesis.

Very warm thanks to all my lab friends in the School of Pharmacy and Pharmaceutical Sciences, TCD that make my study so enjoyable. Thanks all of you for a nice atmosphere in the lab and support during writing of this report.

I would like to acknowledge lecturers, technicians and colleagues from the department that I had a chance to work with who often helped me, especially at the beginning of the project.

I would also like to thank my family, especially my parents. They were always supporting me and encouraging me with their best wishes. Warm thanks to my brothers, sisters and friends. Without their love over the many months none of this would have been possible.

I would like to thank my friend Magdalena Nowak for being there for me.

My apologies to the others who I have not mentioned by name, I am indebted to them for the many ways they helped me.

Acknowledgements to the Lorraine O'Driscoll research group, for a very kind gift of preproinsulin cDNA, which facilitated initial work that was performed within this project.

The author would also like to convey thanks to Merrion Pharmaceuticals, Ireland for funding my project.

PRESENTATIONS ASSOCIATED WITH THIS THESIS

Poster Presentations

"Formulation and *in vitro* characterisation of polymeric nanoparticulate carrier systems for oral delivery of insulin" at 5th World Conference on Drug Absorption, Transport and Delivery (WCDATD), Uppsala 2013 [Maria Dul, Hazel Kelly and Lidia Tajber]

"Developing and characterising new nanoparticulate carrier systems for the oral delivery of insulin" at All-Ireland Schools of Pharmacy Research Conference, Belfast 2013, [Maria Dul, Hazel Kelly and Lidia Tajber]

"Development of a new nanoparticulate system for the oral delivery of insulin" at AAPS Annual Meeting and Exposition, Chicago, 2012, [Maria Dul, Hazel Kelly and Lidia Tajber]

"Investigation into a lab-scale recombinant human insulin production system in *Escherichia coli*" at All-Ireland Schools of Pharmacy Research Conference, Cork 2012, [Maria Dul, Kelly Darragh, Mariusz Kamionka, Astrid Sasse and Lidia Tajber]

"Developing a straightforward recombinant human insulin production system in *E.coli*" at AAPS National Biotechnology Conference 2011, San Francisco, CA, [Maria Dul, Georgios-Charalompos Boutsikaris and Mariusz Kamionka]

"Characterisation of protein expression using various plasmids designed for lab-scale insulin production in *Escherichia coli*" at All-Ireland Schools of Pharmacy Research Conference, Dublin 2011, [Maria Dul and Mariusz Kamionka]

ABBREVIATIONS AND SYMBOLS

-	to
%	percent
°	degree
°C	degree Celsius
~	approximately
®	registered trademark
µm	micrometre
µl	microlitre
A	Adenine
AAK	Alanine alanine lysine
AAL	Alginic acid low viscosity (as sodium salt)
AAM	Alginic acid medium viscosity (as sodium salt)
AAH	Alginic acid high viscosity (as sodium salt)
Ab	Antibody
AE	Association efficiency
ALP	Achromobacter lyticus protease
ANOVA	Analysis of variance
anti-GAD	anti-glutamic acid decarboxylase
bp	base pair
BPTI	Bovine pancreatic trypsin inhibitor
BSA	Bovine Serum Albumin
C	Cytosine
Caco-2	Human colon adenocarcinoma cells
$CaCl_2$	Calcium chloride
cAMP	Cyclic adenosine monophosphate
cDNA	complementary DNA
CH_3CO_2K	Potassium acetate
cm	centimetre
cm^2	square centimetre
CNBr	Cyanogen bromide
CO_2	Carbon dioxide
CPP	Cell Penetrating Peptide
CPβCDs	Cationic β-cyclodextrin polymers
CS	Chitosan
CSII	Continuous subcutaneous insulin infusion
CV	Column volume
DL	Drug loading

DLS	Dynamic light scattering
DNA	Deoxyribonucleic acid
dNTP	deoxynucleoside triphosphate
DsbA	Disulphide oxidoreductase
DTT	Dithiothreitol
e.g.	for example
EDTA	Ethylenediaminetetraacetic acid
EK	Enteokinase
E.coli	*Escherichia coli*
et al.	et alli or et aliae
FaSSIF	Fasted state simulated intestinal fluid
FDA	Food and drug administration
FPLC	Fast protein liquid chromatography
fRMsr	free form of methionine-R-sulphoxide
g	gramme
G	Guanidine
GI	Gastrointestinal tract
GLP-1	Glucagon-like peptide 1
GSH	Glutathione
GSSG	Glutathione disulfide
GST	Glutathione-S-transferase
h	hour
H_2O	water
HCl	Hydrochloric acid
HBSS	Hanks' balanced salt solution
HEPES	4-(2-hydroxyethyl)-1-piperazineethanesulfonic acid
hGh	Human growth hormone
hIFN-c	Human interferon gamma
His tag	Hexahistidine tag
HIV-1Pr	Human immunodeficiency virus type 1 protease
HPLC	High performance liquid chromatography
HPMCP-55	Hypromellose phthalate
HRP	Horseradish peroxidase
HST	$(His)_6$ – tagged sequence
HTLV-1	Human T-cell leukemia virus type 1
IB	Inclusion body
IC	ι-carrageenan
IDDM	Insulin dependent diabetes mellitus

i.e.	that is
IEC	Ion exchange chromatography
IgG	Immunoglobulin G
IGF-I	Insulin-like growth factor
IMAC	Metal ion affinity chromatography
INS	Insulin
IPTG	Isopropyl-1-thio-*β*-*D*-galactopyranoside
k9	oligolysine
KC	κ-carrageenan
kDa	kilodalton
LB	Luria bertani
LC	λ-carrageenan
LDV	Laser doppler velocimetry
M	Moles per litre
mA	milliampere
mAb	Monolonal antibody
MBP	Maltose binding protein
MC	Methyl cellulose
MCD	Methyl β-cyclodextrin
MDI	Multiple daily injections
MEM	Eagle's minimal essential medium
mg	milligram
$MgCl_2$	Magnesium chloride
$MgSO_4$	Magnesium sulphate
min	minute
ml	millilitre
mM	millimolar
MTS	3-(4,5-dimethylthiazol-2-yl)-5-(3-2-(4-carboxymethoxyphenyl) sulfophenyl)-2H tetrazolinum
mV	millivolt
MW	Molecular weight
MWCO	Molecular weight cut-off
N-glut-PE	N-glutaryl-phosphatidylethanolamine
N/A	Not applicable
Na_2SO_3	Sodium sulphite
$Na_2S_2O_3$	Sodium tetrathionate
NaCl	Sodium chloride
NaH_2PO_4	Sodium dihydrogen phosphate

$NaH_2PO_4 \cdot H_2O$	Sodium dihydrogen phosphate monohydrate
NaN_3	Sodium azide
$NaNO_3$	Sodium nitrate
NaOH	Sodium hydroxide
n/d	not determined
ng	nanogramme
NIDDM	Non insulin dependent diabetes mellitus
nm	nanometre
NMR	Nuclear magnetic resonance
NP	Nanoparticle
OD	Optical density
ORI	Origin of replication
p	p-value
P	Protamine
P_{app}	Permeability coefficient
PBS	Phosphate buffer saline
PCP	Poly(methacrylicacid)-chitosan-polyethylene glycol
PCR	Polymerase chain reaction
PdI	Polydispersity index
PEC	Polyelectrolyte complex
PEG	Polyethylene glycol
PEI	Polyethylenimine
PGA	Poly(γ-glutamic acid)
pH	minus logarithm of hydrogen ion concentration
pI	isoelectric point
pmol	picomole
PLA-F127-PLA	Poly(lactic acid)-b-pluronic-b-poly(lactic acid) NPs
PPI	Pre-proinsulin
PVDF	Polyvinylidene fluoride
PVP	Polyvinylpyrrolidone
R^2	Correlation coefficient
r9	oligoarginine
RBI	Ragi bifunctional inhibitor
RH	Relative hypoglycaemia
RNA	Ribonucleic acid
RP HPLC	Reverse phase high performance liquid chromatography
rpm	revolutions per minute
RT	Room temperature

s	second
S. cerevisiae	*Saccharomyces cerevisiae*
SD	Standard deviation
SDS	Sodium dodecyl sulphate
SDS-PAGE	Sodium dodecyl sulphate polyacrylamide gel electrophoresis
SGF	Simulated gastric fluid
SIF	Simulated intestinal fluid
T	Thymine
TAE	Tris Acetate EDTA
TBS	Tris-buferred saline
TEER	Transepithelial electrical resistance
TEMED	N,N,N′,N′-Tetramethylethylenediamine
TFA	Trifluoroacetic acid
TL	Tomato lectin
Tris	Tris(hydroxymethyl)aminomethane
TTB	Towbing Transfer Buffer
UEA1	Ulex europaeus agglutinin 1
UV	Ultraviolet
UV-VIS	Ultraviolet-visible spectroscopy
V	Volt
v/v	volume in volume
WGA	Wheat germ agglutinin
WHO	World health organisation
w/v	weight in volume
w/w	weight in weight
x g	gravitational acceleration constant
$ZnCl_2$	Zinc chloride
ZP	Zeta potential
β-ME	Beta mercaptoethanol
λ	Wavelength
γ-PGA	Poly(γ-glutamic acid)

SUMMARY

The studies in this thesis investigated the preparation of a novel system that would be suitable for the oral delivery of insulin. The genetic modification of insulin gene to establish a simple system of insulin production and formulation of polyelectrolyte complex nanoparticles as potential carriers for the delivery of insulin were examined.
To facilitate further modifications of insulin gene, several plasmids with insulin were designed and prepared. The design of the plasmids was based on the combination of the simplicity of a bacterial expression system with benefits of the expression in yeast, which is achieved by directing the expressed protein with the signal peptide to the oxidation system of the bacterial periplasmic space. Five plasmids with insulin were successfully prepared (pHB1, pHB2, pHB3, pMD2, pMD3) and all of them expressed insulin, however its amount and form was different. Optimisation of expression conditions was further investigated by testing two induction systems: isopropyl β-D-1-thiogalactopyranoside (IPTG) and auto-induction and also various temperatures. The impact of those factors on the solubility and localisation of expressed protein was also examined. Expression of the protein was controlled by measuring the optical density of the culture at 600 nm. Samples prepared for expression, solubility and periplasmic localisation test were tested with SDS-PAGE and Western blot techniques. Two plasmids: pMD2 (protein expressed in the periplasm) and pHB1 (the greatest amount of protein expressed in the insoluble form) were selected for further purification process. Final optimisation of the purification protocols was established for selected plasmids. It involved affinity chromatography (Ni column for purification of His tagged proteins) and Achromobacter lyticus protease (ALP) cleavage for purification of periplasmic fraction of protein expressed by plasmid pMD2. A more complex purification process had to be applied for purification of insoluble form of protein expressed by pHB1 plasmid, as the protein had to be isolated, washed, cleaved, purified and finally renaturated. Moreover, optimisation of the refolding reaction was performed using four various redox conditions: glutathione/glutathione disulfide, β-mercaptoethanol, dithiothreitol and cysteine/cystine, as this reaction was one of the steps that resulted in final low yield of the purification process. The amount of the protein was quantified by BioRad Protein Assay. Additionally samples were analysed with SDS-PAGE and Western blot technique. Prepared plasmids can be used for further genetic modifications as preparing fusions of insulin gene with cell penetrating peptides.
The second approach that has been investigated in the present work development and incorporation of insulin into nanocarriers composed of natural polymers (alginic acid and carrageenan) and protamine as a cell penetrating peptide. Polyelectrolyte complexation was used to manufacture NPs. At first, the conditions for the formation

of insulin-free nanoparticles (NPs) were determined and the manufacture process was optimised by testing the impact of process variables (e.g. the type of polymer used: solution viscosity, concentration and mixing ratio of the polymers) on the properties of NPs. The particle size and size distribution (PdI) were analysed using dynamic light scattering and zeta potential (ZP) was measured with the use of laser Doppler velocimetry. Physical stability of selected formulations was tested upon storage at room temperature and in liquid media at various pH. The impact of the loaded peptide on the physicochemical properties of NPs such as: particle size, ZP, PdI as well as peptide association efficiency (AE), drug loading and *in vitro* insulin release was examined. Cytotoxicity of selected formulations in the Caco-2 cell line was performed. Finally, *in vitro* transport of insulin loaded into prepared nanocarriers through Caco-2 monolayers was examined. Simple, organic solvent and surfactant-free production method by mixing aqueous solutions of polyelectrolytes at room temperature was successfully employed to fabricate novel, cross-linker-free and non-sedimenting NPs. It was possible to obtain NPs with good physical properties (i.e. small and homogenously dispersed) for all of both types of polymers tested. Both, negatively and positively charged NPs, were formed by changing the polymer/protamine weight ratio. Physical stability of NPs upon storage at room temperature and in buffers at various pH was strongly dependent on the initial charge of NPs with better stability of negatively charged NPs in most cases. Two amounts of insulin were loaded into NPs: 100 and 500 µg/ml. Almost 100% AEs were obtained for negatively charged NPs for both doses of insulin loaded. Smaller amounts of insulin were associated with positively charged NPs, with greater AE obtained with alginate-based NPs. Similar *in vitro* release profiles were obtained for all formulations of positively charged NPs, with 90 – 100% of insulin released in first 10 minutes in all of the buffers tested. Release from negatively charged NPs was depended on the formulation, amount of insulin loaded and pH of the buffer. Negatively charged NPs were non-toxic, while 45% - 51% Caco-2 cells (0.5 mg/ml NPs) remained viable after 72 h of incubation with positively charged NPs. The amount and kinetics of insulin transported through Caco-2 monolayers was dependent on the composition of formulation tested.

ORIGIN AND SCOPE

Insulin was the first therapeutic protein produced with recombinant DNA biotechnology and the market for this protein reaches now about 5-6 tons per year (Petrides et al., 1995). Developments in recombinant technology led to the production of native human insulin. The gene encoding insulin is inserted into a suitable vector and expressed in a host organism: *Escherichia coli* or *Saccharomyces cerevisiae* (Cousens et al., 1987, Walsh, 2005). However, the peptide is expressed mainly in the insoluble form as inclusion bodies, which requires several purification and renaturation steps to obtain native functional human insulin. Several studies were conducted in order to improve the expression, purification and overall yield of insulin (Shen, 1984, Murby, 1991, Kang and Yoon, 1994, Samuelsson et al., 1994, Winter et al., 2000, Cho et al., 2001, Tikhonov et al., 2001, Mergulhao et al., 2004, Malik et al., 2007, Min et al., 2011).

Various methods of insulin administration other than injection, have been sought since the discovery of insulin (White et al., 2001). Unfortunately, most attempts have failed to progress beyond the proof of concept stage because of the peptide low bioavailability, dose response variability and other adverse factors. Products for pulmonary (Exubera®, Pfizer) and buccal (Oral-Lyn produced by Generex Biotechnology, only in Ecuador) delivery of insulin have been approved (Beals et al., 2008, Heinemann and Jacques, 2009). However, Exubera® has been withdrawn from the market only one year after its introduction, mainly due to the poor sales of the product (Heinemann, 2008).

Oral delivery is the preferred route of drug administration because it is non-invasive, avoids injections and decreases the risk of infections. None of the numerous therapeutic proteins can be delivered orally at present (Park et al., 2011). One of the reasons is the large size of protein molecules, which is an obstacle to drug absorption in the intestine.

Protein engineering technology could be used as a tool to affect structural and environmental factors that influence absorption of protein therapeutics in the intestine. To achieve that, an approach of producing recombinant human insulin analogues with enhanced bioavailability after oral delivery may be explored. In addition to genetic modifications, there are several strategies employed to enhance transport of macromolecules through epithelial cell layers. These include the use of penetration enhancers or incorporation of macromolecules into carrier systems such as nanospheres or liposomes (Park et al., 2011).

Over the past few years, there has been increasing attention to the use of cell penetrating peptides (CPPs) as penetration enhancers. CPPs are short peptides of about 7-15 aminoacid residues and are cationic or amphiphilic in nature (Sebbage, 2009). CPPs have been used extensively for intracellular delivery of

macromolecules and to facilitate their transport across epithelial barriers (Patel et al., 2009). Polymeric nanoparticles (NPs) demonstrate an interesting approach, mainly because of their ability to entrap macromolecules, protect against degradation and enhance transmucosal transport (de la Fuente et al., 2008). Particularly natural polymers attract increased attention, mainly due to their nontoxic, biocompatible, biodegradable and hydrophilic nature (Sonia and Sharma, 2012). Several techniques are available for the preparation of polymeric NPs (Vauthier and Bouchemal, 2009). Among them, a polyelectrolyte complexation (PEC) method has been recently studied, as especially suited to formulate peptides and proteins. No organic solvents and sonication are needed and the process can be carried out in completely aqueous conditions and at ambient temperature (Hu et al., 2012). Recently, Umerska et al. (2012) presented a range of polyelectrolyte complex-based NPs containing salmon calcitonin and showed modulation of physicochemical properties of such NPs depending on the type of polyelectrolytes used.

The scope of this thesis was:

- Design and preparation of novel DNA constructs combining simplicity of the bacterial expression system and the benefits of yeast expression system
- Optimisation of insulin expression from *E .coli*, isolation and purification of the protein
- Development and characterisation of polyelectrolyte complex nanocarriers composed of naturally occurring, biocompatible macromolecules: alginic acid or carrageenan and protamine and to investigate the influence of different formulation variables on the formation and properties of the carriers
- Loading insulin into the selected nanocarriers with a view of achieving maximum association efficiency of the peptide and nanoparticle physical stability as well as to investigate insulin *in vitro* release profiles
- Assessment of *in vitro* cytotoxicity of nanoparticles and to perform preliminary studies on the transport of insulin from the nanoparticles through Caco-2 monolayers as a model for drug transport across the intestinal mucosa

CHAPTER 1

INTRODUCTION

1.1 Diabetes mellitus

Disturbance of the pancreatic functions occurs in diabetes mellitus. This fact was noted as early as 1788, and in 1889 diabetes mellitus was induced experimentally by disruption of the pancreas (Chien, 1996). The term diabetes mellitus describes a group of metabolic diseases characterised by a high blood sugar (glucose) level. The high blood sugar level can result from defects in insulin secretion, insulin action or both. The effects of diabetes mellitus include long-term damage such as the dysfunction and failure of various organs. Characteristic symptoms of diabetes mellitus are thirst, polyuria, blurring of vision, and weight loss. There are two major types of diabetes, which are referred to as type 1 and type 2 (Alberti and Zimmet, 1998).

Type 1 diabetes (also called Insulin Dependent Diabetes Mellitus (IDDM), or juvenile onset diabetes mellitus), is generally caused by β-cell disruption, often immune mediated, that leads to loss of insulin secretion and absolute insulin deficiency. This may ultimately lead to diabetes mellitus in which 'insulin is required for survival' to prevent the development of ketoacidosis, coma and death (Daneman, 2006). Type 1 diabetes mellitus is usually characterised by the presence of anti-glutamic acid decarboxylase (anti-GAD), islet cell or insulin antibodies which identify the autoimmune processes that lead to β-cell disruption. Without sufficient levels of insulin, patients with type 1 diabetes cannot properly utilise glucose and typically have markedly elevated blood glucose (hyperglycemia), while intracellular glucose levels are generally low (Carino and Mathiowitz, 1999, Le Roith et al., 2004, Alberti and Zimmet, 1998). Currently, insulin therapy administered to control blood sugar levels is the only effective treatment for type 1 diabetes (Carino and Mathiowitz, 1999). Other treatment options are available, such as pancreatic and islets transplants, but these procedures depend on the availability of human donors and moreover, in case of islet transplants, do not ensure permanent insulin independence (Bretzel et al., 2007, Shapiro et al., 2006). Most patients with type 1 diabetes and approximately 27% of type 2 diabetics must take daily insulin treatments administered parenterally, in order to manage the disease (Mayfield et al., 2004). Type 2 diabetes (NIDDM – Non Insulin Dependent Diabetes Mellitus) is characterised by non-responsiveness to insulin. Type 2 diabetes is caused by a combination of genetic and non-genetic factors that result in insulin resistance and insulin deficiency. The specific genes are currently under investigation. Non-genetic factors include increased age, high caloric diet, excess weight, central adiposity and sedentary lifestyle. NIDDM is also characterised by hyperglycemia and shares similar long term complications as IDDM (Carino and Mathiowitz, 1999, Le Roith et al., 2004, Alberti and Zimmet, 1998). Type 2 diabetes can be controlled with

appropriate diet and exercise. With respect to drug therapy, metformin is most widely used medication in treatment of type 2 diabetes. Metformin is the drug of choice to initiate treatment in patients newly given a diagnosis of diabetes type 2 or in patients whose lifestyle modifications fail to attain glycemic control (Irons, 2013). With the emergence of other treatment options, metformin remains underused in as many as 35% of patients. An alternative is to use a thiazolidinedione drug (actos or avandia) that can improve glucose levels by overcoming insulin resistance in the liver or muscle. Sulfonylurea drugs such as glipizide or amaryl and also starlix and prandin lower glucose levels by stimulating the remaining β-cells to produce more insulin (Desai et al., 2012). However, in more advanced cases, insulin therapy is required. Other types of diabetes mellitus are less common. These include a heterogeneous etiologic group that the exocrine includes those cases in which the causes are established or at least partially known. Causes include known genetic defects affecting β-cell function or insulin action, disease of pancreas, endocrinopathies, and drug- or chemical-induced pancreatic changes. These factors comprise approximately 1% to 2% of the cases of diabetic syndrome (Carino and Mathiowitz, 1999, Le Roith et al., 2004, Alberti and Zimmet, 1998). Gestational diabetes mellitus is caused by insulin resistance and relative insulin deficiency associated with pregnancy occurs in approximately 3% to 5% of all pregnancies (Carino and Mathiowitz, 1999, Le Roith et al., 2004, Alberti and Zimmet, 1998).

1.2. Insulin market

Diabetes mellitus is a disease that affects approximately 382 million people worldwide and prevalence continues to increase (IDF, Diabetes Atlas, 2013). In 2004, an estimated 3.4 million people died from consequences of high fasting blood sugar (WHO, 2009). The World Health Organisation (WHO) predicts that by 2030 there will be approximately 366.2 million diabetics world-wide. The US alone has 20.8 million people suffering from diabetes, which equates 6% of the population (Al-Tabakha and Arida, 2008). WHO projects that diabetes will be the 7th leading cause of death in 2030 (WHO, 2011). The global diabetes drugs treatment market was valued at $35.6 billion in 2012. The analysis showed that human insulins and analogues dominated the antidiabetics market in 2012. (Diabetes treatment, 2012-2013).

The key role for insulin in the treatment and management of diabetes and the physiological actions of insulin on glucose and lipid metabolism are clearly established. The first treatments of diabetes mellitus employed insulin purified from animal pancreas (Rosenfeld, 2002). However, insulin obtained from animals has different aminoacid sequence than human insulin and also needed to be purified

from a complex mixture of proteins, which increased the risk of allergic reactions. Additionally, a growing demand for insulin was observed that could not be met utilising just animal sources (Bhatnagar et al., 2006). These issues underpinned the development of recombinant human insulin products, now routinely used in the management of diabetes.

1.3 Insulin structure – biosynthesis and metabolism

The first isolation of insulin in the 1920's by Frederick Banting and Charles Best brought a big relief to many diabetic patients, who before that, were subjected to rigorous starvation and a poor quality of life (Developed by Banting and Best, crude insulin was isolated from canine pancreas, and after several years of improvement it was eventually standardised with the support of the pharmaceutical company Eli Lilly (Sinding, 2002).

Insulin consists of 51 amino acids, subdivided into an A-chain (21 amino acids) and a B-chain (30 amino acids). Both chains are connected by two intermolecular disulfide bonds, A7-B7 and A20-B19. The A-chain contains an additional intramolecular disulfide bond A6-A11 (Chien, 1996). The primary structure of insulin is depicted in Figure 1.1.

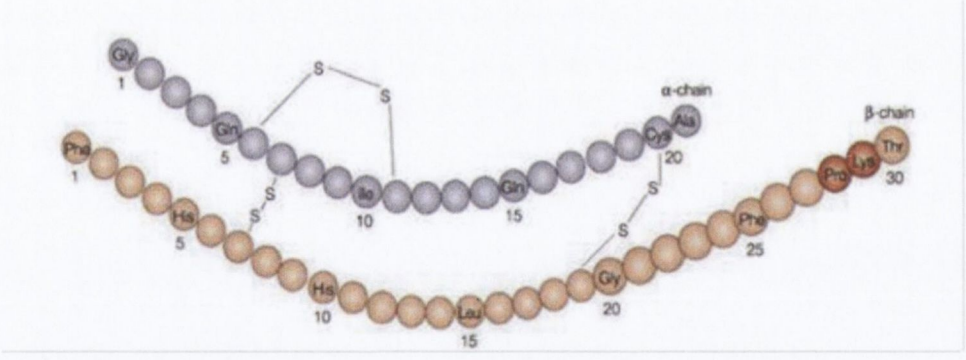

Fig. 1.1 *Primary structure of insulin (adapted from Owens, 2002).*

Insulin from various species confirms this basic structure, while varying slightly in the amino acid sequence. Porcine insulin (5,777 Da) varies from the human form (5,807 Da) by a single amino acid, whereas bovine insulin (5,733 Da) differs by three residues (Walsh, 2007). Variations in the type of amino acid residues among some mammalian insulins are presented in Figure 1.2.

	A – Chain (21 amino acids)			B – Chain (30 amino acids)
Species	**8th**	**9th**	**10th**	**30th**
Human	Thr	Ser	Ile	Thr
Porcine	Thr	Ser	Ile	Ala
Canine	Thr	Ser	Ile	Ala
Sperm Whale	Thr	Ser	Ile	Ala
Rabbit	Thr	Ser	Ile	Ser
Sei Whale	Ala	Ser	Thr	Ala
Bovine	Ala	Ser	Val	Ala
Sheep	Ala	Gly	Val	Ala
Horse	Thr	Gly	Ile	Ala

Ala: Alanine Ser: Serine
Gly: Glycine Thr: Threonine
Iso: Isoleucine Val: Valine

Fig. 1.2 *The species variation in the type of amino acids residues among some mammalian insulins (adapted from Chien, 1996).*

Insulin is a polypeptide hormone which plays an essential role in regulating blood glucose levels. Generally insulin keeps blood glucose levels within narrow defined limits (3.5 – 8.0 $mmol \cdot l^{-1}$). It also has a profound effect on the metabolism of proteins and lipids (Walsh, 2007). Insulin is produced by the β-cells of pancreatic islets of Langerhans as a single chain precursor polypeptide pre-proinsulin. Subsequent proteolytic processing removes the aminoterminal signal peptide, giving rise to proinsulin. Cleavage of an internal 31-residue fragment generates C peptide, A-chain (21 amino acids) and B-chain (30 amino acids) of insulin (Figure 1.3) (Tofteng et al., 2008).

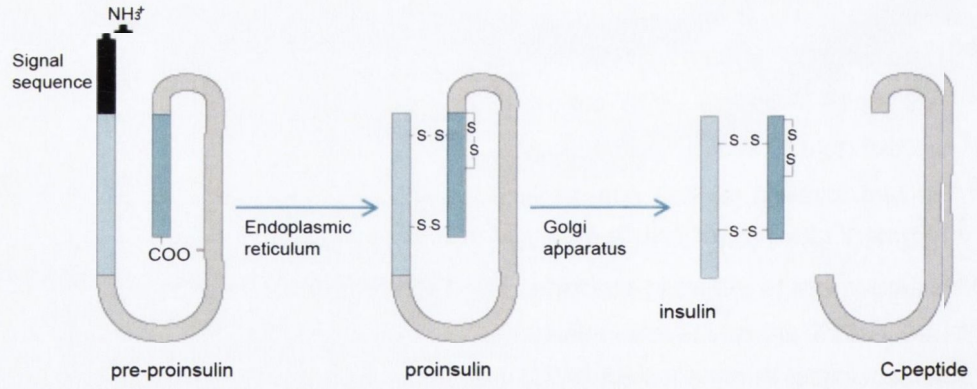

Fig. 1.3 *The biosynthesis of insulin (adapted from Access Science, 2013).*

Structurally, proinsulin is related to insulin-like growth factors I and II. These bind weakly to the insulin receptor. The C-peptide and the mature insulin molecule are stored together and are co-secreted from secretory granules in the β-cells. The C-peptide is cleared more slowly than insulin which makes it a useful marker of insulin secretion and facilitates the discrimination of endogenous and exogenous sources of insulin in the evaluation of hypoglycaemia (Harrison's Principle of Internal

Medicine, 2008). Both insulin and C-peptide are released into the portal venous system by the process of exocytosis. This leads it directly to the liver, which takes up nearly 50% of the excreted insulin. The remainder of insulin is distributed throughout the body. The main stimulant of insulin secretion is glucose (Chien, 1996).

Insulin secretion elicits a biphasic release: an immediate effect of short duration, which is dependent on the amounts available in storage, and a sustained effect. The latter release is prolonged since insulin has to be synthesised, processed, and secreted for the duration of the increase of blood glucose. Additionally, β-cells regenerate the stores of insulin initially depleted in the fast response phase (Nesher and Cerasi, 2002).

The cells of the islets of Langerhans are connected by tight junctions. This allows transferring of ions, secondary messengers or metabolites from one cell to another, and plays an important role in synchronising the secretions (Houamed et al., 2004). Insulin orchestrates a suitable metabolic response to the absorption of glucose and other nutrients in a number of ways:

- Stimulation of glucose transport (and transport of amino acids, K^+ ions and other nutrients) into the cell, reducing their blood concentration in this way;
- Inhibition (or help in inhibition) of catabolic pathways, such as gluconeogenesis;
- Stimulation (or help in stimulation) of intracellular biosynthetic (anabolic pathways, such as glycogen synthesis, that helps to convert the nutrients into the storage form in the cells;
- Stimulation of protein and DNA synthesis (which underlines insulin's growth-promoting activity), (Walsh, 2007).

1.4 Recombinant DNA technology – methods of insulin production

Human insulin was the first mammalian protein produced by recombinant DNA technology and approved for general medical use in 1982 (Dingermann, 2008). It was produced in bacteria in a sequence identical to sequence of insulin obtained from the human pancreas. Collaboration between Eli Lilly (Indiapolis, IN) and Genentech (San Francisco, CA) resulted in achieving expression of a recombinant form of human insulin in *E. coli* (Ladisch and Kohlmann, 1992). Pioneered by Eli Lilly and Genentech, the technique involved inserting chemically synthesised genes into the *E. coli*, fermenting the bacteria, and then harvesting the overexpressed polypeptides prior to cleavage. There are three methods of recombinant human insulin production, which are described below.

1.4.1 Recombinant human insulin production in bacteria

1.4.1.1 Two-chain method

This method entailed the separate expression of chemically synthesised nucleotide sequences coding for insulin A- and B-chains in two *E. coli* production strains. Transformation of *E. coli* with the chimeric plasmid DNA led to the synthesis of hybrid polypeptides, including the sequence of amino acids corresponding to human insulin A- and B-chains (Figure 1.4). Methionine is the N-terminal translation initiator present in *E. coli* expression, that needs to be removed from expressed protein to ensure its proper function and stability (Liao et al., 2004). As human insulin chains have no methionine at the N-terminus, it needs to be cleaved off, with cyanogen bromide. Following separate purification, the two chains are co-incubated under reaction conditions, which promote formation of intact insulin via disulfide bond formation. Purified A- and B-chains are subsequently combined in the form of stable S-sulphonate derivatives and generate native insulin, (Ladisch and Kohlmann, 1992). This "chain combination" procedure was used for producing early commercial recombinant insulins (Walsh, 2005, Chance et al., 1999).

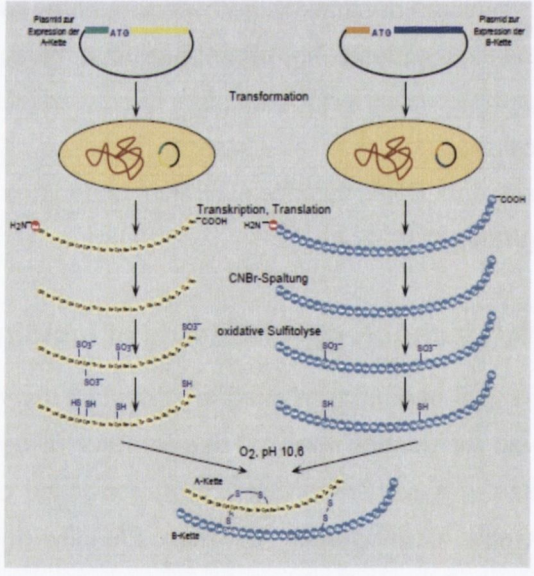

Fig. 1.4 *Recombinant human insulin production in bacteria (E. coli). A- and B-chains produced separately in two strains (adapted from Zündorf and Dingermann, 2001).*

1.4.1.2 Proinsulin method (intracellular)

The second method of recombinant human insulin production using *E. coli* entailed expression of a single chemically synthesised nucleotide sequence coding for native human proinsulin (cytoplasmic synthesis). Appropriate fusion partner for proinsulin

requires either cyanogen bromide (Kroeff et al., 1989) or proteolytic cleavage, (Castellanos-Serra et al., 1996, Nilsson et al., 1996, Jonasson et al., 1996) to separate it through the downstream processing. The purification of expressed polypeptide is followed by proteolytic excision of the C-peptide *in vitro* (Figure 1.5). Proteolytic processing of proinsulin involves the combined utilisation of trypsin and carboxypeptidase B (Castellanos-Serra et al., 1996, Jonasson et al., 1996; Nilsson et al, 1996).

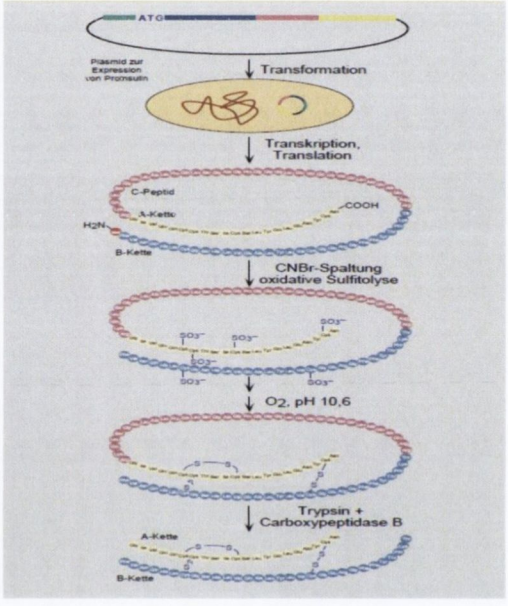

Fig. 1.5 *Recombinant human insulin production in one E. coli strain (adapted from Zündorf and Dingermann, 2001).*

Production of recombinant human insulin according to this method is preferred, largely as a consequence of a requirement for only a single fermentation and subsequent purification protocol. Additionally this process is a substantially more efficient than the two-chain combination approach (Walsh, 2005). Figure 1.6 shows the overview of the industrial-scale production of recombinant insulins produced by the "proinsulin route".

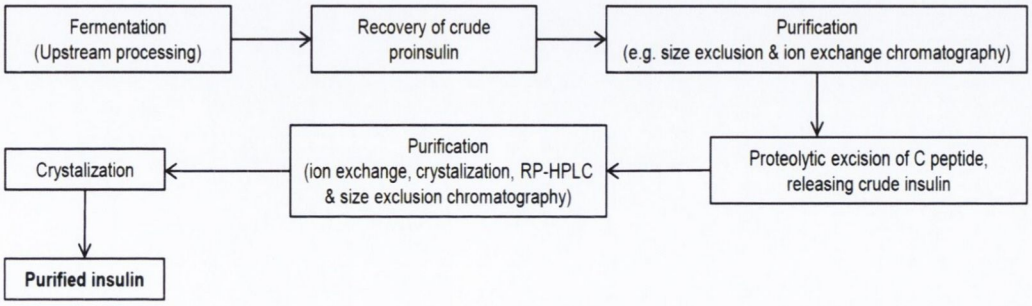

Fig. 1.6 *A generalised overview of the industrial-scale production of modern high-purity recombinant insulins via the "proinsulin route", (Walsh, 2005).*

1.4.2 Recombinant human insulin production in yeast

An alternative biosynthesis method of recombinant human insulin is to insert the genes into the yeast *S. cerevisiae*, which secretes the resulting polypeptide into the culture medium, thus simplifying the purification process (Heller et al., 2007). The aim of this method initialised by Novo Nordisk was to produce a proinsulin extracellulary without any extra residues originating from the host organism (no methionine at the N-terminus). Ultimately a new "artificial gene" called "mini-pro-insulin gene" was inserted instead of C-peptide. This short C-peptide version (3 amino acids residues, AAK), apparently brings the A- and B-chains together into a proximity which allows the yeast cell machinery to produce correct disulfide bridges. To ensure protein secretion out of the cell, a signal peptide sequence is inserted in the front of the gene sequence. The signal peptide is cleaved off by a yeast protease. Production of human insulin using yeast as a host organism has advantages which results from a correct N-terminus (no methionine present as in the case of *E. coli*) and correct disulfide bridges formation. Mini C-peptide (AAK) removal involves the same technology as for changing porcine insulin to human insulin in aqueous environment, where in the presence of threonine-tert-butyl ester the expressed product is exposed to trypsin. Trypsin cleaves initially after every lysine residue and subsequently extends the B-chain in a reverse reaction through transpeptidation with a threonine ester residue. After hydrolysis of the ester, active human insulin is produced (Zündorf and Dingermann, 2001, Ladisch and Kohlmann, 1992). Production of insulin by above method is illustrated in Figure 1.7.

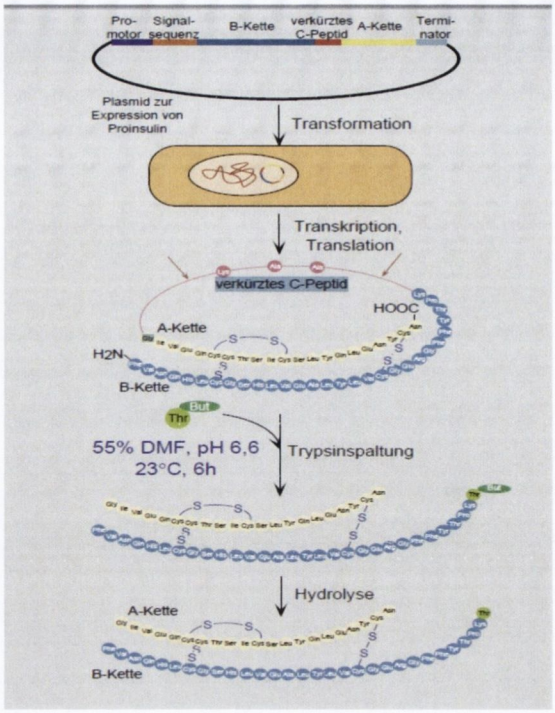

Fig. 1.7 *Recombinant human insulin production in yeast (Saccharomyces cerevisiae) (adapted from Zündorf and Dingermann, 2001).*

Engineered *S. cerevisiae* have been used to produce recombinant human insulin since the mid-1980s and a substantial proportion of current recombinant commercial insulins are produced by expression-optimised yeast systems (Table 1.1).

Table 1.1 *Recombinant human insulin/ engineered insulin currently approved for general medical use in the USA and/ or EU (Walsh, 2005).*

Product	Description	Structure	Company	Approved
Humulin	Recombinant human insulin produced in *Escherichia coli*	Identical to native human insulin	Eli Lilly	1982 (USA)
Novolin	Recombinant human insulin produced in *Saccharomyces cerevisiae*	Identical to native human insulin	Novo Nordisk	1991 (USA)
Insuman	Recombinant human insulin produced in *E. coli*	Identical to native human insulin	Hoechst	1997 (EU)
Actarapid/Velosulin/ Monotard/Insulatard/ Protaphane/Mixtard/ Actaphane/Ultratard	All contain recombinant human insulin produced in *S. cerevisiae* formulated as short/immediate/long-acting product	Identical to native human insulin	Novo Nordisk	2002 (EU)
Humalog (insulin Lispro)	Recombinant short-acting human insulin analogue produced in *E. coli*	Engineered; inversion of native B28-B29 proline-lysine sequence	Eli Lilly	1996 (USA and EU)
Liprolog (insulin Lispro)	Recombinant short-acting human insulin analogue produced in *E. coli*	Engineered; inversion of native B28-B29 proline-lysine sequence	Eli Lilly	1997 (EU)
NovoRapid (insulin Aspart)	Recombinant short-acting human insulin analogue produced in *S. cerevisiae*	Engineered: B28 proline replaced by aspartic acid	Novo Nordisk	1999 (EU)
Novolog (insulin Aspart)	Recombinant short-acting human insulin analogue produced in *S. cerevisiae*	Engineered: B28 proline replaced by aspartic acid	Novo Nordisk	2001 (USA)
Levemir (insulin Detemir)	Recombinant long-acting human insulin analogue produced in *S. cerevisiae*	Engineered: devoid of B30 threonine and a C14 fatty acid is covalently attached to B29 lysine	Novo Nordisk	2004 (EU)
Apidra (insulin Glulisine)	Recombinant rapid-acting insulin analogue produced in *E. coli*	Engineered: B3 asparagine is replaced by a lysine and B29 lysine is replaced by glutamic acid	Aventis Pharmaceuticals	2004 (USA)
Lantus (insulin Glargine; Optisulin)	Recombinant long-acting human insulin analogue produced in *E. coli*	Engineered: A21 asparagine replaced by glycine and B chain elongated by two arginines	Aventis Pharmaceuticals	2000 (USA and EU)

1.5 Expression of proteins in *Escherichia coli* as a host organism

E. coli is the most commonly used organism for the expression of proteins. *E. coli* grows easily, rapidly, and in very large numbers in relatively cheap media. It is a well-established organism for growing proteins, with a large number of biological tools developed for maximising the efficiency of protein production. Plasmid vectors are the key components that regulate protein expression in *E. coli*. They need to have certain features of cloning plasmids and a suitably strong promoter for expressing the gene of interest. Origin of Replication (ORI) is a specific sequence of nucleotide in DNA from which replication begins. When foreign DNA is linked to this particular sequence, then along with vector replication, foreign DNA starts to replicate also. Besides ORI, a cloning vector should have a selectable marker gene. This permits the selection of host cells which bear rDNA from those which do not bear rDNA. An example is antibiotic resistance. The region where the gene of interest will be introduced must be downstream from the promoter. Usually, this will be a multiple cloning sites (polylinker), with DNA sequence where the restriction sites for several enzymes which cut only at this site in the plasmid are present very close to each other. The most important features of the vectors are promoters. A promoter is a region of DNA which initiates transcription of a particular gene. For transcription to take place RNA polymerase must attach to the DNA, promoters provide an initial binding site for these, and the promoter also accommodates transcription factors which are needed for the transcription process to take place. The transcription terminator is a section of DNA sequence that marks the end of the transcription process. Figure 1.8 summarises the most important features of expression vectors.

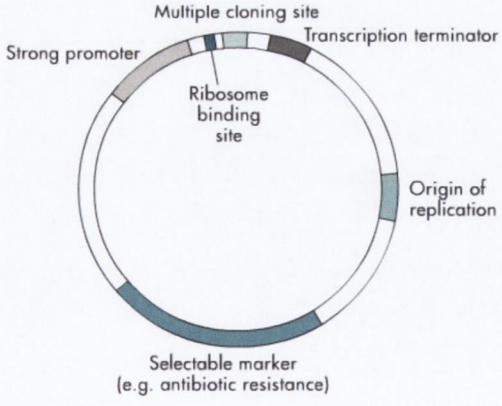

Fig. 1.8 *The key features of a typical vector used for proteins expression (adapted from Lodge et al., 2006).*

As mentioned already, promoters are the most important features of the vector, as they can drive expression of the gene to high levels. The promoter is localised upstream of the gene of interest in a suitable plasmid vector, it directs transcription of

the gene encoding the protein of interest. To obtain a high level of protein expression, the promoter has to be strong, as the stronger the promoter, the more mRNA will be synthesised, and the more protein will result from the translation of this mRNA. The second important feature of the promoter is the degree to which expression from it can be regulated, however as is often the case, high levels of expression of heterologous protein can lead to a decrease in growth of *E. coli*, or even death. The ideal promoter, for most expression experiments, should be strong but at the same time easy to turn down or even off. An example of promoters that are used for protein expression are promoters which are derived from *E. coli* operons, such as the *lac* promoter of the *lac* operon. The expression from the *lac* promoter is regulated by the *lac* repressor protein, *Lac*I. In the absence of lactose *Lac*I is bound to DNA, preventing expression of the gene of the lac operon, which encode proteins for lactose uptake and cleavage. DNA of the *lac* promoter, which contains the binding sites for RNA polymerase can be cloned upstream of any gene, placing the expression of these genes under the control of the signals that usually direct lac gene expression. Expression of proteins from the lac promoter is usually induced experimentally by IPTG. It prevents repression of the *lac* promoter but it is not metabolised by the products of the *lac* operon, so there is no need for continuous replenishment in the medium, as the cells grow. However, before the gene of interest is transcribed, the *lac* repressor (*Lac*I) must fall off the operator DNA sequence in the front of the gene of interest. Additionally, RNA polymerase must be introduced and recognise the T7 promoter in the absence of repressor. The gene coding for T7 RNA polymerase itself has been engineered into many commercially available *E. coli* strains. Instead of a T7 promoter sequence in front of the *lac* operator sequence, there is a *lac* promoter sequence that native *E. coli* RNA polymerase is able to bind. Once the *lac* repressor protein falls off of the *lac* operator sequence of DNA in the host chromosome, T7 RNA polymerase will be transcribed and translated. The *lac* repressor protein evolved to sense the presence of lactose. In the absence of lactose, the *lac* repressor binds to the operator sequence on DNA and bends the DNA by 40°. This blocks access of T7 RNA polymerase to the promoter site and thus prevents leaky transcription of the gene before induction. When lactose binds to *Lac*I it induces a conformational change in the protein structure that renders it incapable of binding to the operator DNA sequence. IPTG is a structural mimic of lactose, in that it resembles the galactose sugar, and it also binds to the *lac* repressor and induces a similar conformational change that greatly reduces its affinity to DNA. Thankfully, IPTG is not part of any metabolic pathways and so will not be broken down or used by the cell. This results in a constant concentration of IPTG, allowing it be a more useful inducer of the lac operon than lactose itself. Once the lac repressor

can no longer bind the operator, native *E. coli* RNA polymerase begins transcribing the T7 RNA polymerase gene engineered into its chromosome. Once the protein is expressed it binds to the T7 promoter sequence upstream of the gene of interest on the plasmid insert and transcribes to the target gene. Figure 1.9 illustrates the action of the lac promoter.

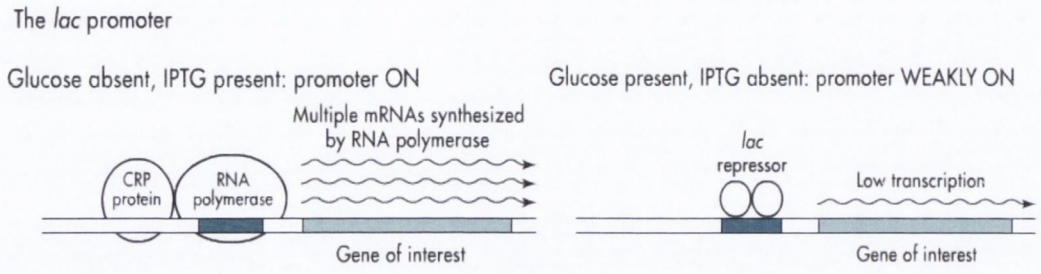

Fig. 1.9 *The mode of action of the lac promoter when on and off (adapted from Lodge et al., 2006).*

The idea of auto-induction was introduced as a convenient way to perform recombinant protein production without inducer addition (IPTG) for *lac* operon controlled expression systems. Auto-induction is a new method where proteins can be expressed effortlessly and with significantly higher yields than can be achieved with IPTG induction. This method, described by Studier, is based on the ability of certain media to induce protein expression in *E. coli* when cells reach saturation (Studier, 2005).

The idea behind auto-induction is to grow the bacteria in a defined medium in which expression of the T7 polymerase is automatically induced in late log-phase growth due to the depletion of carbon sources other than lactose. As the other carbon sources (glucose and glycerol) become depleted, the cells are forced to use lactose. At this point synthesis of the T7 polymerase is turned on. In addition, once glucose is depleted, cAMP (cyclic adenosine monophosphate) levels rise and catabolite repression is relieved. Auto-induction is based on the ability of certain media to induce protein expression in *E. coli* when cells reach saturation. It is a result of the different metabolism states of the bacteria. Auto-induction occurs due to the presence of lactose in the media. Glucose prevents induction by lactose. Auto-induction can be regulated by adjusting the glucose/lactose levels in the media used. The auto-induction system has many advantages, such as: no need to control and monitor the bacterial cultures before the addition of inducer and possibility of overnight incubation since they do not need to be manipulated. Another advantage is a greater cell mass and concomitantly higher yield of expressed proteins, as the media is well buffered and the T7 polymerase is induced in the late log-phase. Moreover this method of induction avoids the high cost of IPTG.

1.6 Recombinant protein production in *Escherichia coli*

E. coli is the most common bacteria, and with the development of recombinant DNA technology it has been used as a host of choice for the manufacture of many non-glycosylated proteins (Blattner et al., 1997, Choi and Lee, 2004, Schumann and Ferreira, 2004). Expressed proteins may be localised in cytoplasm, secreted into periplasm or excreted into the culture media.

1.6.1 Expression of proteins in form of inclusion bodies

Generally, proteins are overexpressed for high production level and further isolation and purification needs to be performed. An overexpression of eukaryotic proteins in the cytoplasm usually leads to accumulation of the protein within the cell in the insoluble fraction, which is commonly known as inclusion bodies (IBs) (Ventura and Villaverde, 2006). The content of the target protein within IBs is up to 90% of the pure form. Insolubility of IBs appears as a result of formation of intracellular protein aggregates of misfolded product (Carrió and Villaverde, 2002, Heebøll-Nielsen et al., 2003). To achieve complete denaturation of the protein it is essential to solubilise the recombinant protein efficiently. Specific renaturation conditions are required to obtain a significant yield of the soluble protein (Radolph and Lilie, 1996; Vallejo and Rinas, 2004).

Expression of proteins in inclusion bodies has certain advantages over expression of free proteins. Large amounts of highly enriched proteins can be expressed in inclusion bodies and, trapped in these insoluble aggregates, these proteins are for the most part protected from proteolytic degradation (Clark, 2001). However manufacturing proteins in the form of IBs is quite expensive due to resolubilisation, denaturation and refolding processes and tends to be reserved for high-value human biotherapeutic agents.

The properties of inclusion bodies as strong, large, dense and highly refractile particles have been exploited for recovery and monitoring processes in industry (Fischer et al., 1993, Georgiou and Valax, 1999, Jin et al., 1994, Singh and Panda, 2005, Taylor et al., 1986). Purification of proteins expressed as inclusion bodies follows a long and highly conserved sequence of operations, which involve: mechanical cell disruption, separation of the insoluble IBs by centrifugation, washing, resolubilisation and denaturation by highly concentrated chaotrope (8 M urea or 6 M guanidine hydrochloride) and several chromatographic purification steps followed by dilution and refolding of the target protein (Singh and Panda, 2005).

Several strategies for production of proinsulin in the cytoplasm of *E. coli* as insoluble inclusion bodies have been developed and are used commercially (Tang and Hu, 1993, Kang and Yoon, 1991, Sung et al., 1986). As mentioned previously, the great

advantage of these approaches is the amount of proinsulin that can be produced, however the complex process of purification and the formation of the correct disulfide bonds during folding are critical cost factors.

Proinsulin expressed in the form of IBs must be isolated, refolded under suitable redox conditions and enzymatically converted to the biologically active insulin. One of the major steps during the purification process is renaturation, which is limited by the formation of the correct disulfide bonds, which are required for biological activity and stability. Sufficiently good refolding yields can be attained by oxidising the reduced insulin precursor (proinsulin) to yield correctly folded proinsulin on renaturation (Tsumoto et al., 2002). The first step of the process is solubilisation of inclusion bodies using chaotropic agents such as urea or guanidine HCl, leading to a flexible and disordered structure of the proteins (Tsumoto et al., 2002). Urea and guanidine HCl show concentration dependent binding to the proteins and in most cases, 6-8 M urea or 6-7 M guanidine HCl are required to achieve extensive binding sufficient to unfold and solubilise the proteins.

For *in vitro* refolding, systems in which the cysteine residues of reduced denatured proteins from inclusion body material are reversibly modified have proven useful (Moroder and Buchner, 2009). It is now a common procedure to convert proinsulin to the S-sulfonate derivative by oxidative sulphitolysis before subsequent refolding in the presence of redox reagents. This step involves the cleavage of disulfide bonds to form one S-sulfonylcysteine residue and one free cysteine residue. In the presence of an oxidising agent (sodium tetrathionate), the oxidative sulphitolysis reaction proceeds to the complete modification of all accessible free cysteines, preventing the formation of potentially incorrect disulfide bonds prior to correct refolding of the proteins under optimal conditions for renaturation. As the reaction is readily reversible, the two S-sulfonated cysteines can form a disulfide bridge in the presence of free thiols (Moroder and Buchner, 2009).

Refolding is the next step in the process. Refolding is usually initiated by reducing the concentration of the denaturant used to solubilise inclusion bodies and so, ideally, transfer of proteins from high denaturant concentrations to aqueous buffer should lead to refolding (Tsumoto et al., 2002). Protein refolding is, however, not a single reaction and competes with other reactions such as misfolding and aggregation. As a result, such a drastic process does often not work and will lead to misfolding and aggregation. The rate of refolding and other reactions is determined both by the procedure to reduce denaturant concentration (Tsumoto et al., 2002). The way by which the denaturant is removed can affect refolding efficiency. A key to refolding is the intermediate concentration of the denaturant (urea), where denaturant concentration is low enough to induce folding and still maintain solubility

and flexibility during the refolding process so any refolding procedure must go through an intermediate denaturant concentration (Tsumoto et al., 2002). Often, 1 M urea is used in the refolding step as an intermediate concentration of denaturant and the protein is added slowly to the reaction buffer.

Proinsulin contains six cysteines which form three disulfide bonds in the native molecule and refolding is usually performed in a buffered redox system (Winter et al., 2002). The yield of proinsulin depends on the redox potential of the refolding buffer, with the yield of refolding increasing in more oxidising buffers (Winter et al., 2002). Fast oxidation of disulfide bonds seems to prevent the formation of intermediates susceptible for aggregation. Aggregation is a non-productive, off-pathway reaction which competes with the correct folding of proinsulin and so the prevention of aggregation can increase the refolding yield (Winter et al., 2002).

The refolding yield of proinsulin is also largely dependent on other factors. The pH of the reaction is a crucial factor in oxidative folding. At basic pH, reduced and denatured proinsulin can be refolded to a yield of about 60%. This increased refolding yield at higher pH is due to faster disulfide bond formation and/or shuffling. In addition, the refolding temperature can also be an important factor, because aggregation, proteolytic degradation and chemical modification are enhanced at elevated temperatures. However proinsulin refolding is not temperature dependent and it has no significant effect on the final yield. Aggregation of proteins is enhanced by increasing protein concentrations. In the case of proinsulin, studies have shown that good yields can be obtained at protein concentrations of up to 0.5 mg/ml and that reasonable yields can be obtained even at protein concentration of 1-2 mg/ml (Winter et al., 2002).

Properly folded proinsulin with correct disulfide bridges is further converted to insulin by enzymatic cleavage whereby the C-peptide is cleaved off and the carboxy-terminus of the B-chain is trimmed. Processing of proinsulin *in vitro* can be performed with trypsin and carboxypeptidase B (Kemmler et al., 1971).

1.6.2 Periplasmic production of proteins

Alternatively, proinsulin has been produced in *E. coli* and secreted by routing the recombinant protein to the periplasmic space using appropriate signal sequences. The periplasm seems to be a better location for the production of large quantities of soluble recombinant proteins (Joly et al., 1998, Laird et al., 2004, Carter et al., 1992, Chen et al., 2004) and offers advantages over the cytoplasmic route. The main advantage of the periplasm is its oxidising environment, which in cooperation with periplasmic proteins assists the formation and isomerisation of disulfide bonds,

which results in a firmly folded structure resistant to proteases (Berkmen et al., 2007, Derman and Beckwin, 1991).

Despite this, as reported previously, the yield of correctly folded proinsulin, which was secreted to the periplasm was very low compared to the yield obtained by intracellularly produced proinsulin (Talmadge et al., 1981; Chan et al., 1981). Beside the oxidising environment, the periplasm also provides proteins of the Dsb family (DsbA, DsbC and DsbG), which are efficient catalysts of disulfide bond formation (Bessette et al., 1999; Raina and Missiakas, 1997). Dsb-dependent protein oxidation and isomerisation is shown in Figure 1.10.

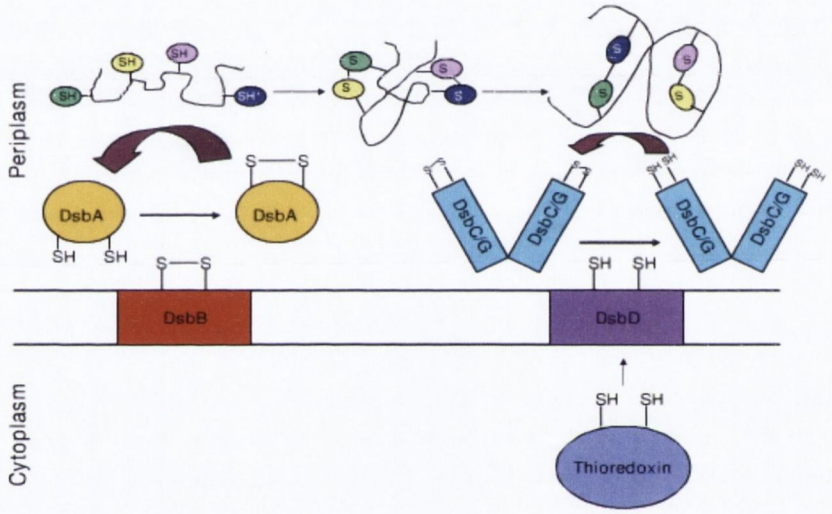

Fig. 1.10 *Dsb-dependent protein oxidation and isomerisation in bacterial periplasm. DsbA couples consecutive cysteines providing the disulfide bonds and is re-charged by the inner membrane DsbB. Incorrect disulfides of oxidised proteins are scrambled by DsbC and DsbG. These isomerases are kept reduced by the inner membrane DsbD, that in return, is reduced by cytoplasmic thioredoxin, (adapted from de Marco, 2009).*

DsbA is the most important oxidase of free sulfhydryl groups in the periplasm. The soluble monomer protein DsbA donates its disulfide bond to newly synthesised polypeptides, that are in the form of intermediates and need disulfide bonds to reach their native structure (de Marco, 2009). It has been reported that it can be useful for *in vitro* folding of disulfide-bonded proteins, such as BPTI (bovine pancreatic trypsin inhibitor), hirudin, a-lactalbumin, alkaline phosphatase, and bovine ribonuclease A (Zapun and Creighton, 1994, Wunderlich et al., 1993; Akiyama et al., 1992). Fusion of an enterokinase to the C-terminus of DsbA facilitated production of high amounts of soluble, native enterokinase in the periplasm (Collins-Racie et al., 1995). However, coexpression of DsbA only yielded periplasmic IGF-I (insulin-like growth factor) inclusion bodies (Joly et al., 1998). The yield of the secreted

α-amylase/trypsin inhibitor RBI (ragi bifunctional inhibitor) was not improved by DsbA coexpression alone but could be significantly increased in combination with the addition of reduced glutathione to the cultivation medium (Wunderlich and Glockshuber, 1993). A study performed by Winter et al., demonstrated that, the yield of native human proinsulin produced in *E. coli* can be significantly increased not only by fusion of proinsulin gene to DsbA, but also by supplementation of the culture with medium additives (Winter et al., 2000).

1.7 Insulin delivery

1.7.1 Subcutaneous delivery of insulin

Insulin discovery in 1922 led to the development not only of different methods of insulin preparation, but also the technology for insulin delivery. Initially, insulin was administered intramuscularly, but soon it became apparent that subcutaneous injections were also effective and moreover less painful (Gupta, et al., 2009). For decades, the syringe was the sole means of insulin delivery. Originally, large and heavy syringes with reusable glass plungers and barrels with a ling, large bore needles were used (Al-Tabakha and Arida, 2008). Today, there are a range of insulin injection syringes available on the market. They are made of lightweight plastic, with disposable and versatile microfine needles. These types of syringes increase patient comfort and offer convenience, thus improving patient compliance (Heller et al., 2007, Al-Tabakha and Arida, 2008).

Over the decades, continuous improvements in insulin syringes were made. Despite this, the syringe injection process still remains inconvenient, painful and time-consuming. Additionally, using a syringe creates a risk associated with the occurrence of dosage errors. In 1987 Novo Nordisk introduced the first insulin pen (NovoPen®) (Al-Tabakha and Arida, 2008). Pen devices combine the insulin container and syringe in a single unit and have smaller-gauge needles which are more comfortable to use. Insulin pens allowed more flexibility, convenience and accurate dosing control. Nowadays there are many technological innovations introduced in insulin pens, such as an audible click when the full dose has been delivered, digital displays and memory functions showing the last administered dose (Sindhu et al., 2011). Several studies confirmed contentment among patients, which found the insulin pens convenient and easy to use (Heller et al., 2007, Al-Tabakha and Arida, 2008).

The main goal of intensive insulin therapy is to achieve near-normal blood glucose control and avoid short-term crises such as hyperglycaemia. This goal can be attained through the administration of multiple daily injections (MDI) of insulin or through insulin pump therapy, which is also known as continuous subcutaneous

insulin infusion (CSII). CSII technology uses a portable pump to deliver fast- or rapid-acting insulin into the subcutaneous tissue. This pump delivers insulin at pre-selected rates, effectively mimicking non-diabetes insulin delivery over 24 h, with patient activated boluses at mealtime. The pump typically consists of a reservoir filled with insulin (e.g. Velosulin® BR), a small battery operated pump and a computer chip, which allows the patient to control the insulin delivery. The CSII pump was introduced in the market in 1974 (Al-Tabakha and Arida, 2008). The worldwide use of insulin pumps has been increasing ever since. Over the years, pumps have become smaller, more durable, easier to use and safer. Advantages of CSII compared with MDI have been demonstrated, including improved control of morning glucose levels and decreased risk of hypoglycaemia (Heller et al., 2007, Al-Tabakha and Arida, 2008).

1.7.2 Non-invasive delivery of insulin

Subcutaneous injection of insulin has many limitations such as local degradation of insulin in the subcutaneous depot, slow absorption from the subcutaneous tissue and high variability in absorption rates (Heinemann, 2010). The parental administration of insulin is still the predominant route of delivery in clinical studies. Since the discovery of insulin, researches have investigated various alternative routes of insulin administration such as pulmonary, intranasal, oral, uterine, intrascrotal, intraperitoneal and intratracheal. From all of these routes only pulmonary administration has proved clinically realistic, so far. Research is still continuing into the novel routes of delivery that could improve the convenience of insulin therapy.

Intranasal administration is another route of insulin administration. Assessments of the efficacy have shown that insulin is quickly absorbed through the nasal mucosa and reaches the systemic circulation. The pharmacokinetic profile indicated a rapid increase and decrease in serum insulin concentration, which is similar to the physiological state. Pharmacodynamic data showed that the onset of action occurs within 10 min (Leary et al., 2008). The peak of the glucose-lowering effect is attained after 20-45 min and the duration of action continues after 20-45 min (Leary et al., 2008). Unfortunately, the mechanism of action has not been well defined yet (Henkin, 2010). Additionally, the results from trials of intranasally administered insulin in patients with diabetes have been disappointing. Bioavailability is also generally low, <10% and addition of permeability enhancers often causes nasal irritation. For all these reasons intranasal insulin is considered unlikely to surpass subcutaneous delivery, in terms of clinically viable routes of administration (Heller et al., 2007, Henkin, 2010).

Pulmonary insulin is another route of delivery that has been extensively studied. The respiratory tree, with an estimated surface area of 140 m^2, is an obvious target for drug delivery and inhaled or pulmonary insulin. The alveolar surface, which account for >95% of the absorptive area, is lined by a very thin vasculated and richly perfused monolayer of epithelial cells. Pulmonary administration allows the delivery of insulin through millions of alveoli in the lungs, where it is rapidly absorbed into the blood supply and has a rapid onset of action (Heller et al., 2007, Owens et al., 2003). Several companies have been working on insulin inhalers, which would work similarly to asthma inhalers. The products fall into two main groups: dry powder formulations and solutions, which are delivered through different patented inhaler systems (Al-Tabakha and Arida, 2008). Exubera® is recombinant human insulin, which was approved for medical use in the USA in 2006. It was indicated for the treatment of diabetes mellitus for the control of hyperglycaemia. It was also the first such product delivered by inhalation technology. The recombinant human insulin was formulated as a powder also containing citrate buffer component, mannitol and glycine as excipients. It was sold as blisters containing 1 mg or 3 mg unit doses, which were administered using a specially designed inhaler (Walsh, 2007). Pharmacokinetic studies (for both healthy and diabetic subjects) showed that the insulin was absorbed as quickly as administered rapid-acting analogues, and thus should be administered within 10 min of mealtime. The maximum effect usually was observed after approximately 2 h and activity duration was approximately 6 h. Exubera was developed by Nectar Inc. and it was marketed under licence by Pfizer (Walsh, 2007). When Exubera was first introduced to the market, it was hoped that this would be the first in a series of novel insulin formulations delivered by this route. Furthermore, it was hoped that inhaled insulin would pave the way for other alternative routes of insulin administration i.e. oral insulin, nasal insulin or transdermal insulin. However Exubera was withdrawn from the market, based on poor sales levels, in October 2007 (Heinemann, 2010). Recent studies demonstrate that this failure was a consequence of poor patient uptake, possible side effects, unattractive device design and concomitant requirement for insulin injections (Mitri and Pittas, 2009). The failure of Exubera was followed by the cessation of nearly all other attempts to develop inhaled insulin formulations. Currently there is just one company (Mann-Kind) which is still working on their TechnoSphere® inhalable insulin formulation called AFREZZA®.

1.8 Oral insulin

Oral administration of insulin would have a considerable advantage as it is easy to administer and would ensure high patient compliance (Chalasani et al., 2007).

Insulin that is absorbed through the gut can be delivered directly to the liver, where it is needed. Oral delivery has the advantage of mimicking the physiological path for therapeutics that could enter the hepatic portal vein from the intestine and travel directly to the liver (Raj et al., 2003). Additionally, direct delivery of insulin to the liver could decrease complications associated with high concentrations and build-ups of insulin in the blood, such as atherosclerosis. While insulin is injected subcutaneously it has to circulate through the body before reaches the liver (Sadrzadeh et al., 2007). Insulin undergoes extensive degradation by proteases in the digestive tract and faces a complete lack of selective transport mechanisms across the intestinal wall (Heller et al., 2007). Dietary proteins do not normally cross the intestinal epithelium intact, but must be first broken down to the constituent amino acids which are then absorbed. Unfortunately, this route of protein absorption destroys all physiological activity of the protein and explains why typical oral bioavailability of the proteins is usually less than 1-2% (Carino and Mathiowitz, 1999). It was estimated that just 0.5% of ingested insulin may reach the systemic circulation and thus very large doses would be required to achieve a useful level of absorption. Furthermore, the transit time of insulin through the gut is unpredictable (Heller et al., 2007). Overcoming natural barriers is the focus of efforts to develop oral insulin delivery systems.

1.8.1 Oral insulin delivery – main barriers

1.8.1.1 The physical barrier to oral protein delivery

The epithelial layer, which lines the gastrointestinal (GI) tract is a tightly bound collection of cells with minimal leakage (Lodish et al., 2000). This forms a physical barrier to absorption. A single layer of columnar epithelial cells supported by the *lamina propria* and *muscularis mucosa*, are tightly bound to one another by the tight junction or *zona occludens*, thus inhibiting the passage between the cells (Wong, 2009). The epithelium folds to form structures composed of villi and microvilli (the brush border), on the epithelial cells, which increase the absorptive area of the intestinal tract by approximately two orders of magnitude. However, this structure also contains digestive enzymes. Additionally glycocalyx and mucus present on the top of epithelial layer are another physical barrier to the transport of the protein (Carino and Mathiowitz, 1999).

1.8.1.2 The enzymatic barrier to oral protein delivery

Another barrier in protein delivery is digestive enzymes. Proteins digestion by protease begins in the stomach and is continued by many different enzymes, which are located throughout the remainder of the GI tract. Pepsins are located in the

stomach. Trypsin, chymotrypsin and carboxypeptidases from the pancreas are located in the small intestinal lumen (Guyton, 1992) and are responsible for only about 20% of the enzymatic degradation of ingested proteins (Pauletti et al., 1996). Additionally, there is also a specific cytosolic enzyme called insulin-degrading enzyme which accomplishes this for insulin. Overcoming the enzymatic barrier is a challenge, because the presence of even one of these enzymes can lead to total denaturation and destruction of the protein drug (Carino and Mathiowitz, 1999).

1.8.1.3 Barriers due to manufacturing of formulation

The final barrier is actual fabrication methods used in formulation. Proteins have a complex internal structure which helps define their biological activity. Any disruption in their primary, secondary, tertiary or quaternary structure can result in the deactivation of the protein. Disruption may be caused even by slight changes in environment such as temperature, pH or solvent. Therefore, although the characterisation of release kinetics of proteins from drug delivery systems has become a common practice in drug delivery, it is more important to understand the stability of the protein (Carino and Mathiowitz, 1999). Figure 1.11 summarises the major barriers to deliver proteins and peptides orally.

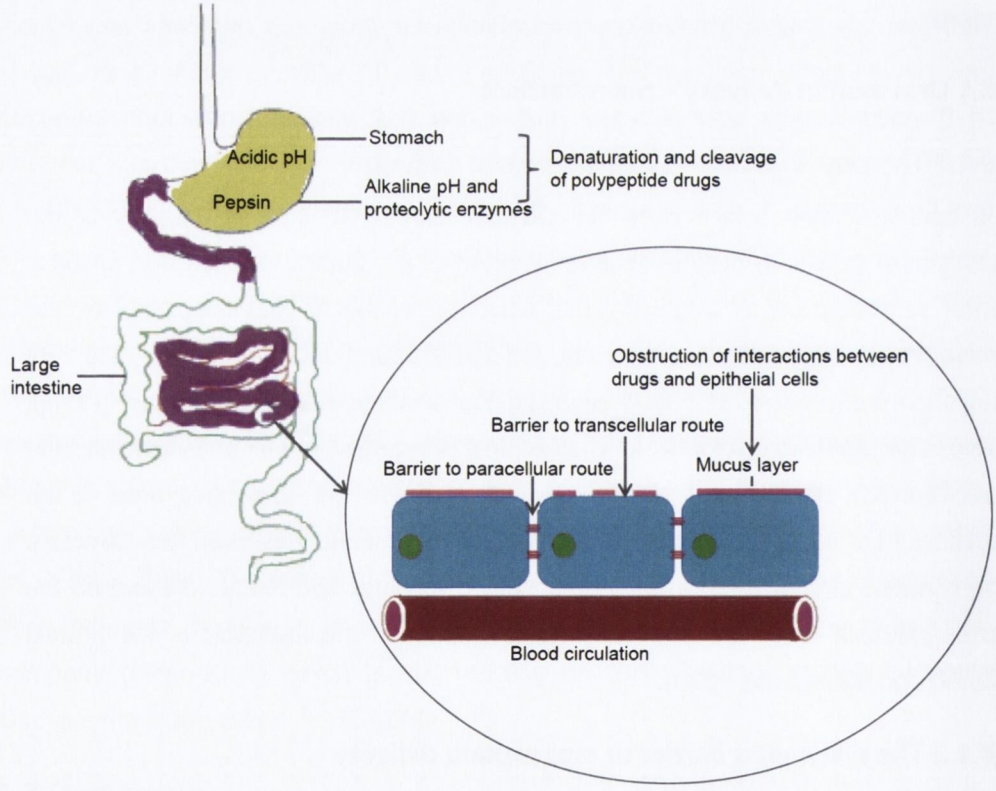

Fig. 1.11 *Barriers to deliver peptide- and protein-based drugs orally (adapted from Ahmad et al., 2012).*

1.8.2 Strategies for oral insulin delivery

The idea of oral insulin has attracted a lot of attention. Various strategies have been employed for formulation of oral insulin. Most often these strategies have focused at surmounting one of the barriers to intestinal absorption, either the epithelial cell layer or the digestive enzymes. These approaches can be divided into four main categories: chemical modification or conjugation to insulin, protease inhibitors, absorption enhancers and particulate delivery (carrier) systems (Khafagy et al., 2007).

1.8.2.1 Chemical modification or conjugation

Chemical modification or conjugation of insulin is used to make it resistant to proteolysis in the gut and in order to increase the bioavailability when administered orally. To achieve this goal, peptide mimetics with suitable substitutions for increased activity and resistance to proteolysis have been designed. One of the approaches is the design of peptide mimetics of insulin on the C-terminal of B-chain (Bhatnagar et al., 2006, Carino and Mathiowitz, 1999). Xia et al. investigated conjugation of insulin with transferrin, which resulted in receptor mediated endocytosis across epithelial cells, leading to a significant hypoglycaemic response comparing to the native insulin (Xia et al., 2000). A report presented by Dave et al., shows modification of insulin by attaching a short-chain methoxypolyethylene glycol derivative to improve its bioavailability (Dave et al., 2008). Another approach was introduced by Emisphere Technologies, which developed a method of a non-covalent complexation with non-acyl amino acids. This type of interaction causes unfolding of insulin structure and exposure of hydrophobic side chains, that promotes superior translocation across the lipid bilayer (Sadrzadeh et al., 2007). The complex dissociates after insulin crosses the membrane and protein appears in its native conformation. Other investigations have been made to examine site-specific oligomeric modifications, which cause increase in insulin half-lives *in vivo* and additionally show greater enzymatic resistance comparing to its native form (Clement et al., 2004). An example could be a report presented by Asada et al., where the acyl insulin derivatives are more resistant to the intestinal enzymes (Asada et al., 1994). Several studies confirmed that conjugation of insulin with cell-penetrating peptides (CPPs) resulted in an increased transport across Caco-2 cell line. Detailed characterisation of this type of enhancers is presented in Section 1.11.2.

1.8.2.2 Protease inhibitors

Co-administration of protease-inhibitors (either peptidic or non-peptidic) was investigated to protect insulin from proteolytic degradation by the enzymes found in

the GI tract. There are known protease inhibitors such as camostat and aprotinin, which confer protection against enzymatic degradation in the large intestine of rats. Sodium glycocholate, bacitracin and inhibitors of insulin degrading enzyme like N-ethylmaleimide, 1,10-phenanthroline and p-chloromercuribenzonate have been shown to increase absorption of insulin from the intestine in a site-dependent manner (Shaji and Patole, 2008). Radwan et al, reported the protease inhibiting effects of permeation enhancers such as glycocholic acid, taurochenodeoxycholate or dimethyl-a-cyclodextrin. Additionally, they investigated that the administration of insulin with capric acid, a fatty acid, had the strongest effect against α-chymotrypsin (Radwan et al., 2001). Study performed by Yamamoto et al. investigated that administration of insulin with soybean trypsin inhibitor or aprotinin increased hypoglycaemic effect in rats (Yamamoto et al., 1994). Researchers Bai et al., however, performed more general studies on the effect of various protease inhibitors. They found that N-ethylmaleimide, 1,10-phenanthroline, ethylenediaminetetraacetic acid, bacitracin and p-chloromercuribenzoate inhibited degradation of insulin completely in intestinal enterocytes. Weaker inhibition effect was observed for aprotinin, leupeptin, chymostatin, and diisopropyl phosphofluoridate (Bai et al., 1995). The same researchers showed that N-ethylmaleimide, p-chloromercuribenzoate and 1,10-phenanthroline improved the transport of insulin across rat ileum, however the mechanism is not known (Bai et al., 1996). However, it was demonstrated that even if the enzyme inhibitors increase oral insulin bioavailability, the permeability is still very low, and thus this method needs to be combined with another approaches (Liang et al., 2005).

1.8.2.3 Permeation enhancers

In order to exert pharmacological effect of a therapeutic agent, it has to cross from the biological membranes into systemic circulation and reach the site of action. Absorption enhancers cause the temporary disruption of the intestinal barrier to improve permeation of these drugs (Shaji and Patole, 2008). Compounds that anchor insulin to the mucosa of the GI tract increase the contact surface and time and thus promote rapid absorption. These types of agents (mucosal permeation enhancers) have been investigated to check their impact on the improvement in the intestinal permeability (Sakai et al., 1997). Bioadhesive compounds, such as: poly(methacrylic acid), polyethylene glycol, poly(methacrylic acid-g-ethylene glycol), alginate, chitosan and plant exudates from the herb Sanguis Draxonis, have been investigated for the intestinal delivery system. Furthermore, compounds like polycarbophil, hydroxypropyl methylcellulose and carbopol 934 have been used to make enteric-coated tablets of insulin (Bhatnagar et al., 2006). A study performed by

Sakai et al., showed that sodium caprate, a fatty acid, and sodium deoxycholate, a bile salt, had an impact on the changes in the transepithelial electrical resistance (TEER) across Caco-2 monolayers. TEER values decreased, while the transepithelial transport increased. The mechanism proposed by these researchers is the reversible opening of the tight junctions and shortening the glycocalyx (overcoming of physical barrier that impedes access to the apical membrane of the epithelial cells in the intestine) (Sakai et al., 1997). Co-administration of insulin with cyclodextrin derivatives have been particularly investigated by Shao et al. (1994). A significant increase in bioavailability was obtained, compared to insulin on its own (Shao et al., 1994). Cyclodextrins are capable of increasing membrane permeability by changing the properties of cellular membrane (Carrier et al., 2007). Other investigators (Li et al., 1992) showed that sodium glycocholate, a bile salt, increased an intestinal permeation by affecting the insulin molecule itself (probably by dissociating oligomers to monomers). Eaimtrakarn et al., showed that an increase in the biological activity can be achieved by using the surfactant, Labrasol®, however it was still low (Eaimtrakarn et al., 2002). Several absorption promoters (cyclodextrins, chelating agents, surfactants, bile salts, fatty acids and terpenes) have been used in various oral insulin delivery systems (Mesiha et al., 2002, Morishita et al., 1993, Scott-Moncrieff et al., 1994, Shao et al., 1994). However, it is important to mention that the safety of those permeation enhancers must be evaluated first, if they are to be employed in pharmaceutical delivery systems (Whitehead et al., 2008).

1.8.2.4 Carrier systems

Particulate delivery systems (microparticles, nanoparticles, liposomes) have been employed to encapsulate insulin as they act as protection and allow for controlled release of the drug. The active insulin can be protected from the extreme pH, hydrolytic conditions or enzyme degradation (Peniche et al., 2003). The release profile and its target location can be modulated by appropriate carrier selection, formulation optimisation and particle engineering. As an example, materials used for mucosal drug delivery should improve epithelial permeability by reversibly opening tight junctions between cells or by increasing contact time with the mucosa through bioadhesive forces (Issa et al., 2006). Several forms of delivery vehicles that have been used for insulin delivery will be described in the following sections.

Currently, continuous development of insulin analogues and derivatives is required in order to provide faster onset, more prolonged action, stability, tissue selectivity, fewer side-effects, decreased immunogenicity and oral availability. It is especially expected that combining several properties into one molecule, e.g. stable, rapid onset oral insulin could lead to many new and effective analogues that could

overcome the shortcomings of presently available therapies. Development of such new analogues would enable truly flexible therapy tailored to the individual requirements of the patient.

1.9 Formulation vehicles used for an oral delivery of insulin

The main objective of oral delivery systems is to protect protein and peptide drugs from acid and luminal proteases in the GI (Shaji and Patole, 2008). Drug delivery systems such as enteric-coated capsules, intestinal patches, liposomes, hydrogel microparticles, microemulsions, hydrogels, niosomes and superporous hydrogel polymers have already been attempted.

1.9.1 Enteric-coated capsules

Enteric-coated capsules were synthesised in an attempt to create a possible oral delivery system by Sonaje et al. (2010). Nanoparticles composed of chitosan and poly(γ-glutamic acid) were placed into an enteric-coated capsule. The internal structure and pH sensitivity of the nanoparticles were preserved and the released insulin molecules did not feature fragmentation or aggregation. The insulin-loaded nanoparticles were released from the enteric coated capsule in the small intestine and avoided the harsh acidic environment of the stomach. Intestinal absorption of insulin was thus enhanced and the relative bioavailability of insulin was found to be approximately 20% (Sonaje et al., 2010). Another attempt was made by Hosny et al., who developed an oral delivery form of insulin in enteric coated capsules containing sodium salicylate. The dosage form design was based on the incorporation of insulin into hard gelatine capsules formulated with sodium salicylate by either physical mixing or wet granulation using 10% polyvinylpyrrolidone (PVP) or in suppository bases polyethylene glycol (PEG 4000) or Witepsol W35. Upon administration to beagle dogs, capsules formulated either by physical mixing or wet granulation with PVP produced similar results, with a relative hypoglycaemia (RH) of 8.7±6.1% and 7.3±2.9% respectively, compared to subcutaneous injection of insulin. Formulation with PEG 4000 produced a RH of 4.7±1.3%. Formulation in Witepsol produced a RH of 12.6±3.2% (Hosny et al., 2002).

1.9.2 Intestinal Patches

Whitehead et al. used mucoadhesive intestinal patches to deliver therapeutic doses of insulin into systemic circulation. The patches localised insulin near the mucosa and protected it from proteolytic degradation by promoting its unidirectional diffusion towards the mucosa. The patches were formulated with a mixture of Carbopol 934, pectin and sodium carboxymethylcellulose. Moreover, it

was found that hypoglycaemia induced by 10 U/kg patches fell between those induced by 1 and 5 U/kg subcutaneous injections, which is considerably high. The patches demonstrated that enteral insulin absorption can result in blood glucose levels comparable to those induced by subcutaneous injections with doses only two to ten times higher than subcutaneous doses (Whitehead et al., 2004). Grabovac et al. designed a similar system for the delivery of insulin using a patch encompassing a mucoadhesive layer, a water insoluble ethylcellulose backing layer and an enteric coating composed of Eudragit. A mean maximum decrease in blood glucose levels of 31.6% was observed after 6 h of administration. The relative bioavailability of insulin compared to subcutaneous injection of the protein was 2.2% (Grabovac et al., 2008).

1.9.3 Hydrogels

Yamagata et al. synthesised insulin-loaded hydrogels composed of poly[methacrylic acid grafted with poly(ethylene glycol)] and tested the mechanisms contributing to oral insulin bioavailability using the gastric and intestinal fluid of rats. It was shown that the hydrogels successfully protected the loaded insulin by forming interpolymer complexes in the gastric fluid. Additionally, it was found that the extent of insulin protection was dependent on the number of carboxylic acid groups in the polymer networks. Despite the interpolymer complexes formed, the rate and extent of insulin release from the hydrogels was unaffected. The polymers also bound Ca^{2+} ions, which was thought to have an inhibitory effect on protease enzymes in the intestinal fluid. It was therefore deduced that this formulation could be promising in the development of a novel oral method of insulin delivery (Yamagata et al., 2006).

1.9.4 Microemulsions

Ma et al. developed a self-emulsifying formulation for the oral delivery of insulin which was approved for entry into clinical trials by the China State Food and Drug Administration (Ma et al., 2006). The formulation featured insulin dissolved in 0.01 M hydrochloric acid and 0.9% w/v sodium chloride solution at pH 3 mixed with polyethylene glycol-8-glycol octanoate, followed by polyglycerol-3-oleate. It was found that after 120 minutes in simulated intestinal conditions, the preparation protected over 40% of the insulin incorporated into it, compared to a control solution of insulin. The bioavailability of insulin was found to be 15.2% compared to its subcutaneous injection in diabetic male beagle dogs (Ma et al., 2006).

1.9.5 Hydrogel Microparticles

Sajeesh et al. produced an oral insulin delivery system featuring poly(methacrylic acid)-chitosan-polyethylene glycol (PCP) microparticles. Insulin was complexed

with methyl β-cyclodextrin (MCD) and incorporated into the PCP microparticles. Studies were then carried out on both insulin-loaded and insulin-MCD loaded microparticles. Although MCD complexation of insulin did not affect loading and release properties from the hydrogel matrix, it was observed that the MCD complexation enhanced insulin transport across Caco-2 cell monolayers. The relative pharmacological bioavailability of insulin from the insulin-loaded and insulin-PCP loaded hydrogel microparticles was 1.8% and 1.5%, respectively (Sajeesh et al., 2010).

1.9.6 Liposomal Formulations

Hydrophobic nature and low toxicity make liposomes an interesting vehicle that has been tested for an oral delivery (Trotta et al., 2005). A number of experimentations on liposomal formulations for oral insulin delivery have been carried out. One example featured in a study by Wu et al, who synthesised insulin-loaded liposomes by reverse-phase evaporation. A chitosan and alginate coating was prepared by mixing a liposomal suspension of insulin with chitosan and sodium alginate solutions. The hypoglycaemic effects of the orally administered liposomes were studied in mice. The chitosan particles were shown to reduce digestion of insulin by trypsin and also to enhance enteral absorption of insulin (Wu et al., 2004).

Xhang et al conducted a similar study to assess the efficacy of lectin-modified liposomes as a drug delivery system. Wheat germ agglutinin (WGA), tomato lectin (TL) and ulex europaeus agglutinin 1 (UEA1) were conjugated by coupling their amino groups to carbodiimide-activated carboxylic groups of N-glutaryl-phosphatidylethanolamine (N-glut-PE). Liposomal dispersions of insulin were prepared by the reverse-phase evaporation and modified with the lectin-N-glut-PE conjugates. Following oral administration of the liposomes modified with WGA, TL and UEA1, the relative bioavailability of each type was found to be 8.5%, 7.3% and 4.9%, respectively. It was therefore deduced that the lectin-modified liposomes could be a promising future method of oral insulin administration (Xhang et al., 2005). However, liposomes typically exhibit poor stability *in vivo*, low drug loading capacities and poor storage properties (Soppimath et al., 2001). A study performed by Degim et al., did not show any increase in the permeability across Caco-2 monolayers in dipalmitoylphosphatidylcholine-insulin liposomes, comparing to insulin alone (Degim et al., 2004). Promising data was reported by Trotta et al., where cetylpalmitate and glyceryl monostrearate liposomes retained over 70% of the total insulin under physiological conditions, but the particles were placed in a systemic-type simulation as opposed to gastrointestinal simulation

(Trotta et al., 2005). There is still much work to be done to investigate the use of liposomes as a vehicle for an oral insulin delivery.

1.9.7 Niosomes

Niosomes are lamellar structures that are composed of non-ionic surfactant of the alkyl or dialkyl polyglycerol ether class and cholesterol with subsequent hydration in aqueous media. Niosomes are now widely studied as an alternative to liposomes (Abhinav et al., 2011). Pardakhty et al. conducted a pharmacokinetic study of insulin-loaded niosomes in diabetic rats. Recombinant human insulin was entrapped in multilamellar niosomes composed of polyoxyethylene alkyl ether surfactants (Brij 52 and Brij 92) or sorbitan monostearate (Span 60) and cholesterol. Proteolytic cleavage studies were carried out in the presence of pepsin, trypsin and α-chymotrypsin. Brij 92 displayed the greatest protective effects against α-chymotrypsin, whereas Span 60 displayed the greatest effects against pepsin and trypsin. The relative bioavailability of insulin obtained from the Brij 92, Brij 52 and Span 60 niosomes were 1.9±0.4%, 1.1±0.6% and 1.5±0.3%, respectively. It was concluded that niosomes could be developed as a possible oral insulin delivery system, however the bioavailability of insulin delivered in this experiment is still too low for this to be currently feasible (Pardakhty et al., 2011).

1.9.8 Nanoparticle delivery systems

Nanoparticles (NPs) are currently being investigated extensively for various medical applications including drug delivery systems for peptides and proteins. There has recently been an increased interest in NPs composed of naturally occurring polymers due to their advantageous biocompatibility, biodegradability, low toxicity and low cost (Mizrahy and Peer, 2012). Also critical factors for their popularity are their diverse structures, a large number of reactive groups and satisfactory stability (Umerska et al., 2012).

A number of attempts have already been made to develop novel drug delivery systems using polymeric NPs. These NPs are solid, colloidal particles of macromolecular substances, which can vary in size from 10 nm to 1000 nm. There are two main types of polymeric NPs: nanospheres or nanocapsules. The production of one type over another depends on the method of preparation. Each has different release properties for the encapsulated drug. Nanospheres are matrix systems in which the drug is uniformly dispersed and are thus said to be polymer-based NPs (Soppimath et al., 2001), whereas nanocapsules are vesicular systems in which the drug is enclosed in a cavity surrounded by a polymer membrane and are thus known as polymer-coated NPs (Mohanraj and Chen, 2006). Nanospheres are capable of undergoing hydrolysis *in vivo*.

Cytotoxicity testing has showed that such NPs can exhibit sustained drug release without exhibiting any cell damage. Polymeric NPs can also be created with an engineered specificity which can allow them to deliver a higher concentration of drug to a specific location. Therefore, polymeric NPs are very interesting candidates for the oral delivery of insulin (Subramani et al., 2012).

A considerable body of research has been carried out on the development of polymeric NPs for the oral delivery of insulin. In a study conducted by Leobandung et al on temperature-sensitive polymer-based nanospheres composed of poly(N-isopropylacrylamide) and poly(ethylene glycol) dimethacrylate, the results indicated that the NPs effectively protected 80% of the encapsulated insulin from elevated temperatures and had an effective insulin loading efficiency of 65% (Subramani et al., 2012, Leobandung et al., 2002). In a study conducted by Lin et al., NPs composed of chitosan (CS) and poly(γ-glutamic acid) (γ-PGA) were prepared by a simple ionic-gelation method for oral insulin delivery. The insulin-loaded NPs were shown to effectively reduce the blood glucose level in a diabetic rat model (Subramani et al., 2012, Lin et al., 2007 a). NPs composed of dextran and chitosan were analysed in a study conducted by Sarmento et al., in which they were shown to lower serum glucose levels of diabetic rats up to 67% and 64% at doses to 50 and 100 IU/kg, respectively, compared to their basal glucose level (Sarmento et al., 2007 a). In a study carried out by Tiyaboonchai et al., NPs composed of dextran sulfate and polyethylenimine (PEI) demonstrated a high insulin entrapment efficiency of 90%, rapid release characteristics in *in vitro* dissolution studies, a prolonged hypoglycaemic effect in a diabetic rat model and an ability to preserve the structure and biological activity of insulin (Tiyaboonchai et al., 2003). In a study conducted by Mesiha et al., insulin-loaded poly (isobutylcyanoacrylate) NPs were shown to increase the oral bioavailability of insulin and significantly lower blood glucose levels compared to the oral delivery of non-encapsulated insulin in a diabetic rat model (Mesiha et al., 2005). Research carried out by Cui et al. demonstrated that insulin-loaded NPs composed of PLGA-Hp55 (HPMCP-55 as hypromellose phthalate, pH sensitive cellulose coating) significantly lowered blood glucose levels in a diabetic rat model. They also displayed excellent insulin entrapment ability (Cui et al., 2007). In a study conducted by Damgè et al, NPs composed of poly(ε-caprolactone) and a polycationic nonbiodegradable acrylic polymer (Eudragit® RS) demonstrated excellent insulin entrapment ability and ability to preserve the biological activity of aspart-insulin. They displayed a hypoglycaemic effect in a diabetic rat model with a maximal effect between 12-24 hours after administration (Damgè et al., 2010). In a study conducted by Xiong et al, insulin-loaded nanoparticles composed of

poly(lactic acid)-b-Pluronic-b-poly(lactic acid) (PLA-F127-PLA) were shown to exhibit a prolonged-hypoglycaemic effect in a diabetic rat model (Xiong et al., 2007). As such, a multitude of research has been carried out on the development of polymeric NPs for the oral delivery of insulin. This included the study of polysaccharide-based NPs such as chitosan, alginate, hyaluronan, dextran, cyclodextrin, arabinogalactan and pullulan-based NPs and polysaccharide-coated NPs such as chitosan, hyaluronan, heparin and dextran-coated NPs (Damgé et al., 2008). Polysaccharides are available from a wide range of natural origins including algal, plant, microbial and animal. Being both structurally and chemically diverse, polysaccharides are at present the polymeric materials of choice for peptide and protein nanocarrier production (Chen et al., 2011). They are safe, non-toxic, sustainable, inexpensive, biodegradable and biocompatible making them ideal candidates for novel NP drug delivery systems. Therefore, the variety of natural polymers available have been utilised to create multiple nanopharmaceutical drug delivery systems (Mizrahy and Peer, 2012).

Chitosan- and alginate-based nanocarriers have been studied extensively for oral insulin delivery (Sarmento et al., 2007 b). Their hydrophilic nature imparts excellent mucoadhesive properties, promoting better contact time with the mucus layer and subsequent drug absorption (Chen et al., 2011). Additionally, their ability to form hydrogels imparts a high affinity to absorb water and as such they display some common physical characteristics to living tissues (Hamidi et al., 2008). As a result, hydrogel NPs, also known as Nanogels (Gonçalves et al., 2010), are being increasingly examined for formation of novel drug delivery systems. They require milder preparative techniques, eliminating the need for organic solvents and as such are more desirable for oral drug delivery. As the potential of biopolysaccharide-based NPs as drug delivery systems is increasingly recognised, the quest for an optimal nanocarrier for oral insulin delivery continues, with hydrophilic biopolysaccharides proving most promising.

1.10 Characterisation of polymers: alginic acid and carrageenan

Polymeric nano/microparticles have been studied over the last past few decades as carriers for an oral insulin delivery (Delie and Blanco-Prieto, 2005). Several biodegradable and non-biodegradable polymer have been investigated, however non-biodegradable polymers cause problems such as: toxicity, difficulty in removal. Biodegradable polymers have the advantage of shielding the encapsulated drug from the external harsh conditions and also might favour uptake by the intestinal cells (Delie and Blanco-Prieto, 2005). Encapsulation of the drug into biodegradable polymeric particles isolates it from external medium, thus protecting the peptide from

peptidases, enabling their uptake by enterocytes. Degradation, sustained and controlled release of the drug strongly depends on the nature of the polymer (Dumitriu and Chornet, 1998). Properties of particles, such as size, surface charge and the nature of the polymer are the crucial parameters involved in the particle uptake by the GI tract. Additionally, the physicochemical properties, release profile of the drug and biological response of polymeric particles can be easily modulated (Sonia and Sharma, 2012).

Natural polymers are considered to be safe *in vivo*, as most of them are already used as excipients in drug formulations. Currently, natural polymers (polysaccharides and proteins) are being widely investigated as carriers for an oral insulin delivery as they show many advantages such as: hydrophilic and biodegradable nature, enzymatic degradation behaviour and good compatibility. Moreover, polysaccharides can be easy modified chemically and biochemically, are safe, stable, nontoxic, with the ability of forming gels, suggesting their usability for oral protein delivery. Polysaccharidic NPs have the potential to be administered by nonparenteral routes, to retain protein stability and to increase the duration of the therapeutic effect of the proteins (Halder et al., 2005). Figure 1.12 shows a selection of natural polymers used for oral insulin delivery and some of their properties.

Natural polymers used for oral insulin delivery	Characteristics of natural polymers used for oral insulin delivery
1. **Polysaccharides** ▪ Chitosan ▪ Alginate ▪ Dextran ▪ Starch ▪ Pectin	▪ Cheap and often extracted from renewable resources ▪ Biodegradable, nontoxic ▪ Purity may vary ▪ Induces a strong immunogenic response ▪ Hydrophilic
2. **Proteins** ▪ Casein ▪ Gelatin	▪ Properties cannot be controlled ▪ Only surface modification possible ▪ Bioadhesive (e.g. chitosan and alginate)

Fig. 1.12 *Natural polymers used for oral insulin delivery and their characteristics.*

1.10.1 Alginic acid

Alginic acid is a linear copolymer with homopolymeric blocks of (1,4)-linked-D-mannuronate (M) and C-5 epimer α-L-guluronate (G) residues, covalently linked in different sequences or blocks. The residue monomers can appear in homopolymeric blocks of consecutive G-residues, known as G-blocks, consecutive M residues, known as M-blocks, alternating M and G residues, known as MG-blocks, or randomly organised blocks (Figure 1.13). The amount of each block type varies with the origin of the alginate. Alternating blocks form

the most flexible chains, whereas G-blocks form stiff chain elements. Two G-blocks of more than six residues each from stable cross-linked junctions with divalent cations, leading to a three-dimensional gel network. Alginic acid powder is white or pale yellow-brown and can be crystalline or amorphous. It swells in water (Tønnesen and Karlsen, 2002).

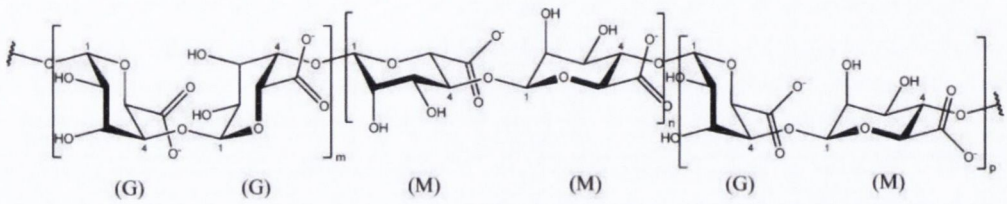

Fig. 1.13 *Structural units of alginate. M – mannurate residue, G – gulutronate residue (adapted from Agulhon et al., 2012).*

The wide availability of alginate and its desirable chemical and physical properties makes it an ideal encapsulation matrix for micro- and nanoparticles. Under mild conditions, alginate forms an inert, biodegradable hydrogel matrix. Porosity of the gel enables high drug diffusion rates, which additionally can be controlled with polymer coatings (Wee and Gombotz, 1998). Similarly to chitosan, alginate possesses mucoadhesive properties due to its carboxyl groups (Raj and Sharma, 2003). Alginate is a water soluble and biocompatible polymer, generally regarded as safe according to the FDA (Food and Drug Administration), (George and Abraham, 2006). Preparation of alginate particles by various methods including: nanoemulsion dispersion, ionotropic gelation and spray drying have been reported in literature (Coppi et al., 2002, Reis et al., 2006, Sarmento et al., 2006 a).

Alginate has the ability to ionically crosslink with multivalent cations, such as calcium, forming a network gel, which is stable at low pH and dissolves in neutral or high pH environments (Augst et al., 2006, George et al., 2006). This feature of hydrogels (pH sensitivity) makes them particularly attractive for oral delivery, as they can contract in the stomach protecting the drug. Passing through the GI, they subsequently swell and release the drug when pH increases. However, the stability of alginate gel usually depends on the M:G ratio, where stronger gels are formed with higher concentrations of G (Gacesa, 1988).

Alginates are widely used in biomedical applications as mucoadhesive, biodegradable and biocompatible polymers (Sinha and Kurmia, 2001). The relatively low encapsulation efficiency of alginates can be improved by interaction with other polymers such as: dextran sulfate, chitosan, pectin or methylcellulose. Sarmento et al., developed alginate-chitosan capsules that have been investigated for their use as oral insulin formulations (Sarmento et al., 2007 b). Nanoparticles were prepared by ionotropic pre-gelation of an alginate core followed by chitosan polyelectrolyte

complexation. The results indicated that the encapsulation of insulin into mucoadhesive nanoparticles was a key factor in the improvement of its oral absorption and oral bioactivity (Sarmento et al., 2007 b). Another group (Ramadas et al., 2000) reported a formulation based on liposome encapsulated alginate-chitosan gel capsules for oral insulin delivery, with increased encapsulation efficiency. The percentage loading of insulin in alginate capsules was only 11%, however the loading was increased to 21.5% when lipoinsulin was encapsulated.The lipid exterior might help to improve the absorption across biological barriers, while the aqueous interior helps to preserve the structure and conformation of insulin. It was reported that an oral administration of lipoinsulin loaded alginate-chitosan capsules reduced the blood glucose level in diabetic rats (Ramadas et al., 2000). Another modification of alginate/chitosan nanoparticles was reported by Zhang et al., where insulin was protected by forming complexes with cationic β-cyclodextrin polymers (CPβCDs). Due to the electrostatic attraction between CPβCDs and insulin, as well the assistance of its polymeric chains, CPβCDs could effectively protect insulin under simulated gastrointestinal conditions. It was notable that the cumulative insulin release in simulated intestinal fluid was significantly higher (40%) than that without CPβCDs (18%) as insulin was mainly retained in the core of the nanoparticles and well protected against degradation in simulated gastric fluid (Zhang et al., 2010). Reis et al., performed investigations into alginates microparticles produced by emulsification/internal gelation method as a promising carrier for insulin delivery. The procedure involved the dispersion of alginate solution with protein into an aqueous phase and further gelation triggered by instantaneous release of ionic calcium from carbonate complex via gentle pH adjustment (Reis et al., 2007). Bioadhesive alginate copolymers as platforms for oral delivery of insulin were reported by Mahkam. Alginate was modified chemically by grafting with acrylic acid at various compositions. The hydrolysis rate and release of insulin was further tested (Mahkam, 2009).

1.10.2 Carrageenan

Carrageenans are a family of hydrophilic sulfated biopolysaccharides extracted from various species of the *Rhodophyta* class of red seaweeds with relatively high molecular weight (Campo et al., 2009). They are potassium, sodium, calcium or magnesium salts of a hydrophilic linear sulfated backbone of alternating 1→3 glycosidic-linked β-D-galactopyransose units and 1→4 glycosidic-linked α-D-galactopyranose units or 1→4 glycosidic-linked 3, 6-anhydro-α-D-galactopyranose units (Figure 1.16) (Berth et al., 2008). Their properties differ depending on the biological origin of the polymer. Three main types of carrageenan exist, namely

Kappa (κ), Iota (ι) and Lambda (λ), which differ respectively by one, two and three sulfate ester groups present on their repeating disaccharide backbones. The proportion of sulfate groups present and their associated cations ultimately determines the water solubility of carrageenans which subsequently determines carrageenan gel strength and solution viscosity (Berth et al., 2008).

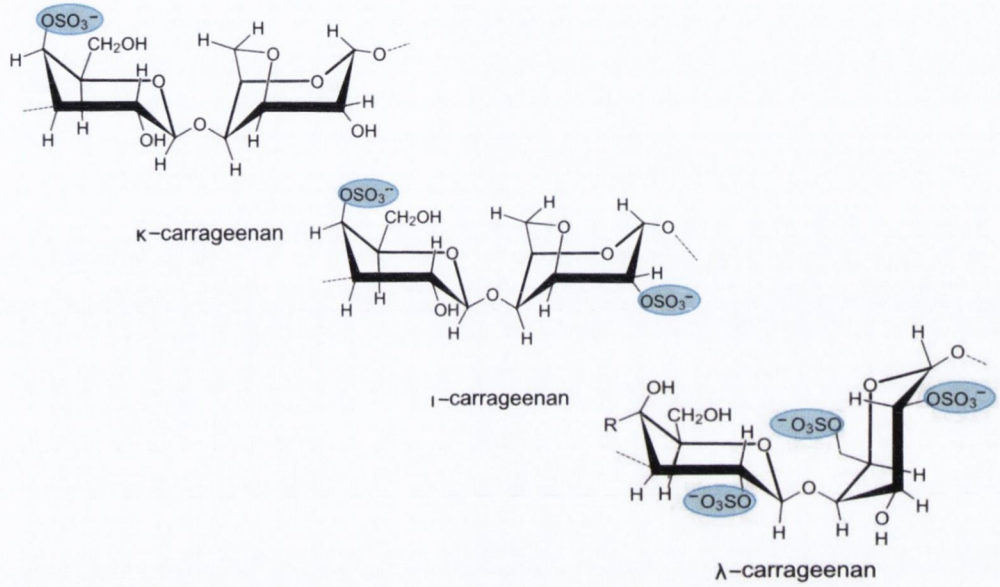

Fig. 1.14 *Chemical structure of κ-, λ- , and ι-carrageenan (Berth et al., 2008).*

κ- and ι- carrageenan share the same backbone, both containing a sulfate group at position 4 of the 1→3 linked D-galactose unit (Figure 1.14). This may explain the similar behaviour of κ- and ι-carrageenan which are both capable of forming thermoreversible gels (Janaswamy and Chandrasekaran, 2002). In the case of λ-carrageenan, the sulfate group present on the 1→3 linked D-galactose unit is at position 2 and may be responsible for its inability to form gels (Berth et al., 2008). In theory, carrageenans should possess some of the same desirable characteristics of previously examined hydrophilic biopolysaccharides such as chitosan and alginate.

Carrageenans have been widely exploited in the food industry and have more recently been adopted for biomedical and pharmaceutical purposes, encapsulating cells, bacteria and fungi (Rinaudo, 2008). They interact with other polymers including chitosan, xanthan, gelatin and locust bean gum to form gel complexes (Pavli et al., 2010). Carrageenan-based microcapsules for encapsulation of isoniazid have been described (Devi and Maji, 2010). In addition, carrageenans have presented sustained drug-release properties when complexed with doxazosin in matrix tablets (Pavli et al., 2010). Thrimawithana et al. have described novel carrageenan/methylcellulose transscleral drug delivery systems (Thrimavithana et al., 2011). More recently, lectin-functionalised carboxymethylated *kappa*-carrageenan microparticles have been

investigated and appear promising as oral insulin delivery systems (Leong et al., 2011).

A variety of polymers/polymer combinations, several choices of formulation and processing techniques make it a very useful tool to overcome delivery challenges and may be readily modified to fit design specifications (Desai and Park, 2005, Zalfen et al., 2008). Polymer properties, the drug to polymer ratio and production method can be used to affect the formulation, which would further affect the stability, bioavailability and drug release profiles. Furthermore, polymers can be engineered through additional coatings and ligands to be site-specific, optimising the dose and subsequent biological response (Bies et al., 2004).

1.11 Cell penetrating peptides in drug delivery

Since the first report of the cell-penetrating peptide (CPP) in 1994 (Derossi et al., 1994), many studies have been performed on these entities. Many types of CPPs have been shown to improve the intracellular delivery of various biologically active molecules into living cells with a high degree of efficiency (El-Andaloussi et al., 2005; Deshayes et al., 2005). CPPs, also called protein transduction domains (PTD), are short peptides (7-15 residues), which are cationic or amphipathic in nature. Cationic CPPs are usually rich in arginine or lysine. Examples of cationic CPP include: the Tat peptide derived from human immunodeficiency virus (HIV)-1 Tat protein, penetratin derived from the third helix of the *Antennapedia* homeodomain protein, and oligomers of arginine or lysine (Murriel and Dowdy, 2006). These types of CPPs have been extensively studied for intracellular delivery of macromolecules, as they have the ability to efficiently translocate across cell plasma membranes without compromising cargo bioactivity (Patel et al., 2007). Their cationic nature helps them to bind extensively to the negatively charged proteoglycans localised on the cell surfaces and consequently have low cell specificity. CPP-mediated drug delivery offers great possibilities to improve intracellular delivery of drugs with poor permeability, especially therapeutic proteins that are unable to cross membranes due to their large size and high hydrophilicity. As reported, CPPs are capable of penetrating a wide variety of mammalian cells, independent of tissue or organism type (Mano et al., 2005), insect cells (Chen et al., 2012), and plants (Chugh and Eudes, 2008, Chang et al., 2007). Certain CPPs can also facilitate targeted delivery to the subcellular structure such as cell nucleus (Niedzielski et al., 2007, Vives et al., 1997, Braddock, 1989). A variety of cargoes such as: small molecules, peptides, proteins, nucleic acids, quantum dots, polysaccharides, liposomes and nanoparticles have been reported to be successfully delivered by CPPs (Morris et al., 2001, Wadia and Dowdy, 2005, Deshayes et al., 2005, Walther et al., 2008, Henriques et al., 2005, Torchilin, 2008, Torchilin, 2007,

Snyder and Dowdy, 2004). It would be expected that the size of the cargo would play an essential role for the CPP-mediated cell delivery, however that is not the case (Vives, 2005), although very large payloads may seem to be less effective in the cell transduction (Zorko and Langel, 2005). Comparison with other polymeric types of transduction agents shows that most CPPs are relatively non-toxic (Splith and Neundorf, 2011). The mechanism of CPP-mediated delivery has not been fully clarified.

1.11.1 Approaches to use cell penetrating peptides in drug delivery

CPP-based delivery systems can be prepared by using four different approaches: genetic fusion of the protein drug with a CPP, covalent linkage of the target drug with CPP, formation of a complex between the cationic CPP and anionic drug, as in case of DNA and siRNA and modification of drug-loaded nanoparticles with CPP.

1.11.1.1 Recombinant fusion protein

To prepare recombinant fusion of CPP with a drug, CPP is integrated into a functional protein as a transduction-enhancing motif. Selective fusion of CPP to a designed site offers a series of advantages in mass manufacturing, quality control and homogenous products. A study performed by Dowdy's group showed for the first time the synthesis of an in-frame TAT bacterial expression vector that could produce the cell-permeable recombinant protein chimeras (Ezhevsky et al., 1997, Nagahara et al., 1998). After that, the application of bacterial expression vectors has become more common in practice to fuse CPP sequence into a therapeutic protein and a general protocol has been successfully established (Dietz and Bahr, 2007). However these recombinant proteins are compatible only for proteins and not applicable for other non-protein molecules as nucleic acids or polymers.

1.11.1.2 Covalent chemical linkage

Several methods can be used to conjugate CPP with cargoes via a stable or cleavable manner such as: thiol-maleimide, amide bond, disulfide and thioester linkages (Heitz et al., 2009). Usually a cleavable bond is selected to ensure further release of the cargos. A disulfide bond could be an example of reversible conjugation, as it can be broken down under a cytosolic environment having several reducing agents, such as glutathione or reductase (Meade et al., 2009). The major disadvantage of the covalent conjugation is the final heterogeneous structure of the product, which causes difficulties in quality control or its characterisation (Meade and Dowdy, 2007). To overcome this problem, site-specific conjugation methods started to be explored. It is a big challenge to create monomeric conjugates of nucleic acid drugs and CPPs, mainly due to strong electrostatic interaction between them (Meade and Dowdy, 2007).

Similar problems were reported with the preparation of CPP-insulin chemical conjugates, because of the anionic structure of insulin (He et al., 2011).

1.11.1.3 Non-covalent method

Non-covalent complexes for CPP-mediated gene delivery, formed via the electrostatic interaction, are often prepared as an alternative for chemical CPP-gene conjugates. Prepared complexes carry net positive charges achieved by adding excessive amount of CPP to ensure their binding with negatively charged proteoglycans and their subsequent cellular uptake. Beside the cell-internalisation, CPP should also facilitate nuclear entry, which is essential for gene expression (Martin and Rice, 2007). However, the small size of CPPs results in relatively poor ability to bind and condense gene drugs, compared to high molecular weight polymers. Thus, the CPP/gene complexes usually show less compact structure and are less favourable for gene transduction.

Non-covalent conjugates were successfully prepared for the effective delivery of quantum dots (Liu et al., 2011) and proteins into mammalian (Hu et al., 2009, Hou et al., 2007 a) and plant cells (Chang et al., 2007, Lu et al., 2010). The possibility for effective delivery was probably due to the permeation enhancer-like functions of CPP, which lead to the membrane destabilisation and enhanced permeability, however detailed mechanism remains unknown.

Intracellular drug delivery via this method seems to be unpredictable and it should be studied on a case by case basis, depending on the sequence of CPP and the nature of cargoes. Another class of CPPs – synthetic amphipathic peptides, which consist of both hydrophobic and hydrophilic domain, was reported to mediate the intracellular protein delivery via the non-covalent conjugation method (Lo and Wang, 2010).

1.11.1.4 Surface modifications of nanoparticle-based drug carriers

The incorporation of CPP into nanoparticle based drug carriers would facilitate the cellular uptake and also would enhance the efficiency of CPP in delivering a larger amount of the loaded drugs, which is an important advantage comparing to CPP-drug conjugate that requires at least one CPP entity for the delivery of one single drug molecule. Furthermore, drugs with different physicochemical properties can be loaded into NPs, where many of those cannot be directly conjugated with CPP. The CPP-modified nanoparticle systems include lipid-based (e.g. liposomes) or polymer-based nanocarriers (e.g. micelles), but also inorganic carriers such as: silver-, iron-based nanoparticles and quantum dots. CPPs could be successfully immobilised on the surface of NPs via either adsorption (usually due to the charge interaction) (Yang et al., 2012, Yan et al., 2012) or chemical conjugation (Liu et al., 2012).

1.11.2 Application of cell penetrating peptides for insulin delivery

The potential of CPPs as modulators that enhance the intestinal uptake of active molecules was also investigated for the non-invasive delivery of insulin. The group of Morishita and co-workers performed an investigation into the intestinal permeability of insulin co-administered with oligoarginine composed of six (R6), eight (R8) or 10 arginine (R10) residues. No insulin absorption was observed following administration of insulin solution alone; however, insulin absorption increased dramatically after co-administration of the D-form of R6 (D-R6) and the form of R6 (L-R6) in a dose-dependent manner. Among oligoarginines composed of six, eight, or 10 arginine residues, D-R8 showed the strongest enhancing effects on insulin intestinal absorption (Morishita et al., 2007). Kamei et al. studied ten selected CPPs (Figure 1.15) for their ability to enhance the intestinal bioavailability of insulin (Kamei et al., 2008).

Peptides	Sequence
Arginine-rich peptides	
Arginine octamer (R8)	RRRRRRRR
Arginine dodecamer (R12)	RRRRRRRRRRRR
HIV-1 Tat (48–60)	GRKKRRQRRRPPQ
HIV-1 Rev (34–50)	TRQARRNRRRRWRERQR
Amphipathic peptides	
Penetratin	RQIKIWFQNRRMKWKK
pVEC	LLIILRRRIRKQAHAHSK
Erns	RQGAARVTSWLGLQLRIGK
RRL helix	RRLRRLLRRLRRLLRRLR
PRL4	PRLPRLPRLPRL
Random composition peptides	
Random peptide	GLSASPNLQFRTV

A: Alanine, E: Glutamic acid, F: Phenylalanin, G: Glycine, H: Histidine, I: Isoleucine, K: Lysine, L: Leucine, M: Methionine, N: Asparagine, P: Proline, Q: Glutamine, R: Arginine, S: Serine, T: Threonine, V: Valine, W: Tryptophan.

Fig. 1.15 *Selected CPPs studied for the intestinal bioavailability of insulin (Kamei et al., 2008).*

The results obtained indicated that L-penetratin showed the most significant enhancement effect for ileal insulin absorption among CPPs tested in the study.

The effect of selected CPPs (L-penetratin, D-penetratin, D- form of R8 (D-R8), and L- form of R8 (L-R8) on the nasal absorption of insulin and the resultant hypoglycaemic effect was also investigated (Khafagy et al., 2009). These researchers demonstrated that insulin absorption was greater after treatment with L- and D-penetratin, and compared to D- or L-R8. D- and L-penetratin significantly increased the bioavailability, which is related to the extent of absorption and demonstrated the greatest increase in nasal insulin absorption to insulin solution alone more markedly than D- and L-R8 (Khafagy et al., 2009). CPP-insulin hybrids were prepared and tested for improvement of the intestinal absorption of insulin. Tat

(CGGGYGRKKRRQRRR) peptide was selected for the modification of insulin. As reported, the intestinal efficiency of CPP hybridised insulin was 6-8 times increased compared to normal insulin as tested on Caco-2 cell monolayer (Liang and Yang, 2005). Patel et al., investigated the conjugation of insulin with CPPs for the enhancement of its absorption rate across alveolar epithelial barrier. Insulin (INS) was conjugated to series of cationic CPPs, such as: Tat peptide, oligoarginine (r9) or oligolysine (k9) via disulfide bridge to a D-isoform cysteine (c) present at the N-terminal of the peptide sequence yielding INS-c-TAT, INS-cr9 and INS-ck9, respectively. The order of the transport of INS and INS-CPPs across primary cultured rat alveolar epithelial cell monolayers was as follow: INS-cr9 > INS-cTat > INS-ck9 > INS, with 27-, 19- and 4-fold increase compared to native INS, respectively. Additionally, it was reported that transport of INS-cr9 was temperature- and time-dependent. Intratracheal instillation of INS-cr9 in diabetic rats resulted in a steady decrease in blood glucose level that was more sustained over time when compared with INS (Patel et al., 2009).

1.11.3 Characterisation of protamine sulfate

Protamines are highly cationic peptides with molecular weights of approximately 5 kDa, an unusually high level of arginine (~66% on a molar basis) with an isoelectric point of pH 12–13 (Suzuki and Ando, 1972). Protamine sulfate (PROT), usually extracted from the sperm or roe of *Salmonidae* or *Clupeidae* species of fish, is comprised of the sulfates of basic arginine-rich peptides (European Medicines Agency, 2012), Protamine is a small cationic peptide that binds and precipitates DNA and it can be employed in the removal of DNA from protein samples or the purification of DNA binding proteins. PROT shows antimicrobial properties (Johansen, 1995) and it inhibits pepsin activity (Mekras, 1989). It binds with heparin in solution and inhibits its anticoagulant activity (Sie, 1989). It has been employed in subcutaneous insulin formulations, along with zinc, to prolong the action of insulin e.g. in intermediate acting Neutral Protamine Hagedorn (NPH) (Gualandi-Signiorini and Giorgi, 2001). Prolonged release insulin formulations are of utmost importance for treatment of diabetes to minimise the frequency of subcutaneous administration. Reynolds et al. have reported an *in vitro* membrane-translocating ability of protamine believed to be associated with its positively charged polyarginine chains (Reynolds et al., 2005). Thus, protamine was considered here for its potential to form novel membrane-translocating NPs to facilitate the successful transport of insulin to its site of action. In addition, protamine has proved a promising non-toxic entity for the enhanced cellular uptake of large protein molecules into tumours, a property which could be transferrable to cellular uptake of insulin (Choi et al., 2010).

CHAPTER 2

MATERIALS AND METHODS

2.1 Materials

Reagent	Supplier/Manufacturer
Acetic acid, glacial (>99.85%)	Sigma-Aldrich
Acetonitrile, HPLC grade	Fisher Scientific UK
Achromopeptidase from *Lysobacter* sp.	Sigma-Aldrich
Acrylamide/Bis-acrylamide 30% solution	Sigma-Aldrich
Advantage cDNA PCR Kit and Polymerase Mix	Clontech
Agarose multi – purpose	Bioline
Alginic acid, sodium salt, low viscosity (AAL) from *Macrocystis perifera* (Kelp)	Sigma-Aldrich
Alginic acid, sodium salt, medium viscosity (AAM) from *Macrocystis perifera* (Kelp)	Sigma-Aldrich
Alginic acid, sodium salt, high viscosity (AAH) from *Macrocystis perifera* (Kelp)	Sigma-Aldrich
Ammonium chloride	BDH Laboratory Supplies
Ampicillin sodium salt	Sigma-Aldrich
Anti Mouse IgG, HRP-linked antibody	Cell Signalling Technology
Ammonium peroxodisulphate	Merck
Ammonium sulphate	BDH Laboratory Supplies
Anti-mouse IgG-HRP	ISIS
Aspartate	Sigma-Aldrich
*BamH*I restriction enzyme	Invitrogen
Bio-Rad protein assay	Bio-Rad
Boric acid	Sigma-Aldrich
Buffer solution pH 4	Fluka, Germany
Buffer solution pH 7	Fluka, Germany
Buffer solution pH 10	Fluka, Germany
Calcium chloride	Sigma-Aldrich
Carbenicillin disodium salt	Molekula
CellTiter96 Aqueous One Solution Cell Proliferation Assay Kit	Promega Corp.
Cobalt (II) chloride hexahydrate	Sigma-Aldrich
Coomassie brilliant blue R-250	Sigma-Aldrich
Copper (II) chloride dehydrate	Sigma-Aldrich
Disodium hydrogen phosphate	Merck
DL-Dithiothreitol	Sigma-Aldrich
dNTP mix	Stratagene-Agilent technologies
Donkey anti-goat IgG-HRP	Santa Cruz Biotechnology

*Dpn*I restriction enzyme	Stratagene-Agilent technologies
Dried skimmed milk	Marvel
Ethidium bromide	Sigma-Aldrich
Ethylenediaminetetraacetic acid (EDTA)	Sigma-Aldrich
FaSSIF	Biorelevant.com
Fluorescein sodium salt	Sigma-Aldrich
Gentamycin sulphate	Sigma-Aldrich
Glucose	Sigma-Aldrich
Glutathione oxidised form disodium salt	Sigma-Aldrich
Glycerol	Sigma-Aldrich
Glycine	Molekula/ Sigma-Aldrich
Hanks' balanced salt solution	Sigma-Aldrich
HEPES (4-(2-hydroxyethyl)-1-piperazineethanesulfonic acid)	Sigma-Aldrich
HiSpeed® Plasmid Maxi kit	Qiagen
HisTrap™ HP column	GE Healthcare
His Tag Antibody, Purified Rabbit Polyclonal (Mab)	Abgent
His Tag Antibody, Purified Mouse Monoclonal (Mab)	Abgent
Hydrochloric acid 37%	Sigma-Aldrich
HyperLadder I and IV	Bioline
Imidazole	Sigma-Aldrich
Insulin A (C-12) goat polyclonal IgG	Santa Cruz Biotechnology
Insulin B (N-20) goat polyclonal IgG	Santa Cruz Biotechnology
Insulin, human recombinant	SAFC
Insulin human recombinant, expressed in *E. coli*	Sigma-Aldrich
Iron (III) chloride	Sigma-Aldrich
Isopropyl-1-thio-*β*-*D*-galactopyranoside (IPTG)	Molekula
Kanamycin sulphate	Calbiochem
Laemmli SDS-PAGE Loading buffer, 2x	Sigma-Aldrich
L-Cysteine	Sigma-Aldrich
L-Cystine	Sigma-Aldrich
L-Glutathione reduced	Sigma-Aldrich
Lyophilised Protein Assay Standard BSA	BioRad Laboratories GmbH
Luria Bertani (LB) agar	Sigma-Aldrich
Luria Bertani (LB) broth	Sigma-Aldrich
Magnesium chloride	Riedel-DeHaen
Magnesium sulphate	Sigma-Aldrich

Manganese (II) chloride tetrahydrate	Sigma-Aldrich
Methanol	Fisher Scientific UK
Methyl cellulose	Sigma-Aldrich
Minimal Essential Medium Eagle	Sigma-Aldrich
Monoclonal Anti-Insulin mouse IgG, Clone K36AC10	Sigma-Aldrich
*Msc*I restriction enzyme	Invitrogen
Non-radioactive Cell Proliferation Assay	Promega Corporation USA
*Nco*I restriction enzyme	Invitrogen
*Nde*I restriction enzyme	Invitrogen
Nickel (II) chloride hexahydrate	Sigma-Aldrich
N,N,N′,N′-Tetramethylethylenediamine	Sigma-Aldrich
N-A amine AS	Sigma-Aldrich
Oligonucleotides	Eurofins MWG Operon
Penicillin G sodium salt	Sigma-Aldrich
pET-19b plasmid DNA	Novagen
pET-22b plasmid DNA	Novagen
pET-39b plasmid DNA	Novagen
Phosphate buffered saline	Sigma-Aldrich
Phosphoric acid, 85%	Sigma-Aldrich
Potassium dihydrogen phosphate	BDH Laboratory Supplies
Protamine sulphate salt, from salmon	Sigma-Aldrich
Protease inhibitor cocktail tablets	Roche
Protein Assay dye concentrate	BioRad Laboratories GmbH
Protein Assay Standard BSA, 1.45 mg/ml	BioRad Laboratories GmbH
QIAprep® Spin Miniprep kit	Qiagen
QIAquick® Gel Extraction kit	Qiagen
Rapid DNA Ligation Kit	Roche
SDS PAGE, ruler plus prestain protein ladder	Fermentas Life Sciences
SeeBlue® plus2 prestained standard	Invitrogen
Simulated Intestinal Fluid (SIF) powder	Biorelevant
Sodium azide	Sigma-Aldrich
Sodium bicarbonate	Sigma-Aldrich
Sodium chloride	Sigma-Aldrich
Sodium dodecyl sulphate	Sigma-Aldrich
Sodium hydrogen phosphate	Sigma-Aldrich
Sodium hydroxide	Sigma-Aldrich
Sodium molybdate dehydrate	Sigma-Aldrich
Sodium pyruvate solution	Sigma-Aldrich

Sodium selenite pentahydrate	Sigma-Aldrich
Sodium sulphate	Sigma-Aldrich
Sodium sulphite	Sigma-Aldrich
Sodium tetrathionate	Sigma-Aldrich
Streptomycin solution	Sigma-Aldrich
Sucrose	Sigma-Aldrich
Tricine	Alfa Aesar
Trifluoroacetic acid	Sigma-Aldrich
Trizma base	Sigma-Aldrich
Trizma HCl	Sigma-Aldrich
Trypsin – EDTA solution	Sigma-Aldrich
Tween 20	Sigma-Aldrich
Ultrapure water	Purite Prestige Analyst HP
Urea	Merck/ Sigma-Aldrich
Virkon	Day-impex limited
Visualizer^{TM} Western blot detection kit, mouse	Millipore
*Xho*I restriction enzyme	Invitrogen
Yeast extract	Sigma-Aldrich
Zinc chloride	Sigma-Aldrich
Zinc sulphate heptahydrate	Sigma-Aldrich
α-Lactose monohydrate	Sigma-Aldrich
β-Mercaptoethanol	Sigma-Aldrich
ι-carrageenan (IC)	Sigma-Aldrich
κ-carrageenan (KC)	Sigma-Aldrich
λ-carrageenan (LC)	Sigma-Aldrich

2.2 Bacterial strains and plasmids

Name	Supplier
BL21 (DE3) (BF^{-}*dcm ompT hsdS* $r_B^{-}m_B^{-}$)	Stratagene-Agilent technologies
XL2 – Blue Ultracompetent Cells	Stratagene-Agilent technologies
pHB1 plasmid, (145.5 ng/μl, stock solution)	(prepared by Boutsikaris, 2009)
pHB2 plasmid, (110 ng/μl, stock solution)	(prepared by Boutsikaris, 2009)
pHB3 plasmid, (102 ng/μl, stock solution)	(prepared by Boutsikaris, 2009)

2.3 Equipment

Instrumentation	Manufacturer
Agarose gel electrophoresis apparatus, PerfectBlue™	PegLab
BL310 Laboratory Balance	Sartorius
Centrifuge 5810R	Eppendorf
Centrifuge 5415R	Eppendorf
Centrifuge RT 6000D	Sorvall
ChemiDoc® XRS	BioRad
Chromatography purification system	BUCHI
CO_2 incubator, series 8000DH	Thermo Scientific
Electrophoresis power supply PowerPac Basic	BioRad
FLUOstar Optima microplate reader	BMG labtech
FPLC system "AKTA"	GE Healthcare
Haraeus Fresco 17 centrifuge	Thermo Scientific
Heat-stir SD162 hotplate	Stuart
Hi LoadTM 26/60, SuperdexTM 75 pg column	GE healthcare
Ika vortex genius 3	Ika
Incubator Shaking apparatus, MAXI 14	Medical Supply CO
Incubator B-10	Memmert
LC-10 Arp Series HPLC system	SHIMADZU
Magnetic stirrer, Yellow MagMS	Yellow line
MT5 Microbalance	Mettler
Microson ultrasonic cell disruptor, XL2000	Misonix
Mini Gyro –rocker SSM3	Stuart
Mini-Protean TetraCell Electrophoresis system	BioRad
Orion 42A pH meter	Thermo Electron Corporation
pH meter, Seven Easy	Mettler Toledo
PCR Primus 96	PegLab
Power Pac basic	BioRad
Scientific Reciprocal Shaking Bath Model 25	Precision
Semi Dry Blotting apparatus AE 6675 (Horizblot)	ATTO corporation
Spectrophotometer ND-1000, Nanodrop	ThermoScientific
Spectrophotometer PharmaSpec UV-1700	Shimadzu
Thermomixer comfort / Thermomixer R	Eppendorf
Thermomixer compact 5350	Eppendorf
Trans-blot SD Semi-Dry cell	BioRad
Vibro Viscometer SV-10	A&D

Yellow MAG MS7 stirring plate	Yellow line
Zetasizer Nano ZS	Malvern
Z1 Coulter Counter Particle Counter	Beckman Coulter

2.4 Methods

2.4.1 Methods - preparation, expression and purification of insulin plasmids

2.4.1.1 Preparation of solutions

Table 2.1 *Solutions used in described methods.*

Solution	Composition
Solutions used for transformation, inoculation and induction	
Carbenicillin salt	stock solution 100 mg/ml
Kanamycin salt	stock solution 30 mg/ml
LB (Luria Bertani) agar plates	35% w/v LB agar, 1:1000 of antibiotic (carbenicilin or kanamycin)
NZY (+) broth	20% w/v LB broth, pH 7.5, supplemented with 12.5 mM $MgCl_2$, 12.5 mM $MgSO_4$, 0.4% w/v glucose
IPTG (Isopropyl-1-thio-*β-D*-galactopyranoside)	stock solution 1 M
Solutions used for auto-induction system Each solution was autoclaved (except the solution containing iron)	
MDG	2 mM $MgSO_4$, 1:5000 1000x metals, 0.5% w/v glucose, 0.25% w/v aspartate, 1:50 50x M
NPSx 20	1 M Na_2HPO_4, 1 M KH_2PO_4, 0.5 M $(NH_4)_2SO_4$
NZ-Amine	1% w/v NZ amine, 0.5% w/v yeast extract
1000x metals	50 mM $FeCl_3$, 20 mM $CaCl_2$, 10 mM $MnCl_2 \cdot 4H_20$, 10 mM $ZnCl_2 \cdot 7H_20$, 2 mM $CoCl_2 \cdot 6H_2O$, 2 mM $CuCl_2 \cdot 2H_2O$, 2 mM $NiCl_2 \cdot 6H_2O$, 2 mM $Na_2MoO_4 \cdot 2H_2O$, 2 mM $Na_2SeO3 \cdot 5H_2O$, 2 mM H_3BO_3
50x M	1.25 M Na_2HPO_4, 1.25 M KH_2PO_4, 2.5 M NH_4Cl, 0.25 M Na_2SO_4
50x 5052	5% w/v glycerol, 0.5% w/v glucose, 0.2% w/v α-lactose monohydrate
ZYM-5052	95.8% v/v NZ-Amine, 2 mM $MgSO_4$, 1:5000 1000x metals, 1:50 50x 5052, 1:50 50x M
ZYP-5052	95.8% v/v NZ-Amine, 2 mM $MgSO_4$, 1:5000 1000x metals, 1:50 50x 5052, 1:20 20x NPS

Table 2.1 *Solutions used in described methods.*

Solution	Composition
Solutions used for samples preparation for expression, solubility and periplasmic localisation test	
0.5 M EDTA	0.5 M EDTA, pH 8.0
Washing buffer	30 mM Tris HCl, 20% w/v sucrose, pH 8.0
Urea buffer	8 M urea, 0.1 M $NaH_2PO_4 \cdot H_2O$, 0.01 M Tris base, pH 8.0
Buffers used for Histag column purification	
Starting (binding) buffer	50 mM NaH_2PO_4, 300 mM NaCl, 20 mM imidazole, pH to 7.4
Elution buffer	50 mM NaH_2PO_4, 300 mM NaCl, 500 mM imidazole, pH 7.4
Agarose gel electrophoresis solutions	
10x Tris acetate EDTA (TAE) Buffer	0.4 M Tris base, 0.011% v/v glacial acetic acid, 0.01 M EDTA, pH8
Glycine SDS-PAGE electrophoresis solutions	
5x Tris-glycine electrophoresis buffer	25 mM Tris base, 250 mM glycine (electrophoresis grade), pH 8.3, 0.1% w/v SDS
1.5 M Tris buffer pH 8.8	1.5 M Tris base, pH 8.8
1.0 M Tris buffer pH 6.8	1.0 M Tris base, pH 6.8
Staining solution	0.0025% w/v solution of Coomassie Brilliant Blue R-250 dissolved in destaining solution
Destaining solution	Methanol: acetic acid (glacial):H_2O mixed in ratio 5:1:4
4x SDS-PAGE sample loading buffer	40% w/v glycerol, 0.24 M Tris pH 6.8, 8% w/v SDS, 0.04% w/v bromophenol blue, 5% w/v β-ME
Western blot solutions	
Washing buffer	0.1% w/v Tween20 in PBS
Blocking buffer	5% w/v solution of dry milk in PBS
Primary antibodies in a blocking buffer	The concentration of primary antibodies was 1:1000, unless otherwise indicated
Towbing transfer buffer (TTB)	0.025 M Tris base, 0.2 M glycine, 0.0005% w/v SDS, 20% w/v methanol

All employed molecular biology protocols, if not mentioned here, were used exactly like described in Sambrook and Russell (Sambrook and Russel, 2001).

2.4.1.2 Transformation

The XL2 ultracompetent cells were thawed on ice. 1 µl of the plasmid DNA (appropriate vector) was added to 40 µl aliquot of cells, mixed and incubated on ice for 30 min. After the incubation prepared mixture was heat-pulsed at 42°C in water bath (thermomixer) for 40 s. The duration of the heat pulse was critical for maximum efficiency. Afterwards the tube was incubated on ice for 2 min. 900 µl of NZY^+ broth preheated to 42°C were added to the tube with cells and the tube was incubated at 37°C for 1 h with shaking. 20 µl and 200 µl of the transformation mixture were plated on 2 LB agar plates containing antibiotic. The plates were incubated at 37°C overnight.

2.4.1.3 Inoculation and bacterial culture

A single colony from each freshly streaked selective plate was picked and starter cultures of 2 ml LB broth containing antibiotic were inoculated. Tubes prepared in this way were incubated for approximately 8 h at 37°C with vigorous shaking. The starter cultures (precultures) were diluted 1:500 into selective LB broth. The cultures were grown at 37°C with vigorous shaking (approx. 300 rpm) for 12 - 16 h.

2.4.1.4 Plasmid amplification – Maxi Prep Kit

To amplify the vector Qiagen HiSpeed Plasmid Maxi Kit was used. All the amplification were used exactly like described in the Qiagen MaxiPrep Protocol.

2.4.1.5 Enzymatic digestion of DNA

Cleavage mixture containing one restriction enzyme contained: 5 µl of enzyme buffer 10x, 30 µl of the appropriate vector maxi prep DNA, 13 µl of sterile H_2O and 2 µl of restriction enzyme. Prepared mixture was carefully mixed with the pipette and incubated overnight at 37°C.

2.4.1.6 Agarose gel electrophoresis

Agarose gel electrophoresis is a method mainly used for analysis or separation of DNA and RNA molecules. Separation of the molecules of nucleic acids is achieved by moving negatively charged molecules through an agarose gel in an electric field. 0.8% w/v agarose gel, which is standard type agarose suitable for size range of DNA fragments 500 bp - 15 kbp was used. Electrophoresis buffer was TAE (Tris-acetate EDTA, pH 8.0). Before loading into the gel samples were mixed with loading buffer. To enable accurate sizing of DNA two types of Hyper Ladders (I and IV) with

Loading Buffer were used. Solution of agarose in electrophoresis buffer (1x, TAE working solution) was prepared at concentration 0.8% w/v. The beaker was heated in a microwave oven until the agarose was dissolved. When the molten gel was cooled to ~55°C, ethidium bromide (1 µg/ml) was added. The comb was positioned 0.5-1.0 mm above the plate and the warm agarose solution was poured into the mould, so after setting the gel wells were formed. Then the electrophoresis buffer (TAE, 1x) was poured to cover the gel to depth of ~1 mm and the comb was removed very carefully. Samples were loaded into the slots of the submerged gel using a micropipette. The lid of the tank was closed and the electrical leads were attached. A voltage of 100 V was applied. The gel was running until dyes (the bromophenol blue and xylene cyanol FF) were migrated in appropriate distance through the gel. The image of the gel was captured by digital camera ChemiDoc XRS using UV light source at 254 nm.

2.4.1.7 Gel extraction

The QIAquick gel extraction kit was used to extract DNA from the agarose gel. All the steps of gel extraction were used exactly like described in the QIAquick gel extraction kit protocol. Purified DNA was stored in -20°C.

2.4.1.8 PCR – Polymerase Chain Reaction

PCR was carried out in the PCR apparatus, model PCR Primus 96. The synthesis reaction for thermal cycling was prepared in a sterile tube. The components were added as follows: 40 µl distilled water, 5 µl reaction buffer 10x, 1 µl dNTP mix, 1 µl forward primer working solution (10 pmol/µl), 1 µl reverse primer working solution (10 pmol/µl), 1 µl DNA template and 1 µl of Advantage Polymerase. Prepared PCR synthesis reaction was mixed by pipetting gently the solution, before and after addition of the polymerase. The reaction was cycled by using the cycling parameters outlined in the Table 2.2.

Table 2.2 *Cycling parameters of PCR reaction.*

Segment	Cycles	Temperature	Time
1 Initialisation step	1	94°C	2 min
2 Denaturation	30	94°C	30 s
3 Annealing – Extension/elongation		68°C	3 min
4 Final elongation	1	15°C	15 min
5 Final hold		4°C	∞

2.4.1.9 Ligation

Rapid DNA Ligation Kit was used to ligate vector with insert. Appropriate amounts of vector and insert were added to the same sterile tube (final volume of mixture was 8 µl). 2 µl of 5x DNA dilution buffer and 10 µl of 2x T4 DNA ligation buffer were added step by step. Finally 1 µl of T4 DNA ligase was added to the mixture and the total content of the tube was mixed carefully with a pipette. The tube was incubated for 1 h at RT.

2.4.1.10 Clone isolation

QIAprep spin miniprep kit was used to isolate prepared clones. The bacterial cells were harvested by centrifugation at >8000 rpm in a conventional table-top microgentrifuge for 3 min at RT. All the steps of clone isolation were performed exactly like described in the QIAprep spin miniprep kit manual.

2.4.1.11 DNA concentrations UV analysis

To determine DNA concentration of prepared construct the NanoDrop, model Spectrophotometer ND-1000 (ThermoScientific), was used. The UV analysis was carried out at 260 nm. First blank measurement was taken by adding 1 µl of H_2O (RNase free). Afterwards 1 µl of desired sample was added and the DNA concentration was measured. Additionally the ratio of absorbance at 260 nm and 280 nm was measured to assess the purity of DNA.

2.4.1.12 Preparation of pMD2 plasmid

The following cloning strategy was used to prepare desired plasmid.

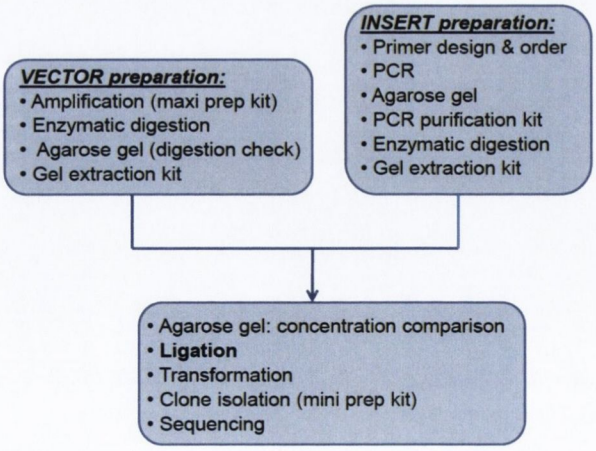

Fig 2.1 *Cloning strategy.*

2.4.1.12.1 Vector preparation

pET-39b vector was used to prepare pMD2 construct composed of:

DsbA–B CHAIN–AAK–A CHAIN–STOP

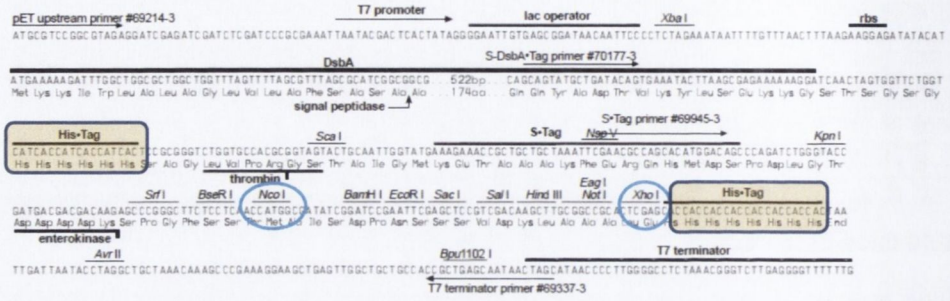

pET-39b(+) cloning/expression regions

The following sequence was cloned into the pET-39b vector:

(NcoI)tttgtgaaccaacacctgtgcggctcacacctggtggaagctctctacctagtgtgcggggaacgaggcttctt ctacacacccaagaccGCGGCGAAAggcattgtggaacaatgctgtaccagcatctgctccctctaccagctg gagaactactgcaactag(XhoI)

B chain AAK linker A chain STOP codon

Restriction enzymes selected:*

N-terminus: *Nco*I

5′...C▼CATGG...3′
3′...GGTAC▲C...5′

C-terminus: *Xho*I

5′...C▼TCGAG...3′
3′...GAGCT▲C...5′

* The enzymes are confirmed not to have any cleavage sites in the insulin precursor gene.

To amplify the vector pET-39b bacterial culture was prepared (transformation, inoculation, bacterial culture and plasmid amplification, Sections: 2.4.1.2 – 2.4.1.4). Kanamycin antibiotic was used during all the steps of pMD2 plasmid preparation. Then vector pET-39b was digested with selected enzymes (*Nco*I and *Xho*I, Section 2.4.1.5). To check digestion of the vector agarose gel electrophoresis was performed (Section 2.4.1.6). DNA of digested vector was extracted from agarose gel (Section 2.4.1.7) and stored at -20°C.

2.4.1.12.2 Insert preparation

Primer design and order is the first step of insert preparation. The sequence of a forward primer pMD1 was as follows:

*Nco*I Insulin...

5'-CGACCATGGTTTGTGAACCAACACCTGTGCGG-3'

The sequence of a reverse primer pMD1 was as follows:

*Xho*I S Insulin...

5'-CCGCTCGAGCTAGTTGCAGTAGTTCT-3'

PCR reaction was carried out with pHB3 (102 ng/µl) template (diluted 1:20) and previously described primers (Section 2.4.1.8). Product of PCR reaction was analysed with agarose gel electrophoresis (Section 2.4.1.6). Purification of the PCR reaction product was carried out by using QIAquick gel extraction kit, Qiagen (Section 2.4.1.7). Purified insert was digested by *Xho*I & *Nco*I restriction enzymes.

2.4.1.12.3 Ligation

To estimate the approximate DNA concentration of the digested vector and prepared insert agarose gel electrophoresis was performed (Section 2.4.1.6).

Rapid DNA Ligation Kit was used to ligate prepared vector pET-39b with prepared insert (Section 2.4.1.9). 7.3 µl of DNA (vector pET-39b) and 0.7 µl of DNA (insert pHB3) were added to the ligation mixture. Ligation mixture was then transformed into XL2 ultracompetent cells. Transformation was performed according to protocol 2.4.1.2, with different volume of NZY^+ broth, which was 500 µl. Additionally, at the beginning ultracompetent cells were split into two tubes and 1 µl and 4 µl of the DNA ligation mix were added to each. Ultimately 0.25 ml of each transformation mixture was placed on two different LB agar plates. To prepare culture for mini-prep a single colony from each freshly streaked selective plate was picked and a starter culture of 5 ml LB broth containing kanamycin were inoculated. The same procedure was repeated to seven other tubes (two colonies from each plate). Prepared tubes were incubated for 12 - 16 h at 37°C with vigorous shaking. Clone isolation was performed according to 2.4.1.10 protocol. To confirm the sequence of prepared clones, eight plasmids were sent for sequencing analysis. Results were compared with reference sequences DNA by using software "clustalx-2.0".

2.4.1.12.4 Mutation

To further improve the obtained pMD2 plasmid:

DsbA–frame corr.-ALP cleav. site-B CHAIN–AAK–A CHAIN–STOP

insertion of GCAAG was required. GC was introduced to correct the reading frame (with the previous G makes GGC => Glycine) and AAG were added to introduce the ALP protease cleavage site (Lysine).

Sequence before mutagenesis was as follow:

gatgacgacgacaagagcccgggcttctcctcaaCCATGGtttgtgaaccaacacctgtgcggctcacacctgg
tggaagctctctacctagtgtgcggggaacgaggcttcttctacacacccaagaccGCGGCGAAAggcattgtg
gaacaatgctgtaccagcatctgctccctctaccagctggagaactactgcaactag

vector seq – NcoI – insulin B chain ...

While, sequence after mutagenesis was:

gatgacgacgacaagagcccgggcttctcctcaaCCATGG**GCAAG**tttgtgaaccaacacctgtgcggctc
acacctggtggaagctctctacctagtgtgcggggaacgaggcttcttctacacacccaagaccGCGGCGAAA
ggcattgtggaacaatgctgtaccagcatctgctccctctaccagctggagaactactgcaactag

The QuikChange site-directed mutagenesis was performed in four steps to insert the required five base pairs:

1: Plasmid preparation (parental DNA plasmid)

Plasmid pMD1 was amplified by using Maxiprep preparation (2.4.1.4). The culture of the plasmid was prepared according to the protocols which are described in points 2.4.1.2 – 2.4.1.4, but instead of vector pET-39b, 1 µl of plasmid pMD1 (31.0 ng/µl) diluted 1:10 was used during the transformation step.

2: PCR reaction (mutagenic primers)

To insert desired mutation two synthetic oligonucleotide primers were designed. The sequence of the forward primer pMD2 was as follow:

NcoI Insulin...

5'-CTTCTCCTCAACCATGG**GCAAG**TTTGTGAACCAACACC-3'

The sequence of a reverse primer pMD2 was as follow:

Insulin *NcoI*

5'-GGTGTTGGTTCACAAA**CTTGC**CCATGGTTGAGGAGAAG-3'

DNA template was pMD1 plasmid and primers discussed above were used. There were some differences in the cycling parameters, which are summarised below.

Table 2.3 *Cycling parameters of PCR reaction.*

Segment	Cycles	Temperature	Time
1	1	95°C	30 sec
2	18	95°C (denaturation)	30 sec
		55°C (annealing)	1 min
		68°C (extension synthesis)	7 min (1 min/kb of plasmid length)
3		4°C	∞

PCR reaction allowed the oligonucleotide primers to generate a mutated plasmid containing staggered nicks.

3: Digestion

Product of the PCR reaction was digested by *Dpn*I endonuclease, enzyme which is specific for methylated and hemimethylated DNA. 1 µl of *Dpn*I restriction enzyme (10 U/µl) was added directly to 45 µl volume of PCR reaction mixture. The reaction mixture was mixed gently and thoroughly by pipetting the solution up and down

several times. The tube was incubated at 37°C for 1 h to digest the parental (nonmutated) ds-DNA.

4: Transformation

Prepared plasmid was transformed into ultracompetent cells, purified and sequenced (Eurofins MWG Operon). Results were compared with reference sequences DNA by using software "clustalx-2.0". DNA concentration of amplified pMD2 plasmid was determined by UV-Vis analysis (Section 2.4.1.11).

2.4.1.13 Preparation of pMD3 plasmid

2.4.1.13.1 Vector preparation

pET-19b vector was used to prepare pMD3 construct composed of:

Histag–EK site–B CHAIN–AAK–A CHAIN–STOP

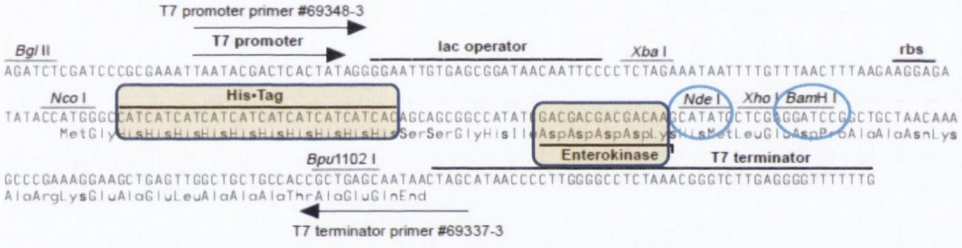

pET-19b cloning/expression region

The following sequence was cloned into the pET-19b plasmid:

tttgtgaaccaacacctgtgcggctcacacctggtggaagctctctacctagtgtgcggggaacgaggcttcttctaca
cacccaagaccgcggcgaaaggcattgtggaacaatgctgtaccagcatctgctccctctaccagctggagaacta
ctgcaactag

B chain AAK linker A chain STOP codon

Restriction enzymes selected:*

N-terminus: *Nde*I	C-terminus: *BamH*I
5′...CA▼TATG...3′	5′...G▼GATCC...3′
3′...GTAT▲AC...5′	3′...CCTAG▲G...5′

* The enzymes are confirmed not to have any cleavage sites in the inserted DNA.

Preparation of the new plasmid pMD3 covered the same steps as described previously for plasmid pMD2. The pET19b vector was digested by selected enzymes, i.e. *Nde*I and *BamH*I. Agarose gel electrophoresis was performed to check digestion process and isolation of digested DNA (Section 2.4.1.6). Extracted DNA was stored at -20°C.

2.4.1.13.2 Insert preparation

Primer design and order is first step in insert preparation. The sequence of the forward primer pMD3(1) was as follow:

*Nde*I Insulin...

5'-AAGCATATGTTTGTGAACCAACACCTGTGCGG-3'

The sequence of a reverse primer pMD3(1) was as follow:

*BamH*I Insulin...

5'-CGGGGATCCCTAGTTGCAGTAGTTCTCCAGCT-3'

The next step in the insert preparation was PCR (Section 2.4.1.8). Template pMD2 (106.7 ng/µl) was diluted 1:20 at 5.3 ng/µl final concentration. Cycling parameters were the same as summarised in 2.4.1.8 protocol. Product of PCR reaction was analysed with agarose gel electrophoresis. Purification of the PCR reaction product was carried with QIAquick gel extraction kit, Qiagen (Section 2.4.1.7). Purified insert was digested by *Nde*I & *BamH*I restriction enzymes.

2.4.1.13.3 Insert preparation

To estimate the approximate DNA concentration of digested vector and prepared insert agarose gel electrophoresis was performed (Section 2.4.1.6). Rapid DNA Ligation Kit was used to ligate pET-19b vector with pMD2 insert. 3 µl of vector pET-19b DNA and 5 µl of insert pMD2 DNA were added to a sterile tube. Subsequent steps of preparation were the same as in Section 2.4.1.9. After the ligation, transformation and clone isolation, the sequencing of prepared samples was performed. After comparison of the sequence pMD3(1) plasmid was amplified (Maxi prep kit, Section 2.4.1.4).

Finally six bases (CATATG) encoding two extra residues (His-Met) were deleted to ensure a "clean" sequence at the N-terminus of insulin. Sequence in the N-terminal part of the cloning area after mutagenesis is as follow:

EK insulin
...AAGTTTGTG...
LysPhe...



QuikChange site-directed mutagenesis kit was used to delete 6 bases. Procedure was the same as for pMD1 plasmid mutagenesis, although there were a few differences. To insert desired mutation two synthetic oligonucleotide primers were designed. The sequence of the forward primer pMD3(2) was as follows:

5'- gacgacgacgacaagtttgtgaacacctgt-3'

The sequence of the reverse primer pMD3(2) was as follows:

5'-acaggtgttcacaaacttgtcgtcgcgtcc -3'

The next step of the vector mutagenesis was a thermal cycling, PCR reaction with DNA template pMD3(1). Cycling parameters were the same as for pMD1 plasmid mutagenesis, but the number of cycles was decreased to 16. PCR reaction product was analysed with agarose gel electrophoresis.

Product of the PCR reaction was digested by *Dpn*I endonuclease. Digested vector pMD3(2) was transformed into ultracompetent cells and purified. After conformation of the sequence (Eurofins MWG Operon, software "clustalx-2.0"), pMD3(2) plasmid was amplified (Maxi prep kit, Section 2.4.1.4) and the DNA concentration of prepared plasmid was determined by UV analysis (Section 2.4.1.11).

2.4.1.14 Glycine SDS-PAGE protein electrophoresis

2.4.1.14.1 Gel preparation

15% resolving (separating) gel composed of 15% w/v acrylamide, 0.17 M Tris buffer, pH 6.8, 0.1% w/v SDS, 0.1% w/v APS and 0.0004% v/v TEMED.

Stacking gel composed of 5% w/v acrylamide, 0.19 M Tris buffer pH 8.8, 0.1% w/v SDS, 0/1% w/v APS and 0.1% w/v TEMED.

2.4.1.14.2 Sample loading

Prior to the gel loading prepared electrophoresis samples were heated at 95°C for 10 min to denature the proteins. 5 µl of marker (SeeBlue Plus PreStained Standard, Figure 2.2, used in order to determine molecular weight of the proteins) and 10 µl (unless otherwise indicated) of the appropriate samples were loaded into the pockets of the gel.

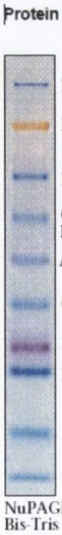

Protein	Approximate Molecular Weights (kDa)				
	Tris-Glycine	Tricine	NuPAGE® MES	NuPAGE® MOPS	NuPAGE® Tris-Acetate
Myosin	250	210	188	191	210
Phosphorylase	148	105	98	97	111
BSA	98	78	62	64	71
Glutamic Dehydrogenase	64	55	49	51	55
Alcohol Dehydrogenase	50	45	38	39	41
Carbonic Anhydrase	36	34	28	28	n/a
Myoglobin Red	22	17	17	19	n/a
Lysozyme	16	16	14	14	n/a
Aprotinin	6	7	6	n/a	n/a
Insulin, B Chain	4	4	3	n/a	n/a

NuPAGE® Novex Bis-Tris 4-12% Gel

Fig 2.2 *SeeBlue® Plus PreStained Standard, Invitrogen.*

The electrophoresis chamber was closed and the electrodes were connected. The electrophoresis run was performed at 150 V until the blue dye was washed out from the gel (1.5 h – 2 h).

2.4.1.14.3 Staining with Coomassie

After completion of the run, stacking gel was removed and resolving gel was placed in a container filled with staining solution Coomassie Brilliant Blue G for 30 min. After staining Coomassie dye solution was recovered. The gel was destained 3x 10 min and finally 2x 30 min in destaining solution. The image of the destained gel was captured by digital camera using EPI light source.

2.4.1.15 Western blot

- Transfer

Semi Dry Blotting apparatus AE 6675 - Horizblot was used to transfer proteins from the gel the carrier membrane. After electrophoresis completion the gel was placed in a container filled with TTB. In another TTB-filled container Blot paper (Extra Thick Blot paper Mini blot size, Biorad) was placed. Immun-Blot PVDF membrane (Biorad) was cut, activated in methanol for 30 s and transferred to TTB for 5 min. Prepared parts of the transfer were placed in Transblot SD device in the following order: a sheet of a blot paper was placed on a metal surface and covered with membrane. Gel was placed on the membrane and covered with another sheet of paper. The apparatus was closed and connected to 120 mA for 60 min.

- Blocking

Membrane was transferred to container filled with a blocking buffer. The membrane was agitated overnight at Mini Gyro rocker at 4°C.

- Reaction with antibodies

Blocking buffer was replaced with 10-15 ml of washing buffer. The membrane was washed for 5 min with 40 rpm at RT. Then washing buffer was replaced with the solution of primary antibodies in blocking buffer. The membrane was agitated in a solution of primary antibodies for 2 h at RT with 20 rpm. After that the solution of primary antibodies was collected and the membrane was washed 3 times (15 min each washing) in 10-15 ml of washing buffer at 40 rpm. After a third washing, buffer was replaced by the solution of secondary antibodies in blocking buffer. The membrane was agitated at RT for 1 h with 20 rpm. After that the solution of antibodies was removed and the membrane was washed 3 times with washing buffer at 40 rpm.

- Visualisation

Visualisation solution was prepared by mixing one volume of Visualiser^{TM} Detection Kit Reagent A with two volumes of Visualiser^{TM} Detection Kit Reagent B. Membrane

was placed on the plastic tray and covered with 3 ml of visualisation solution. The incubation time was 5 min. Finally, the membrane was placed in a plastic folder, air bubbles were removed and the photograph was developed with digital camera using Chemi Hi sensitivity light.

2.4.1.16 Preparation of samples for expression test

2.4.1.16.1 Expression induced by IPTG

Transformation of the plasmid was performed according to protocol 2.4.1.2 with the following modifications. *E. coli* BL21 (DE3) was used as a host strain. 1 µl of diluted 1:10 plasmid was incubated with cells. Mixture of colonies from a freshly streaked selective plate containing 200 µl transformation mixture of the plasmid was picked and a starter culture of 40 ml LB broth containing appropriate antibiotic was inoculated. Prepared mixture was incubated overnight at 37°C with vigorous shaking (approx. 300 rpm). 3 ml (1:100) of bacterial suspension from preculture flask were transferred into the flask with 300 ml of LB broth with appropriate antibiotic (1:1000). Flasks were incubated at 37°C with vigorous shaking (approx. 300 rpm). After 2 h of incubation 1 ml of bacterial suspension was taken from each flask and OD was measured by using a disposable cuvette at UV-Vis spectophometer at 600 nm. LB broth solution was used as a blank sample. OD_{600} measurements were performed to monitor the cell density and the growth of the culture. They were repeated every 30 min until value of absorbance reached ~ 0.7. IPTG (1 mM), was added to each flask and the incubation was continued. The samples from OD_{600} measurements were transferred to Eppendorf tubes and were centrifuged for 10 min at RT. Supernatant was removed by pipetting until all medium was drained and the pellet was re-suspended by adding 50 µl of SDS-PAGE Loading buffer. The tube was heated at 95°C for 10 min and stored at -20°C. The same procedure was repeated every 1 h after adding IPTG to the bacterial culture for the next 4 h. The last sample was taken after overnight incubation. In this case volume of the loading buffer was 100 µl. Prepared for SDS-PAGE electrophoresis samples were stored in -20°C. Harvested by centrifugation bacterial cells were stored at -20°C, until used for further assays (periplasmic localisation 2.4.1.17 and solubility test 2.4.1.18).

2.4.1.16.2 Expression in the auto-induction system

Transformation step was the same as mentioned for IPTG induced expression. Two colonies from each freshly streaked selective plate were picked and starter cultures of 2 ml MDG containing antibiotic (1:1000) were inoculated. Prepared mixtures were incubated overnight at 37°C with shaking. 50 µl of bacterial suspension from preculture flasks (MDG) was transferred to 50 ml of fresh media: ZYM-5052 or ZYP-

5052 containing appropriate antibiotic (1:1000). Prepared flasks were incubated at 37°C with vigorous shaking (300 rpm). After 1 h, 1 ml of bacterial suspension from each flask was taken and the optical density was measured, using a disposable cuvette at UV-Vis spectrophotometer at 600 nm. Medium was used as blank solution. Optical density measurements were repeated after 3, 4, 5, 6, 24 hours. When OD_{600} value reached ~0.4 the temperature was adjusted as appropriate (16°C - 37°C).

2.4.1.17 Preparation of samples for periplasmic localisation test

The bacterial cells (from 2.4.1.15 above) were harvested by centrifugation at 4000 x g for 20 min. The cell pellet was re-suspended thoroughly in 30 ml of 30 mM Tris-HCl, 20% sucrose, pH 8.0, washing buffer. Then 0.5 M EDTA, pH 8.0 (final concentration of 1 mM) was added. A stirring bar was added and the solution was stirred slowly on ice for 10 min. After that the cells were collected by centrifugation at 4°C for 10 min at 10000 x g. Supernatant was removed and discarded. The pellet was thoroughly resuspended in 30 ml of ice-cold 5 mM $MgSO_4$ and the cell suspension was stirred slowly for 10 min on ice. During this step the periplasmic proteins were released into the buffer. Prepared suspension was centrifuged at 4°C for 10 min at 10000 x g. After centrifugation (periplasmic fraction) supernatant was concentrated by using Stirred Ultrafiltration Cells (Millipore, Model 8010, 8050) and 3000 Da ultrafiltration membranes (Millipore). 50 µl of periplasmic fraction were mixed with 50 µl SDS-PAGE Loading buffer and the mixture was heated at 95°C for 5 min. Prepared SDS-PAGE samples were stored at -20°C. Periplasmic fraction samples were stored at 4°C.

2.4.1.18 Preparation of samples for solubility test

The pellet obtained from the preparation of the periplasmic fraction was used to prepare the soluble (cytoplasmic fraction) and insoluble (inclusion body) fraction. To extract the proteins present in the pellet sonication method was used. The pellet was resuspended in 5 ml PBS and sonicated 2 x 2 min (50% of maximum power) with ultrasound needle (Microson Ultrasonic cell). During this step the suspension was kept on ice. The suspension was centrifuged for 1 h at 4°C. Supernatant (soluble fraction) was separated from pellet (insoluble fraction). To prepare samples for electrophoresis 50 µl of the supernatant (soluble fraction) were mixed with 50 µl SDS-PAGE Loading buffer and the sample was heated at 95°C for 20 min. The pellet was resuspended in 5 ml Urea buffer. 50 µl of the resuspended solution (insoluble fraction) were mixed with 50 µl SDS-PAGE Loading buffer and the tube was heated at 95°C for 5 min. Prepared samples were tested by SDS-Polyacrylamide Gel Electrophoresis and Western blot technique and stored at -20°C.

2.4.1.19 Purification of proteins with His tag column

HisTrap™ HP (5 ml, GE Healthcare) column, prepacked with precharged Ni Sepharose™ High Performance, was washed with 3 column volumes (one column volume – CV is 5 ml) of elution buffer. Recommended fast-flow was used: 5 ml/min (corresponds to approx. 120 drops/min). After washing the column, it was equilibrated with starting (binding) buffer. The pre-treated sample (concentrated periplasmic fraction obtained from 2.1.17, 5 ml) was applied to the column by using a 5 ml syringe. The column was washed with 3 CV of starting buffer (flow-through fractions) and then with 3 CV of elution buffer (flow-rate fractions), 2 ml fractions were collected. The amount of the protein obtained in each fraction was analysed by BioRad Protein Assay. Selected fractions were finally analysed by SDS-PAGE electrophoresis and Western blot.

2.4.1.20 Bio-Rad Protein Assay

The Bio-Rad Protein Assay is a simple and accurate procedure for determining concentration of the protein, which is based on the Bradford method. The Bio-Rad protein assay is a dye-binding assay (involves the addition of acidic dye to the protein solution) in which differential colour change of the dye occurs in response to various concentrations of protein present.

Working solution of BioRad Protein assay was prepared by dilution of stock solution 1:5. Calibration curve for BioRad Protein Assay was performed by using BSA at the following concentrations: 2.0, 1.0, 0.5, 0.25, 0.125, 0.0625 mg/ml. 625 µl of BioRad working solution was mixed with 400 µl of PBS and 10 µl of protein. Composition of blank sample was the same, but instead of protein sample 10 µl of PBS was added. Absorbance of prepared samples was measured at 595 nm by Spectrophotometer UV-1700 (Shimadzu). Example of calibration curve that was applied for protein quantification is shown in Figure 2.3.

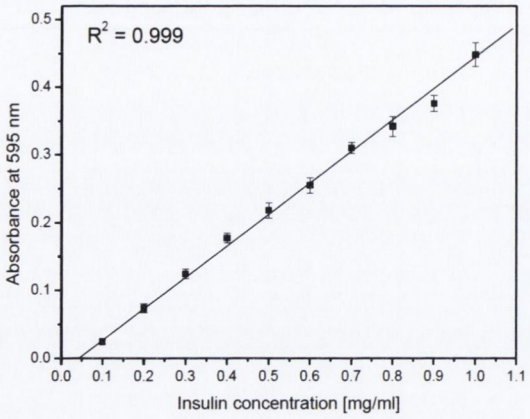

Fig 2.3 *Calibration curve prepared with lyophilised insulin.*

2.4.1.21 Dialysis

Dialysis is a separation technique that facilitates the removal of small, unwanted compounds from macromolecules by allowing diffusion of only the small molecules through selectively permeable membranes. The dialysed solution is placed in a sealed dialysis membrane and immersed in an appropriate buffer. Small molecules such as buffer salts pass freely through the membrane, reducing the concentration of those molecules in the sample; however the movement of the solvent is in the opposite direction, what can result in sample dilution. Changing the dialysis buffer removes the small molecules that are no longer in the sample and allows more contaminants to diffuse into the dialysate. To remove the imidazole from the sample (elution fractions) dialysis was carried out against TBS buffer. The sample was transferred to dialysis membrane (Spectra/Por Dialysis membrane 3000 Da) and stirred in a beaker filled with 2 L of dialysis buffer TBS for 2 h at 4°C. The buffer was changed once and the sample was dialysed overnight at 4°C.

2.4.1.22 Digestion by ALP protease

Achromopeptidase is a lysyl endopeptidase with a MW of ~27 kDa. It is useful for lysis of Gram-positive bacteria that are resistant to lysozyme. ALP cleaves peptide bonds at the carboxy-terminal of lysine residues with a high degree of specificity, making it a valuable tool for analysis of peptide and protein primary structure and for enzymatic synthesis of Lys-X compounds.

To check activity of ALP protease (dissolved in TBS buffer) different concentrations (0 – 1 unit) and incubation times (2.5 min – 240 min) were tested. Before digestion by ALP protease, protein concentration was measured by using Bio-Rad Protein Assay. ALP protease (appropriately diluted) was added to the sample containing

periplasmic fraction of pMD2 plasmid purified by His tag column. 150 µl of the sample were taken and 250 µl of the inhibitor cocktail solution (1 tablet dissolved in 1.5 ml of water) were added to inhibit the activity of the enzyme. Prepared mixture was incubated for 10 min at RT and samples were withdrawn after 2.5 min, 5 min and 10 min for electrophoresis (50 µl + 50 µl SDS-PAGE Loading buffer). The sample was heated at 95°C for 10 min. Digestion process was determined by SDS-PAGE protein electrophoresis and Western blot technique.

2.4.1.23 Optimisation of refolding reaction

Sample of misfolded protein (obtained after testig the purification of proinsulin from pHB1 plasmid) was used to optimise the refolding reaction. Four different refolding reagents were tested using the same protocol. After protein quantification with BioRad Protein Assay and division into equal aliquots the following steps were carried out:

2.4.1.23.1 Denaturation of proinsulin

Samples with misfolded proinsulin were diluted 10x with water and precipitated by lowering pH to 5.0 with 1 M HCl. Pellets obtained after centrifugation (at 6000 rpm) were diluted in denaturing buffer (20 mM Tris-HCl, 1 mM EDTA, 8.0 M Urea, pH 9.5) to final protein concentration of 5 mg/ml. The mixture was incubated with gentle stirring for 2 h at RT.

2.4.1.23.2 Oxidative sulfitolysis reaction

Sodium sulphite (Na_2SO_3) and sodium tetrathionate ($Na_2S_2O_3$) were added to final concentrations of 0.2 M and 20 mM, respectively, to start sulphitolysis reaction. The mixtures were gently agitated for 12 h at 4°C. The reaction was stopped by diluting 10-fold with water and adjusting pH to 4.5 using 1 M HCl. Samples were centrifuged at 6000 rpm for 30 min to obtain the protein pellet.

2.4.1.23.3 Refolding reaction

300 ml of refolding buffer (1 M Urea, 50 mM glycine, pH 10.6) was prepared for each sample and then tested. Pelleted proteins were solubilised in deionised water with pH adjusted to 10.6 to ensure its solubility. Prepared samples were injected in droplets to the refolding buffer to a final concentration of 0.1 mg/ml. The reaction was performed for 16 h at 4°C. The samples were then acidified to pH 2.9 to precipitate misfolded protein. Supernatant containing properly folded proinsulin was saved for further assays. Pelleted misfolded proteins (centrifugation at 6000 rpm for 30 min) were resuspended in deionised water with pH adjusted to 10.6 and quantified with BioRad Protein Assay. At each stage of process samples for quantification and SDS-PAGE electrophoresis and Western blot were collected.

2.4.1.24 Purification of pHB1 inclusion bodies – optimised protocol

The optimised protocol for inclusion bodies purification expressed by pHB1 plasmid was established with the following steps.

2.4.1.24.1 Cells harvesting, disruption and washing

Culture of pHB1 plasmid was performed at 30°C. After overnight incubation cells were harvested by low-speed centrifugation. First, periplasmic fraction was prepared (Section 2.4.1.17). Remained pellet of inclusion bodies was resuspended in 30 ml of washing buffer (50 mM Tris-HCl, pH 7.5, 10 mM EDTA, and 0.02% lysozyme). The pellet was lysed by sonication (3 x 2 min) and centrifuged at 6000 rpm for 30 min. Pelleted inclusion bodies were resuspended in buffer (20 mM Tris-HCl, pH 7.5, 1% Triton X, 2 M Urea) and centrifuged at 6000 rpm for 30 min. Inclusion bodies pellet was then washed another three times by re-suspension in PBS and subsequent centrifuged.

2.4.1.24.2 Solubilisation and oxidative sulfitolysis

Washed proteins were solubilised in buffer (20 mM Tris-HCl, 1 mM EDTA, 8.0 M Urea) at protein concentration of 10 – 15 mg/ml. To enhance solubility of the protein pH of the solution was adjusted to 11 and then readjusted to 9.5. To start sulphitolysis reaction 200 mM sodium sulphite and 20 mM sodium tetrathionate (final concentration) were added and prepared mixture was incubated with gentle stirring for 12 h at 4°C. The reaction was stopped by diluting 10x with water. To precipitate sulphonated forms of proinsulin pH of solution was adjusted to 4.5.

2.4.1.24.3 CNBr cleavage

Precipitates were dissolved in 8 M Urea, 0.3 M HCl buffer at concentration 10 mg/ml and cleaved by adding 400 M excess of CNBr and incubating for 16 h at RT in the dark. Proteins were precipitated by dilution 10x with water and adjustment of pH to 4.5.

2.4.1.24.4 Cation exchange purification

The precipitates of CNBr-cleaved product were solubilised in 7 M Urea, 20 mM formic acid, pH 4 buffer and loaded onto the Sepharose cation exchange column (Pierce Strong Cation Exchange Spin Columns, Maxi) equilibrated with the same buffer. The elution of the column was performed at rate of 3 ml/min using a linear gradient of 0, 0.1, 0.2, 0.3, 0.4 and 0.5 M NaCl in 7 M Urea (pH 4.0). Flow through and flow rate (eluate) fractions were analysed by BioRad Protein Assay, SDS-PAGE electrophoresis and Western blot.

2.4.1.24.5 Dialysis and refolding reaction

Purified fractions of proinsulin were mixed and dialysed against refolding buffer: 1 M Urea, 50 mM glycine, pH 10.6. Refolding reaction was carried out with 1 mM GSH/ 5 mM GSSG as a refolding agent. After 16 h incubation at 4°C the reaction was stopped by acidifying the solution to final pH of 2.9±0.1 with 2 M HCl.

2.4.1.24.6 Proteolytic cleavage of proinsulin

Concentrated sample of properly folded proinsulin was specifically cleaved with trypsin (1000:1 proinsulin: trypsin ratio, by mass) and carboxypeptidase B (2000:1 proinsulin to a carboxypeptidase B ratio, by mass). The mixture was incubated for 30 min at 37°C. To stop the reaction inhibition cocktail mix was added and pH was adjusted to 3 with TFA.

2.4.2 Methods – nanoparticle (NP) preparation and characterisation

2.4.2.1 Preparation and characterisation of protamine sulphate and polymer solutions

2.4.2.1.1 Alginic acid (as sodium alginate) solutions

100 ml of 0.2%, 0.1% and 0.05% w/v solutions of alginic acid (as sodium salts) high viscosity (AAL), medium viscosity (AAM) and low viscosity (AAL) were prepared with DI H_2O. Polymers as powders were dissolved at 25°C and stirred for 30 min on a magnetic stirrer until clear solutions were obtained. Prepared polymer solutions were further characterised by pH and viscosity measurements.

2.4.2.1.2 Carrageenan solutions

100 ml of 0.2%, 0.1% and 0.05% w/v solutions of ι-carrageenan (IC), κ-carrageenan (KC) and λ-carrageenan (LC) were prepared with DI H_2O. LC was dissolved at 25°C and stirred for 30 min on a magnetic stirrer until a clear solution was obtained. For KC and IC, the polymers were first dissolved with vigorous stirring in H_2O at 80°C. When clear solutions were obtained, the polymer solutions were removed from the heat and stirred until the temperature returned to 25°C. The volume of KC and IC solutions was made up to 100 ml to account for any evaporation, which occurred during the heating. Prepared polymer solutions were further characterised by pH and viscosity measurements.

2.4.2.1.3 Protamine (as protamine sulphate) solutions

100 ml of 0.2%, 0.1% and 0.05% w/v solutions of protamine sulphate (P) were prepared and characterised by pH and viscosity measurements. Protamine was dissolved in DI H_2O at 25°C and vigorously stirred on a magnetic stirrer for 30 min. Protamine solutions at pH=2 (P_pH2) and pH=3 (P_pH3) were also prepared to

ensure insulin solubility. In these experiments, protamine sulphate was dissolved in 90 ml of DI H_2O. The required pH was adjusted by adding a required volume of 1 M HCl and the final volume of the protamine solution was brought to 100 ml.

2.4.2.2 Synthesis of empty nanoparticles (NPs)

2.4.2.2.1 Synthesis and characterisation NPs composed of alginic acid and protamine

0.1% w/v solution of alginic acid low viscosity (AAL), 0.1% w/v solution of alginic acid medium viscosity (AAM) and 0.1% w/v solution of protamine (P) were prepared according to the methods described above. Alginic acid (AAL or AAM)/P solutions were combined together at various ratios v/v at RT and mixed under magnetic stirring for around 10 min to allow stabilisation of the system. The resultant nanoparticle dispersions were then evaluated. Size, polydispersity and zeta potential of NPs with different polymer/protamine weight ratios were measured. Additionally, the prepared nanodispersions were analysed by measuring their pH and viscosity.

2.4.2.2.2 Synthesis and characterisation NPs composed of carrageenan and protamine

0.1% and 0.05% w/v solutions of ι-carrageenan (IC), κ-carrageenan (KC), λ-carrageenan (LC) and protamine (P) were prepared according to the method described above. Polymer/protamine solutions were combined together in various v/v ratios at RT and mixed under magnetic stirring for around 10 min to allow stabilisation of the system. The resultant nanoparticle dispersions were then assessed. Size, polydispersity and zeta potential of NPs with different protamine/polymer weight ratio were measured. Additionally, the prepared nanodispersions were analysed by measuring their pH and viscosity.

2.4.2.3 Methods of NPs formation

- Various sequence of mixing both components

Method 1A. An aliquot of protamine solution was added to the aliquot of polymer solution under magnetic stirring. Stirring was continued for 10 min at RT.

Method 1B. An aliquot of polymer was introduced to the aliquot of protamine under magnetic stirring for 10 minutes at RT.

- Various speed of addition of one component to the other

Method 2A. An aliquot of protamine was slowly (drop by drop, within 15 s) added to the aliquot of polymer.

Method 2B. An aliquot of protamine was fast (within 2 sec) added to the aliquot of polymer.

2.4.2.4 Synthesis of insulin loaded NPs

Insulin was first dissolved in 0.1% w/v P solution at pH 3 (P_pH3), to give the final insulin concentration in NP dispersion of 100 μg/ml or 500 μg/ml. An aliquot of the insulin/protamine solution was then rapidly added to the appropriate volume of the polymer solution (method 2B, Section 2.4.2.3) and the system was stirred for 10 min at RT. Size, polydispersity and zeta potential of NPs with different polymer/protamine weight ratios were subsequently measured. Additionally, the prepared nanodispersions were analysed by measuring their pH and viscosity.

2.4.2.5 Size, polydispersity and zeta potential analyses

The mean particle size (particle size diameter [nm]) and polydispersity index (PdI) of both: empty and insulin-loaded polyelectrolyte complexes were determined by Dynamic Light Scattering (DLS) with the use of 173° backscatter detection. The electrophoretic mobility values measured by Laser Doppler Velocimetry (LDV) were converted to zeta potential (ZP) using the Smoluchowski equation. Both measurements (DLS and LDV) were performed on a Zetasizer Nano ZS series Nano-ZS ZEN3600 fitted with a 633 nm laser (Malvern Instruments Ltd., UK). Samples without any dilutions were placed directly into a clear plastic zeta cell (DTS 1061) and equilibrated for 2 min at 25°C prior to the measurement. The readings for each sample were performed at least 3 times and at least 3 batches of each sample were prepared and analysed. The results are given as an average of size ± std dev, polydispersity (PdI) ± std dev and zeta potential (ZP) ± std dev.

2.4.2.6 pH measurements

Thermo Electron Orion 420A$^+$ Basic pH/mV/ORP 25°C, Thermo Electron Corporation pH meter equipped with an Orion Rose^{TM} 8103SC glass body pH semi-micro electrode was used to perform pH analyses. pH measurement of each sample was conducted in triplicate at 25°C. The pH meter was calibrated with standard buffer solutions at pH 4, 7 and 10 before each batch of sample measurements. The results are given as an average value of three measurements ± strd dev.

2.4.2.7 Viscosity measurements

Low frequency vibration viscometer (SV-10 Vibro Viscometer, A&D Company Limited, Japan) was employed to measure the viscosity of polymer solutions and nanoparticles suspensions. Before use the viscometer was calibrated with DI H_2O. Viscosity measurement of each sample was carried out in triplicate at 25±0.2°C. Water bath (Reciprocal Shaking Bath Model 25, Precision Scientific, UK) was used

to equilibrate the samples prior to the measurement. The results are given as an average ± std dev.

2.4.2.8 Influence of different cations on the formation of empty carrageenan-based NPs

To check the impact of divalent cations on IC/P NPs formation, $CaCl_2$ (final concentration of 0.05 M and 0.1 M) and $ZnCl_2$ (final concentration of 0.01 M) were dissolved in 0.1% w/v solution of P. The pH of the solution was then adjusted to 3 using 1 M HCl. Polymer and protamine with an additional cation solutions were combined together in various v/v ratios at RT and mixed under magnetic stirring for around 10 min to allow stabilisation of the system. Size, PdI and ZP of NPs were subsequently measured. Obtained NPs were compared with NPs prepared using P solution with no divalent cations present.

2.4.2.9 Physical stability of empty NPs

Each NP formulation was visually inspected immediately after preparation, prior to carrying out any measurements. The presence/absence of aggregation was recorded. Stability of prepared NPs was determined by measuring changes in the mean particle size, PdI and ZP over time. Measurements and visual observations were performed directly after sample preparation (day 0) and were continued every day for further 3 days.

2.4.2.10 Physical stability of NPs in different liquid media

The physical stability of empty NPs was determined in the following liquid media: 0.01 M HCl, 0.1 M HCl, 0.1 M acetate buffer pH 4.5, 0.1 M HEPES pH 6.5, 0.1 M PBS, 0.01 M PBS, 0.1 M NaOH, 0.01 M NaOH as well as Minimum Essential Medium (MEM). An aqueous suspension of NPs prepared as described in Section 2.4.2.3 (method 1A) was diluted with a suitable liquid medium in the ratio of 1:1 v/v. Stability of the prepared NPs was determined by measuring changes in mean particle size, PdI and ZP over time. Measurements and visual observations were performed directly after sample preparation (day 0) and were continued for another 3 days.

2.4.2.11 Separation of non-associated insulin

The association efficiency of insulin in NPs was calculated by the difference between the total amount of insulin used to prepare the complexes and the remaining amount of free insulin remaining in the aqueous medium (Equation 2.1).

$$AE = \left[\frac{A-B}{A}\right] * 100\% \qquad \text{(Equation 2.1)}$$

Where: A - the total amount (mass) of insulin

B - the mass of non-associated insulin

Drug loading (DL) was calculated according to the following equation:

$$AE = \left[\frac{A-B}{C}\right] * 100\% \qquad \text{(Equation 2.2)}$$

Where: C - the total weight of all the components of NPs

The amount of free insulin was determined in the supernatant by Reverse Phase High Performance Liquid Chromatography (RP-HPLC) (Section 2.4.2.12) following separation of NPs from the aqueous medium by a combined ultrafiltration–centrifugation technique (Amicon Ultra-15, MWCO of 50 kDa, Millipore USA). Briefly, 5 ml sample was placed in the sample reservoir of a centrifugal filter device and centrifuged (5810R centrifuge, Eppendorf, UK) for 60 min at 3000 rpm. The filtrate was collected, its volume measured and the amount of insulin quantified by RP-HPLC. This quantity of the peptide is referred as non-associated insulin. Insulin NPs were characterised by Zetasizer Nano ZS before and after its reconstitution with DI H_2O.

2.4.2.12 Release studies

In vitro release of insulin from NPs was determined at 37 °C in 0.01 M HCl, 0.1 M acetate buffer pH 4.5, 0.01 M PBS and Fasted State Simulated Intestinal Fluid (FaSSIF, prepared according to the manufacturer's protocol) under shaking (60 cpm, Reciprocal Shaking Bath Model 25, Precision Scientific). Methylcellulose at concentration of 0.001% w/v was added to the release media to prevent adsorption to the plastic vessel (Jelvehgari et al., 2010, Hwang et al., 2000). 1 ml of insulin loaded NP dispersions (prepared as described in Section 2.4.2.4) was added to 19 ml of the appropriate release medium at 37°C. Additionally, a control containing the equivalent amount of insulin as that in the NPs and in the same medium as that used for NP release studies was established. At pre-determined time points (10, 20, 30, 60, 120, 180, 240 and 360 min) 1 ml of the release mixture was withdrawn and replaced with 1 ml of plain medium. 1 M HCl was added to the collected release mixtures to acidify the solutions for further RP-HPLC analysis (20 µl to samples collected from 0.01 M PBS, FaSSIF and 60 µl to the samples collected from 0.1 M acetate buffer pH 4.5). The amount of released insulin was determined by RP-HPLC method described in Section 2.4.2.12. All experiments were performed at least in triplicate. Prepared insulin NPs were characterised by its size, polydispersity and zeta potential measured with Zetasizer Nano ZS before and after release studies.

Release studies data was fitted to the first order equation (Equation 2.3, Corrigan et al., 2006) using Origin ver. 7 software.

$$W = W_{\infty}(1 - e^{-kt}) \qquad \text{(Equation 2.3)}$$

Where: W - insulin amount released at time t

W_{∞} - insulin amount released at infinity

k - the release rate constant

2.4.2.13 RP-HPLC method for insulin quantification

The method for quantitative determination of insulin was adapted from Xu et al., (2006). The HPLC system consisted of LC-10 AT VD liquid chromatograph pump system, SIL - 10 AD VP autoinjector, FCV-10 AL VP low pressure gradient flow - control valve, DGU - 14A degasser, SPD-10A VP photodiode array UV-VIS detector and SCL - 10A VP system controller (Shimadzu). Data was collected and processed using Shimadzu CLASS-VP software (version 6.10). Chromatographic separations were carried out on a C18 Phenomenex column (250x4.6 mm, 5 µm). Standard solutions of insulin were prepared in 0.01 M HCl. 50 µl standards (0.5 - 100 µg/ml) or samples were injected and isocratic elution was carried out at a flow rate of 0.8 ml/min, with a mobile phase consisting of 0.2 M sodium sulphate adjusted to pH 2.3 with phosphoric acid and acetonitrile (74:26, v/v). Samples were monitored at a UV absorbance of 214 nm. Data collection and integration were accomplished using Shimadzu CLASS-VP software (version 6.10).

2.4.2.14 Cell culture studies

Caco-2 cells, human colon carcinoma cell line (passage 20) was obtained from European Collection of Cell Cultures. The Caco-2 cells were routinely cultured as a monolayer in 75 cm^2 cell culture flasks in Eagle's Essential Medium (MEM, Sigma-Aldrich), supplemented with 20% fetal bovine serum, 0.006 mg/ml penicillin, 0.01 mg/ml streptomycin, 0.005 mg/ml gentamycin, 2.2 g/L sodium bicarbonate and 0.11 g/L sodium pyruvate, in an atmosphere of 5% CO_2 at 37^{0}C (CO_2 incubator, series 8000DH, Thermo Scientific). pH of culture medium was adjusted to 7.4 by 1M NaOH or 1 M HCl solutions. The culture medium was replaced with fresh medium every second day until the cells reached 70-80% confluence. Confluent cells were passaged by detaching from the culturing flask with EDTA – trypsin (0.25%) solution twice a week. All the studies were performed on the cells with the passage number in the range of 22 - 40.

2.4.2.15 Cytotoxicity MTS assay

Cytotoxicity of prepared nanoformulations was determined by using the CellTiter96 Aqueous One Solution Cell Proliferation Assay Kit (Promega Corp.) which is a colorimetric method for determining the number of viable cells. The soluble tetrazolium salt (3-(4,5-dimethylthiazol-2-yl)-5-(3-carboxymethoxyphenyl)-2-(4-sulfophenyl)-2H-tetrazolium, MTS) is bioreduced by cells into a formazan product. The absorption of a purple formazan product is proportional to the number of living cells in the culture. Caco-2 cells were seeded into flat-bottom 96-well plates in 100 µl of MEM with 20% FBS, at a density of 25,000 cells per well (cells were previously counted with the aid of Z1 Coulter Particle Counter, Beckman Coulter) and incubated at 37°C and 5% CO_2 for 24 h. The medium was then replaced with 100 µl of the sample (solution of empy NPs) dispersed or dissolved in serum-free medium and incubated for 72 h. After incubation, the supernatant was removed from the wells and replaced with serum-free media. 20 µl of the MTS reagent prepared according to the manufacturer protocol was then added into each well; in case of positive control (0% viability) the media was replaced by 10% SDS solution in serum-free media 30 min before the addition of MTS reagent. After 4 hours the UV absorbance of the formazan product was measured spectrophotometrically (FLUOstar Optima microplate reader, BMG Labtech) at 492 nm. Positive control was treated as a blank and its value was subtracted from each reading. The cells viability was calculated by dividing the absorbance value for a particular sample and the absorption value of negative control, which was assumed to have 100% viability.

2.4.2.16 Transport of insulin through Caco-2 monolayer

2.4.2.16.1 Seeding and growing Caco-2 cells on Transwell® plates

Caco-2 cells were cultured as described in Section 2.4.2.13. Experimental for seeding and transport study was adopted from Hubatsch et al., (2007). Caco-2 cells, with passage numbers 25 - 38, were used for cultivation on filter supports and insulin transport experiments. The cells were cultured on polycarbonate membrane filters (pore size 0.4 µm, cell growth area 1.12 cm^2) in Corning Transwell® 12-well plates (Corning Incorporated, Europe) at seeding density of 300,000 cells for each well. The culture medium (Eagle's Essential Medium (MEM), 20% FBS, pH 7.4) was added to both apical (0.5 ml) and basolateral (1.5 ml) compartments and was changed every second day for 21 - 24 days. The cells were maintained at 37°C, in the atmosphere of 95% air and 5% CO_2.

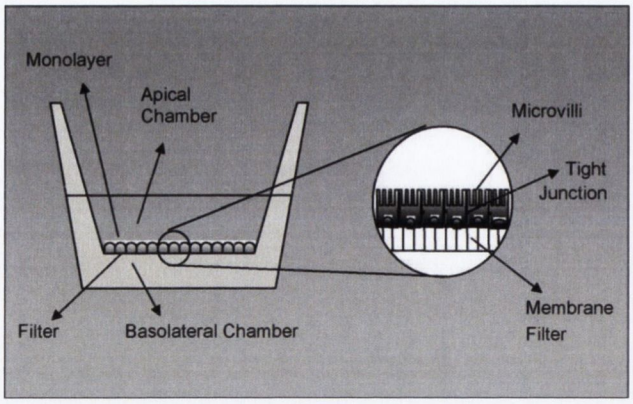

Fig 2.4 *Experimental setup for transport studies using Caco-2 permeability assay (Kavimandana and Peppas, 2008).*

The transepithelial electrical resistance (TEER) was measured using a Milicell ERS meter (Millipore Corp. Bedford, MA, USA) connected to a pair of chopstick electrodes to ensure integrity of the monolayers formed on the filters and tight junction formation. Measurements were taken every other day.

2.4.2.16.2 Sample preparation

500 µg/ml insulin loaded NPs were prepared according to the method described in Section 2.4.2.4. Additionally, insulin standard solutions (500 µg/ml) dissolved in 0.01 M HCl and in 0.1% w/v P solution pH 3 were tested.

2.4.2.16.3 Transport study – procedure

30 minutes before the experiment the culture medium was removed from the apical and basolateral chamber and replaced with pre-warmed HBSS (Hank's Balanced Salt Solution, Sigma) after first washing both chambers with HBSS. TEER measurements were taken before and after replacing medium with HBSS. Equilibrated monolayers were then threated with samples: insulin loaded NPs, insulin standards solution dissolved in 0.01 M HCl and in 0.1% w/v P solution at pH 3. Controls (non-treated wells) were employed. 200 µl of a sample was withdrawn from the basolateral part at predetermined time of 60, 120, 240 and 360 min and replaced with an equal volume of fresh HBSS. pH of samples withdrawn was adjusted with 1 M HCl and samples were analysed for the insulin content using the RP-HPLC method described in Section 2.4.2.12.

2.4.2.16.4 Integrity of Caco-2 monolayers

TEER measurements were also performed during the experiment (just before collecting the samples) to check the effect of prepared NPs and P on opening the tight junctions. The permeability of passive paracellular flux marker, sodium

fluorescein, was additionally tested during the transport study as a more sensitive method than TEER measurements. Fluorescein sodium salt stock solution (1 mg/ml) was added to the samples applied to Caco-2 cells monolayers (apical compartment) to form the final concentration of 10 µg/ml. The diffusion of sodium fluorescein into the basal compartment was determined by measuring the fluorescence integrity (excitation 492 nm, emission 520 nm, FLUOstar Optima microplate reader, BMG labtech). All experiments were done at least in triplicate.

2.4.2.16.5 Permeability coefficient (P_{app}) caluclation

The apparent permeability coefficient (P_{app}, [$cm \cdot s^{-1}$]) was determined from the amount of compound transported in time, according to the following equation:

$$P_{app} = \left(\frac{dQ}{dt}\right) \cdot \left(\frac{1}{AC_0}\right) \qquad \text{(Equation 2.4)}$$

Where: ($\frac{dQ}{dt}$) - permeability rate (steady state transport rate) obtained from the transport time profile of the substrate

A - surface area of the filter (cm^2)

C_0 - initial concentration in the donor chamber

2.4.2.17 Statistical analysis

The statistical significance of the differences between samples was determined using one-way analysis of variance (ANOVA) Origin software version 7 was employed for all analyses. Differences were considered significant at $p<0.05$.

CHAPTER 3

OPTIMISATION OF PROINSULIN EXPRESSION AND PURIFICATION FROM NEWLY DESIGNED PLASMIDS

3.1 Introduction

Human insulin is the first therapeutic protein produced by recombinant DNA technology, which was approved for general use in 1982. There are different methods of recombinant human insulin production in *E. coli*, which are more detailed in Section 1.4 of this thesis. Two of the methods are based on the intracellular insulin production in *E.coli* (Walsh, 2005). An alternative method of recombinant human insulin production is based on the insulin gene insertion into the yeast *S. cerevisiae*, which secretes expressed polypeptide into the culture medium, and thus simplifies the purification process (Heller et al., 2007).

The aim of this study was to develop a straightforward laboratory scale expression system for recombinant human insulin to enable insulin gene modification, which could have potential application in oral delivery. Having such a system would not only provide the material for further studies but would also enable easily engineered alternative versions of recombinant human insulin, which would exhibit the desired characteristics. At first, the design and cloning of various DNA constructs that will be used for insulin expression in *E. coli* had to performed. A major benefit of newly designed constructs was the combination of the simplicity of a bacterial expression system with benefits of the expression in yeast which is achieved by directing the expressed protein with the signal peptide to the oxidation system of the bacterial periplasmic space. Another modification of the insulin gene, which was introduced, was a shorter C-peptide (3 amino acid residues, AAK), which brings A- and B-chains of insulin closer, thus allowing production of correct disulfide bridges. As reported by Chang et al. (1998) the short-turn forming sequence is more effective in the refolding process than the much longer C-peptide. Short C-peptide (AAK) removal involves a site-specific cleavage (Zündorf et al., 2001, Ladisch and Kohlmann, 1992). It is expected that these novel DNA constructs will have several advantages including low cost, convenience and speed of the method. Furthermore, there are fewer post-processing steps because of the periplasmic localisation, which may ensure both correct disulfide bridges and correct N-terminus (no need for methionine removal). Development of a new method will facilitate further modifications of insulin such as: isotopically labelling of insulin for structural NMR studies or creating fusions with cell penetrating peptides (CPP).

In the next step the expression of proinsulin from prepared clones had to be optimised. There are two various methods of protein induction from genes regulated with *Lac* promoter. IPTG is the most common inducer of expression from the *lac* promoter. IPTG prevents repression of the *lac* promoter, but it is not metabolised by the product of *lac* operon, so there is no need for continuous replenishment in the medium as cells grow. Although the *lac* promoter is widely used, it is not always is

the best choice for expression of heterologous proteins in *E. coli* (Lodge at al., 2006). An alternative system for induction of protein expression was described by Studier (Studier, 2005) and is known as an auto-induction system. An auto-induction expression system is a convenient way to perform recombinant protein production without addition of inducer such as IPTG for *lac* controlled expression systems. This method is based on the ability of certain media to induce protein expression in *E. coli* when the cells reach saturation (Studier, 2005). The aim of this study was to define conditions, which are suitable for the expression of human proinsulin from different plasmids. MDG as a non-inducing medium was used to grow *E. coli* in a starter culture. Then two auto-induction media were tested for proinsulin expression, ZYP-5052 and ZYM-5052. Since several studies suggest that a temperature shift during incubation increases the yield of expressed protein in bacteria, various temperatures were studied in order to find optimal conditions to achieve a high yield of soluble proinsulin expression in *E. coli* (Son et al., 2007).

Having the confirmation of an overexpression of proinsulin from prepared plasmids, the purification protocol had to be established. Depending on the form in which proinsulin would be expressed (soluble expression in periplasm or insoluble cytoplasmic form) and the composition of the plasmid (presence of purification tags and cleavage sites) various purification steps would have to be employed.

3.2 Design and preparation of proinsulin plasmids

3.2.1 Composition of plasmids pHB1-3

pHB1, pHB2 and pHB3 plasmids were prepared earlier by Georgios Boutsikaris and the details of their preparation are described in a Masters thesis entitled "Establishing a novel laboratory scale expression system for recombinant human insulin in bacteria" (Boutsikaris, 2009). Short description of those plasmids is presented below, as they underwent further analysis.

pET-22b vector was chosen as it carried an N-terminal pelB signal sequence for potential periplasmic localisation and optional C-terminal His tag sequence. In the first step insulin precursor (preproinsulin) DNA was inserted into chosen vector (pET-22b).

The final composition of **pHB1** plasmid is presented in Figure 3.1.

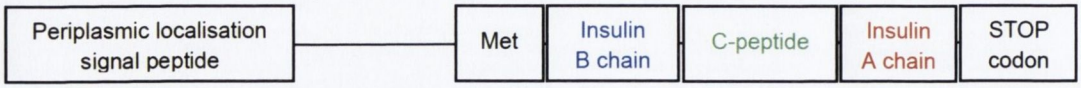

Fig. 3.1 *pHB1 construct components.*

Next step of the expression construct cloning strategy was deletion of ATG codon (methionine), which would result in clean insulin end at N-terminus after cleavage with signal peptidase. Signal peptidases are indispensable enzymes, catalysing the cleavage of the amino-terminal signal-peptide sequences from preproteins, which are translocated across biological membranes (Tuteja, 2005).

The final composition of **pHB2** plasmid is presented in Figure 3.2.

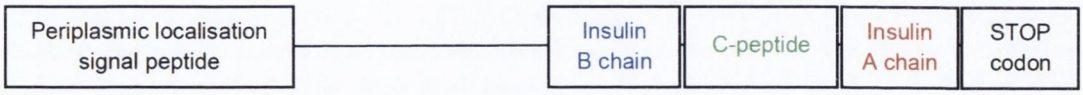

Fig. 3.2 *pHB2 construct components.*

In the final step of the insulin expression construct cloning strategy, the C-peptide was replaced by a short AAK sequence peptide.

The final composition of **pHB3** plasmid is presented in Figure 3.3.

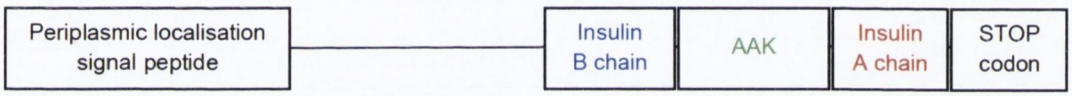

Fig. 3.3 *pHB3 construct components.*

3.2.2 pMD2 insulin construct preparation

To increase the probability of biological activity by export to the periplasm the vector pET-39b (Novagen) was selected. Vector pET-39b encodes for a DsbA tag, which contains a signal sequence that directs the signal protein to the periplasm and catalyses the formation and isomerisation of disulfide bridges. In addition, pET-39b contains a His tag sequence, which is useful during the purification step. The cloning/expression region of the coding strand is transcribed by T7 RNA polymerase. Preparation of desired plasmid, which contains:

DsbA–B chain–AAK–A chain–STOP is described in details in Section 2.4.1.12.

The final composition of prepared plasmid pMD2 is presented in Figure 3.4.

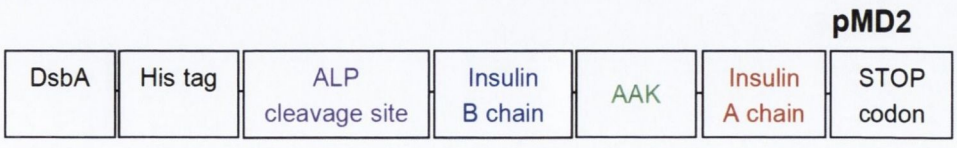

Fig. 3.4 *pMD2 construct components.*

3.2.3 pMD3 insulin construct preparation

For the preparation of the new construct

Histag–EK site–B CHAIN–AAK–A CHAIN–STOP,

the vector pET-19b (Novagen) was selected. This vector carries an N-terminal His tag sequence followed by an enterokinase site (EK site), which allows for a straight-forward digestion and purification of the plasmid. The cloning/expression region of the coding strand is transcribed by T7 RNA polymerase. Preparation of desired plasmid pMD3 is described in detail in Section 2.4.1.13.

The final composition of prepared plasmid pMD3 is presented in Figure 3.5.

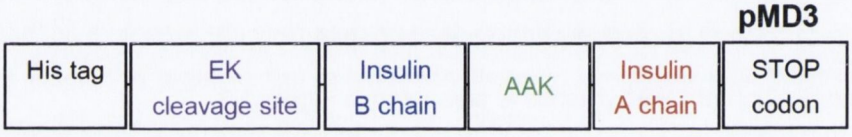

Fig. 3.5 *pMD3 construct components.*

3.3 Expression/ auto-induction of proinsulin from prepared plasmids

The expression of prepared plasmids (described above) induced by IPTG and auto-induced and the cellular localisation was established.

3.3.1 Expression and cellular localisation of proteins expressed by IPTG induction

Cultured cells with pHB1 plasmid were incubated at 37°C. Expression of proinsulin was induced by IPTG when OD_{600} reached ~ 0.7 (Section 2.4.1.16.1). Comparison of proinsulin expression from plasmids pHB1, pHB2 and pHB3 at 37°C is shown in Figure 3.6.

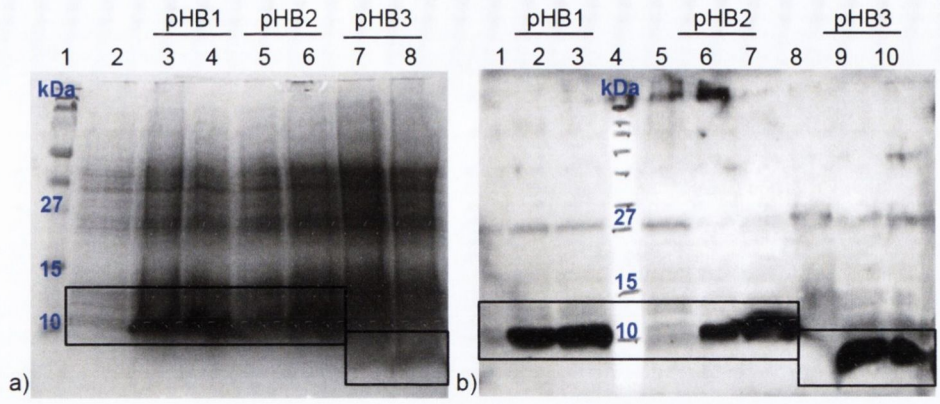

Fig 3.6 ***a)*** *SDS-PAGE and* ***b)*** *Western blot analysis of pHB1, pHB2 and pHB3 plasmid expression, (1st Ab Monoclonal Anti-insulin Mouse IgG: 1:1000, 2nd Ab Anti-mouse IgG HRP: 1:5000).*

(a): lane 1: molecular mass marker, 2: non-induced cultured cells with pHB1 plasmid, lanes 3-4: pHB1 plasmid, lanes 5-6: pHB2 plasmid, lanes 7-8: pHB3 plasmid, : 3,5,7: culture after 2 h of IPTG induction, 4,6,8: culture after 4 h of IPTG induction, b): lanes 1-3: pHB1 plasmid, lane 2: molecular mass marker, lanes 5-7: pHB2 plasmid, lanes 8-10: pHB3 plasmid, : 1,5,8: non-induced cultured cells, 2,6,9: culture after 2 h of IPTG induction, 3,7,10: culture after 4 h of IPTG induction). Test performed by Boutsikaris, 2009.

Shortening the C-peptide resulted in smaller size obtained for pHB3 plasmid of 8.3 kDa (lane 9 and 10, Figure 3.6 a) comparing to plasmid pHB1 (11.8 kDa, lane 2 and 3, Figure 3.6 b). Western blot analysis confirmed good expression of proinsulin for all of the plasmids tested (Figure 3.6 b). Solubility of expressed proinsulin was determined next. Prepared cytoplasmic fractions (soluble) and inclusion body fractions (insoluble) (Section 2.4.1.18) for pHB1, pHB2 and pHB3 plasmid were analysed by Western blot (Figure 3.7).

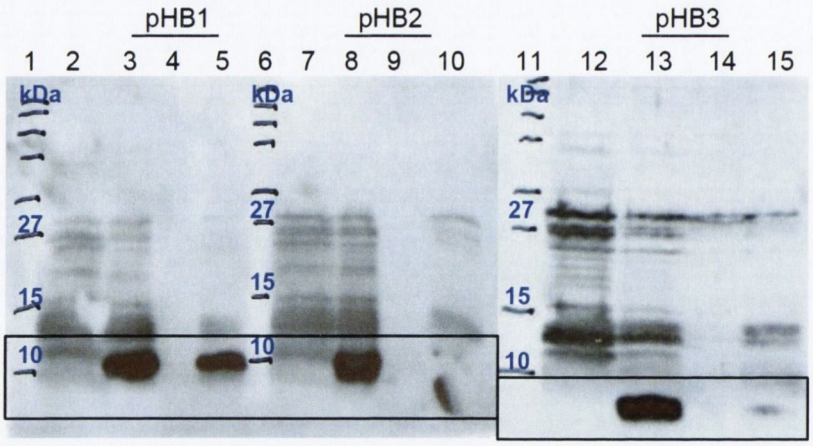

Fig 3.7 *Western blot analysis of solubility of proteins expressed by pHB1, pHB2 and pHB3 plasmid, (1st Ab Monoclonal Anti-insulin Mouse IgG: 1:1000, 2nd Ab Anti-mouse IgG HRP-linked: 1:5000).*
(lanes 1, 6 and 11: molecular mass marker, lanes 2-5: pHB1 plasmid, lanes 7-10: pHB2 plasmid, lanes 12-15: pHB3 plasmid, : 2,7,12: non-induced cultured cells, 3,8,13: culture after 4 h of IPTG induction, 4,9,14: cytoplasmic (soluble) fraction), 5,10,15: IBs (insoluble) fraction). Test performed by Boutsikaris, 2009.

Results obtained from Western blot showed the absence of the band for proinsulin in the soluble part (cytoplasmic fraction) for all of tested plasmids (lanes: 4, 9 and 14, Fiure 3.7). This indicated that protein was mostly expressed in form of insoluble inclusion bodies (lanes 5, 10, 15, Figure 3.7). Insoluble fraction of proinsulin expressed by plasmid pHB2 and pHB3 (lanes 10 and 15) was very small, which would suggest a low yield of extraction technique, which should be further optimised. Denaturing conditions were then used for further purification process. As pHB3 plasmid was chosen for further proinsulin expression and purification studies, further test were performed. To check the cellular localisation, periplasmic localisation test was carried out (Section 2.4.1.17). SDS-PAGE and Western blot analysis summarising expression, cellular localisation and solubility of pHB3 plasmid are shown in Figure 3.8.

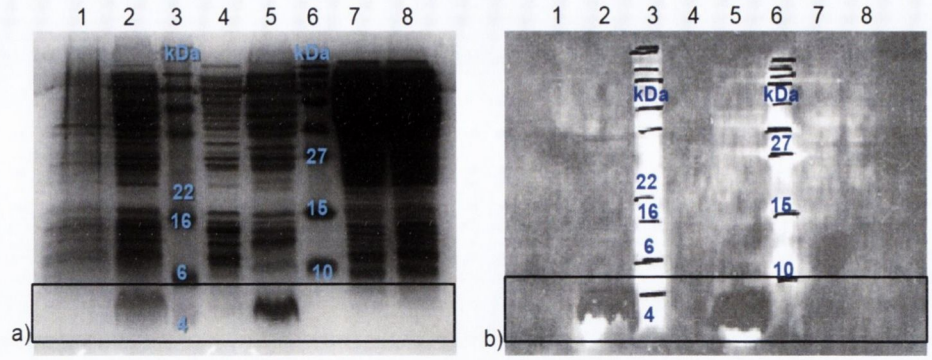

Fig 3.8 ***a)*** *SDS-PAGE and* ***b)*** *Western blot analysis of expression, solubility and cellular localisation of pHB3 plasmid, (1st Ab Monoclonal Anti-insulin Mouse IgG: 1:1000, 2nd Ab Anti-mouse IgG HRP: 1:5000).*
(lane 1: non-induced cultured cells with pHB3 plasmid, 2: culture with pHB3 plasmid after 4 h of IPTG induction, 3: molecular mass marker 1, 4: cytoplasmic (soluble) fraction of pHB3 plasmid, 5: IBs (insoluble) fraction of pHB3 plasmid, 6: molecular mass marker 2, 7 and 8: periplasmic fraction of pHB3 plasmid).

SDS-PAGE and Western blot analysis confirmed that the target protein was mostly expressed in the insoluble form. Additionally, periplasmic localisation test excluded the presence of proinsulin in this fraction.

To increase the export of expressed proinsulin to the periplasm, a new plasmid (pMD2) with DsbA protein was designed and prepared (Section 3.2.2). DsbA is a periplasmic protein that is required for the formation of disulfide bonds in proteins secreted in *E. coli* (Zapun and Creighton, 1994). Additionally, it was reported that fusion of target protein with DsbA increases its periplasmic yield (Winter et al., 2000). Expression of a polypeptide of expected size (35.6 kDa), cellular localisation and solubility was demonstrated with SDS-PAGE (Figure 3.9 a) and confirmed by Western blot analysis (Figure 3.9 b).

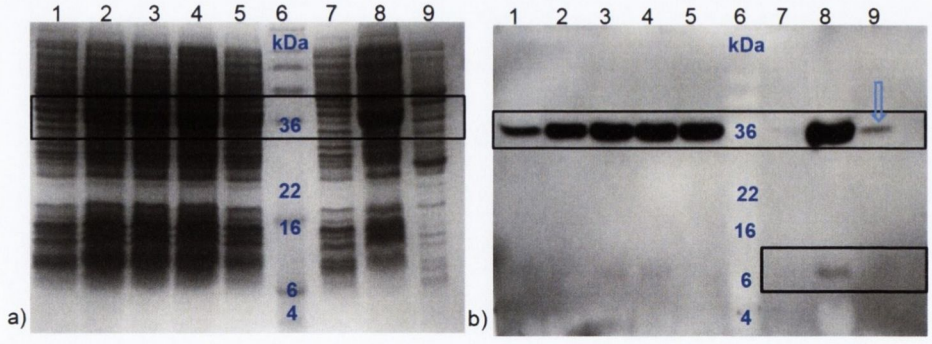

Fig 3.9 ***a)*** *SDS-Page and* ***b)*** *Western blot analysis of expression, solubility and cellular localisation of pMD2 plasmid, (1st Ab Monoclonal Anti-insulin Mouse IgG: 1:1000, 2nd Ab Anti-mouse IgG HRP: 1:5000).*
(lane 1: non-induced cultured cells with pMD2 plasmid, 2, 3, 4 and 5: culture with pMD2 plasmid after 1, 2, 3 and 4 h of IPTG induction, respectively, 6: molecular mass marker, 7: cytoplasmic (soluble) fraction of pMD2 plasmid, 8: IBs (insoluble) fraction of pMD2 plasmid, 9: periplasmic fraction of pMD2 plasmid).

Analysis of SDS-PAGE and Western blot results confirmed high expression of pMD2 plasmid. The band present in the non-induced cultured cells (lane 1, Figure 3.9 b) is probably the part of the fraction that is present in lane 2. As intended, prepared plasmid pMD2 successfully secreted the desired protein (DsbA+proinsulin) into the periplasm (lane 9). Western blot analysis showed a small fraction of proinsulin present (lane 9), which was probably digested by cytoplasmic proteolytic enzymes (Maurizi, 1992). To further improve the yield of the fusion protein, especially in the periplasm, optimisation of protein expression conditions was carried out by lowering the temperature of the culture to 30°C. Obtained data will be described in the next chapter as part of the purification protocol optimisation.

Expression of protein from plasmid pMD3 was tested in parallel. pMD3 plasmid was prepared in order to simplify digestion (enterokinase cleavage site) and purification (His tag) of the expressed product, for both, the soluble or insoluble fraction. Determination of expression level (culture at 30°C) and solubility was assessed by SDS-PAGE and Western blot were performed. Results obtained are presented in Figure 3.10.

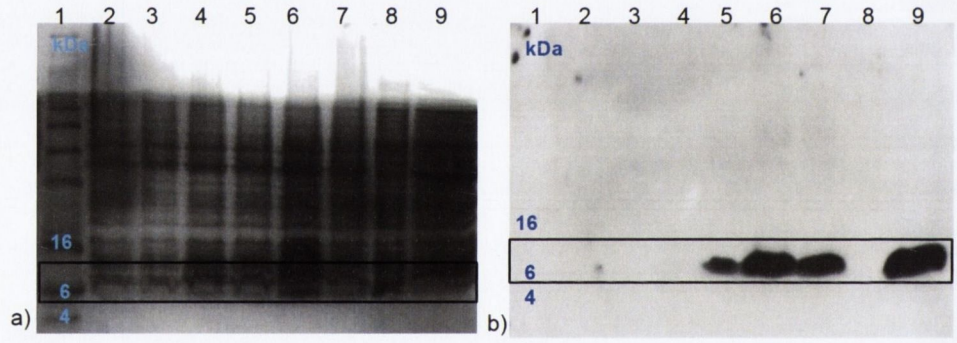

Fig 3.10 ***a)*** *SDS-Page and* ***b)*** *Western blot analysis of expression and solubility of pMD3 plasmid, (1st Ab Monoclonal Anti-insulin Mouse IgG: 1:1000, 2nd Ab Anti-mouse IgG HRP: 1:5000).*

(lane 1: molecular mass marker, 2: non-induced cultured cells with pMD3 plasmid, 3, 4, 5 and 6: culture with pMD3 plasmid after 1, 2, 3 and 4 h of IPTG induction, respectively, 7: culture with pMD3 after overnight incubation, 8: cytoplasmic (soluble) fraction of pMD3 plasmid, 9: IBs (insoluble) fraction of pMD3 plasmid).

Western Blot analysis (Figure 3.10 b) confirmed expression of proinsulin and its presence in the insoluble form. It was noticed that the greatest amount of proinsulin was expressed after 4 h of incubation after IPTG induction, suggesting that 4 hours is the optimum culturing period for pMD3 plasmid. To further optimise expression of proinsulin several cultures were carried out. Despite various optimisation attempts, the amount of expressed product was not repeatable and insufficient for further experiments.

The results obtained from IPTG induced expression of proinsulin from prepared plasmids are summarized in Figure 3.11.

Construct	DNA sequence confirmed	Expression level	Identity confirmed with Western blot	Molecular weight confirmed with SDS-PAGE	Inclusion bodies production	Periplasmic space localisation
pHB1	OK	+++	OK	OK	+	-
pHB2	OK	+++	OK	OK	+	-
pHB3	OK	+++	OK	OK	+	-
pMD2	OK	++	OK	OK	+	+
pMD3	OK	+	OK	OK	+	-

Fig. 3.11 *Expression and cellular localisation of proteins induced by IPTG.*

3.3.2 Development of an auto-induction system for high level expression of proinsulin

Further optimisation of expression conditions by using auto-induction system (Studier, 2005) was performed for pHB1 and pHB3 plasmids as they showed the highest yield of proinsulin expression (expressed in the form of inclusion bodies (insoluble form)). Two auto-induction media were tested: ZYP-5052 and ZYM-5052 for proinsulin expression, which differed in the concentration of phosphate buffer in the medium. Optimisation of the auto-induction system was performed under my supervision by Caroline de Grully as a research project: "Development of an auto-induction system in *E. coli* for high level expression of modified human insulin for oral delivery" (de Grully, 2012).

3.3.2.1 pHB1 plasmid expression by using auto-induction

A series of experiments were performed in ZYP-5052 media culturing four different colonies of pHB1 plasmid. During the culturing at 37^{0}C, optical density measurements (at 600 nm, OD_{600}) were performed to check the increased growth of the cultures. To check the expression of the four different colonies of pHB1 plasmid during auto-induction SDS-PAGE was performed. Gels are presented in Figure 3.12.

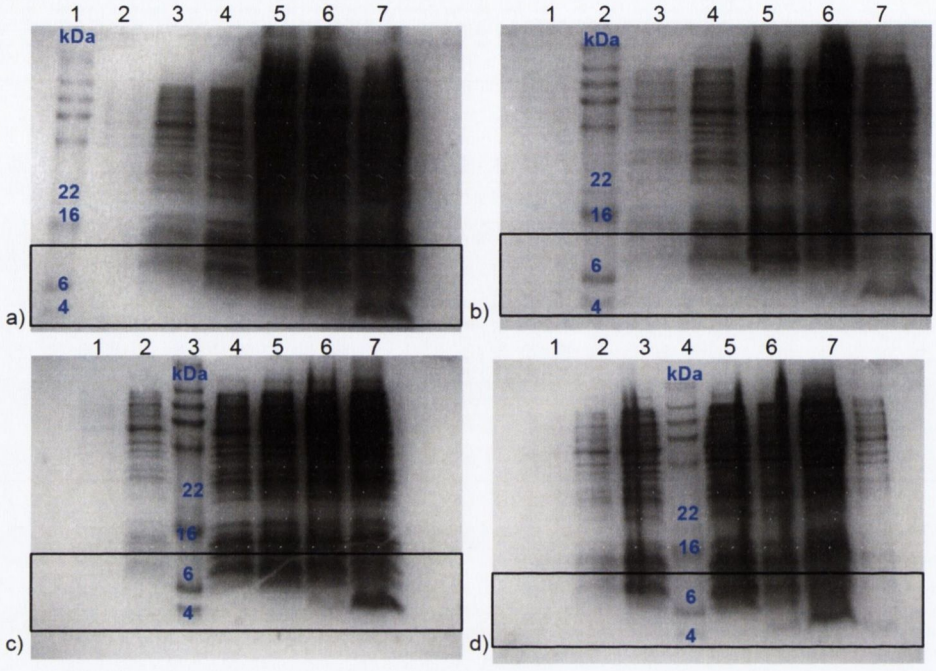

Fig 3.12 *SDS-PAGE analysis of pHB1 plasmid expression during auto-induction in ZYP-5052 media at 37°C.*
(a) 1st colony (lane 1: molecular mass marker, 2, 3, 4, 5 and 6: culture after 1 h, 2 h, 3 h, 4 h and 6 h of incubation, respectively, 7: culture after overnight incubation), b) 2nd colony (lane 1: culture after 1 h of incubation, 2: molecular mass marker, 3, 4, 5 and 6: culture after 2 h, 3 h, 4 h and 6 h incubation, respectively, 7: culture after overnight incubation), c) 3rd colony (lane 1 and 2: culture after 1 h and 2 h of incubation, respectively, 3: molecular mass marker, 4, 5 and 6; culture after 3 h, 4 h and 6 h of incubation, respectively, 7: culture after overnight incubation), d) 4th colony (lane 1, 2 and 3; culture after 1 h, 2 h and 3 h of incubation, respectively, 4: molecular mass marker, 5 and 6: culture after 4 h and 6 h of incubation, respectively, 7: culture after overnight incubation). Test performed by de Grully, 2012.

Confirmation of expression for all four colonies of pHB1 plasmid during auto-induction allowed further assays of cellular localisation and solubility of expressed proteins to be performed. SDS-PAGE and Western blot techniques were used to analyse obtained samples (Figure 3.13 and 3.14).

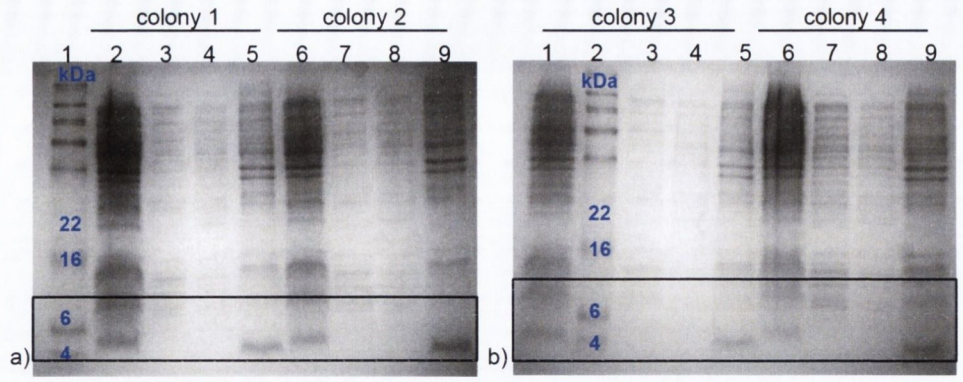

Fig 3.13 *SDS-PAGE analysis of cellular localisation and solubility of pHB1 plasmid expressed by auto-induction in ZYP-5052 media at 37°C.*
(a) colony 1 and 2 (lane 1: molecular mass marker, lanes 2-5 colony 1, lanes 6-9 colony 2, : 2,6: bacterial culture after overnight incubation, 3,7: periplasmic fraction, 4,8: cytoplasmic (soluble) fraction, 5,9: insoluble (IBs fraction) of colony, b) colony 3 and 4 (lane 1,6: bacterial culture after overnight incubation, 2: molecular mass marker, 3,7: periplasmic fraction, 4,8: cytoplasmic (soluble) fraction, 5,9: insoluble (IBs fraction). Test performed by de Grully, 2012.

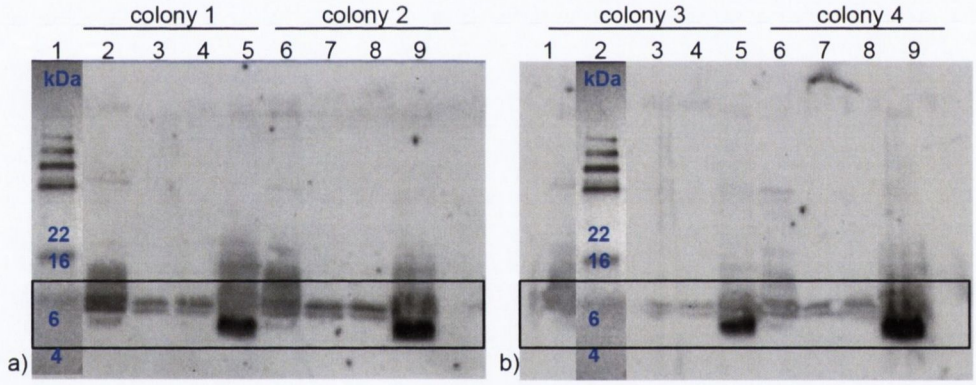

Fig 3.14 *Western blot analysis of cellular localisation and solubility of pHB1 plasmid expressed by auto-induction in ZYP-5052 media at 37°C, (1st Ab: Insulin A (C-12) goat polyclonal IgG: 1:1000, 2nd Ab: Donkey anti-goat IgG-HRP: 1:5000).*
(a) colony 1 and 2 analysis, b) colony 3 and 4 analysis). Sequence of samples loading was the same as for SDS-PAGE electrophoresis (Figure 4.9). Test performed by de Grully, 2012.

As presented in Figure 3.14, the size of proinsulin (proinsulin+signal peptide) expressed by plasmid pHB1 varied from its calculated value of 11.8 kDa, which might suggest that the periplasmic localisation signal peptide was cleaved off during overnight incubation, thus only proinsulin with a size of 9.4 kDa is visible in lanes 2, 6 (Figure 3.14 a) and 1, 6 (Figure 3.14 b). Additionally, it was noticed that the size of the protein after extraction from inclusion bodies (lanes 5 and 9) was lower compared to the size of the protein extracted after overnight culturing (lanes 2 and 6, Figure 3.14 a, lanes 1 and 6, Figure 4.13 b), suggesting degradation of proinsulin during the sonication process.

Based on presented data, colony 1 of pHB1 plasmid expressed in ZYP-5052 media was chosen as it expressed the highest amount of the proinsulin (Figure 3.13). The selected colony was conserved in glycerol (1 ml of MDG solution with 0.1 ml of glycerol), frozen at -20 °C or -80°C and used as a stock for further assays.

However, before colony 1 was selected for further analysis, all prepared cultures of pHB1 plasmids had been stored at 4°C. Western blot (Figure 3.14) confirmed that the protein expressed by pHB1 plasmid was mostly insoluble (inclusion bodies formed) for all of tested colonies. However there was a small amount of protein present in the periplasmic fraction. The next step of the optimisation process was comparison of two different auto-induction media: ZYP-5052 and ZYM-5052 for pHB1 plasmid expression. Expression of pHB1 plasmid was carried out in both media at 16°C. To control the growth of the culture OD measurements at 600 nm was carried out. Obtained results indicated that there was no difference in the OD of colony 1 in two different media: ZYP-5052 and ZYM-5052. However, relatively low OD value was obtained after 6 h of incubation (~ 2), which could be explained by low temperature of the culture since initial growth was carried out at 37°C, but after 4 h of incubation temperature was lowered to 16°C. Expression of pHB1 plasmid (colony 1) in the two media was analysed by SDS-PAGE. In the next step periplasmic localisation and solubility test was performed and samples were analysed by SDS-PAGE and Western blot (data not shown). Western blot results showed very low expression of colony 1 of pHB1 plasmid in both media. The sample was probably stored for too long before best colony was selected and analysed, which might be the reason for low OD value after overnight incubation (de Grully, 2012).

3.3.2.2 pHB3 plasmid expression by using auto-induction

A series of experiments was performed with four different colonies containing pHB3. The bacteria were initially cultured at 37°C. After 4 h the temperature was decreased to 22°C. During culturing, optical density measurements were performed to check growth of the cultures. Figure 3.15 shows the increase in OD600 versus time (samples were diluted 1:10 when OD value was over 1).

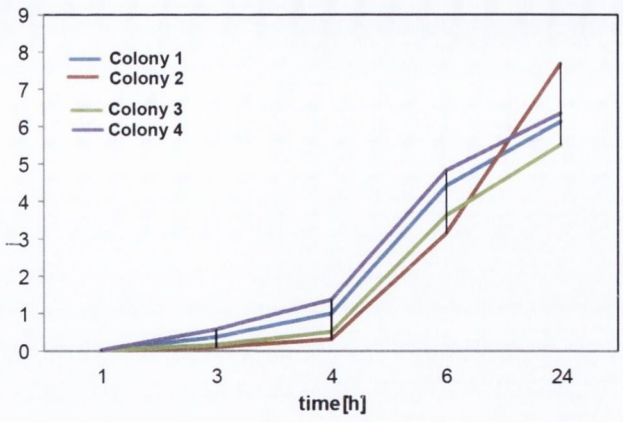

Fig 3.15 *Optical density measurements for four colonies of pHB3 plasmid cultured in ZYP-5052 media at 37 °C, after 4 h temperature was lowered to 22 °C.*

A similar growth was observed for colony 1, 3 and 4. Colony 2 showed initially the lowest OD value, but after overnight incubation it reached the highest OD. Expression of four different colonies of pHB3 plasmid in ZYP-5052 media at 22°C was analysed by SDS-PAGE (Figure 3.16).

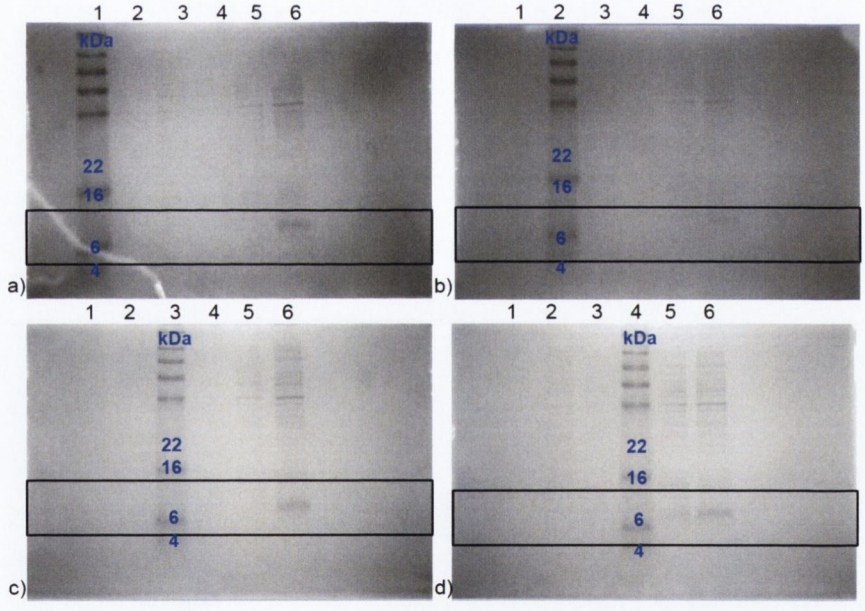

Fig 3.16 *SDS-PAGE analysis of pHB3 plasmid expression during auto-induction in ZYP-5052 media at 22°C.*

(a) 1st colony (lane 1: molecular mass marker, 2, 3, 4, and 5: culture after 1 h, 3 h, 4 h and 6 h of incubation, respectively, 6: culture after overnight incubation), b) 2nd colony (lane 1: culture after 1 h of incubation, 2: molecular mass marker, 3, 4 and 5: culture after 3 h, 4 h and 6 h incubation, respectively, 6: culture after overnight incubation), c) 3rd colony (lane 1 and 2: culture after 1 h and 3 h of incubation, respectively, 3: molecular mass marker, 4 and 5; culture after 4 h and 6 h of incubation, respectively, 6: culture after overnight incubation), d) 4th colony (lane 1, 2 and 3; culture after 1 h, 3 h and 4 h of incubation, respectively, 4: molecular mass marker, 5: culture after 6 h of incubation, respectively, 6: culture after overnight incubation). Test performed by de Grully, 2012.

Confirmation of pHB3 plasmid expression (size of 8.3 kDa, proinsulin+shortened C-peptide) in ZYP-5052 medium at 22°C allowed further analysis to be performed. Periplasmic, cytoplasmic (soluble) and inclusion body (insoluble) fractions were prepared and analysed by SDS-PAGE (Figure 3.17) and Western blot (Figure 3.18).

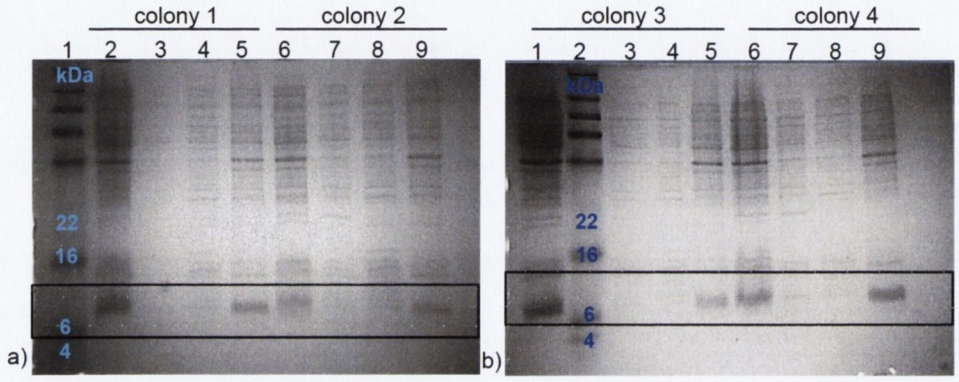

Fig 3.17 *SDS-PAGE analysis of cellular localisation and solubility of pHB3 plasmid expressed by auto-induction in ZYP-5052 media at 22°C.*
(a) colony 1 and 2 (lane 1: molecular mass marker, lanes 2-5 colony 1, lanes 6-9 colony 2, : 2,6: bacterial culture after overnight incubation, 3,7: periplasmic fraction, 4,8: cytoplasmic (soluble) fraction, 5,9: insoluble (IBs fraction) of colony, b) colony 3 and 4 (lane 1,6: bacterial culture after overnight incubation, 2: molecular mass marker, 3,7: periplasmic fraction, 4,8: cytoplasmic (soluble) fraction, 5,9: insoluble (IBs fraction). Test performed by de Grully, 2012.

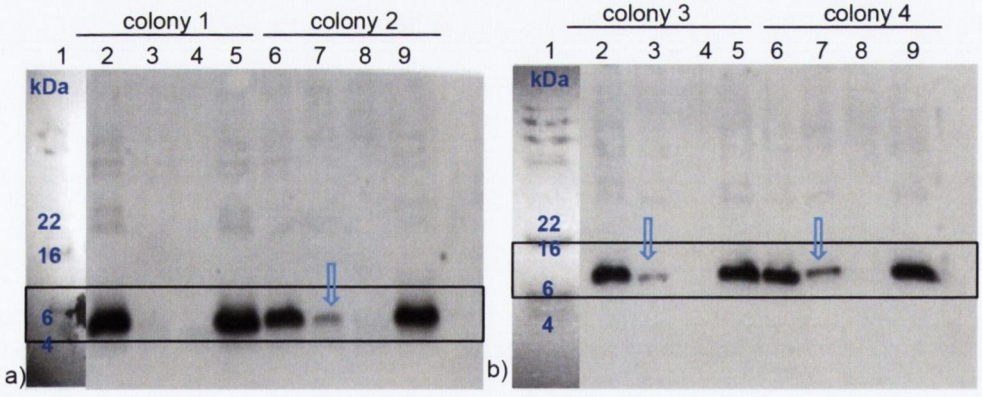

Fig 3.18 *Western blot analysis of cellular localisation and solubility of pHB3 plasmid expressed by auto-induction in ZYP-5052 media at 22°C, (1st Ab: Insulin A (C-12) goat polyclonal IgG: 1:1000, 2nd Ab: Donkey anti-goat IgG-HRP: 1:5000).*
(a) colony 1 and 2 (lane 1: molecular mass marker, lanes 2-5 colony 1, lanes 6-9 colony 2, : 2,6: bacterial culture after overnight incubation, 3,7: periplasmic fraction, 4,8: cytoplasmic (soluble) fraction, 5,9: insoluble (IBs fraction) of colony, b) colony 3 and 4 (lane 1: molecular mass marker, lanes 2-5 colony 3, lanes 6-9 colony 4, : 2,6: bacterial culture after overnight incubation, 3,7: periplasmic fraction, 4,8: cytoplasmic (soluble) fraction, 5,9: insoluble (IBs fraction). Test performed by de Grully, 2012.

Interesting results were obtained with Western blot analysis. As indicated in Figure 3.18 only colony 1 did not express protein in the periplasm. All of the protein was

present in the form of insoluble inclusion bodies. However, colony 2, 3 and 4 expressed the protein as inclusion bodies but there was a fraction present in the periplasm as well. The greatest amount of protein present in the periplasmic fraction was noticed for colony 4. For that reason colony 1 and 4 were selected and conserved in glycerol (1 ml MDG solution with 0.1 ml of glycerol – frozen at -80°C) for further assays. After a week the chosen colonies were used for culturing in different media: ZYP-5052 and ZYM-5052. During the first 4 h culturing was performed at 37°C. After that, temperature was lowered to 16°C. During the culturing optical density measurements were performed to check growth of the cultures (de Grully, 2012). There was no difference in the growth of colony 4 in the two media tested. In case of colony 1 higher OD_{600} values were obtained after overnight incubation in ZYM-5052 media compared to ZYP-5052. Expression of plasmid pHB3 in the two media was analysed by SDS-PAGE (Figure 3.19).

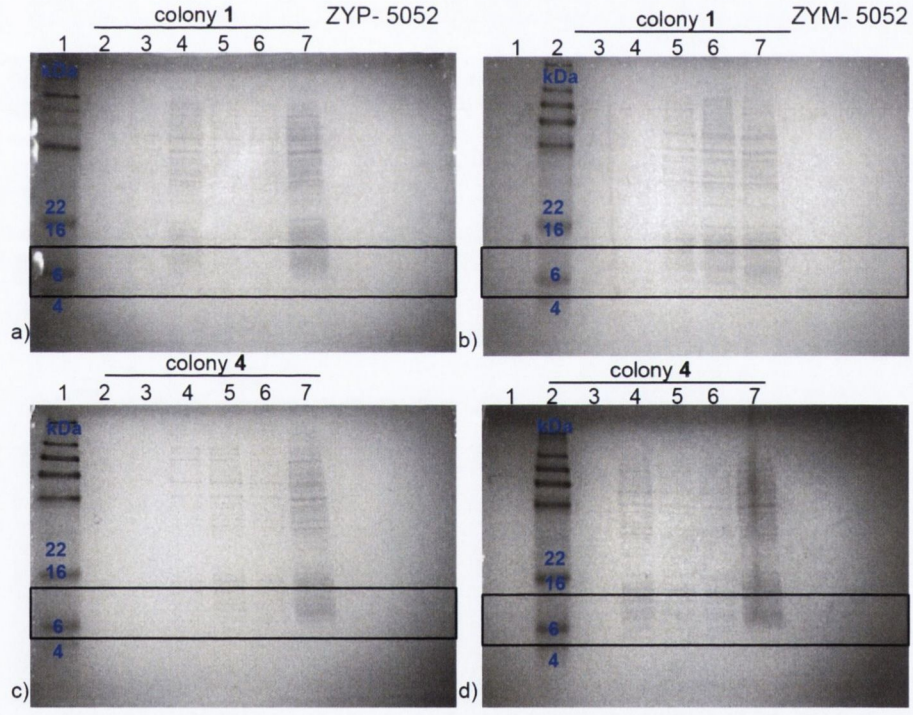

Fig 3.19 *SDS-PAGE analysis of pHB3 plasmid expression (1st and 4th colony) during auto-induction at 16°C in ZYP-5052 and ZYM-5052 media.*
(a) ZYP-5052 media, colony 1 (lane 1: molecular mass marker, 2, 3, 4, 5, 6: culture after 1 h, 3 h, 4 h, 5 h and 6 h of incubation, respectively, 7: culture after overnight incubation), b) ZYM-5052 media, colony 1 (lane 1: culture after 1 h of incubation, 2: molecular mass marker, 3, 4, 5 and 6: culture after 3 h, 4 h, 5 h and 6 h of incubation, respectively, 7: culture after overnight incubation), c) ZYP-5052 media, colony 4 (lane 1: molecular mass marker, 2, 3, 4, 5 and 6: culture after 1 h, 3 h, 4 h, 5 h and 6 h of incubation, respectively, 7: culture after overnight incubation), d) ZYM-5052 media, colony 4 (lane 1: culture after 1 h of incubation, 2: molecular mass marker, 3, 4, 5 and 6: culture after 3 h, 4 h, 5 h and 6 h of incubation, respectively, 7: culture after overnight incubation). Test performed by de Grully, 2012.

SDS-PAGE analysis confirmed an expression of all of the pHB3 colonies tested. There was no noticeable difference between the amounts of proinsulin expressed in two media, even if the OD_{600} was different in case of colony 1. The next step was isolation and analysis of periplasmic, cytoplasmic (soluble) and inclusion bodies (insoluble) fraction of expressed protein. Prepared fractions were loaded into SDS-PAGE (Figure 3.20) and additionally analysed by Western blot (Figure 3.21).

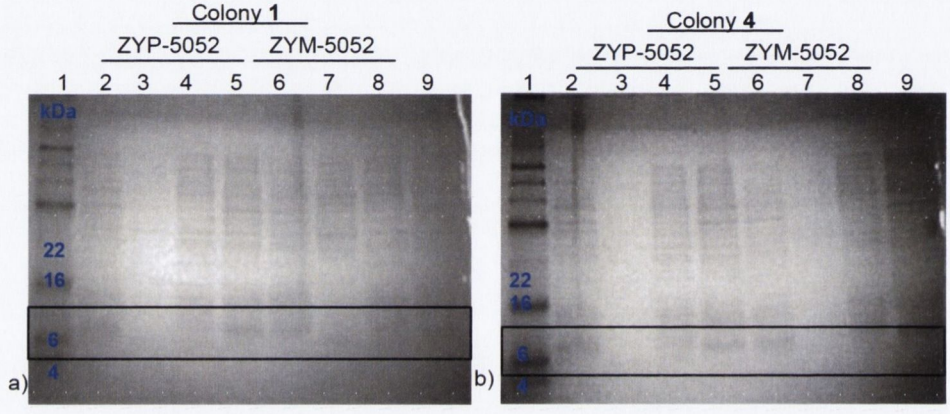

Fig 3.20 *SDS-PAGE analysis of cellular localisation and solubility of pHB3 plasmid expressed by auto-induction in ZYP-5052 and ZYM-5052 media at 22°C.*
(a) colony 1 (lane 1: molecular mass marker, lanes 2-5 ZYP-5052, lanes 6-9 ZYM-5052, 2,6: bacterial culture after overnight incubation, 3,7: periplasmic fraction, 4,8: cytoplasmic (soluble) fraction, 5,9: insoluble (IBs fraction), b) the same order of samples loading as for colony 1). Test performed by de Grully, 2012.

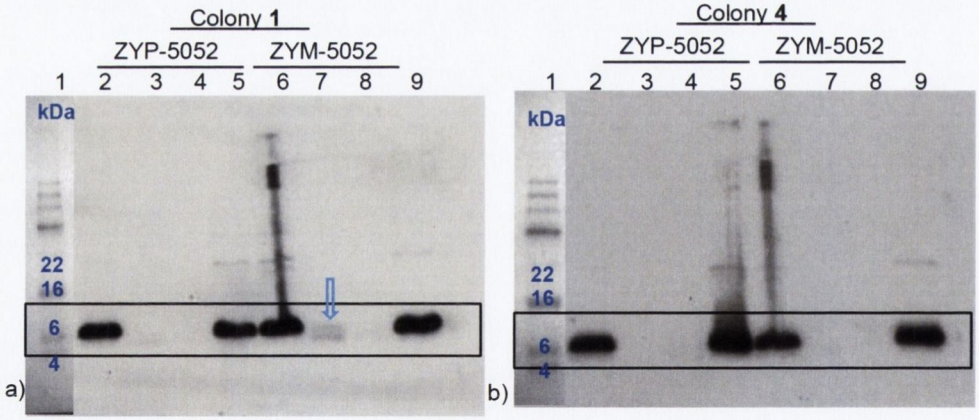

Fig 3.21 *Western blot analysis of cellular localisation and solubility of pHB3 plasmid expressed by auto-induction in ZYP-5052 and ZYM-5052 media at 22°C, (1st Ab: Insulin A (C-12) goat polyclonal IgG: 1:1000, 2nd Ab: Donkey anti-goat IgG-HRP: 1:5000).*
(a) colony 1 (lane 1: molecular mass marker, lanes 2-5 ZYP-5052, lanes 6-9 ZYM-5052, 2,6: bacterial culture after overnight incubation, 3,7: periplasmic fraction, 4,8: cytoplasmic (soluble) fraction, 5,9: insoluble (IBs fraction), b) the same order of samples loading as for colony 1). Test performed by de Grully, 2012.

Analysis of data obtained by Western blot showed that the first colony of pHB3 plasmid was expressed mostly in form of inclusion bodies, however there was a small amount of protein present in the periplasm. Different data were obtained for colony 4 of pHB3 plasmid, where just inclusion bodies were presented in both media.

It is difficult to compare pHB1 and pHB3 plasmids because there was no good expression of pHB1 plasmid obtained after selecting colony 1 for further tests. It is important to highlight no difference in expression of proinsulin in two tested auto-induction media: ZYP-5052 and ZYM-5052. Both of them expressed similar amount of protein.

On the other hand, it was concluded that temperature plays an important role in the protein expression. When the bacteria were cultured at 37°C all of the protein was expressed in the insoluble form of inclusion bodies. However, when the temperature was decreased to 22°C after 4 hours (when the OD_{600} is around 0.4), the protein was mostly expressed in the form of inclusion bodies, but there was also protein present in the periplasm.

A high concentration of expressed proteins in *E. coli* often leads to the appearance of insoluble inclusion bodies (Palmer and Wingfield, 2012). After lysis of the bacteria, the inclusion bodies can be recovered by centrifugation and solubilised in order that proteins can regain conformation. With the periplasmic fraction, fewer steps are needed for protein purification.

ZYP-5052 media was used for further experiments, but different temperatures were tested after 4 h incubation at 37°C (i.e. when the OD is approximately 0.4) in order to compare the expression of proinsulin.

3.3.3 Impact of temperature on proinsulin expression by pHB1 and pHB3 plasmid using auto-induction system

Since several studies suggest that temperature shift during incubation increases protein production in bacteria, including *E. coli* (Schmidt et al., 1999, Son et al., 2007), various temperatures were studied to optimise the conditions for the highest yield of proinsulin expression by auto-induction for pHB1 and pHB3 plasmids. Optimisation of the temperature factor was performed under my supervision by Eduards Pulks as a Master degree project: "Temperature impact on insulin expression in *E. coli* bacteria" (Pulks, 2012).

Two colonies of pHB1 plasmid and two colonies of pHB3 plasmid were cultured at different temperatures (16°C, 22°C, 28°C and 37°C). Afterwards, periplasmic, cytoplasmic (soluble) and inclusion bodies (insoluble) fractions were isolated for each culture and were tested by SDS-PAGE and Western blot analysis. pHB1 plasmid (colony 1 and 2) and pHB3 plasmid (colony 3 and 4) were tested and

compared. Since expression of colony 1 of pHB1 plasmid was very low, data is not shown.

Comparison of samples after overnight expression and inclusion bodies for colony 2 of pHB1 plasmid shows Figure 3.22 a (SDS-PAGE) and 3.22 b (Western blot).

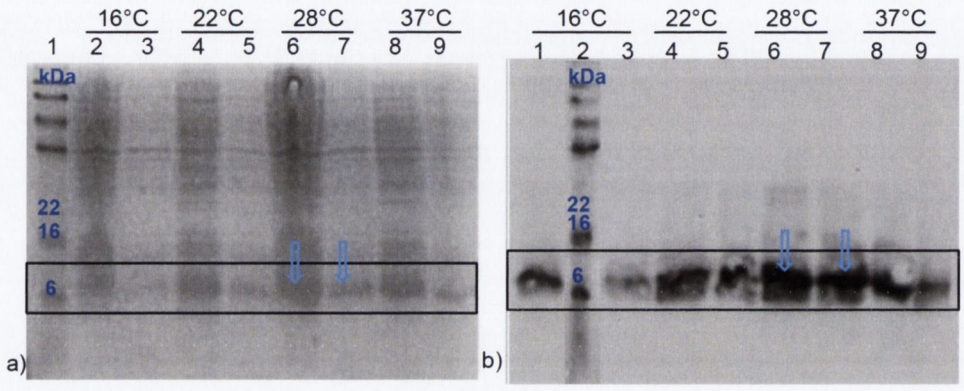

Fig 3.22 ***a)*** *SDS-PAGE and* ***b)*** *Western blot analysis of pHB1 (colony 2) expression and Inclusion bodies (IB) production at various temperatures, (1st Ab: Insulin A (C-12) goat polyclonal IgG: 1:1000, 2nd Ab: Donkey anti-goat IgG-HRP: 1:5000).*
(a) lane 1: molecular mass marker, lanes 2-3: bacterial culture at 16 °C, lanes 4-5, bacterial culture at 22 °C, lanes 6-7: bacterial culture at 28 °C, lanes 8-9: bacterial culture at 37 °C, : 2,4,6,8: bacterial culture after overnight incubation, 3,5,7,9: insoluble (IBs fraction, b) colony 4, (lane 1 and 3: bacterial culture at 16 °C, lane 2: molecular mass marker, lanes 4-5, bacterial culture at 22 °C, lanes 6-7: bacterial culture at 28 °C, lanes 8-9: bacterial culture at 37 °C, : 1,4,6,8: bacterial culture after overnight incubation, 3,5,7,9: insoluble (IBs fraction). Test performed by Pulks, 2012.

To obtain a better comparison of bands present in Western blot, relative density of each band was measured with ImageJ software (Wayne Rasband, National Institutes of health, USA) (Pulks, 2012). Based on Western blot analysis (Figure 3.22 b) maximum proinsulin expression of colony 2 of pHB1 plasmid was obtained when temperature was lowered to 28°C. SDS-Page analysis confirmed that overall protein production of the tested temperatures was at its peak as using 28°C.

Similar studies were performed for colony 3 and colony 4 of pHB3 plasmid. Samples after overnight incubation and inclusion bodies for each tested temperature were loaded onto SDS-PAGE. Additionally, Western blot was carried out for the results comparison (Figure 3.23 a – colony 3 of pHB3 plasmid analysis, Figure 3.23 b – colony 4 of pHB3 plasmid analysis).

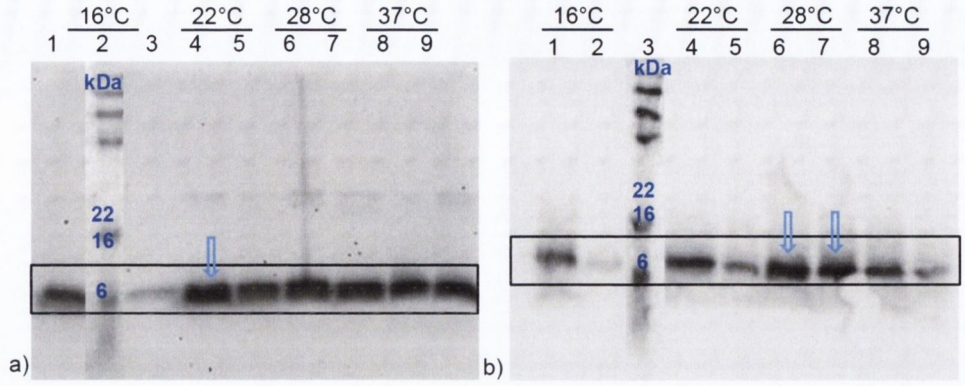

Fig 3.23 *Western blot analysis of expression and Inclusion bodies (IB) production at various temperatures for pHB3 plasmid a) colony 3, b) colony 4, (1st Ab: Insulin A (C-12) goat polyclonal IgG: 1:1000, 2nd Ab: Donkey anti-goat IgG-HRP: 1:5000).*
a) colony 3, (lane 1 and 3: bacterial culture at 16°C, lane 2: molecular mass marker, lanes 4-5, bacterial culture at 22°C, lanes 6-7: bacterial culture at 28°C, lanes 8-9: bacterial culture at 37°C, : 1,4,6,8: bacterial culture after overnight incubation, 3,5,7,9: insoluble (IBs fraction), b) colony 4, (lanes 1-2: bacterial culture at 16°C, lane 3: molecular mass marker, lanes 4-5, bacterial culture at 22°C, lanes 6-7: bacterial culture at 28°C, lanes 8-9: bacterial culture at 37°C, : 1,4,6,8: bacterial culture after overnight incubation, 2,5,7,9: insoluble (IBs fraction). Test performed by Pulks, 2012.

Relative density of bands present on Western blot was measured by using ImageJ software. Colony 3 of pHB3 plasmid showed similar proinsulin expression when 22°C, 28°C or 37°C were used as induction temperature (Figure 3.23 a). However the highest amount of the protein was expressed at 22°C. When temperature was lowered to 16°C, proinsulin was expressed the least. Similar comparison was performed for expression of proinsulin from colony 4 of pHB3 (Figure 3.23 b). Analysis of Western blot results showed that when 28°C was used as temperature during expression, proinsulin was obtained in greater amounts than in case of cultures performed at 22°C or 37°C. When expression temperature was lowered to 16°C, proinsulin was expressed in much lower amounts. Colony 4 showed a noteworthy difference of proinsulin expression between overnight (lanes 1, 4, 6 and 8, Figure 3.23 b) and IB fractions (lanes 2, 5, 7 and 9, Figure 3.23 b). As in previous tests 22°C and 28°C showed the most promising results, one more induction temperature was chosen: 25°C. pHB1 plasmid (colony 2) and pHB3 plasmid (colony 3) were further tested. SDS-PAGE and Western blot analysis of samples collected after overnight incubation and inclusion bodies fractions were performed. Comparison of following temperatures: 22°C, 25°C, 28°C and 37°C at Western blot presents Figure 3.24 a (plasmid pHB1 – colony 2) and Figure 3.24 b (plasmid pHB3 – colony 3).

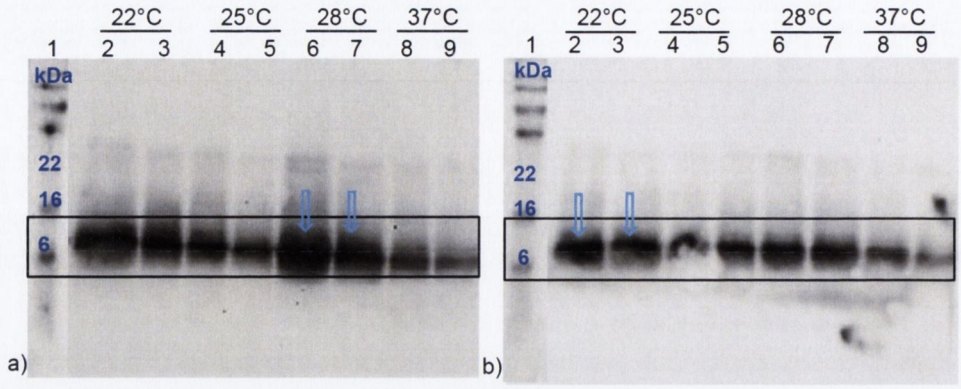

Fig 3.24 *Western blot analysis of expression and Inclusion bodies (IB) production at various temperatures a) for pHB1 plasmid – colony 2, b) for pHB3 plasmid – colony 3, (1st Ab: Insulin A (C-12) goat polyclonal IgG: 1:1000, 2nd Ab: Donkey anti-goat IgG-HRP: 1:5000).*
(a) pHB1 plasmid – colony 2, (lane 1: molecular mass marker, lanes 2-3: bacterial culture at 22 °C, lanes 4-5, bacterial culture at 25 °C, lanes 6-7: bacterial culture at 28 °C, lanes 8-9: bacterial culture at 37 °C, : 2,4,6,8: bacterial culture after overnight incubation, 3,5,7,9: insoluble (IBs fraction), b) pHB3 plasmid – colony 3 – samples were loaded in the same sequence as for Figure 4.20 a). Test performed by Pulks, 2012.

To compare the bands on Western blot picture relative density was measured with ImageJ software. In case of pHB1 plasmid (Figure 3.24 a) a maximum proinsulin expression is shown in samples of 28°C, following 22°C and then 25°C. Overall proinsulin production was similar in all of the tested cases. Colony 3 of pHB3 plasmid (Figure 3.24 b) showed that the maximum proinsulin expression was obtained for 22°C followed by 28°C. Unfortunately, the sample after overnight incubation in western blot was damaged (lane 4, Figure 3.24 b) so the results of 25°C experiments are incomplete.

3.4 Establishing protocols for purification of expressed proinsulin

3.4.1 Purification and ALP protease cleavage of proinsulin expressed by pMD2 plasmid

3.4.1.1 His tag column purification of periplasmic fraction of pMD2 plasmid

Having good expression of the plasmid in *E. coli*, the periplasmic localisation and solubility of expressed protein were determined. The data is presented in Section 3.3.1 of the thesis. Fusion of proinsulin with DsbA protein resulted in the expression of the protein in the periplasm. However, the main part was expressed in the form of insoluble inclusion bodies. Since the amount of protein present in the periplasmic fraction was very small (Figure 3.9 b), an optimisation of expression conditions was carried out. Based on a literature review (Winter et al., 2000), the temperature of the culture after IPTG induction was decreased to 30°C in order to improve the yield of

the protein sent to the periplasm. Periplasmic fractions from cultures held at two temperatures (30°C and 37°C) were isolated. Having the His tag region allowed for simplification of the purification process. Prepared periplasmic fractions of proteins expressed by the pMD2 plasmid were purified by using Ni^{2+} binding (Histrap) column (Section 2.4.1.19). Purified periplasmic fractions of pMD2 plasmid were compared by SDS-PAGE (Figure 3.25 a) and Western blot (Figure 3.25 b).

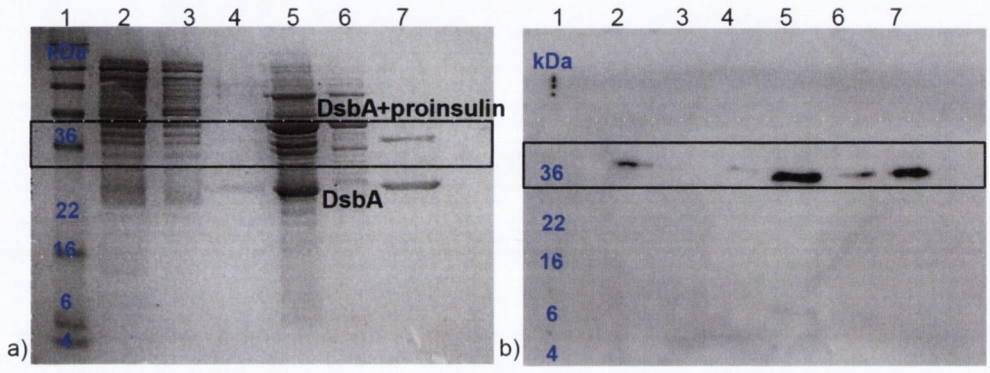

Fig 3.25 ***a)*** *SDS-PAGE and* ***b)*** *Western blot analysis of Ni column binding test for periplasmic fractions of pMD2 plasmid cultured at 30°C and 37°C (IPTG induction), (1st Ab Monoclonal Anti-insulin Mouse IgG: 1:1000, 2nd Ab Anti-mouse IgG HRP: 1:5000).*

(both gels were loaded in the same order, as follows: lane1: molecular mass marker, 2: periplasmic fraction of pMD2 plasmid cultured at ***37°C*** *before Ni column,3: flow through fraction of sample in lane 2, 4: eluate of sample in lane 2, respectively, 5: periplasmic fraction of pMD2 plasmid cultured at* ***30°C*** *before Ni column, 6: flow through fraction of sample in lane 2, 7: eluate of sample in lane 2).*

Analysis of SDS-PAGE and Western blot confirmed that the decrease of temperature to 30°C led to an increase in the amount of protein present in the periplasm. Thus, for further experiments, bacteria were cultured at 30°C. There was a small amount of the protein that remained in the flow through fraction (protein not bound to the Histrap column), which might be due to the fast rate of the purification process. Figure 3.26 shows a typical SDS-PAGE gel with eluate (proteins bound to the Ni^{2+} column) fractions after purification of the periplasmic fraction the proteins expressed by pMD2 on Ni^{2+} column.

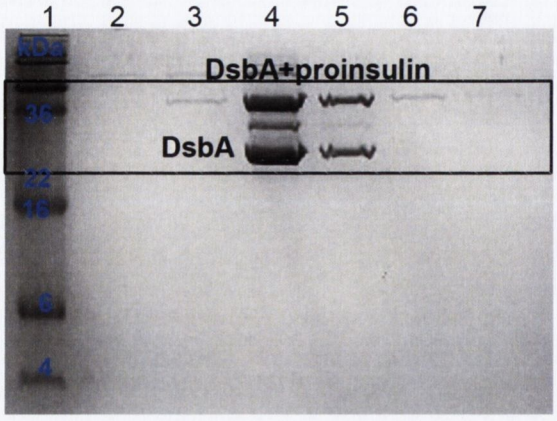

Fig 3.26 *SDS-PAGE analysis of eluate fractions after Ni^{2+} binding for periplasmic fraction of pMD2 plasmid (culture at 30 °C, IPTG induction).*
(lane 1: molecular mass marker, 2, 3, 4, 5, 6 and 7: eluate fractions after purification).

Fractions with the greatest amount of the protein (fraction 4 and 5) were combined and stored at 4°C for further experiments.

3.4.1.2 ALP protease digestion

The next step of the purification process was the cleavage of proinsulin from the DsbA protein. ALP protease was used as a specific enzyme, which cleaves proteins at the C-terminus of lysine. Series of experiments were performed to optimise the ALP cleavage conditions, i.e., concentration of the protease and incubation time (Section 2.4.1.22).

Different dilutions of ALP in TBS buffer were prepared (0.0001 U – 1 U) and the Ni^{2+} column purified sample of pMD2 periplasmic fraction was treated with the cleavage enzyme for 5 minutes. The initial test showed an approximate concentration of ALP enzyme required for cleavage of insulin from DsbA protein, which was between 0.01 U and 0.1 U. In the next step, the range of ALP concentration was narrowed down to 0.01 U – 0.1 U. Time of reaction remained the same (5 minutes). The ALP cleavage was analysed with SDS-PAGE (Figure 3.27 a) and Western blot (Figure 3.27 b).

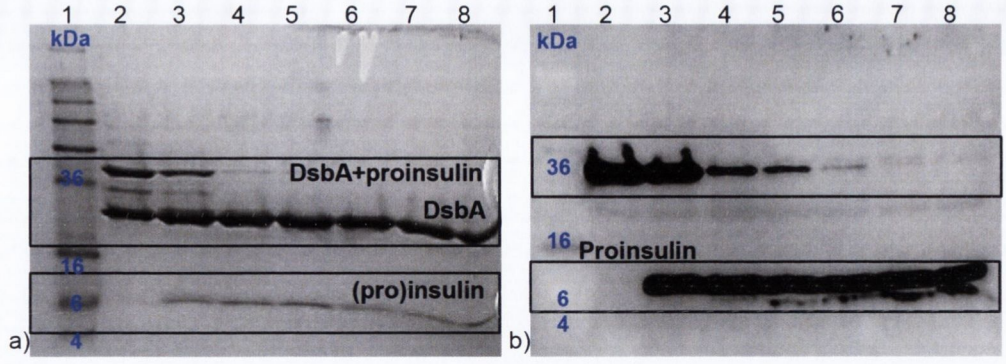

Fig 3.27 ***a)*** *SDS-PAGE and* ***b)*** *Western blot analysis of concentration dependent ALP digestion (incubation time 5 mins) of purified periplasmic fraction of pMD2 (culture at 30 °C, IPTG induction), (1st Ab Monoclonal Anti-insulin Mouse IgG: 1:1000, 2nd Ab Anti-mouse IgG HRP: 1:5000).*

(lane 1: molecular mass marker, 2: purified periplasmic fraction of pMD2 before enzyme digestion, 3: 0.01 U, 4: 0.03 U, 5: 0.05 U, 6: 0.07 U, 7: 0.09 U, 8: 0.1 U of ALP).

The experiment was repeated in order to obtain fresh fractions of insulin after cleavage and to confirm obtained results.

Based on performed experiments optimum ALP cleavage conditions were established (concentration of ALP was 0.05 U and incubation time 5 minutes).

In order to localise the His-tag during the cleavage and purification steps, SDS-PAGE (Figure 3.28 a) and Western blot (Figure 3.28 b) analysis was performed with a His tag anti-mouse antibody.

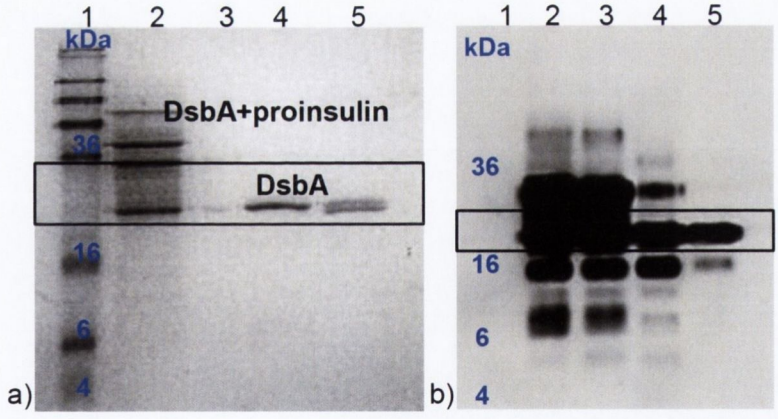

Fig 3.28 ***a)*** *SDS-PAGE and* ***b)*** *Western blot analysis of purified samples of pMD2 plasmid cleaved with ALP, (1st Ab: His tag mouse monoclonal: 1:1000, 2nd Ab: Anti-mouse IgG HRP: 1:5000).*

(both gels were loaded in the same order, as follows: lane 1: molecular mass marker, 2: periplasmic fraction of pMD2 plasmid before loading to Ni column, 3: sample before ALP cleavage, 4: sample treated with 0.05 U of ALP, 5: combined fractions of samples cleaved with 0.03 – 0.1 U of ALP).

Analysis of SDS-PAGE showed the presence of cleaved DsbA protein after the ALP proteolytic cleavage (lane 4 and 5, Figure 3.28 a). Western blot performed with His tag anti-mouse antibodies showed the presence of proteins with different molecular weights having the His tag. There was a band with a molecular weight of ~20 kDa, which corresponds to the DsbA protein (21.1 kDa) observed after ALP protease cleavage (lane 5), confirming the separation of DsbA from proinsulin. ALP protease is an enzyme, which cleaves specifically at C-terminus of lysine, which suggests many cleavage sites. As a result of the cleavage, proteins with a range of sizes were formed, as seen on the Western blot (Figure 3.28 b).

To ensure that insulin was not degraded by ALP protease during incubation, standard of insulin was incubated with the enzyme. 0.05 U of ALP was used as before. The incubation time was 10, 20 and 30 minutes. The reaction was stopped by adding the protease inhibitor cocktail. Additionally, samples obtained after cleavage of proteins present in the periplasmic fraction of the protein expressed by pMD2 were characterised. Analysis of the samples was performed with SDS-PAGE (Figure 3.29 a) and Western blot (Figure 3.29 b).

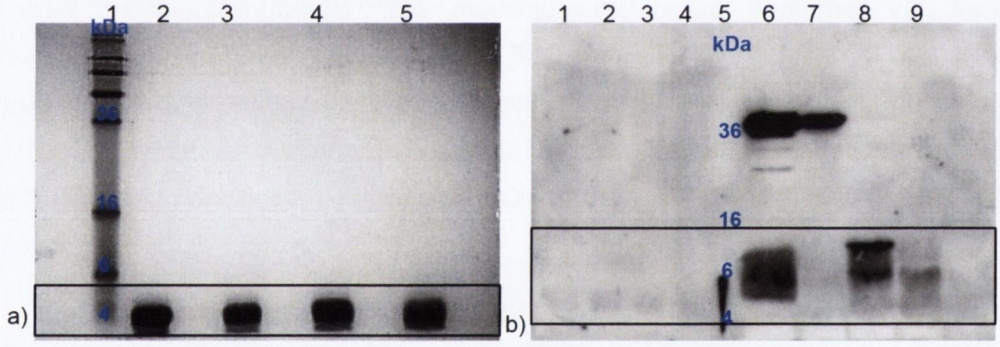

Fig 3.29 a) SDS-PAGE and **b)** Western blot analysis of insulin standard and purified samples of pMD2 plasmid cleaved with ALP, *(1st Ab: Insulin A (C-12) goat polyclonal IgG: 1:1000, 2nd Ab: Donkey anti-goat IgG-HRP: 1:5000).*
(a) lane 1: molecular mass marker, 2: 1 mg/ml of insulin standard, 3: 1 mg/ml of insulin standard with 0.05 U of ALP, 10 min incubation, 4: 1 mg/ml of insulin standard with 0.05 U of ALP, 20 min incubation, 5: 1 mg/ml of insulin standard with 0.05 U of ALP, 20 min incubation, b) lane 1: 1 mg/ml of insulin standard, 2: 1 mg/ml of insulin standard with 0.05 U of ALP, 10 min incubation, 3: 1 mg/ml of insulin standard with 0.05 U of ALP, 20 min incubation, 4: 1 mg/ml of insulin standard with 0.05 U of ALP, 20 min incubation, 5: molecular mass marker, 6: periplasmic fraction of pMD2 plasmid before loading to Ni column, 7: sample before ALP cleavage, 8: sample treated with 0.05 U of ALP, 9: combined fractions of samples cleaved with 0.03 – 0.1 U of ALP).

Analysis of SDS-PAGE showed good stability of insulin after its incubation with the ALP protease. However, Western blot did not confirm the presence of insulin standard, also without the enzyme (lane 1), which would suggest that insulin A-chain antibody did not recognise the insulin standard (lanes 1 – 4), although the antibody

seems to have recognised proinsulin bound to DsbA and cleaved proinsulin (lanes 6 – 9). A weaker band was seen when the fractions obtained after ALP cleavage were mixed, which could suggest instability and degradation of the protein during the cleavage process.

Further gel filtration is suggested as a final step of the purification process. Additionally, mass spectrometry should be performed to estimate the size of purified protein.

3.4.2 Purification of pHB1 plasmid expressed in the form of insoluble inclusion bodies

In parallel, the optimisation for the purification of inclusion bodies expressed by pHB1 plasmid was explored, as a significantly larger amount of the protein was expressed in this form. More complex purification protocol had to be performed, as the protein had to be isolated, washed, cleaved, purified and finally renaturated to obtain its native structure.

3.4.2.1 Establishment of an optimised method for proinsulin refolding reaction

Many protocols have been described to refold misfolded proinsulin produced by recombinant DNA technology utilising different refolding reagents. To obtain a high yield of proinsulin after refolding reaction, four different refolding reagents were tested in this study and compared. Optimisation of refolding reaction was performed under my supervision by Darragh Kelly as part of a Senior Sophister research project: "Development of an optimised method for proinsulin refolding" (Kelly, 2011). A fraction of misfolded proinsulin (collected after refolding reaction carried out as a part of pHB1 purification protocol) was divided into six equal portions. Four of them were used for refolding reaction test with four different refolding reagents. Details of the refolding reaction procedure are described in Section 2.4.1.23. The process consisted of: denaturation of the sample with 1 mM EDTA and 8 M urea (Section 2.4.1.23.1), sulfitolysis reaction using 0.2 M sodium sulphite and 20 mM sodium tetrathionate (Section 2.4.1.23.2) and final refolding (Section 2.4.1.23.3) with one the following reagents:

1) 1 mM GSH/5 mM GSSG
2) β-mercaptoethanol 18 M/mol of protein (MW of proinsulin = 9394.6 Da)
3) 5 mM DTT
4) 0.5 mM cysteine/4.5 mM cystine

At each stage of the process (denaturation, oxidative sulfitolysis and refolding), a sample was collected and quantified with BioRad Protein Assay. Additionally, obtained samples were analysed by SDS-PAGE (Figure 3.30).

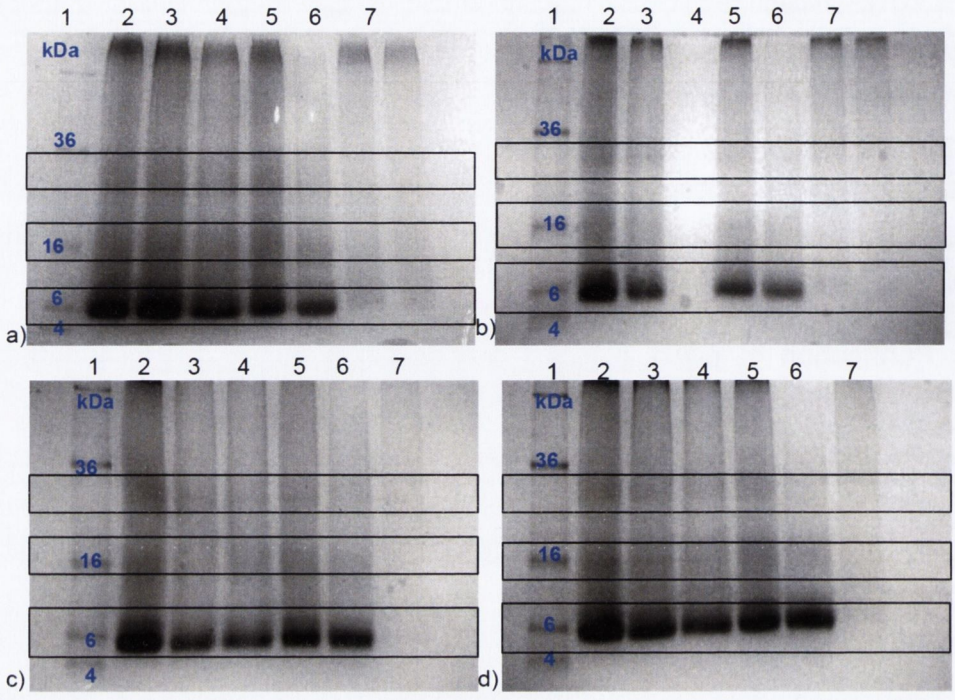

Fig 3.30 *SDS-PAGE analysis of refolding reaction process using refolding reagent:* ***a)*** *1 mM GSH/ 5 mM GSSG,* ***b)*** *β-ME,* ***c)*** *5 mM DTT,* ***d)*** *0.5 mM cysteine/4.5 mM cysteine.*

(samples in each gel were loaded in the same order as follows: lane 1: molecular mass marker, 2: sample of misfolded protein before starting the refolding process, 3: sample after denaturation process, 4: sample after sulfitolysis reaction, 5: resuspended pellet before refolding reaction, 6: sample after refolding reaction (properly folded protein), 7: sample after refolding reaction (misfolded protein).

Analysis of the gels shows that there was a strong band of proinsulin observed in each of the gels. MW of the band (~6 kDa) was however smaller than that of proinsulin (~9.4 kDa), which might be due to the low resolution of the gels. Additionally, each of the samples taken before refolding reaction showed a reasonable degree of a background noise indicating that there were aggregates and contaminants present in the sample. In particular, faint bands could be observed at ~18 kDa and ~27 kDa, which correspond to oligomeric proinsulin species such as dimers and trimers. It was noticed that the bands of samples taken directly after refolding were clearer, which might suggest that some of the non-native species present in the samples before refolding were refolded correctly. An additional purification step is a suggestion for future work (i.e., gel filtration chromatography) in order to remove remaining aggregates and to obtain a higher yield of pure and properly folded proinsulin.

To assess the difference between the percentage yields of the refolding reaction, samples of the protein were collected at various points of the process for protein quantification assay. The absorbance at 595 nm was recorded, averaged and used

to estimate the amount of the protein (Section 2.4.1.20). The results of the BioRad Protein Assay are summarised in Table 3.1.

Table 3.1 *Protein amount at different stages of the refolding process.*

	GSH/GSSG	β-ME	DTT	Cysteine/Cystine
Sample before starting refolding process	25.8 mg	22.7 mg	32.1 mg	27.3 mg
Sample after denaturation with Urea / EDTA	22.7 mg	20.3 mg	31.1 mg	26.4 mg
Sample after sulfitolysis reaction	22.4 mg	n/a	25.4 mg	22.4 mg
Resuspended pellet before refolding reaction	21.3 mg	19.8 mg	20.9 mg	20.7 mg
Sample taken after refolding reaction (properly folded reaction)	11.9 mg	8.2 mg	8.8 mg	11.3 mg
Sample taken after refolding reaction (misfolded protein)	11.3 mg	9.5 mg	7.6 mg	9.0 mg
Yield of the process	**55.7%**	**41.3%**	**42.0%**	**54.6%**

As shown in Table 3.1, a small amount of the protein was lost at each stage of the process, most likely due to the transfer between tubes or in process losses. BioRad quantification confirmed the presence of misfolded protein, which was not visible on the Western blot. It might be due to the properties of the antibody used, which did not recognise the misfolded protein that was formed during the refolding process. In order to accurately compare the efficacy of the refolding reactions, percentage yields were calculated using quantities of the samples directly before and directly after the refolding reaction. Comparable percentage yields were obtained using GSH/GSSG (~56%) and cysteine/cystine (~55%). Yields of ~41% and 42% were attained using β-ME and DTT, respectively.

3.4.2.2 Establishement of final protocol for pHB1 inclusion bodies purification

Having optimised all aspects of the purification process of proinsulin, a final protocol for pHB1 inclusion bodies purification was established and tested (Section 2.4.1.24). IPTG was used to induce expression of proteins (Section 2.4.1.16.1). Culturing was performed at 30°C. The bacterial culture with pHB1 plasmid was harvested and periplasmic fraction was isolated first. The remaining pellet containing inclusion bodies was solubilised and lysed by sonication (Section 2.4.1.24.1). Inclusion bodies were washed with PBS and resuspended in pH adjusted buffer (first pH 11, then pH

9.5). In the next step oxidative sulfitolysis (Section 2.4.1.24.2) and CNBr cleavage (Section 2.4.1.24.3) were carried out. SDS-PAGE electrophoresis (Figure 3.31 a) and Western blot (Figure 3.31 b) analysis were performed to monitor the purification process.

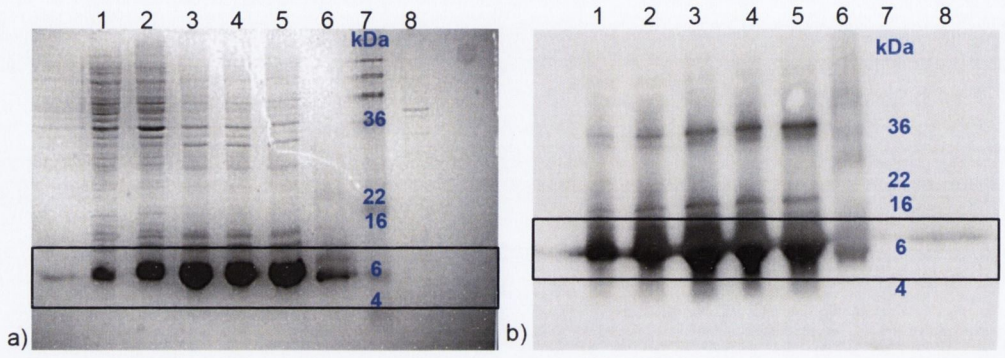

Fig 3.31 ***a)*** *SDS-PAGE and* ***b)*** *Western blot analysis of pHB1 inclusion bodies purification process, (1st Ab: Insulin A (C-12) goat polyclonal IgG: 1:1000, 2nd Ab: Donkey anti-goat IgG-HRP: 1:5000).*
(both gels were loaded as follows: lane 1: solubilised pellet before sonication, 2: inclusion bodies washed in PBS, 3: solubilised inclusion bodies after pH adjustment, 4; sample before sulfitolysis reaction, 5: sample after sulfitolysis reaction, 6: sample after CNBr cleavage, 7: molecular mass marker, 8: pHB1 periplasmic fraction).

SDS-PAGE and Western blot analysis showed a small amount of proinsulin present in the periplasm, but most of the protein was expressed in the form of insoluble IBs. There was a strong band of proinsulin observed during all purification steps. Furthermore, CNBr cleavage was confirmed by two bands observed (proinsulin and insulin). It was observed that there was a smaller amount of the protein after its cleavage with CNBr. As reported, the efficiency of this bond cleavage is greater than 90% in most of the cases (Kaiser and Metzka, 1999). A further optimisation of the cleavage reaction is a suggestion for future work (optimisation of CNBr concentration, reaction time, buffer composition and pH). Since there were many other proteins with higher molecular weights present in the sample, cation exchange chromatography was carried out to purify the sample. The sample was divided into four parts and purified in parallel in four columns used in cation exchange chromatography (Section 2.4.1.24.4). Gradient concentration of salt (NaCl) was used to elute the sample from the column. All fractions were collected and analysed with SDS-PAGE (Figure 3.32 a and 3.32 c). Purified proteins were also analysed with Western blot as a more sensitive method than SDS-PAGE (Figure 3.32 b and 3.32 d).

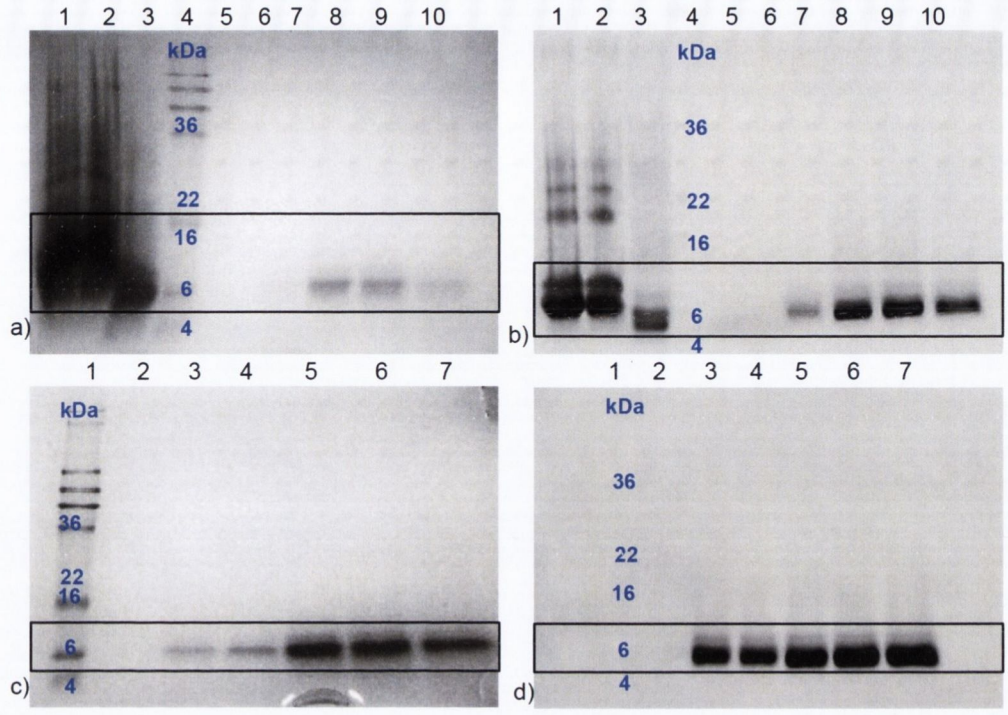

Fig 3.32 *SDS_PAGE (**a)** and **c)**) and Western blot (**b)** and **d)**) analysis of samples obtained after cation exchange purification, (1st Ab: Insulin A (C-12) goat polyclonal IgG: 1:1000, 2nd Ab: Donkey anti-goat IgG-HRP: 1:5000).*
(gels were loaded as follows: gel a and b: lane 1 and 2: samples before CNBr cleavage, 3: sample after CNBr cleavage, 4: molecular mass marker, 5: flow through fraction, 6: 6: eluate with 100 mM NaCl, 7: eluate with 250 mM NaCl, 8: eluate with 500 mM NaCl, 9: eluate with 750 mM NaCl, 10: eluate with 1000 mM NaCl), (gel c and d: lane 1: molecular mass marker, 2: flow through fraction, 3: eluate with 100 mM NaCl, 4: eluate with 250 mM NaCl, 5: eluate with 500 mM NaCl, 6: eluate with 750 mM NaCl, 7: eluate with 1000 mM NaCl).

Western blot analysis confirmed the presence of proinsulin in the eluate, which appeared as a clean band. There was a small and very faint band with larger molecular weight, which corresponds to the sample before CNBr cleavage. Refolding reaction was performed next in order to obtain the proper disulfide bridges for proinsulin. To remove the salt present in the sample after elution, dialysis against refolding buffer was performed (Section 2.4.1.21). Based on the previous findings (Section 3.4.2.1), GSH/GSSG was used as the refolding reagent since it showed the best yield. Properly folded proinsulin was concentrated and cleaved with proteolytic enzymes: trypsin and carboxypeptidase B (Section 2.4.1.24.6). SDS-PAGE and Western blot of analysed samples is presented in Figure 3.33.

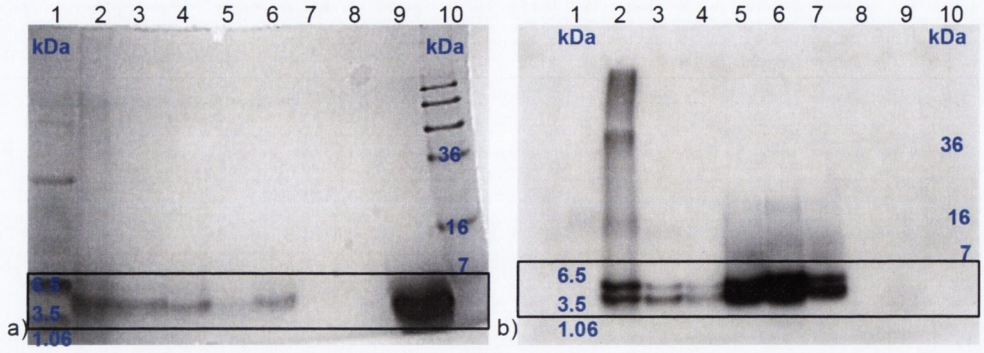

Fig 3.33 ***a)*** *SDS-PAGE and* ***b)*** *Western blot analysis of proinsulin refolding and proteolytic cleavage, (1st Ab: Insulin A (C-12) goat polyclonal IgG: 1:1000, 2nd Ab: Donkey anti-goat IgG-HRP: 1:5000).*

(gel a and b was loaded in the same sequence as follows: lane 1: molecular mass marker for tricine gels (colour marker ultra-low range), 2: sample before loading to the column, 3: sample 1 after cation exchange, 4: sample 2 after cation exchange, 5: sample after dialysis and before refolding, 6: sample after refolding and concentration, 7: 1/5 part of sample before proteolytic cleavage, 8: sample after proteolytic cleavage, 9: insulin standard 7 mg/ml, 10: molecular mass marker).

Analysis of the SDS-PAGE gel and Western blot showed that a pure sample was obtained after purification by cation exchange chromatography. A large and strong band was observed on the Western blot after the refolding process (lane 6). Since insulin A chain antibodies were applied to the Western blot analysis, two bands were visible each time. One of them corresponds to the proinsulin and the other to A-chain of insulin. It was noticed that the size of proinsulin present on the gels was smaller than ~9.4 kDa, as it appeared below the band at 6.5 kDa. It might be due to the resolution of the gels, as it is quite difficult to obtain good separation for proteins with low MW. There was no band of insulin standard (lane 9, Figure 3.33 b) and insulin after proteolytic cleavage (lanes 8, Figure 3.33 b) present on the Western blot. The insulin A-antibody did not recognise the insulin standard, however it recognised insulin A-chain in the proinsulin.

The comparison of purification protocols established for proinsulin expressed by plasmid pMD2 and pHB1 shows Figure 3.34.

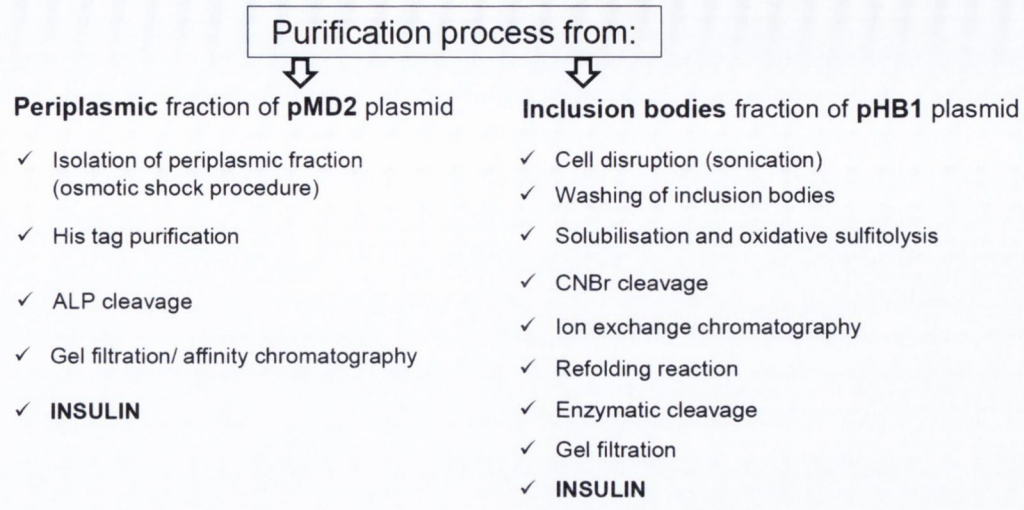

Fig. 3.34 *Purification process for protein expressed in periplasm by pMD2 plasmid, and protein expressed in the form of inclusion bodies by pHB1 plasmid.*

3.5 Conclusions

Currently, insulin is produced by recombinant DNA technology, using *E. coli* or yeast as a host organism. To facilitate further modifications of the insulin gene, several plasmids with insulin were designed and prepared. The preparation strategy was based on the combination of the simplicity of the bacterial expression system, which is fast to work with, cheap and easy with the benefits from the yeast expression system, i.e., fewer post-processing steps as periplasmic localisation can ensure correct disulfide bridges (Missiakas and Raina, 1997) and only one proteolytic cleavage step would be required. Five plasmids with insulin were prepared with various combinations, to obtain the best possible yield in the desired form. Figure 3.35 summarizes the composition of prepared plasmids.

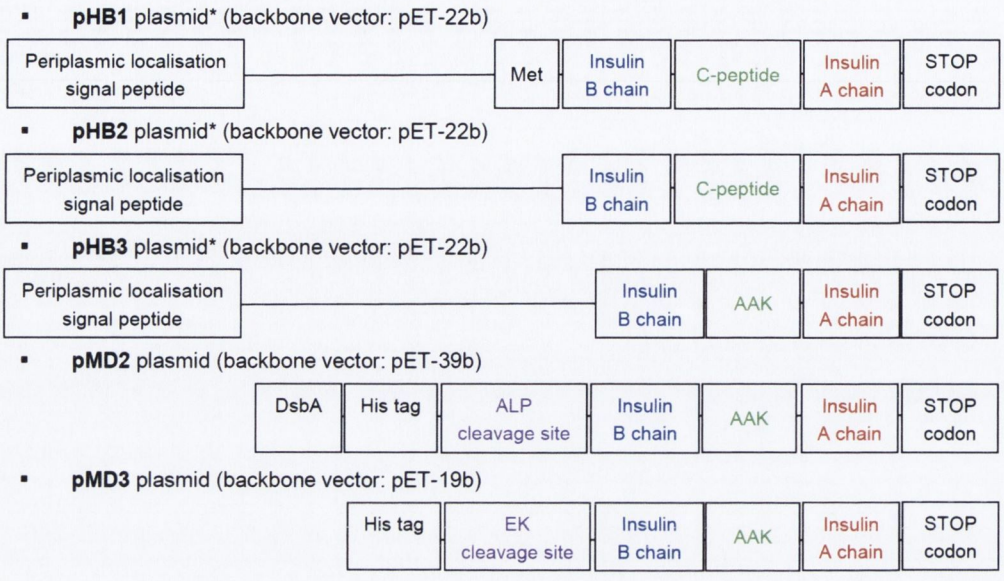

Fig. 3.35 *Summary of prepared plasmids.*
* Plasmids pHB1-3 were prepared as an M.Sc. project: "Establishing a novel laboratory scale expression system for recombinant human insulin in bacteria" (Boutsikaris, 2009).

Optimisation of expression conditions was further investigated by testing two different induction systems: IPTG and auto-induction, and also various temperatures. The impact of those factors on the solubility and the localisation of expressed protein was also examined.

Initially, expression for all of five plasmids was induced by IPTG, as a commonly used induction system. Expressed proteins were further tested for their cellular localisation (cytoplasmic/periplasmic) and the form in which was expressed (soluble/insoluble (inclusion bodies)). Prepared plasmids successfully expressed proinsulin, however the amounts of expressed proteins and its solubility was highly variable. A higher expression level was obtained for plasmids pHB1-3, however the protein was expressed only in the form of inclusion bodies. Fusion to DsbA (plasmid pMD2) successfully enhanced protein expression in the periplasm, although the amount of expressed protein was smaller compared to plasmid pHB1. In case of pMD3, the amount of protein expressed in the form of inclusion bodies was not sufficient for further study.

Next, expression of proteins was induced by using system characterised by Studier et al., called auto-induction (Studier, 2005). A study reported by Sivashanmugam et al. (2009) showed an impact of the induction system used for heterologous protein overproduction. However no such a study was performed on proinsulin expression. pHB1 and pHB3 plasmids were tested as they showed the highest expression level. Expression of four colonies was tested. Similarly to the induction by IPTG,

expression of pHB1 plasmid occurred in the form of inclusion bodies, however interesting results were obtained for pHB3 plasmid. Colony 1 was expressed in form of inclusion bodies, although colony 2, 3, and 4 expressed protein mostly in the form of inclusion bodies, but there was a fraction present in the periplasm as well. These results confirmed that optimisation of expression conditions is a very important step, which needs to be optimised for each protein. As reported in Section 4.3.2 the type of media tested: ZY-5052 and ZYM-5052 had no impact on the yield and form of expressed protein.

Additionally it was noted that temperature of culture plays an important factor. When pHB3 was cultured at 37°C, the protein was expressed in form of inclusion bodies. Lowering the temperature to 22°C increased the yield of protein expressed in the periplasm. The results described in details in Section 4.4 suggest that there is not one temperature that will be optimum for all of the plasmids, as different conditions were better for each of the plasmids tested. The best yield of protein expression was obtained if the temperature ranged from 22°C to 28°C.

Final optimisation of the purification protocols was established. Prepared plasmids can be used for further genetic modifications such as fusions of insulin gene with cell penetrating peptides.

In our case the form of protein expression played an important role for further purification. As mentioned previously, the expression in the periplasm was achieved for pMD2 plasmid, although at low level. Further optimisation of expression conditions (lowering temperature of culture to 30°C) increased the yield of soluble protein expressed in periplasm. The purification of expressed protein was performed using the advantage of incorporated His tag and ALP cleavage site. Expression in the periplasmic fraction ensured proper folding of the protein, however the yield was significantly lower, compared to the plasmid pHB1. Figure 9.4 compares the periplasmic fraction of pMD2 plasmid, after its isolation, further purification with His tag and cleavage with ALP protease. In parallel, the optimisation for the purification of inclusion bodies expressed by pHB1 plasmid was explored, as a significantly larger amount of the protein was expressed in this form. More complex purification protocol had to be performed, as the protein had to be isolated, washed, cleaved, purified and finally renaturated to obtain its native structure. Moreover, optimisation of the refolding reaction was performed, as it was one of the steps that had an impact on final yield of the purification process.

CHAPTER 4

CHARACTERISATION AND STABILITY OF ALGINATE/PROTAMINE CARRIERS

4.1 Introduction

Recent advances in nanotechnology are focused on using polymeric nanoparticulate systems as carriers for peptide drugs (Delie and Blanco-Prieto, 2005). Nanoparticles (NPs) formulated from natural polymers have attracted considerable interest as protein carriers. They have many advantages, such as the potential to retain protein stability, increase duration of therapeutic effects of proteins and they can be administered by nonparenteral routes (Sarmento et al., 2007 a). Different nanoparticulate formulations used for oral delivery of insulin have been reviewed by Damgè et al. (2008). These include nanoparticles which are based on chitosan, alginate or chitosan/alginate or alginate/chitosan/poly(ethylene glycol) (PEG) (Damgè et al., 2008). Another approach for peptide drug delivery that has been extensively studied over past two decades is the use of cell-penetrating peptides (Temsamani and Vidal, 2004, Snyder and Dowdy, 2004). Cell penetrating peptides (CPPs) are relatively short (up to 30 amino acids in length), cationic and/or amphipathic peptides that are derived from natural sources such as animal toxins or synthetically designed constructs (Xia et al., 2011). Oligoarginine rich CPPs have been reported as enhancers of intestinal absorption of insulin (Morishita et al., 2007). Silva et al., developed alginate microspheres coated with chitosan prepared by an emulsification/internal gelation method with a mean diameter that ranged from 65 to 106 µm (Silva et al., 2006). An ionic pregelation method of alginate with calcium chloride, followed by complexation between alginate and chitosan was used to prepare nanoparticles loaded with insulin. Particle size ranged from 764 to 2209 nm, with decreasing chitosan to alginate mass ratio (Sarmento et al., 2006 a). Polyelectrolyte complex formation using alginate and chitosan as oppositely charged polymers has been reported by Saether et al. As reported, the net charge ratio between chitosan and alginate, and the molecular weights (MW) of both the alginate and chitosan samples were the most significant parameters that influenced the particle size, zeta potential (ZP) and pH (Saether et al., 2008). A similar study was conducted by Sarmento's research group, where colloidal carriers prepared by complexation of two oppositely charged polymers: dextran sulphate (as an anionic polymer) and chitosan (as a cationic polymer) were used as a carrier for insulin (Sarmento et al., 2007 a).

The polyelectrolyte complexation method (PEC) of nanoparticle preparation has received increasing attention as NPs formed by this method have several characteristic advantages for cellular uptake and colloidal stability, including suitable diameter and surface charge, spherical morphology and low polydispersity index (Pdl) (Avadi et al., 2011). Furthermore, the preparation of NPs by PEC methods can be carried out in completely aqueous conditions and at ambient temperature, so the

stability and biological activity of loaded peptides would not be affected (Hu et al., 2012).

The aim of this work was to prepare and characterise cross-linker free and stable NPs composed of only alginate and protamine as CPP. To achieve this goal, the alginate/protamine manufacturing process was comprehensively investigated, including an examination of the type of polymer, polymer mixing ratio, sequence of mixing the polymers and speed of polymer addition was carried out. The physical stability of the nanoparticle dispersion on storage at room temperature and upon the exposure to different pH values was also examined.

4.2 Formulation of empty alginic acid/ protamine NPs

4.2.1 Physicochemical properties of NP components: alginic acid and protamine

The viscosity and pH of nanoparticle component solutions were characterised prior to starting formulation experiments. Protamine (P) and three different types of alginic acid solutions were prepared at the following concentrations: 0.2%, 0.1% and 0.05% w/v. The data is presented in Table 4.1.

Table 4.1 *pH and viscosity of alginic acid and protamine solutions. AAH – alginic acid high viscosity (14.000 cps for 2% w/v solution*), AAM – alginic acid medium viscosity (3.500 cps for 2% w/v solution*), AAL – alginic acid low viscosity (250 cps for 2% w/v solution*).*
** - manufacturer data*

Component	Concentration [%]	pH	Viscosity [mPa·s]
AAH	0.05	6.35	3.49±0.11
	0.1	6.53	6.50±0.26
	0.2	6.80	11.47±0.54
AAM	0.05	6.33	2.85±0.06
	0.1	6.37	4.19±0.14
	0.2	6.36	6.55±0.10
AAL	0.05	6.33	1.00±0.03
	0.1	6.39	2.72±0.10
	0.2	6.25	3.60±0.20
PROTAMINE	0.05	5.47	0.81±0.02
	0.1	5.81	0.97±0.06
	0.2	6.00	0.88±0.06

Analysis of the data obtained showed that the viscosity of the above solutions decreased in the following order AAH>AAM>AAL>P for a given concentration. Higher viscosity values were measured for solutions with higher concentrations. The concentration of polymer had an impact on its pH for AAH only ($p<0.001$). For the two other types of polymer (AAM and AAL) only small changes in pH values were observed ($p>0.05$). In the case of P solution a decrease in the concentration caused

a decrease in pH values. There was a significant difference between viscosity of P solutions prepared at various concentrations ($p<0.01$).

As reported by Carneiro-da-Cunha et al. (2011), polymer concentration is one of the factors that has an impact on the mean hydrodynamic diameter and ZP of edible polysaccharide solutions (sodium alginate, carrageenan and chitosan), that were envisaged for use in multilayer film production. The authors studied sodium alginate at concentrations 0.2 – 0.6% w/v showing that an increase of polysaccharide concentration led to an increase of the average particle size. However, lowering the concentration of polymer to 0.2% w/v decreased the surface area and final loading capacity (Carneiro-da-Cunha et al., 2011). Therefore, in this work, to balance desirable NP characteristics and high efficiency of loading, 0.1% w/v solutions of alginic acid and protamine were used for further formulation testing.

4.2.2 Preliminary studies on the formation of alginic acid/protamine nanoparticles

Preliminary studies were performed to test whether alginic acid can form nanocomplexes with P. 0.1% w/v solution of AAL and 0.1% w/v solution of P were used. NPs were prepared by adding P solution to a stirred aliquot of AAL solution (method 1A, Section 2.4.2.3). Screening a wide range of AAL/P weight ratios was performed to check the impact of the component mixing ratio on NP formation and properties. Particle size, PdI and ZP of formed PECs were measured and are presented in Figures 4.1.1 and 4.1.2. Values presented in the graphs are summarised in Table A.1 (Appendix A). Mixing 0.1% w/v AAL with 0.1% w/v P resulted in the formation of NPs with different surface charge. Negatively charged NPs were formed for the AAL/P weight ratios 15 to 0.87. ZP values of those NPs ranged from -67.2 mV to -36.7 mV (Figure 4.1.1).

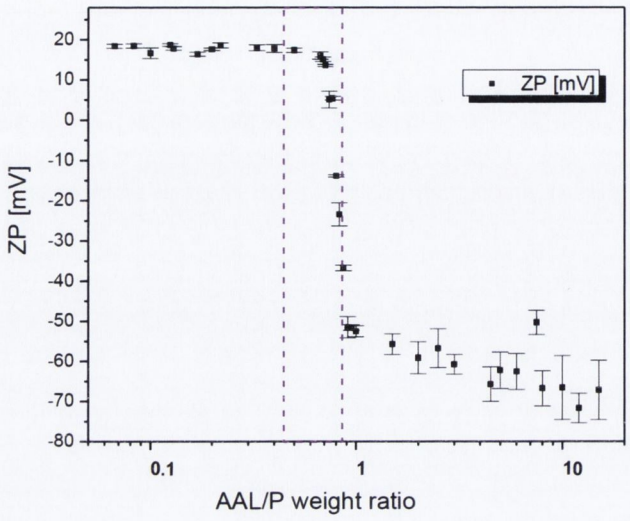

Fig. 4.1.1 *Zeta potential of NPs composed of AAL and P (---- - aggregates formed).*

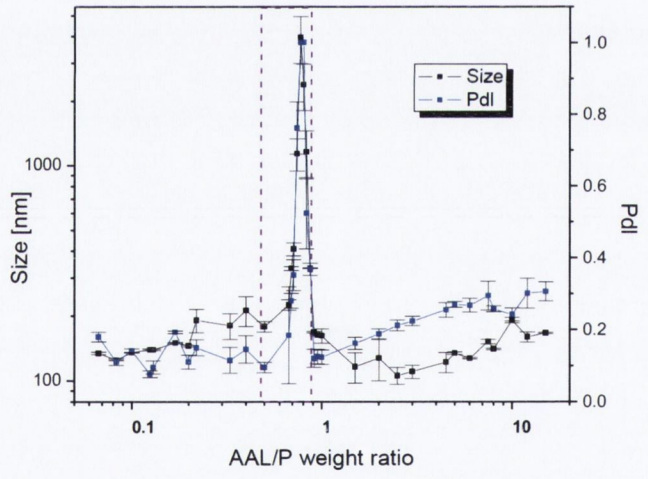

Fig. 4.1.2 *Particle size and polydispersity index of NPs composed of AAL and P (------ - aggregates formed).*

The particle size of negatively charged NPs was 105 – 332 nm with PdI of 0.120 – 0.368 (Figure 4.1.2). PdI values correlated with the AAL content - NPs with higher amounts of the polymer had greater PdI values. This could be explained by the fact that not all of the polymer was able to interact with P and so the excess alginic acid resulted in heterogeneity of the systems formed. A rapid increase in the size occurred when the net charge of NPs was close to being neutralised, which resulted in aggregation of the NPs and/or the formation of micron-sized entities (AAL/P weight ratio 0.83 – 0.50). Mixing AAL/P at weight ratios of 0.40 – 0.067 resulted in the formation of positively charged NPs with quite consistent ZP of 17.8 – 18.7 mV.

The size of those NPs was between 125 – 212 nm and PdI in the range of 0.077 – 0.180.

Generally, the negatively charged NPs were larger and associated with greater PdI values because of the presence of surplus polymer, which did not fully react. An increase in NP size and PdI value was observed when charge neutralisation of both components occurred. Positively charged NPs were characterised by a stable charge of ~18 mV and smaller size. Physicochemical characterisation of prepared NPs was also performed by measuring pH and viscosity of the dispersions (Table A.1, Appendix A). The pH of negatively charged NPs ranged between 6.46 and 6.02 for the AAL/P weight ratios of 15 – 0.87 and pH of 5.74 – 5.60 was measured for AAL/P NPs with weight ratios of 0.40 – 0.067 (positively charged NPs). Viscosity data is presented in figure 4.1.3.

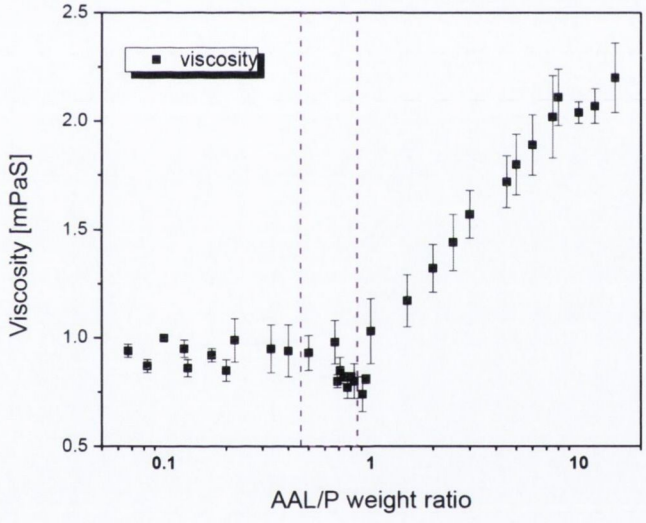

Fig. 4.1.3 *Viscosity of nanoparticles composed of AAL and P (---- - aggregates formed).*

The viscosity of nanoparticle suspensions prepared was related to the polymer/P weight ratio. Increasing the amount of polymer resulted in higher viscosity values of the continuous medium. Negatively charged NPs reached a viscosity value of 2.20 mPa·s for the greatest AAL/P weight ratio tested (15), which was lower than the viscosity of the 0.1% w/v solution of AAL (2.72 mPa·s, Table 4.1). It was observed that the viscosity of NPs decreased with increasing P content. Viscosity values of positively charged NPs were comparable, at ~0.90 mPa·s, which was similar to the viscosity of P solution (0.97 mPa·s, Table 6.1). The lowest viscosity value of 0.77 mPa·s, corresponding to the viscosity of water at RT, was measured for the system with an AAL/P weight ratio of 0.77. It can therefore be assumed that no excess

components were present in the continuous phase and at this particular component ratio full charge neutralisation was achieved.

4.2.3 Influence of formulation process on the properties of NPs

4.2.3.1 Sequence of alginic acid/protamine solution addition on NPs characteristics

To check the impact of the sequence of polymer addition in the preparation of P solutions, NPs prepared by two different methods were compared. Both of the methods are described in detail in Section 2.4.2.3. Table 4.2 compares the particle size, PdI and ZP of tested NPs.

Table 4.2 *Comparison of properties of AAL/P NPs prepared using two different modes of addition of NP components.* ***Method 1A****: an aliquot of P solution was added to the aliquot of polymer solution under magnetic stirring.* ***Method 1B****: an aliquot of polymer solution was introduced to the aliquot of P solution under magnetic stirring. Statistical analysis: # - no significant difference, *p<0.05, **p<0.01, ***p<0.001.*

AAL/P weight ratio	Particle size [nm]		PdI		ZP [mV]	
	Method of preparation:					
	1A	1B	1A	1B	1A	1B
5	134±2	236±1	0.270±0.008	0.242±0.016	-62.2±4.5	-67.9±2.0
	***		*		*	
3	110±8	213±2	0.224±0.013	0.207±0.008	-60.8±2.5	-64.4±0.7
	***		*		*	
1.5	116±19	424±4	0.162±0.017	0.376±0.011	-55.8±2.6	-60.3±0.7
	***		***		**	
1	162±12	167±1	0.123±0.019	0.114±0.010	-52.5±1.4	-52.2±0.8
	#		#		#	
0.67	225±13	245±4	0.185±0.135	0.216±0.013	16.0±0.9	16.1±0.5
	**		#		#	
0.33	180±25	144±2	0.115±0.036	0.122±0.028	18.0±0.7	17.2±0.6
	**		#		#	
0.20	145±1	113±2	0.111±0.019	0.215±0.008	17.6±0.3	18.0±0.5
	***		***		#	

Analysis of the particle size shows that there was a significant difference in the particle size for all of the formulations tested, with exception of the formulation with an AAL/P weight ratio of 1. NPs with a larger negative charge were formed using method 1B. A significant difference in PdI of NPs prepared by method 1A and 1B was noticed for negatively charged NPs and for one type of positively charged NP (AAL/P weight ratio of 0.2). The mixing sequence had a significant impact on the charge of NPs formed in the case of the three negatively charged formulations (Table 4.2). The order of solution addition may have an impact on NP formation perhaps due to microenvironmental pH changes around negatively charged polymer solution and positively charged protamine (Qiu and Park, 2001). Based on the above

results, method 1A was chosen for further studies as NPs formed by this method were generally smaller in size.

4.2.3.2 Slow/fast protamine solution addition to alginic acid

To examine the impact of the speed at which the protamine solution was added to the stirred aliquot of alginic acid, NPs were prepared by two different methods. Both of the methods are described in detail in Section 2.4.2.3. Size, PdI and ZP of the prepared NPs was compared (Table 4.3). Two formulations of negatively charged NPs were selected for these trials as the significant difference in the particle size within those formulation had previously been noted (Section 4.2.3.1).

Table 4.3 *Comparison of properties of AAL/P NPs prepared using two different speeds of addition of P solution to polymer solution.* ***Method 2A****: an aliquot of P solution was* ***slowly*** *added to the aliquot of polymer solution,* ***Method 2B****: an aliquot of P solution was* ***quickly*** *(within 2 sec) added to the aliquot of polymer solution. Statistical analysis: # - no significant difference, *p<0.05, **p<0.01, ***p<0.001.*

AAL/P weight ratio	Particle size [nm]		PdI		ZP [mV]	
	Method of preparation:					
	2A	2B	2A	2B	2A	2B
5	269±5	146±1	0.312±0.032	0.380±0.018	-71.8±1.3	-64.9±4.2
	***		**		*	
4.5	254±2	110±1	0.239±0.010	0.233±0.012	-66.8±3.3	-66.8±3.3
	***		#		#	

A significant difference in the size of NPs was noticed. NPs which were smaller in size were formed when P solution was added quickly to the aliquot of AAL solution in comparison to the slow method. A difference in the PdI and ZP was also observed for NPs at an AAL/P weight ratio of 5. NPs, which were greater in size and which had lower zeta potential values, were formed when P solution was added slowly to the aliquot of polymer solution tested.

Based on the above studies on the sequence of solution mixing and speed of addition, the final method of AAL/P NPs formation was established as a fast addition of P solution (method 2B, which was used in all further experiments) to a stirred aliquot of AAL solution (method 1A).

4.2.4 Impact of changing solution pH on properties of NPs

4.2.4.1 Properties of NPs using alginic acid solution at pH 2

Insulin is soluble in diluted mineral acids (British Pharmacopoeia, 2012). The pI of insulin is approximately 5.3 (Alberti et al., 1997) and at pH lower than pI insulin is positively charged (Sarmento et al., 2006 b). This may further facilitate insulin loading efficiency via stronger electrostatic interactions with the NPs. For this reason,

the pH of one of the NP component solutions needs to be made acidic to facilitate entrapment of insulin when polyelectrolyte complexes are formed. At first, the pH of alginate solution was adjusted to 2. A range of weight ratios (15 to 0.10) using 0.1% w/v solution of AAL at pH 2 and 0.1% w/v P solution were tested to examine if NPs can be formed. However, only aggregates/microparticles were formed immediately after mixing the two solutions. Analysis of alginate properties shows pH dependent stability of this polymer. It has been shown that the viscosity of sodium alginate solution is nearly constant in the pH range of 6 - 8. Following a pH decrease, viscosity increases and reaches a maximum at pH of 3 – 3.5, as carboxylate groups in the alginate backbone become protonated and form hydrogen bonds (Lee and Mooney, 2012). Solutions of alginic acid at higher concentrations form a physical gel at this pH where hydrogen bond attractions predominate over electrostatic repulsions. The intrinsic pK (no charge on the polyelectrolyte) of alginic acid is 3 (Andriamanantoanina and Rinaudob, 2010).

4.2.4.2 Properties of NPs using protamine solution at pH 2

As no NPs were formed when pH of the AAL solution was adjusted to 2, further manipulations with solution pH were performed for P solution. pH 2 was chosen as it would result in complete insulin solubility (solubility of insulin is 10 mg/ml in pH 2-3) (Fischel-Ghodsian et al., 1988). Similarly to the previous studies (presented in Sections 4.2.3.1 and 4.2.3.2) two various sequences of the components mixing were tested.

Method 1A. An aliquot of P solution at pH 2 was added to the aliquot of polymer solution under magnetic stirring. Table A.2 (Appendix A) summarises the properties of NPs obtained.

Particle size of formed NPs ranged from 228 to 283 nm and PdI had values between 0.205 and 0.284. An increase in the amount of polymer resulted in an increase in the size of NPs. Compared to NPs formed with P solution without adjusting the pH, NPs were larger in size (below 200 nm for NPs made of pH unadjusted P solution) and had greater PdI. Aggregates/microparticles were formed at a AAL/P_pH2 weight ratios of 2.5 and lower. In the case of AAL/P (pH of P solution unadjusted) NPs, sedimentation was observed for the 0.83 – 0.50 AAL/P weight ratio. The ZP of prepared NPs ranged from -59.3 mV to -25.2 mV. It decreased with higher P content and at a value of -25.2 mV value aggregation occurred.

The pH of NP dispersions ranged from 4.64 to 2.96 for 15 – 2.5 AAL/P_pH2 weight ratios. The viscosity of the formulations ranged from 1.69 to 0.83 mPa·s for 15 – 2.5 AAL/P_pH2 weight ratios (Figure 4.1.4). Compared to AAL/P (pH of P solution

unadjusted), the viscosity of nanodispersions made using P solution with pH 2 decreased, which may be due to changing polymer/protamine interactions as the pH of P solution was lowered. Additionally, the pH of P solution was adjusted by HCl (1 M solution), which resulted in an excess of negatively charged ions (Cl^-). The addition of protamine at pH 2 may cause stronger interaction between polymer/P and lower viscosity of the continuous medium. However, using excess P at pH 2 may cause partial/local deprotonation of alginic acid and formation of aggregates by hydrogen bond interactions (Lee and Mooney, 2012).

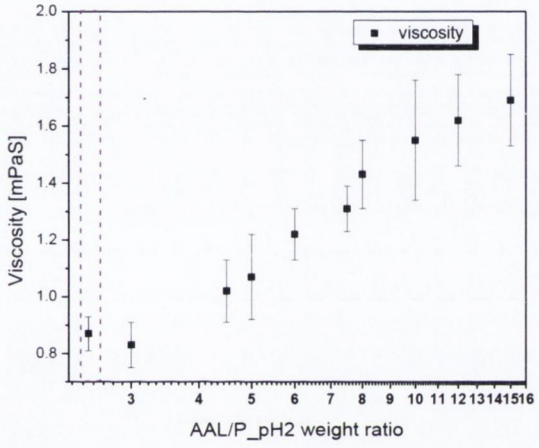

Fig. 4.1.4 *Viscosity of NPs composed of AAL and P (P_pH2). Preparation method: 1A. (---- - aggregates formed).*

Method 1B. An aliquot of polymer solution was introduced to the aliquot of protamine solution at pH 2 under magnetic stirring. The data is summarised in Table A.3 (Appendix A).

Comparison of the particle size, PdI and ZP of NPs formed using methods 1A and 1B was performed. Additionally, statistical significance of this data was evaluated. Figure 4.1.5 compares the size of NPs composed of 0.1% w/v solution of AAL and 0.1% w/v solution of P at pH 2. Significant differences in the size of NPs formed by these two different methods were measured. In the case of method 1B, NPs were formed in the higher weight ratio range (3 - 0.067). Aggregates/microparticles occurred at a AAL/P_pH2 weight ratio of 3, while NPs prepared according to method 1A were in the nano-size range. Additionally, NPs prepared by method 1B were generally greater in size (over 330 nm for the smallest NPs formed).

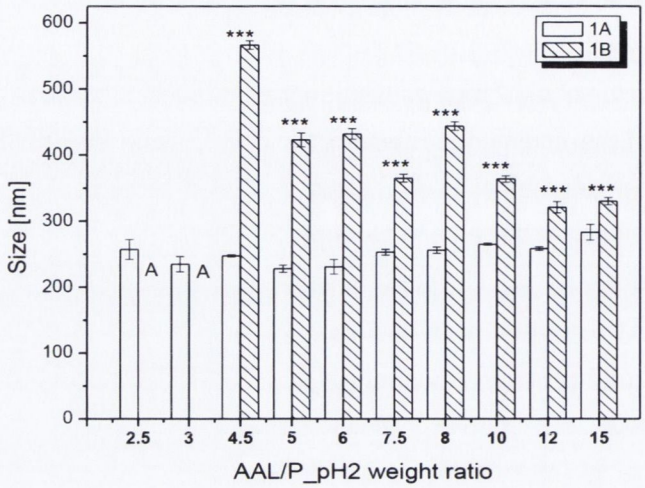

Fig. 4.1.5 *Comparison of particle size values for NPs composed of AAL and P (P_pH2) and formed by two different methods. (A - aggregates formed, statistical analysis: # - no significant difference, *p<0.05, **p<0.01, ***p<0.001).*
*(Method **1A**: an aliquot of P solution at pH 2 was added to the aliquot of AAL solution under magnetic stirring, method **1B**: an aliquot of AAL solution was introduced to the aliquot of P solution at pH 2 under magnetic stirring).*

PdI of NPs formed using methods 1A and 1B is compared in Figure 4.1.6. PdI analysis indicated that NPs with significantly greater PdI values were obtained when polymer solution was added to the aliquot of P solution (method 1B). The greatest difference occurred for an AAL/P_pH2 weight ratio of 4.5 perhaps as this ratio is close to the ratio of 3, where NP aggregation was observed.

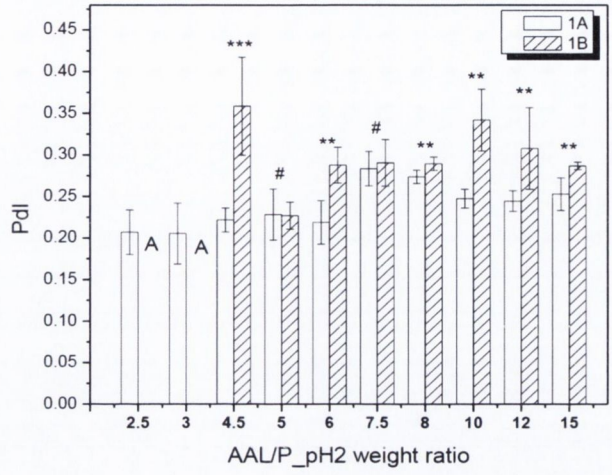

Fig. 4.1.6 *Comparison of polydispersity index values for NPs composed of AAL and P (P_pH2) formed using two different methods, (A - aggregates formed, statistical analysis: # - no significant difference, *p<0.05, **p<0.01, ***p<0.001).*
*(Method **1A**: an aliquot of P solution at pH 2 was added to the aliquot of AAL solution under magnetic stirring, method **1B**: an aliquot of AAL solution was introduced to the aliquot of P solution at pH 2 under magnetic stirring).*

As was observed in the case of method 1A, no positively charged NPs were formed when protamine solution at pH 2 was used (Figure 4.1.7). The preparation method did have an impact on ZP values of NPs prepared. Greater ZP was obtained with method 1A. Furthermore, there was a difference in the mass mixing ratio at which the first occurrence of aggregates was noticed. It can be assumed that there will be a different interaction scheme depending on which component was added as first. Generally, particles larger in size and with greater PdI, having lower ZP were obtained when the aliquot of AAL solution was introduced to the aliquot of P solution under magnetic stirring. As mentioned previously, pH of P was lowered using HCl (1 M solution). The introduction of extra negatively charged residues may cause deprotonation and destabilisation of alginate. The amount of cationic groups present could be too limited to interact with the excess of anionic groups present, which results in the formation of only negatively charged NPs. Based on the data obtained, method 1A would be suggested for further studies.

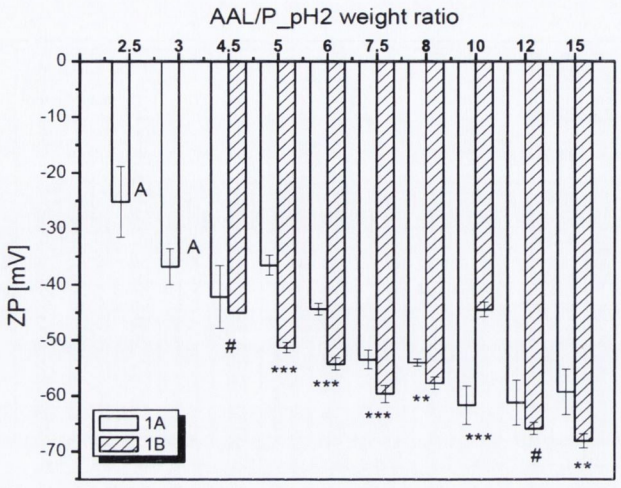

Fig. 4.1.7 *Comparison of zeta potential values for NPs composed of AAL and P (P_pH2) formed by two different methods, (---- - aggregates formed, statistical analysis: # - no significant difference, *p<0.05, **p<0.01, ***p<0.001).*
*(Method **1A**: an aliquot of P solution at pH 2 was added to the aliquot of AAL solution under magnetic stirring, method **1B**: an aliquot of AAL solution was introduced to the aliquot of P solution at pH 2 under magnetic stirring).*

4.2.5 Formation of NPs using protamine solution at pH3 and alginic acid

As described in Section 4.2.4.2, decreasing pH of P solution to 2 caused formation of only negatively charged NPs. To enhance the possibility that NPs with positive surface charge will also be formed, the pH of protamine solution was adjusted to 3 as increasing the pH of solution does not change the solubility of insulin, which is 10 mg/ml at pH 2-3 (Fischel-Ghodsian et al., 1988). As for experiments involving the use of P solution at pH 2, two methods of component solution mixing were tested.

Method 1A. An aliquot of P solution at pH 3 was added to the aliquot of polymer solution under magnetic stirring. Characteristics of NPs prepared by this method are summarised in Table A.4 (Appendix A).

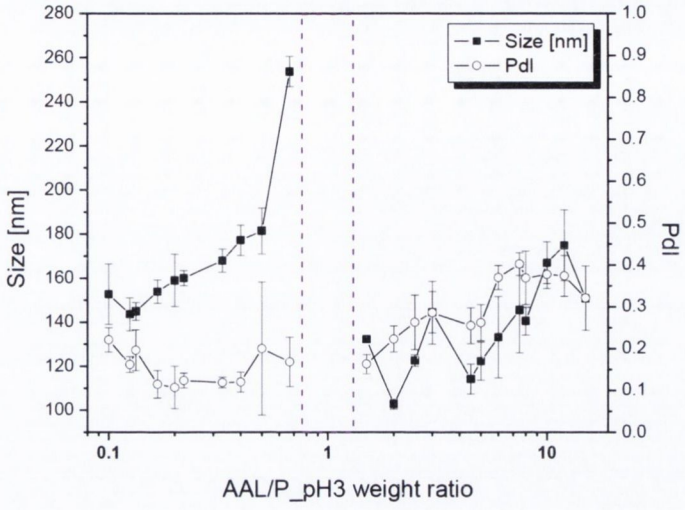

Fig. 4.1.8 *Particle size and polydispersity index of NPs composed of AAL and P (P_pH3). Preparation method **1A**: protamine solution at pH 3 added to an aliquot of alginic acid, (---- - aggregates formed).*

The particle size of NPs prepared varied from 103 to 254 nm (Fig. 4.1.8). An increase in the particle size and PdI was noticed when aggregates/microparticles were formed at an AAL/P_pH3 weight ratio of 1.0. NPs with greater PdI were obtained when a greater amount of polymer was used (negatively charged NPs). NPs with more homogeneous size distribution (with lower PdI) were formed when the content of P increased. Lowering the pH of P solution to 3 resulted in the formation of both negatively and positively charged NPs (Figure 4.1.9). Negatively charged NPs had a charge between -51.2 mV and -65.4 mV. Aggregates/microparticles were formed when ZP reached a value of -20.3 mV. ZP of positively charged NPs reached the value of 20 mV for AAL/P_pH3 weight ratios in the range of 0.33 - 0.1 (Figure 4.1.9).

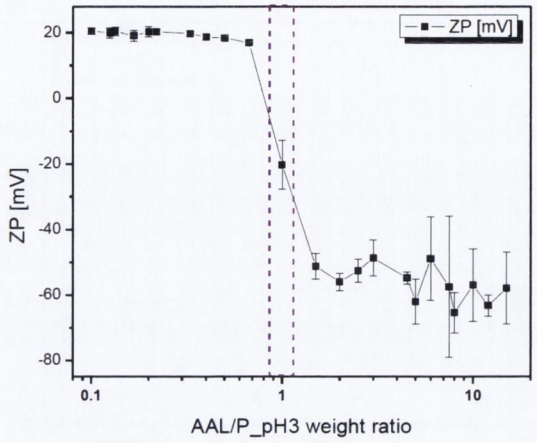

Fig. 4.1.9 *Zeta potential of NPs composed of AAL and P (P_pH3). Preparation method **1A**: protamine solution at pH 3 added to an aliquot of alginic acid, (---- - aggregates formed).*

The pH of NPs prepared had values between 5.96 to 3.26, depending on the AAL/P weight ratio. Viscosity values of NPs formed are presented in Figure 4.1.10. Viscosity increased with increasing amount of polymer and had values between 0.86 to 2.25 mPa·s for negatively charged NPs and 0.74 – 0.84 mPa·s for positively charged NPs.

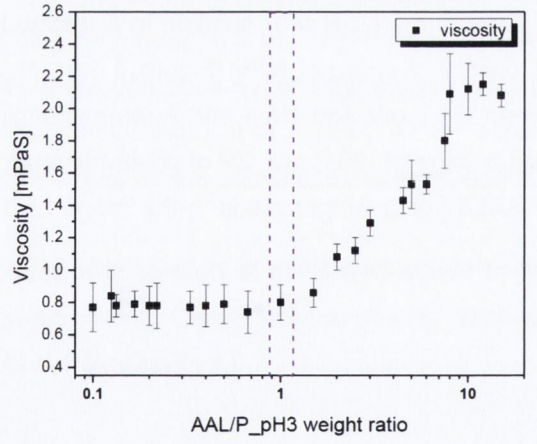

Fig. 4.1.10 *Viscosity of NPs composed of AAL and P (P_pH3). Preparation method **1A**: protamine solution at pH 3 added to an aliquot of alginic acid, (---- - aggregates formed).*

Method 1B. An aliquot of polymer solution was introduced to the aliquot of protamine at pH 3 under magnetic stirring. Characteristics of NPs are summarised in

Table A.5 (Appendix A). Comparison of the particle size, PdI and ZP of NPs formed by methods 1A and 1B was performed. Figure 4.1.11 presents the particle size of NPs composed of 0.1% w/v solution of AAL and 0.1% w/v solution of P at pH 3.

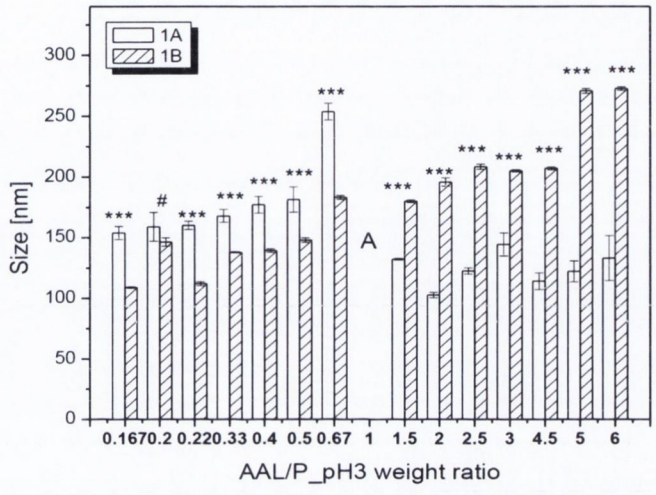

Fig. 4.1.11 *Comparison of particle size values for NPs composed of AAL and P (P_pH3) formed by two various methods, (A - aggregates formed, statistical analysis: # - no significant difference, *p<0.05, **p<0.01, ***p<0.001).*
*(Method **1A**: an aliquot of P solution at pH 3 was added to the aliquot of AAL solution under magnetic stirring, method **1B**: an aliquot of AAL solution was introduced to the aliquot of P solution at pH 3 under magnetic stirring).*

There was a significant difference in the NP size depending on the preparation method. Negatively charged NPs prepared by adding AAL solution to P solution (method 1B) were much larger in size (average size of 120 nm for NPs prepared by method 1A and over 200 nm for NPs prepared by method 1B, Fig. 4.1.11). Smaller positively charged NPs were obtained when method 1B was used for preparation, compared to method 1A. Therefore, the sequence of component mixing had a significant impact on NP size. Smaller NPs were obtained for greater AAL/P_pH3 weight ratios (1.5 – 6) when method 1A was utilised. However, in the case of 0.167 - 0.67 weight ratios, method 1B resulted in the formation of NPs which were smaller in size, when compared to method 1A (Figure 4.1.11). For the two methods of preparation, aggregation and particle size increase was observed for the same AAL/P_pH3 weight ratio of 1. The introduction of polymer solution to the protamine solution at pH 3, might deprotonate the polymer first, before the interaction with protamine occurs, resulting in the larger particle size.

Considering homogeneity (polydispersity) of NPs formed, there was no significant difference for most of the formulations prepared (Figure 4.1.12). Generally,

negatively charged NPs had greater PdI values compared to those of the positively charged NPs, for both of the methods tested. Relatively high standard deviations obtained for AAL/P_pH3 NPs prepared by method 1A are the consequence of many repetitions that were performed, as those NPs were further used for insulin entrapment.

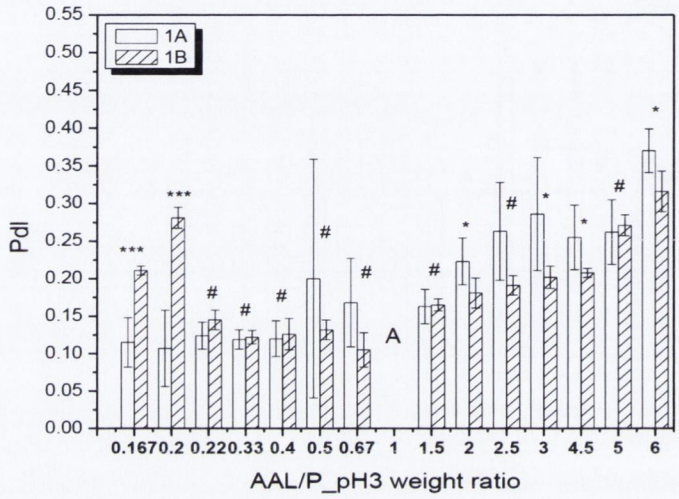

Fig. 4.1.12 *Comparison of polydispersity index values for NPs composed of AAL and P (P_pH3) formed by two different methods, (A - aggregates formed, statistical analysis: # - no significant difference, *p<0.05, **p<0.01, ***p<0.001).*
*(Method **1A**: an aliquot of P solution at pH 3 was added to the aliquot of AAL solution under magnetic stirring, method **1B**: an aliquot of AAL solution was introduced to the aliquot of P solution at pH 3 under magnetic stirring).*

In general, the preparation method had an impact on the charge of NPs prepared (Figure 4.1.13). AAL/P_pH3 weight ratios of 0.1 – 0.5 resulted in positively charged NPs (16.5 – 20.3 mV). Mixing the same volumes of polymer/protamine (AAL/P_pH3 weight ratio=1) caused aggregation of NPs formed, as neutralisation of the charges occurred. Negatively charged NPs -45.2 – -62.0 mV were obtained using AAL/P_pH3 weigh ratios of 1.5 – 6.

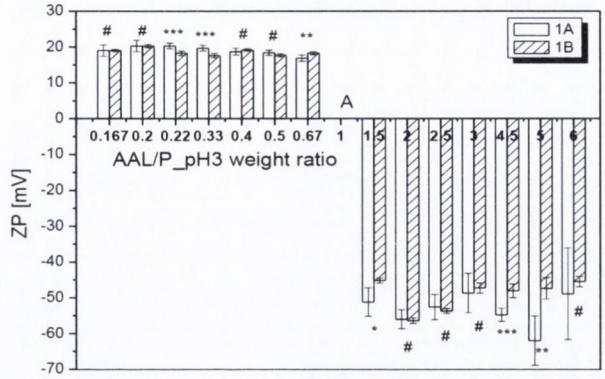

Fig. 4.1.13 *Comparison of zeta potential values for NPs composed of AAL and P (P_pH3) formed by two different methods, (A - aggregates formed, statistical analysis: # - no significant difference, *p<0.05, **p<0.01, ***p<0.001).*
*(Method **1A**: an aliquot of P solution at pH 3 was added to the aliquot of AAL solution under magnetic stirring, method **1B**: an aliquot of AAL solution was introduced to the aliquot of P solution at pH 3 under magnetic stirring).*

Adjusting the pH of protamine to 3 resulted in the formation of both negatively and positively charged NPs. Interaction between negatively charged AAL and positively charged P occurred, as perhaps the amount of Cl^- ions (from HCl) that was used for pH adjustment was lower, compared to P at pH 2.
Based on experiments described in this Section, the final preparation method for nanocarriers composed of 0.1% w/v solution of AAL and 0.1% w/v solution of P at pH 3 (P_pH3) was established. The most favourable NP characteristics (small size, low polydispersity and various ZP) were obtained when 0.1% w/v P solution at pH 3 was added to the stirred aliquot of 0.1% w/v AAL solution (Method 1A).

4.2.6 Evaluation of nanoparticles composed of AAM and P

In addition to the evaluation of the suitability of AAL in the formation of NPs, alginic acid medium viscosity (AAM) was also tested. 0.1% w/v solution of AAM and 0.1% w/v solution of P were used. A range of AAM/P weight ratios was tested to examine the likelihood of NP formation. Two methods using a different sequence of mixing both components for NP preparation were tested.

Method 1A: An aliquot of P solution was added to the aliquot of polymer solution under magnetic stirring.
The particle size, PdI and ZP of the formed PEC were measured (Table A.6, Appendix A). Figure 4.1.14 shows the particle size and PdI of tested NPs.

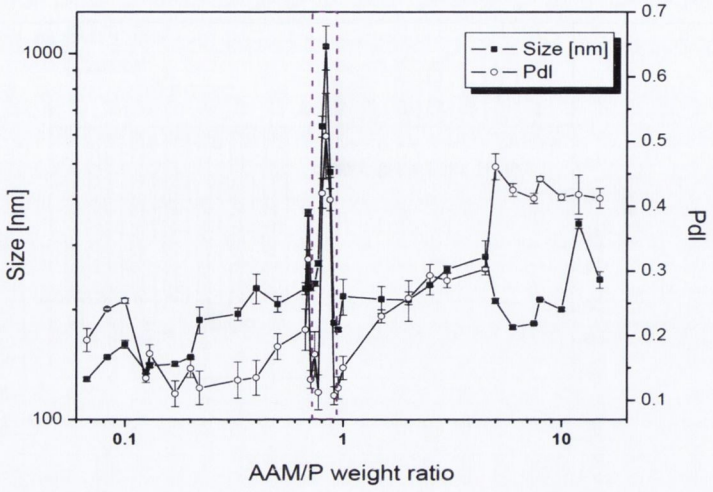

Fig. 4.1.14 *Particle size and polydispersity index of NPs composed of AAM and P. Preparation method **1A**: P solution was added to an aliquot of alginic acid, (---- - aggregates formed).*

The particle size and PdI of NPs obtained was strongly dependent on the AAM/P weight ratio. NPs that were smaller in size and with lower PdI were obtained when more P than polymer was used. Increasing the content of AAM resulted in the formation of NPs which were larger in size and less homogeneous, as not all of the polymer was able to interact with P and the excess of alginic acid resulted in heterogeneity of the systems formed. A rapid increase in the particle size and PdI occurred when the net charge of NPs was close to being neutralised, which resulted in aggregation of the NPs and/or the formation of micron-sized entities (AAM/P weight ratio 0.87 – 0.77).

Both negatively and positively charged NPs were formed (Figure 6.1.15). Negatively charged NPs were obtained when 0.91 – 15 AAM/P weight ratios were employed. The particle size of these NPs was 176 – 343 nm, where greater size corresponded to greater AAM/P weight ratios. PdI varied from 0.107 – 0.461, where lower values correlated with lower AAM/P weight ratios. ZP of negatively charged NPs was -47.3 – -72.8 mV. Aggregation occurred when the charge of positively charged amino groups of protamine and negatively charged carboxyl groups of polymer were neutralised, which was in the range of AAM/P weight ratios of 0.77 – 0.87. Positively charged NPs were formed for AAM/P weight ratios of 0.067 – 0.74. The size of these NPs varied from 129 to 368 nm with PdI variations between 0.110 – 0.318. ZP of positively charged NPs had values between 16 – 20.6 mV.

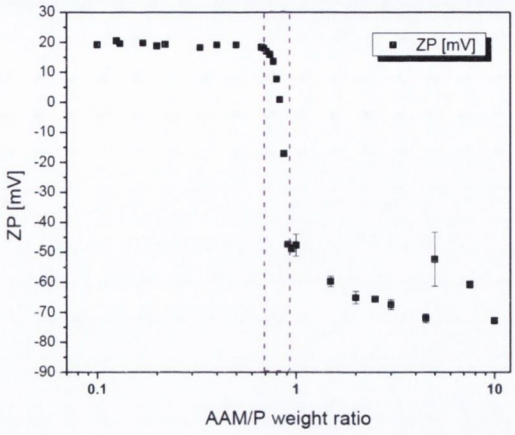

Fig. 4.1.15 *Zeta potential of NPs composed of AAM and P. Preparation method **1A**: P solution was added to an aliquot of alginic acid, (---- - aggregates formed).*

The particle sizes of NPs formed from AAL and AAM had similar values (ranging from 106 to 332 nm for AAL/P NPs, and from 129 to 343 nm for AAM/P NPs). PdI values of NPs prepared with AAM were greater (in the range of 0.107 – 0.461) compared to those of NPs formed from the polymer at low viscosity (AAL, in the range of 0.077 – 0.368). The charge of NPs obtained from AAL and AAM had similar values (-72 – +19 mV for AAL/P NPs, and -73 – 21 mV for AAM/P NPs). The neutralisation point and aggregation of NPs occurred at wider range of polymer/protamine weight ratios for NPs composed of AAL (0.83 – 0.50), comparing to the AAM/P NPs (0.87 – 0.77).

The pH of negatively charged NPs ranged from 6.37 to 6.69 and from 6.01 to 6.26 for positively charged AAM/P NPs (Table A.6, Appendix A). Figure 4.1.16 shows the viscosity of nanodispersions formed.

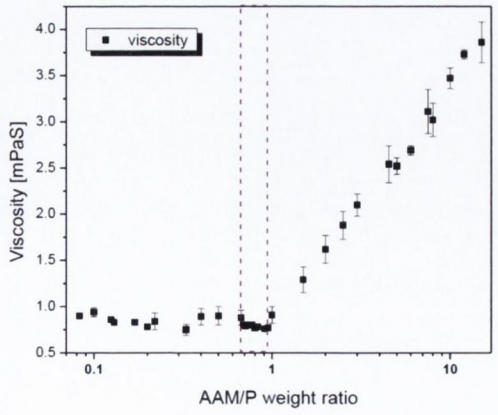

Fig. 4.1.16 *Viscosity of NPs composed of AAM and P. Preparation method **1A:** protamine solution was added to an aliquot of alginic acid, (---- - aggregates formed).*

The viscosity of the dispersions was strongly related to the AAM/P weight ratio. The viscosity of positively charged formulations (~0.90 mPa·s) was similar to that of 0.1% w/v P solution (0.97 mPa·s, Table 4.1). Neutralisation of alginic acid and protamine resulted in the lowest viscosity value of 0.75 mPa·s, which corresponds to the viscosity of water at room temperature (RT). The viscosity of dispersions increased with increasing AAM/P weight ratio (in the range of weight ratios between 1-15), most likely due to excess of AAM. At the AAM/P weight ratio of 15 the dispersion viscosity was comparable to that of the 0.1% w/v solution of polymer (Table 4.1).

In **method 1B** an aliquot of polymer solution was introduced to the aliquot of P solution under magnetic stirring. The data is summarised in Table A.7 (Appendix A). Figure 4.1.17 compares the particle size values of NPs composed of 0.1% w/v solution of AAM and 0.1% w/v solution of P prepared using Method 1A and 1B.

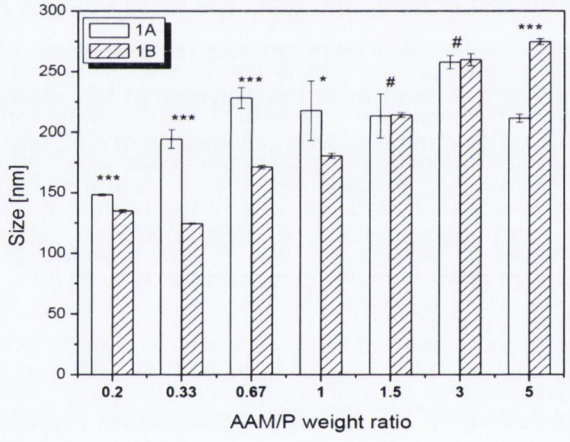

Fig. 4.1.17 *Comparison of particle size values for NPs composed of AAM and P formed by two various methods, (statistical analysis: # - no significant difference, *p<0.05, **p<0.01, ***p<0.001).*
*(Method **1A**: an aliquot of P solution was added to the aliquot of AAM solution under magnetic stirring, method **1B**: an aliquot of AAM solution was introduced to the aliquot of P solution under magnetic stirring).*

There was almost no difference in the particle size of negatively charged AAM/P NPs, but positively charged NPs that were smaller in size ($p<0.001$) were formed when polymer solution was added to the stirred aliquot of protamine solution (method 1B) (Figure 4.1.17). PdI values were similar although statistical difference was observed for some formulations (Figure 4.1.18).

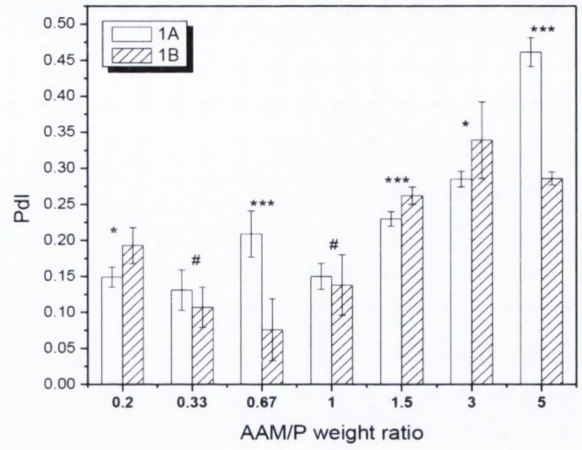

Fig. 4.1.18 *Comparison of polydispersity index values for NPs composed of AAM and P formed by two different methods, (statistical analysis: # - no significant difference, *p<0.05, **p<0.01, ***p<0.001).*
*(Method **1A**: an aliquot of P solution was added to the aliquot of AAM solution under magnetic stirring, method **1B**: an aliquot of AAM solution was introduced to the aliquot of P solution under magnetic stirring).*

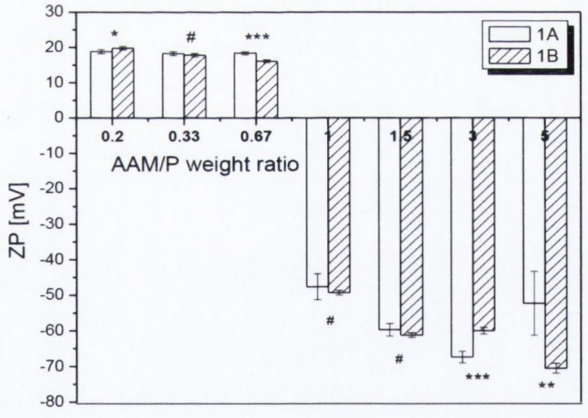

Fig. 4.1.19 *Comparison of zeta potential values for NPs composed of AAM and P formed by two different methods, (statistical analysis: # - no significant difference, *p<0.05, **p<0.01, ***p<0.001).*
*(Method **1A**: an aliquot of P solution was added to the aliquot of AAM solution under magnetic stirring, method **1B**: an aliquot of AAM solution was introduced to the aliquot of P solution under magnetic stirring).*

Analysis of the surface charge of NPs formed using methods 1A and 1B shows that the NPs had comparable ZP values, although a statistical difference was observed for a few formulations (Figure 4.1.19).

Comparison of two methods of AAM/P NPs preparation shows no significant changes within the PdI and ZP. However, smaller positively charged NPs were

obtained by method 1B. Similar results were obtained for positively charged AAL/P_pH3 NPs, although in this case smaller negatively charged NPs were formed by method 1A, which was chosen for further preparations. The excess of protamine results in the formation of particles that are smaller in size, as the polymer interacts completely with protamine after its introduction.

4.2.7 Formation of NPs using protamine solution at pH 3 and AAM

NPs composed of 0.1% w/v solution of AAM and 0.1% w/v solution of P at pH 3 (P_pH3) were also evaluated, similar to the experiments with AAL/P_pH3 NPs (Section 6.2.7).

Method 1A: An aliquot of P solution at pH 3 was added to the aliquot of polymer solution under magnetic stirring. Particle size, PdI and ZP of PECs formed were measured (Table A.8, Appendix A). Figure 4.1.20 summarises the particle size and PdI of NPs obtained.

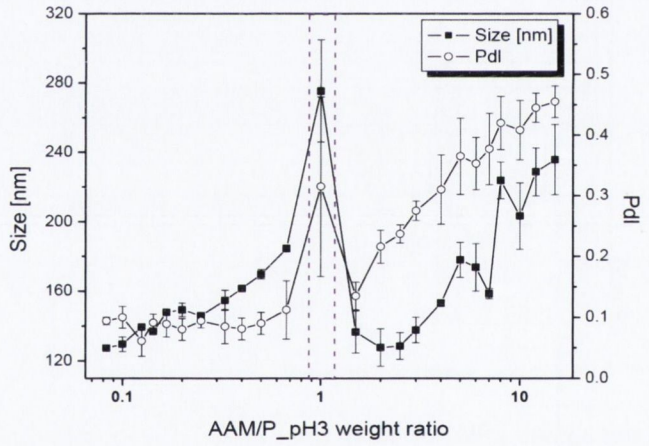

Fig. 4.1.20 *Particle size and polydispersity index of NPs composed of AAM and P (P_pH3). Preparation method **1A**: protamine solution at pH 3 was added to an aliquot of alginic acid, (---- - aggregates formed).*

It was observed that the AAM/P_pH3 weight ratio had a strong impact on the particle size and PdI of the NPs. NPs larger in size and with greater PdI values were obtained when greater AAM/P weight ratios were used. The size of negatively charged NPs was 128 – 236 nm with the PdI value of 0.135 – 0.455 for AAM/P_pH3 weight ratios of 1.5 – 15. Aggregation occurred when equal volumes of AAM and P_pH3 solutions were mixed (AAM/P weight ratio of 1). AAM/P_pH3 weight ratios of 0.083 – 0.67 resulted in the formation of positively charged NPs with very narrow

particle size distributions (low PdI value – below 0.100) and small particle size (127 – 184 nm).

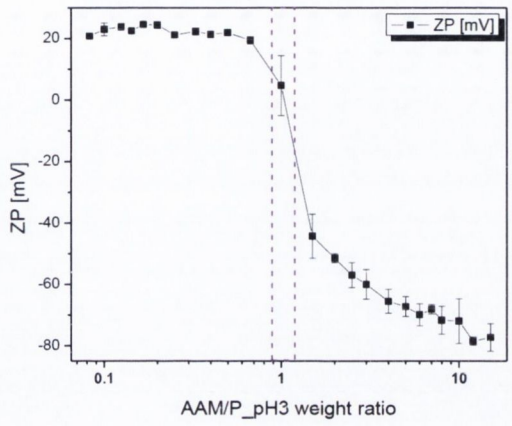

Fig. 4.1.21 *Zeta potential of NPs composed of AAM and P (P_pH3). Preparation method **1A**: protamine solution at pH 3 was added to an aliquot of alginic acid, (---- - aggregates formed).*

Both negatively and positively charged NPs were formed. ZP of the AAM/P_pH3 NPs varied from -77.3 mV (for negatively charged NPs) to 23.8 mV (for positively charged NPs). The pH and viscosity of NPs prepared were measured (Table A.8, Appendix A). The NPs had pH values of 3.01 – 5.82. Similarly to the NPs composed of AAM and P (pH of P solution was unadjusted), the viscosity of nanodispersions obtained was strongly dependent on the AAM/P weight ratio. Viscosity values were much higher for negatively charged NPs (0.94 – 3.17 mPa·s) and were 0.77 – 0.94 mPa·s for NPs with positive charge (Figure 4.1.22).

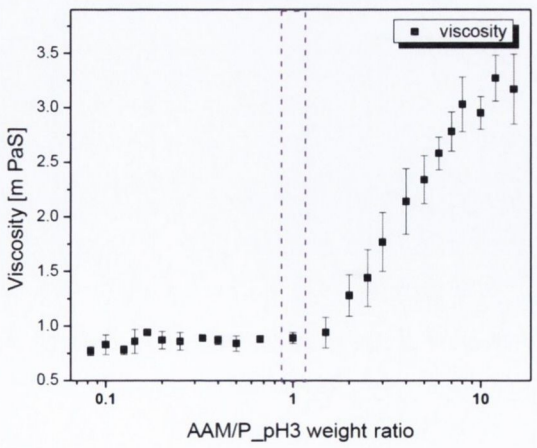

Fig. 4.1.22 *Viscosity of NPs composed of AAM and P (P_pH3). Preparation method **1A**: protamine solution at pH 3 was added to an aliquot of alginic acid, (---- - aggregates formed).*

To elucidate the impact of the sequence in which polymer/protamine at pH 3 solutions were mixed, NPs prepared according to method 1A and 1B were compared. In **method 1B** an aliquot of polymer solution was introduced to the aliquot of protamine solution at pH 3 under magnetic stirring. The physical properties of the formulations are presented in Table A.9 (Appendix A). Figure 4.1.23 shows the particle size of NPs composed of 0.1% w/v solution of AAM and 0.1% w/v solution of P at pH 3.

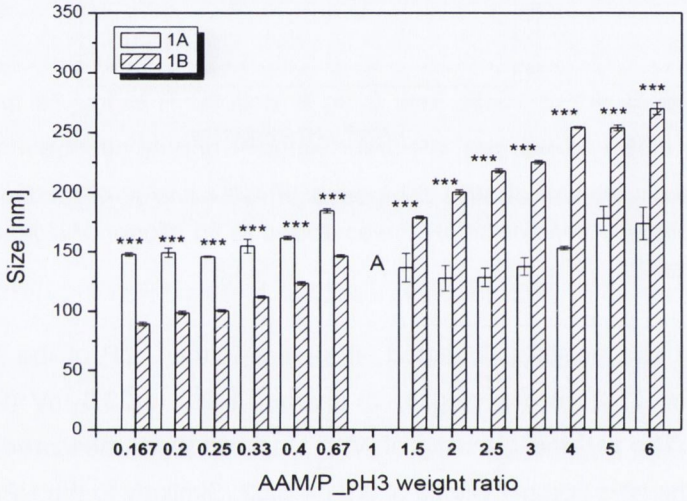

Fig. 4.1.23 *Comparison of particle size values for NPs composed of AAM and P (P_pH3) formed by two various methods, (A - aggregates formed, statistical analysis: # - no significant difference, *p<0.05, **p<0.01, ***p<0.001).*
*(Method **1A**: an aliquot of P solution at pH 3 was added to the aliquot of AAM solution under magnetic stirring, method **1B**: an aliquot of AAM solution was introduced to the aliquot of P solution at pH 3 under magnetic stirring).*

Size comparison of NPs prepared using methods 1A and 1B shows that a significant difference can be noted for all formulations tested. However, when P solution at pH 3 was added to an aliquot of polymer solution (method 1A) smaller negatively charged NPs were formed. In the case of positively charged NPs, smaller particles were obtained when NPs were prepared using method 1B (polymer solution was added to the stirred aliquot of protamine solution at pH 3). Comparison of PdI (Figure 4.1.24) showed no significant difference for most of the formulations tested. It can be seen that greater PdI values in general were measured for negatively charged NPs.

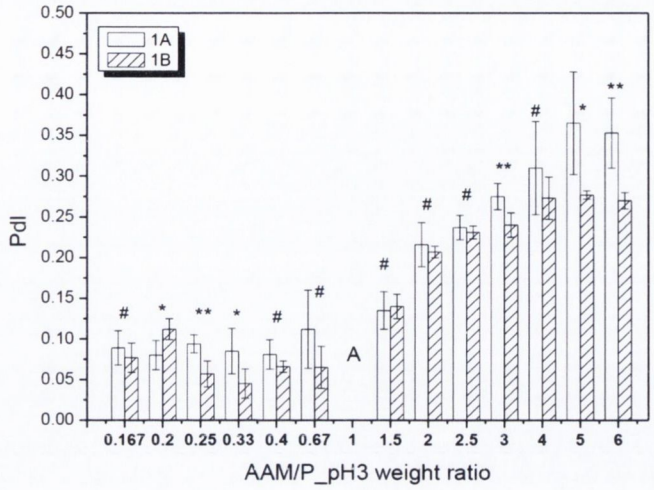

Fig. 4.1.24 *Comparison of polydispersity index values for NPs composed of AAM and P (P_pH3) formed by two various methods, (A - aggregates formed, statistical analysis: # - no significant difference, *p<0.05, **p<0.01, ***p<0.001).*
*(Method **1A**: an aliquot of P solution at pH 3 was added to the aliquot of AAM solution under magnetic stirring, method **1B**: an aliquot of AAM solution was introduced to the aliquot of P solution at pH 3 under magnetic stirring).*

The preparation method had no impact on ZP values of the NPs formed in most cases (Fig. 4.1.25). However, greater ZP values were obtained for positively charged NPs when method 1A was used, as opposed to method 1B. Neutralisation of positive groups of P and negative groups of AAM occurred for the same AAM/P_pH3 weigh ratio equal to 1, regardless of the method used.

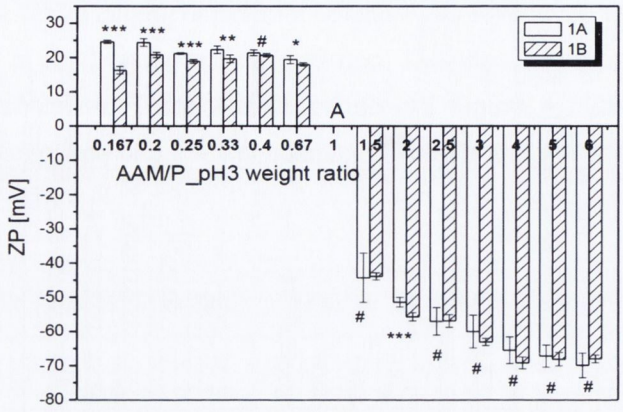

Fig. 4.1.25 *Comparison of zeta potential values for NPs composed of AAM and P (P_pH3) formed by two different methods, (A - aggregates formed, statistical analysis: # - no significant difference, *p<0.05, **p<0.01, ***p<0.001).*
*(Method **1A**: an aliquot of P solution at pH 3 was added to the aliquot of AAM solution under magnetic stirring, method **1B**: an aliquot of AAM solution was introduced to the aliquot of P solution at pH 3 under magnetic stirring).*

Analysis of the results obtained for NPs formed by two different methods: 1A and 1B show similar results for both types of polymers tested: AAL and AAM. Generally method 1A formed only negatively charged NPs which were smaller in size and had lower PdI. In the case of positively charged NPs, smaller NPs were obtained by method 1B. As reported, the method of preparation had no significant impact on the NP charge for most of the formulations tested. The order of solution addition may have an impact on NP formation, perhaps due to microenvironmental pH changes around negatively charged polymer solution and positively charged protamine (Qiu and Park, 2001). Generally, NPs with smaller sizes and with lower PdI were obtained, when the excess of the polymer was stirred while other polymer was added. Therefore, method 1A was selected for further studies.

4.3 Physical stability of AAL/P_pH3 NPs

A challenging and very important aspect of nanoparticle characterisation is to measure the stability of formulations under conditions that resemble *in vitro* and *in vivo* environment. Stability and the level of NP aggregation in physiological conditions or different media important for biotechnological applications (e.g. cell culture media) are important parameters to be characterised. Properties of NPs such as size and surface charge determine quality and applicability of given NPs.

Therefore, the physical stability of the most promising formulations in buffers/solutions at various pH and ionic strength was investigated. Six types of AAL/P_pH3 (5, 2.5, 1.5, 0.5, 0.3 and 0.2 AAL/P_pH3 weight ratio) were selected for further stability studies in media at various pH. The selection of candidates was based on their most favourable characteristics (NPs with the smallest size and PdI, with a variety of surface charge (ZP)). Particle size, PdI and ZP were measured directly after NP preparation, buffer addition and up to 3 days of storage at RT for each buffer/solution tested.

4.3.1 Stability of AAL/P_pH3 NPs up to 72 h storage at RT

Stability of NPs composed of 0.1% w/v solution of AAL and 0.1% w/v solution of P at pH 3 (P_pH 3) was tested up to 72 h of storage at RT. Particle size, PdI and ZP of prepared NPs was measured after preparation and every 24 h. Figure 4.2.1 presents the size of NPs upon storage of the native dispersion at RT.

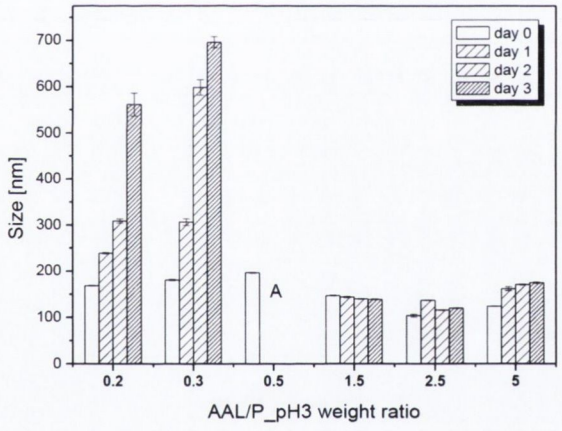

Fig 4.2.1 *Stability of NPs composed of AAL and P_pH3 up to 72 h of storage at RT – particle size measurements, (A – aggregates formed).*

Stability of NPs prepared was strongly dependent on the surface charge of NPs (AAL/P weight ratio). Negatively charged NPs (weight ratios of 1.5, 2.5 and 5) containing more polymer than P remained stable up to 72 h of storage at RT (only a small increase in size was observed). A considerable increase in the particle size of positively charged NPs (weight ratios of 0.2, 0.3 and 0.5) was observed, while in case of a AAL/P weight ratio of 0.5 aggregates (particles with size larger than 1 µm) were formed after 24 h of storage at RT. Similar changes were observed for PdI of the NPs (Figure 4.2.2). A small increase in the PdI values was observed for all types of negatively charged NPs, while a continuous growth in PdI of positively charged NPs was measured, which confirmed instability of such NPs and formation of aggregates upon storage.

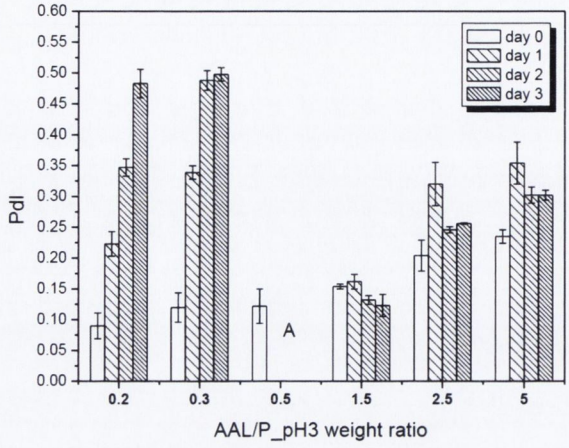

Fig 4.2.2 *Stability of NPs composed of AAL and P_pH3 up to 72 h of storage at RT - polydispersity measurements, (A – aggregates formed).*

ZP values of positively charged NPs remained stable over time, while a small increase in ZP values was observed for negatively charged NPs (Figure 4.2.3).

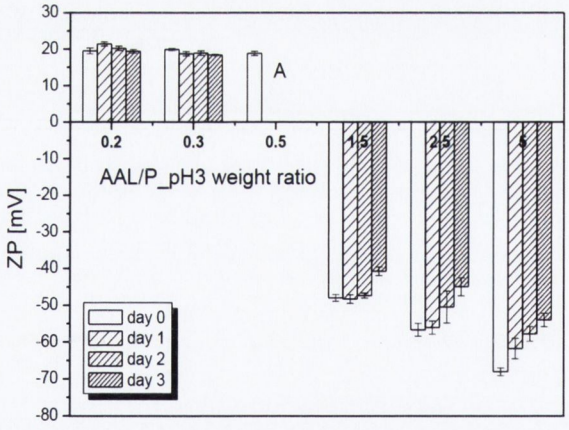

Fig 4.2.3 *Stability of NPs composed of AAL and P_pH3 up to 72 h of storage at RT – zeta potential measurements, (A – aggregates formed).*

The surface charge of NPs is most important factor that has an impact on their stability. Negatively charged NPs remained stable, as their particle size and PdI value did not change upon storage. However, an increase in the ZP of those NPs was noticed, which might be due to depolymerisation of the polymer caused by acid catalysed hydrolysis and an alkaline hydrolysed mechanism (Holme et al., 2003, 2008). In the case of positively charged NPs, an increase in the particle size and PdI was observed, however the charge of those NPs remained stable. It was noticed that

the least stable formulation was that with 0.5 AAL/P_pH3 weight ratio, as its charge was the closest to the neutralisation point. An increase in the particle size and PdI might be caused by the interaction between protamine residues.

4.3.2 Stability of AAL/P_pH3 NPs in 0.1 M and 0.01 M HCl

Stability of AAL/P_pH3 NPs was tested in HCl at concentrations of 0.1 and 0.01 M. It was noticed that positively charged NPs remained more stable at low pH comparing to the negatively charged NPs. A rapid increase in the particle size of negatively charged NPs was observed after addition of HCl solution at both concentrations tested (Figure 4.2.4). This behaviour of negatively charged NPs containing more AAL than P could be explained by the instability of alginic acid at low pH, caused by a proton catalysed hydrolysis (Draget et al., 2005).

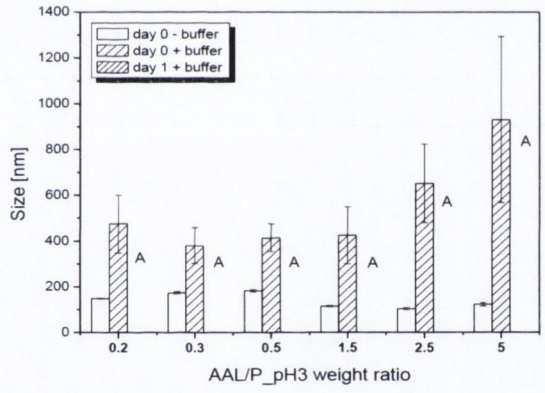

a)

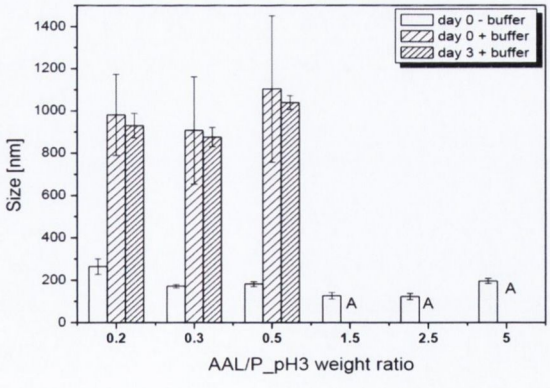

b)

Fig 4.2.4 *Stability of NPs composed of AAL and P_pH3 in* ***a)*** *0.1 M HCl and* ***b)*** *0.01 M HCl – particle size measurements, (A – aggregates formed).*

An increase in the PdI values was observed after adding HCl solution at both concentrations to the NPs tested (Figure 4.2.5). Smaller PdI values were obtained for positively charged NPs comparing to those of negatively charged NPs, which

suggests that they have greater stability in acidic environments. PdI reached a value of 1 when aggregates were formed.

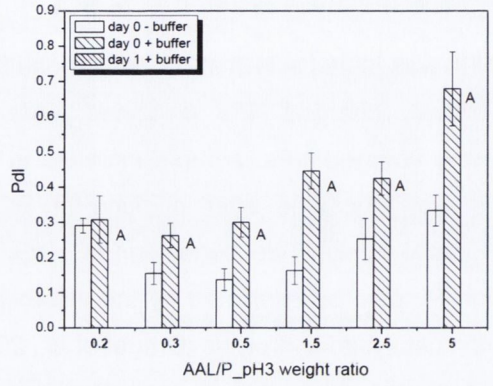

a)

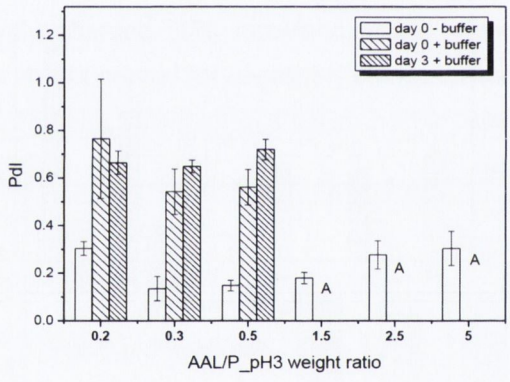

b)

Fig 4.2.5 *Stability of NPs composed of AAL and P_pH3 in* ***a)*** *0.1 M HCl and* ***b)*** *0.01 M HCl – polydispersity index measurements, (A – aggregates formed).*

Analysis of the ZP of NPs after adding HCl solution showed an impact of HCl concentration (Figure 4.2.6). When 0.1 M HCl was added to the NPs, the surface charge reached a value of ~0 mV for all types of NPs tested (Figure 4.2.6 a). Using more diluted HCl (0.01 M) caused a small increase in the ZP of positively charged NPs. An increase in the surface charge of negatively charged NPs was also observed, however this increase was dependent on the polymer/P weight ratio in the formulation. For the formulation with an AAL/P_pH3 weight ratio of 1.5, zeta potential changed from a negative value to a positive value after the addition of 0.01 M HCl. For the other two formulations with AAL/P weight ratios of 2.5 and 5 a smaller increase in the ZP value was observed (Figure 4.2.6 b).

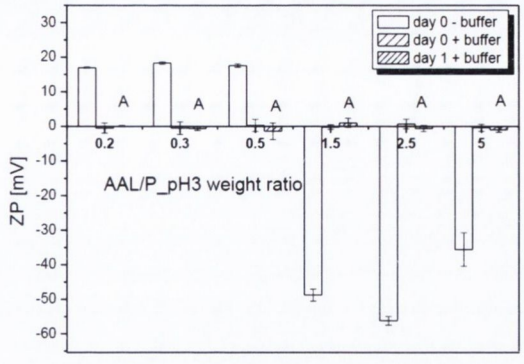

a)

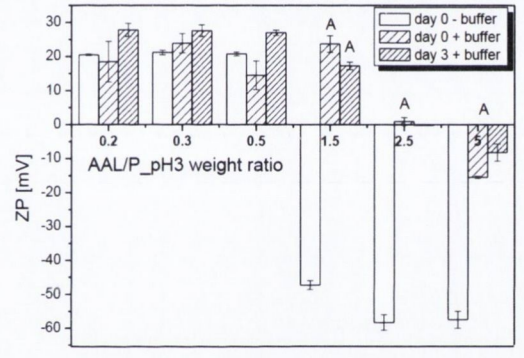

b)

Fig 4.2.6 *Stability of NPs composed of AAL and P_pH3 in* ***a)*** *0.1 M HCl and* ***b)*** *0.01 M HCl – zeta potential measurements, (A – aggregates formed).*

4.3.3 Stability of AAL/P_pH3 NPs in 0.1 M acetate buffer at pH 4.5

In order to check the behaviour and stability of selected NPs at various pH values, 0.1 M acetate buffer at pH 4.5 was then tested, as the pH of the human gastrointestinal tract varies greatly. The pH of the stomach is 1.5 – 5, while in the small intestine pH values of 7 – 8 may be present (Belzer and de Vos, 2012).

Figure 4.2.7 shows changes in the particle size of NPs after mixing with acetate buffer at pH 4.5. The stability of NPs in acetate buffer at pH 4.5 strongly depends on the polymer/protamine weight ratio. An increase in the size of negatively charged NPs was observed after addition of the buffer and upon storage, but the size remained in the nano-range even after 3 days of incubation. The greatest change in particle size over time was seen for NPs at an AAL/P_pH3 weight ratio of 5. Positively charged NPs were less stable in acetate buffer at pH 4.5 than negatively charged NPs and aggregates were formed directly after mixing of the NPs with the buffer.

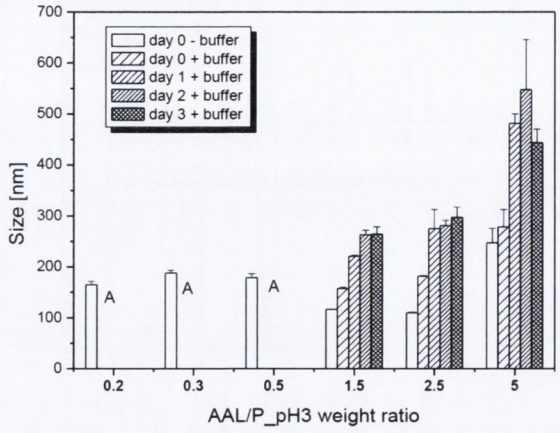

Fig 4.2.7 *Stability of NPs composed of AAL and P_pH3 in 0.1 M acetate buffer pH 4.5 – particle size measurements, (A – aggregates formed).*

A rise in PdI values was also observed (Figure 4.2.8). A small increase in PdI values of negatively charged NPs was seen, confirming that they have good stability at pH 4.5. A rapid increase in PdI values of positively charged NPs was observed as aggregates were formed immediately after mixing with the buffer.

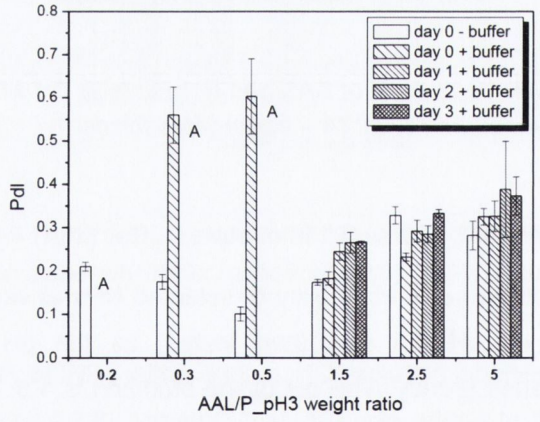

Fig 4.2.8 *Stability of NPs composed of AAL and P_pH3 in 0.1 M acetate buffer pH 4.5 – polydispersity measurements, (A – aggregates formed).*

ZP values of positively charged NPs did not change after buffer addition, however aggregation was observed (Figure 4.2.9). ZP value decreased upon storage and reached a value ~0 mV after 48 h of storage in acetate buffer at pH 4.5. An increase in the ZP values of two formulations containing negatively charged NPs was observed (AAL/P_pH3 weight ratios of 1.5 and 2.5). In the case of the formulation with an AAL/P weight ratio of 5, the ZP value decreased to -6.6 mV directly after mixing with acetate buffer at pH 4.5 and then increased to ~0 mV.

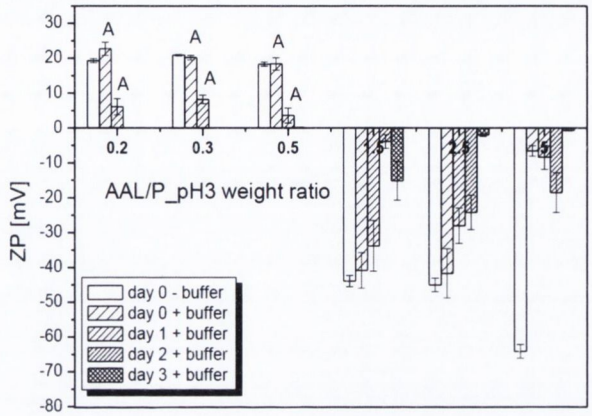

Fig 4.2.9 *Stability of NPs composed of AAL and P_pH3 in 0.1 M acetate buffer pH 4.5 – zeta potential measurements, (A – aggregates formed).*

4.3.4 Stability of AAL/P_pH3 NPs in 0.1 M HEPES at pH 6.5

The stability of prepared NPs in HEPES buffer at pH of 6.5 was tested next, as similar pH is present in the small intestine of the gastrointestinal tract (GIT).

A small increase in particle size was observed after addition of the buffer (Figure 4.2.10). Negatively charged NPs remained stable even after 3 days of storage at RT (however a small increase in the particle size was noticed). An increase in the size of positively charged NPs was noticed after 24 h of storage, but the NPs remained in nano-size. Storage for longer periods of time resulted in the formation of aggregates.

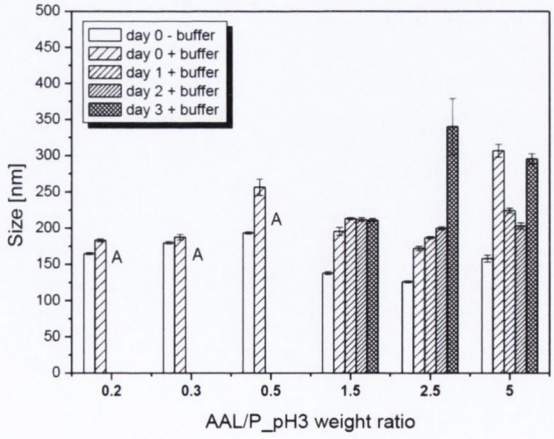

Fig 4.2.10 *Stability of NPs composed of AAL and P_pH3 in 0.1 M HEPES buffer pH 6.5 – particle size measurements, (A – aggregates formed).*

Similar to the size, an increase in PdI was noticed (Figure 4.2.11). The lowest PdI value was measured for NPs with an AAL/P_pH3 weight ratio of 1.5 (it changed from

0.165 to 0.232 after mixing with described buffer). Greater PdI values were seen for the other two formulations of negatively charged NPs, but they remained stable after addition and storage in the buffer. A small increase in PdI values was observed after mixing positively charged NPs with HEPES buffer at pH 6.5 (day 0), (from 0.11 to 0.207 for AAL/P_pH3 weight ratio of 0.2), however further storage showed that the formation of aggregates occurred (Figure 4.2.11).

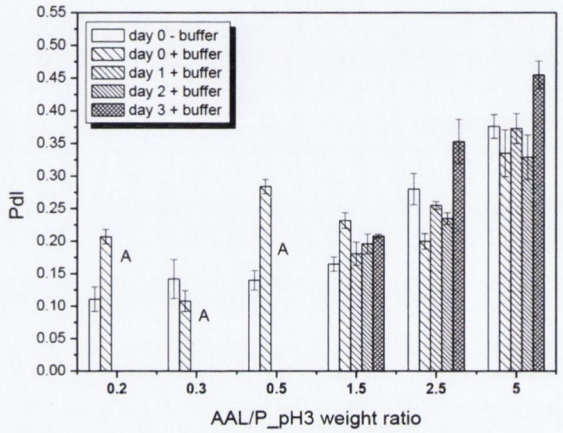

Fig 4.2.11 *Stability of NPs composed of AAL and P_pH3 in 0.1 M HEPES buffer pH 6.5 – polydispersity measurements, (A – aggregates formed).*

ZP of positively charged NPs increased after addition of 0.1 M HEPES buffer at pH 6.5 (from 17.2 mV to 28.1 mV for NPs with an AAL/P_pH3 weight ratio of 1.5) and it remained relatively stable over time, even if aggregates were formed. ZP of negatively charged NPs had values from -44.8 mV to -46.7 mV, which increased during storage in the buffer (Figure 4.2.12).

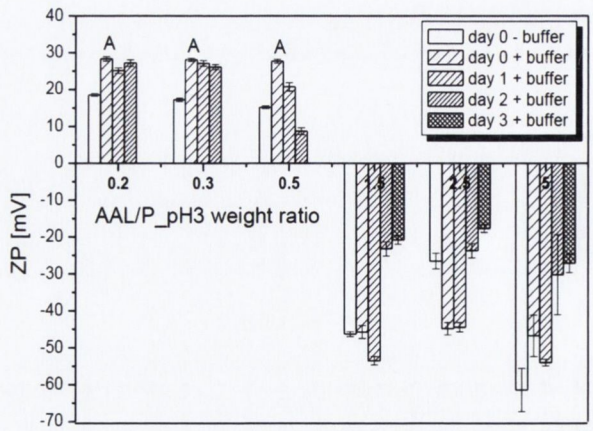

Fig 4.2.12 *Stability of NPs composed of AAL and P_pH3 in 0.1 M HEPES buffer pH 6.5 – zeta potential measurements, (A – aggregates formed).*

4.3.5 Stability of AAL/P_pH3 NPs in 0.01 M PBS at pH 7.4

Stability in 0.01 M phosphate buffer saline (PBS) at pH 7.4 was tested next. Changes in size of NPs after addition and storage in the buffer are shown in Figure 4.2.13. Stability of NPs in 0.01 M PBS at pH 7.4 was strongly dependent on the type of NP (negatively or positively charged). As indicated in figure 4.2.13, micron sized aggregates were formed immediately after adding 0.01 M PBS to the formulation with positively charged NPs. There was a small increase in the particle size for negatively charged NPs (from 157 to 210 nm, for AAL/P_pH3 weight ratio of 2.5) after mixing with PBS and upon the storage, but the size remained in the nano-range after 72 h. The most stable NP formulation was that with an AAL/P_pH3 weight ratio of 1.5 (no changes in PdI and a small increase in the size). Aggregates were formed immediately after adding 0.01 M PBS to the positively charged NPs as shown by the high PdI values (Figure 4.2.14).

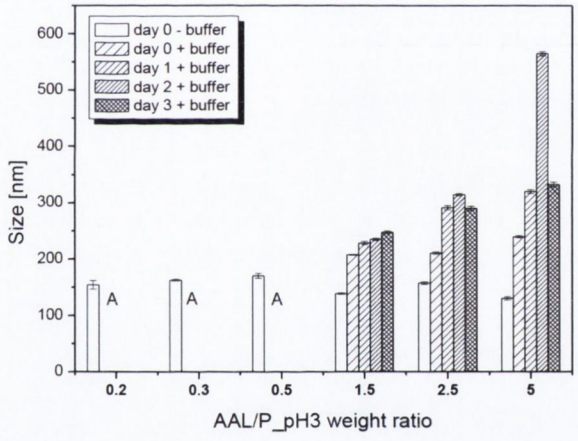

Fig 4.2.13 *Stability of NPs composed of AAL and P_pH3 in 0.01 M PBS pH 7.4 – particle size measurements, (A – aggregates formed).*

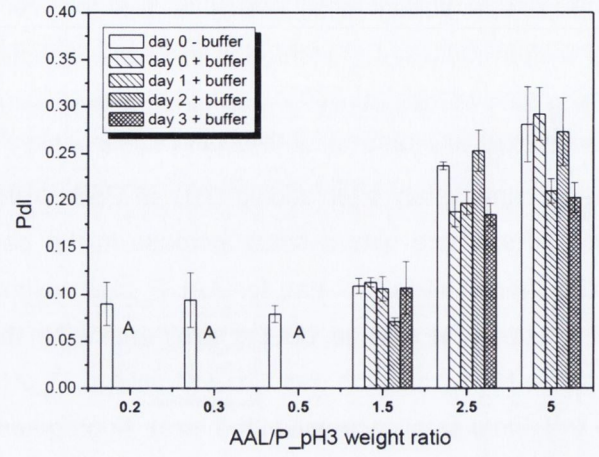

Fig 4.2.14 *Stability of NPs composed of AAL and P_pH3 in 0.01 M PBS pH 7.4 – polydispersity measurements, (A – aggregates formed).*

Addition of 0.01 M PBS caused a decrease in ZP of positively charged NPs (reaching values of 4.0 mV - 6.3 mV). A small increase in ZP values was observed after mixing negatively charged NPs with 0.01 M PBS (Figure 4.2.15). The ZP values ranged between -27.7 mV and - 29.2 mV and did not change considerably over time.

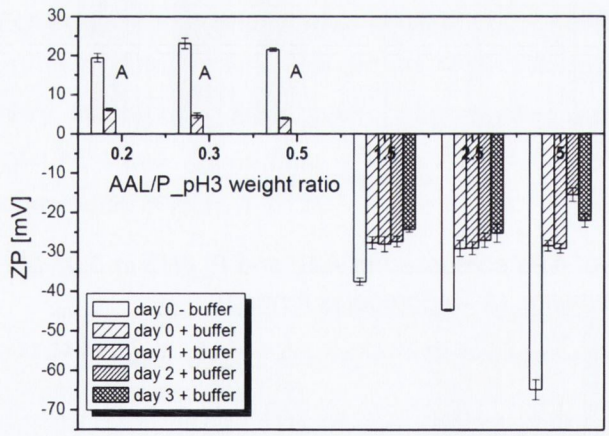

Fig 4.2.15 *Stability of NPs composed of AAL and P_pH3 in 0.01 M PBS pH 7.4 – zeta potential measurements, (A – aggregates formed).*

4.3.6 Stability of AAL/P_pH3 NPs in 0.1 M and 0.01 M NaCl

To check the impact of ionic strength on the stability of NPs, two concentrations of NaCl were tested: 0.1 M and 0.01 M. Figure 4.2.16 shows changes in the size of NPs after mixing with NaCl solution. The concentration of NaCl solution had an impact on the stability of prepared NPs. NPs were more stable when diluted NaCl

(0.01 M) was used (Figure 6.2.12 b) indicating that NPs are more stable in environments with a lower ionic strength. A small increase in the size of negatively charged NPs was observed after mixing with 0.01 M NaCl (from 140 to 182 nm for AAL/P_pH3 weight ratio of 5). The size of positively charged NPs remained stable after mixing with 0.01 M NaCl, but aggregates were formed after 24 h of storage. More concentrated NaCl (0.1 M) caused aggregation of positively charged NPs directly after mixing. Larger in size negatively charged NPs were formed when 0.1 M NaCl was used, compared to the diluted NaCl solution (0.01 M). Aggregates were formed in the formulation containing NPs at an AAL/P_pH3 weight ratio of 1.5 after 3 days of storage in 0.1 M NaCl.

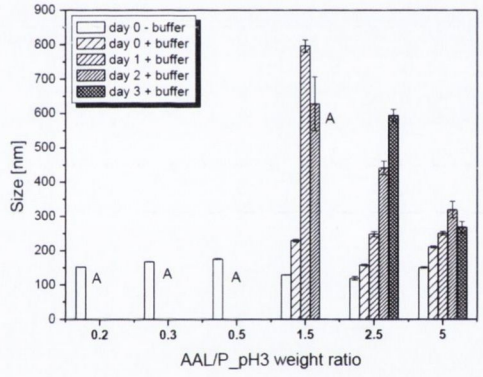

a)

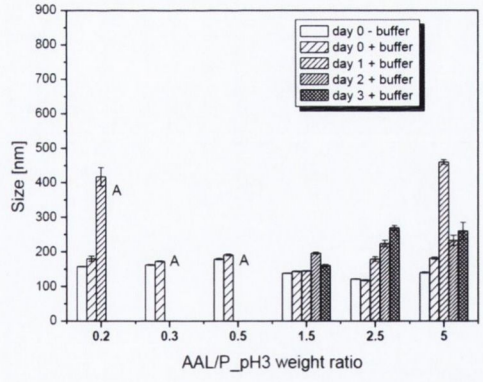

b)

Fig 4.2.16 *Stability of NPs composed of AAL and P_pH3 in* ***a)*** *0.1 M NaCl and* ***b)*** *0.01 M NaCl - particle size measurements, (A – aggregates formed).*

PdI of NPs had lower values when 0.01 M NaCl solution was added, compared to more concentrated NaCl solution (0.1 M). A small increase in PdI values was observed for all of the formulations tested after mixing negatively charged NPs with 0.01 M NaCl (Figure 4.2.17 b). PdI of positively charged NPs remained steady after mixing with 0.01 M solution of NaCl, but it increased upon storage. More

concentrated solution of NaCl (0.1 M) led to a greater increase in the PdI values. A small increase was observed for negatively charged NPs with AAL/P_pH3 weight ratios of 2.5 (from 0.194 to 0.366) and 5 (from 0.247 to 0.264), while a greater increase was shown for NPs with an AAL/P_pH3 weight ratio of 1.5, which was the least stable of all negatively charged NPs tested.

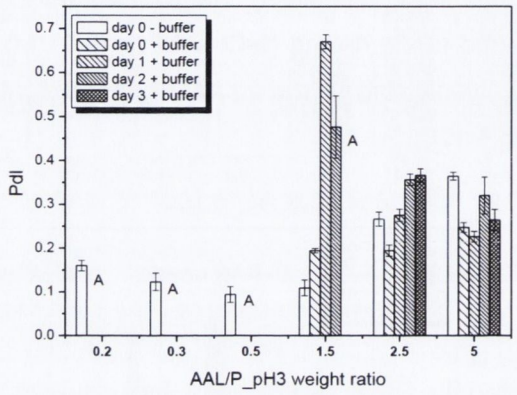

a)

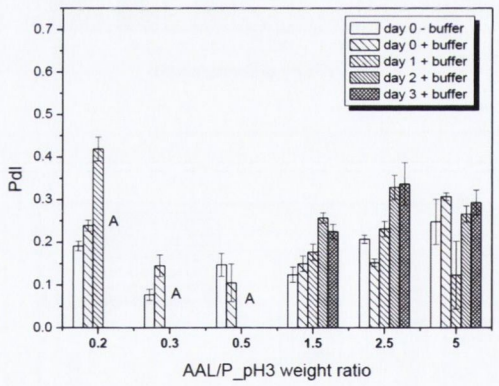

b)

Fig 4.2.17 *Stability of NPs composed of AAL and P_pH3 in* ***a)*** *0.1 M NaCl and* ***b)*** *0.01 M NaCl - polydispersity measurements, (A – aggregates formed).*

Mixing of positively charged NPs with 0.1 M NaCl caused a decrease in ZP, which was related to the rapid aggregation of these NPs (Figure 4.2.18 a). The diluted solution of NaCl (0.01 M) caused a small increase of ZP for positively charged NPs (values reached 22.7 mV - 25.9 mV). A decrease in ZP values was observed when aggregation occurred. There was an increase in ZP of negatively charged NPs, which reached values of -25.3 mV to -28.2 mV after addition of 0.1 M NaCl. A further increase in ZP values was observed upon storage in 0.1 M NaCl. A similar increase in ZP values of negatively charged NPs was observed after adding 0.01 M NaCl

(reaching values of -33.9 mV to -44.4 mV). Further storage resulted in an increase in ZP values, which were ~0 mV after 72 h of storage (Figure 4.2.18 b).

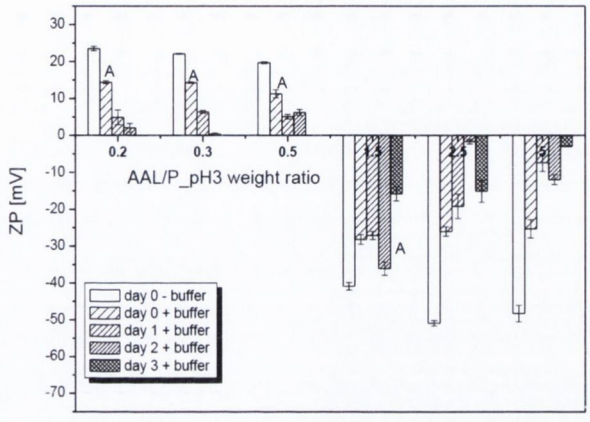

a)

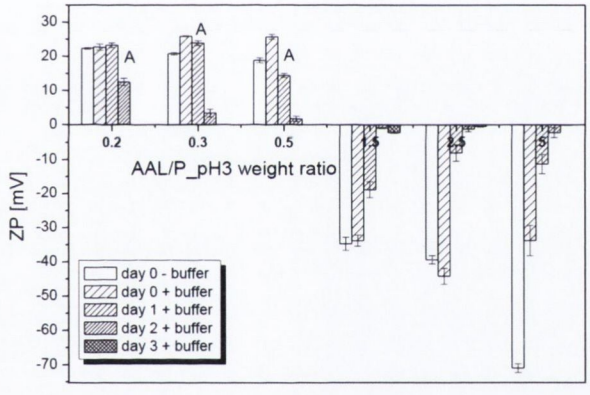

b)

Fig 4.2.18 *Stability of NPs composed of AAL and P_pH3 in* ***a)*** *0.1 M NaCl and* ***b)*** *0.01 M NaCl – zeta potential measurements, (A – aggregates formed).*

As reported, (Shu et al., 2009), low salt concentration favours the formation and growth of polyelectrolyte complex NPs, whereas a higher salt concentration may drastically interfere with the electrostatic attraction between oppositely charged polymer chains by masking the oppositely charged groups thus reducing their interaction, which was the case for positively charged NPs.

4.3.7 Stability of AAL/P_pH3 NPs in cell culture medium

Stability studies in cell culture medium (Minimum Essential Medium Eagle, MEM, pH 7.4) were performed as further studies included experiments with Caco-2 cells. Two formulations of NPs with AAL/P_pH3 weight ratios of 5 (negatively charged) and 0.2 (positively charged) were diluted with the liquid medium. Particle size, PdI and ZP,

measured after dilution and after 1 day of storage at RT is presented in Table 4.4. Dilution of NPs with the cell culture medium caused an increase in the size and PdI of negatively charged NPs. A greater increase in the size was noticed when lower concentrations of NPs were tested. ZP values of negatively charged NPs increased upon dilution in the medium (Table 4.4). Negatively charged NPs remained stable in the medium up to 24 h of storage. Positively charged NPs formed aggregated immediately after dilution with the liquid medium.

To ensure that the osmolarity of NPs diluted in the culture medium corresponded to the osmolarity of normal saline solution, glucose was added to reach the final osmolarity 280 mOsm/L. Size, polydispersity and zeta potential of NPs diluted with culture medium without and with the addition of glucose was measured as the data is shown in Table 4.5.

Adjusting the osmolarity of NP dispersion in cell culture medium led to a small increase in the size and PdI of negatively charged NPs, but it had no impact on the charge of tested NPs. Aggregates were formed after dilution of positively charged NPs with the culture medium.

Table 4.4 *Stability of AAL/ P_pH3 NPs in 0% MEM.*

AAL/P_pH3 weight ratio	NPs concentration in 0%MEM [mg/ml]	Particle size [nm]		PdI		ZP [mV]	
		in 0% MEM		**in 0% MEM**		**in 0% MEM**	
		after preparation	next day	after preparation	next day	after preparation	next day
5	1.0	136±1	-	0.236±0.008	-	-58.6±2.0	-
	0.5	210±2	267±3	0.253±0.059	0.269±0.025	-25.1±2.7	-22.0±1.6
	0.25	242±9	292±5	0.278±0.032	0.273±0.025	-23.9±1.0	-13.4±3.1
	0.1	325±5	310±6	0.206±0.026	0.316±0.029	-21.2±2.2	-20.1±1.2
0.2	1.0	145±1	-	0.127±0.028	-	20.0±0.7	-
	0.5	A	A	A	A	A	A
	0.25	A	A	A	A	A	A
	0.1	A	A	A	A	A	A

A - aggregates formed

Table 4.5 *Stability of AAL/ P_pH3 NPs in 0% MEM after adding glucose.*

AAL/P_pH3 weight ratio	NPs concentration in 0%MEM [mg/ml]	Particle size [nm]		PdI		ZP [mV]	
		in 0% MEM		**in 0% MEM**		**in 0% MEM**	
		after preparation - glucose	after preparation + glucose	after preparation - glucose	after preparation + glucose	after preparation - glucose	after preparation + glucose
5	1.0	177±1	-	0.218±0.009	-	-66.4±2.1	-
	0.5	240±2	294±4	0.159±0.016	0.223±0.009	-28.7±0.9	-26.7±0.8
	0.4	254±1	289±4	0.178±0.017	0.192±0.019	-26.4±1.5	-27.8±0.9
	0.3	308±9	316±110	0.263±0.008	0.255±0.022	-27.9±0.9	-28.0±1.4
	0.2	278±3	-	0.195±0.021	-	-28.0±2.1	-
	0.1	307±4	-	0.198±0.012	-	-25.3±0.5	-
0.2	1.0	183±2	-	0.222±0.016		21.8±0.4	-
	0.5	A	A	A	A	A	A
	0.4	A	A	A	A	A	A
	0.3	A	A	A	A	A	A
	0.2	A	-	A	-	A	-
	0.1	A	-	A	-	A	-

A - aggregates formed

4.4 Conclusions

A wide range of NPs composed of alginic acid with low viscosity (AAL)/protamine (P) and alginic acid medium viscosity (AAM)/protamine (P) were prepared and characterised by measuring their particle size, polydispersity and zeta potential. Both polymers and protamine were dissolved in water at a concentration of 0.1% w/v and were mixed in various polymer/protamine weight ratios. Different methods of NP preparation were tested, including the sequence in which both components were mixed (method 1A and 1B) and the speed of polymer addition (method 2A and 2B).

The fast addition of P solution to the stirred solution of polymer resulted in the formation of NPs that were smaller in size and with lower PdI values. Also, a different sequence of addition of one solution to the other was tested. Generally, NPs which were smaller in size and with lower PdI values and negatively charge were obtained when P solution was added to the polymer solution. For positively charged NPs, the method of preparation did have an impact, as slightly better results were obtained when polymer solution was added to the solution of P. The final method selected to prepare further NP formulations was the addition of P solution to the stirred aliquot of alginate solution.

To facilitate insulin entrapment in the NPs, it was decided that the pH of one of the NP component solutions had to be lowered. At first the pH of alginate solution was adjusted to 2, however only aggregates/microparticles were formed after mixing with P solution for all of the weight ratios tested. This is because of the instability of alginic acid at low pH, which is deprotonated in these conditions. As no NPs were formed when the pH of AAL solution was adjusted to 2, further manipulations with pH of P solution were performed. Adjustment of P solution to 2 resulted in the formation of only negatively charged NPs. Furthermore, excess of P caused formation of aggregates. When pH of P solution was adjusted to 3, two types of differently charged (negatively and positively) NPs were formed by combining 0.1% w/v solution of AAL and 0.1% w/v solution of protamine at pH 3 at various volume ratios. Since not many differences between properties of NPs formed from alginic acid at low viscosity and medium viscosity were observed, NPs composed of AAL were selected for further testing.

The most promising formulations (with the lowest size and PdI) were chosen for further stability testing: three formulations containing negatively charged NPs with AAL/P_pH3 weight ratios of 5, 2.5 and 1.5 and three formulations containing positively charged NPs at AAL/P_pH3 weight ratios of 0.5, 0.3 and 0.2. Stability of the NPs tested was strongly dependent on the initial charge of the formulation. Physical stability of NPs upon storage at RT showed very good stability of negatively

charged NPs, while an increase in particle size and PdI was observed for all formulations of positively charged NPs.

Rapid increase in the NP size and PdI was observed following addition of HCl (0.1 and 0.01 M), however better stability was noticed for positively charged NPs, compared to those with a negative charge. The instability of negatively charged NPs at low pH could be explained by the properties of alginic acid, which forms a high-viscosity "acid gel" under the conditions tested. An increase in pH of the tested buffer (acetate buffer pH 4.5) caused instability of positively charged NPs, which formed aggregates directly after adding acetate buffer (interactions between positively charged groups of P and negatively charged acetate groups lead to the neutralisation of the charge and formation of aggregates), while negatively charged NPs were more stable. An increase in the stability of positively charged NPs was observed after adding HEPES buffer at pH 6.5, as NPs formed aggregates after 24 h of storage in the buffer. Good stability of negatively charged NPs in the acetate buffer pH 4.5 and HEPES buffer pH 6.5 could be explained by the properties of alginate, which is reported to be chemically stable at pH values between 5 and 10. Interactions between positively charged moieties of P and negatively charged groups of acetate or HEPES leads to the formation of aggregates and instability of those NPs in tested buffers. Similar behaviour was observed after testing in 0.01 M PBS buffer at pH 7.4.

To investigate the impact of ionic strength on the stability of NPs, NaCl at concentrations of 0.1 M and 0.01 M was tested. Negatively charged NPs remained stable in NaCl, while positively charged NPs formed aggregates. Finally, stability in cell culture medium was tested. Negatively charged NPs remained stable, while aggregates were formed for all dilutions of positively charged NPs. The addition of glucose had no impact on the stability of NPs tested.

Generally, negatively charged NPs showed better physical stability in most of the buffers/solutions studied. The exception was HCl solutions, leading to the formation of aggregates in the case of negatively charged NPs and better stability in the case of positively charged NPs.

CHAPTER 5

CHARACTERISATION AND STABILITY OF CARRAGEENAN/PROTAMINE CARRIERS

5.1 Introduction

Data presented in Chapter 4 of this thesis shows the ability to form polyelectrolyte complexes between negatively charged polymer – alginic acid and positively charged protamine. Based on those results another type of nanocarrier based on the PEC principle, using carrageenan as a negatively charged polymer and protamine as a positively charged cell penetrating peptide was designed and prepared.

Shumilina and Shchipunov tested interactions between carrageenan and chitosan (Shumilina and Shchipunov, 2002). It was shown that the nature or type of carrageenan considerably influenced the characteristics of the PEC that was formed with chitosan. The mechanical strength of PEC gels formed between chitosan and different carrageenans were in order λ- > ι- > κ-carrageenan. Moreover, the gels obtained for ι- and κ-carrageenan were temperature sensitive, due to the helix-coil conformational transitions in their molecules (Shumilina and Shchipunov, 2002). An investigation was performed on the potential of PEC between κ-, ι-, λ-carrageenan and chitosan to form controlled release systems for glucose oxidase (Briones and Sato, 2010). The complex between chitosan and κ-carrageenan showed high encapsulation efficiencies for glucose oxidase while having the lowest release rate for this compound. Furthermore, this complex was able to protect the encapsulated glucose oxidase against degradation in pH 1.2 solution, in a chitosanase solution and in a pepsin solution (Briones and Sato, 2010). Another example of chitosan/carrageenan PECs used for delivery of protein drug has been reported (Li at al., 2013). As characterised by Li et al., in acidic solution, negatively charged sulphate groups of carrageenan (κ in this case) binded to positively charged amino groups of chitosan and formed acid-base PEC. When the pH was increased, amino groups deionised so the binding activity between both became weaker, which resulted in swelling and disintegration of PEC and final release of the drug. Modulation of drug release to the target site was possible by adjusting the factors that cause swelling properties of PEC (Li et al., 2013). A study reported by Leong et al., show the encapsulation of insulin into lectin-funcionalised carboxymethylated κ-carrageenan microparticles. Insulin-loaded microparticles were prepared by ionotropic gelation process. The size of prepared particles ranged from 700±100 μm to 1300±200 μm. Results obtained by this research group clearly showed that insulin entrapped into described microparticles was protected from hydrolysis and proteolysis by stomach acids and enzymes (Leong et al., 2011).

It is important to highlight that in the colloid conformation, the sulphate groups of carrageenans are further apart than in the helix conformation so long range intermolecular forces between the sulphate groups are weaker in the colloid formation (Thrimawithana et al., 2011). The anionic character of carrageenans when

present in the helix conformation would appear more important for PEC formation. Therefore, based on the above, polyelectrolyte complex NPs composed of carrageenan (as an anionic polymer) and protamine (a positively charged CPP) were designed and characterised to select the most favourable formulation. Prepared carrier NPs were characterised regarding their particle size, surface chemistry/charge and aggregation propensity. Next, physical stability studies of NPs with the most promising physical characteristics were performed. To determine the quality and applicability of prepared carriers for oral delivery stability studies in buffers at various pH was carried out.

5.2 Formulation of empty carrageenan/ protamine NPs

5.2.1 Solubility and physicochemical properties of carrageenans

* Physicochemical properties of protamine solutions were already characterised in Section 4.2.1 of this thesis.

The presence of sulphate groups on the hydrophobic backbone of carrageenan polymer facilitates the solubility of carrageenans in water. It was reported that kappa carrageenan (KC) and iota carrageenan (IC) can undergo thermal and salt – induced coil – helix transitions, forming double helices prior to gel formation (Hugerth et al., 1997). For that reason solubility of all three types of carrageenans was first assessed. Adequate quantities of carrageenans were dissolved in deionised water at RT to achieve a final polymer concentration of 0.1% w/v. As expected, LC dissolved completely to the clear solution due to the greater sulphate groups content (Pavli et al., 2011). It was noticed that KC and IC were not dissolved completely at RT. The final dissolution method for these polymers (KC and IC) was established to be in water at a temperature of 80 °C, which was confirmed by literature (British Pharmacopoeia, 2012). Three different concentrations of each type of polymer was prepared and the pH and viscosity was measured (Table 5.1).

Table 5.1 *Preparation, pH and viscosity of carrageenan solutions at various concentrations. LC – lambda carrageenan, KC – kappa carrageenan, IC – iota carrageenan. Measurements were carried out at RT.*

Component	Preparation method	Concentration [%]	pH	Viscosity [mPa·s]
LC	in H_2O at RT	0.05	7.15	4.58±0.06
		0.1	7.89	6.06±0.19
		0.2	8.43	8.78±0.04
KC	in H_2O at 80°C	0.05	6.66	3.62±0.13
		0.1	7.19	5.49±0.04
		0.2	7.44	8.49±0.16
IC	in H_2O at 80°C	0.05	6.25	2.63±0.05
		0.1	6.59	4.34±0.01
		0.2	6.97	7.52±0.13

As summarised in Table 5.1, both viscosity and pH value of carrageenan solutions decreased in the following order: LC> KC> IC, for each concentration investigated. The highest viscosity was measured for LC solutions and this type of carrageenan also has the higher sulphate content. The viscosity and pH of the solutions decreased with respect to the concentration. The pH of the polymer solutions was neutral or slightly basic, which is more desirable due to the polymer instability in acidic solutions (Phillips and Williams, 2000).

5.2.2 Preliminary studies on the formation of carrageenan/protamine nanoparticles

Preliminary studies were performed with 0.1% w/v solution of each carrageenan and 0.1% w/v solution of protamine to check their ability to form PECs. Prepared nanocomplexes were characterised by particle size, polydispersity (PdI) and zeta potential (ZP), (Table B.1 (KC/P NPs), Table B.2 (LC/P NPs) and Table B.3 (IC/P NPs), Appendix B). Figure 5.1.1 compares the particle size of NPs prepared by using three different types of carrageenan.

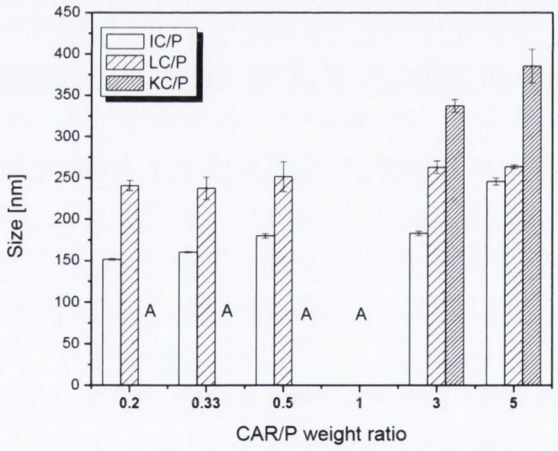

Fig. 5.1.1 *Comparison of particle size values for NPs composed of various types of carrageenans (CAR) (KC, IC, LC) and protamine (P), (A – aggregates formed).*

It was reported that KC has been recently used to prepare colloidal nano-formulations made by the spontaneous emulsification (using KC and dodecyltrimethylammonium) and ionic interaction (between KC and chitosan) method (Rosas – Durazo et al., 2011; Pinheiro et al., 2012). Based on that it would be expected that PECs at nano-dimensions will be formed between KC/P, however that was not the case. Aggregates (micron-sized particulates) were formed for most of the KC/P weight ratios tested (0.2 – 1). Formation of aggregates was further highlighted by very high PdI values (Figure 5.1.2). NPs with the particle size of

~250 nm were formed from LC/P (Figure 5.1.1). However, aggregation occurred for LC/P weight ratio of 1. Generally, LC/P NPs were larger in size and had greater PdI for LC/P weight ratio lower than 1 (bigger content of polymer resulted in negatively charged NPs). Thus the more positively charged LC/P NPs presented smaller particle sizes and lower PdI. NPs with the smallest particle size and with the lowest PdI were obtained for IC/P (Figure 5.1.1 and Figure 5.1.2). It was noticed that particle size and PdI of those NPs increased with increasing content of polymer. Aggregates were formed at the same weight ratio as for LC/P NPs, which was 1.

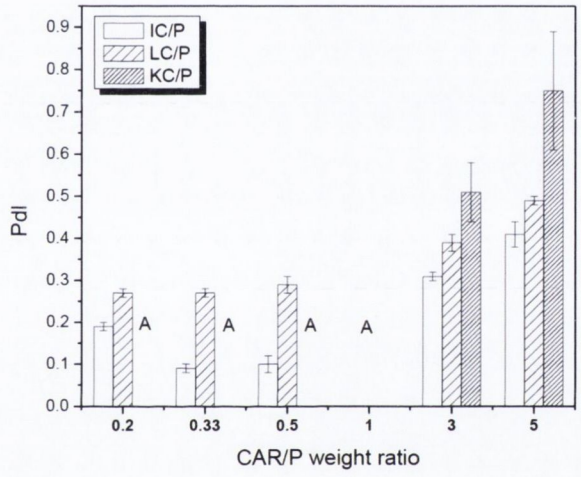

Fig. 5.1.2 *Comparison of polydispersity index values for NPs composed of various types of carrageenans (CAR) (KC, IC, LC) and protamine (P), (A – aggregates formed).*

Figure 5.1.3 compares the surface charge of prepared NPs. Both: negatively and positively charged NPs were formed for each of the polymers tested. ZP of positively charged NPs had similar values for each type of NP, due to the P contribution, which was similar in each case. Negatively charged NPs composed of KC/P and LC/P had similar ZP values (~ -60 mV). Lower charge was obtained for negatively charged IC/P NPs (~ -40 mV). As expected the lowest ZP value was obtained for LC/P NPs as LC has three sulphate groups per disaccharide unit, whereas KC has just one. It was expected that KC/P should show the greatest ZP within negatively charged NPs, however that was not the case. As indicated aggregates were formed for all of the weight ratios of KC/P tested, which would suggest weak interactions between KC and P. Although in case of IC/P NPs nanocomplexes between IC (two sulphate groups per disaccharide unit) and P were formed, which explains their greater ZP compared to other polymers.

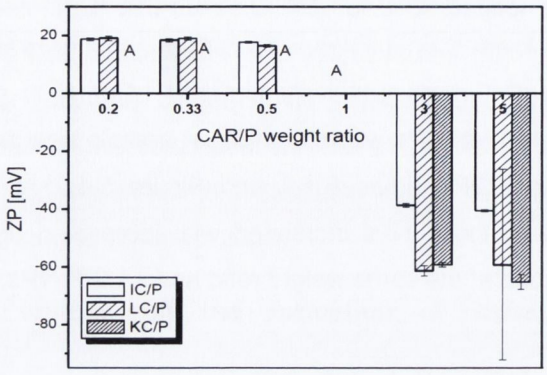

Fig. 5.1.3 *Comparison of zeta potential values for NPs composed of various types of carrageenans (CAR) (KC, IC, LC) and protamine (P), (A – aggregates formed).*

Within all three different types of carrageenans NPs formed from IC/P displayed the most promising results in terms of obtaining NPs with the smallest particle sizes (Figure 5.1.1) and lowest PdI values (Figure 5.1.2). NPs at IC/P weight ratio of 2 and 3 showed very similar characteristics within negatively charged NPs, with a particle size of 180 – 190 nm (Table C.3, Appendix C). The PdI for those NPs was 0.26 and 0.31. Positively charged formulations were smaller in size (below 180 nm) and had lower PdI, averaging below 0.2.

Prepared nanodispersions were characterised by pH and viscosity measurements and the results are tabulated (Table B.1, B.2 and B.3 for KC/P, LC/P and IC/P NPs, respectively). It was noticed that pH of the solution decreased with decreasing content of carrageenan. In the case of viscosity (Figure 5.1.4) the values for NPs were lower than the viscosity of respective carrageenan solution alone for each formulation tested. This could be indicative of PEC formation rather than gel formation and might be attributed to the formation of independent carrageenan/protamine domains causing a reduction in solution viscosity. For three different types of carrageenan, IC/P formulations displayed the lowest values for negatively charged NPs and the highest for positively charged NPs, while there were no differences between LC and KC. It was noticed that there was a proportion of increased pH and viscosity values with increased content of carrageenan present for all of three types of carrageenan being tested.

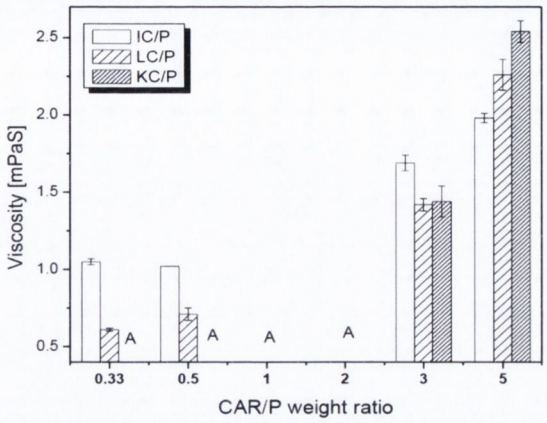

Fig. 5.1.4 *Comparison of viscosity values for NPs composed of various types of carrageenans (CAR) (KC, IC, LC) and protamine (P), (A – aggregates formed).*

5.2.3 Influence of carrageenan/protamine concentration on NPs formation

As reported by Rao and Geckeler (2011), the concentration of polymer used can influence the NPs formation and can play an important role in the control of particle size. Therefore, a solution of KC was prepared at two various concentrations: 0.05% w/v and 0.1% w/v and was combined with 0.05% w/v and 0.1% w/v solution of P. KC was chosen as the most problematic showing aggregates at almost all KC/P weight ratio range. NPs formulated by combining 0.05% w/v solutions of KC and P were characterised by particle size, PdI and ZP. Additionally, properties of formed nanocomplexes (pH and viscosity) were measured. (Table B.4, Appendix B). Comparison of the NPs characteristics formed with two various concentrations of KC and P (particle size, PdI and ZP) was carried out. Figure 5.1.5 illustrates the comparison of the particle size KC/P NPs formed from two various concentrations of polymer solutions. Dilution of KC and P solution allowed the formation of particulates at nano size for all formulations tested (KC/P weight ratio of 0.22 – 5), (Figure 5.1.5).

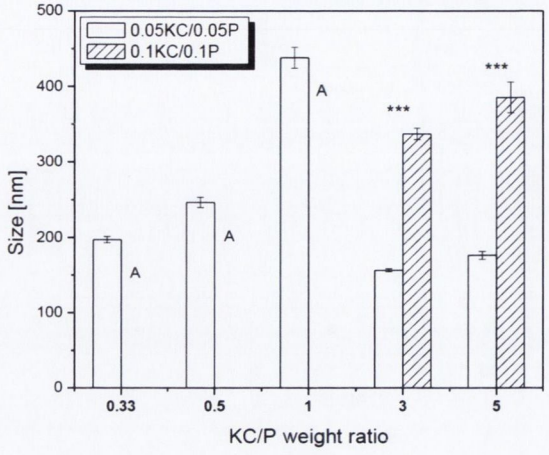

Fig. 5.1.5 *Comparison of particle size values for NPs composed of two different concentrations of KC and P, (A – aggregates formed, statistical analysis: # - no significant difference, *p<0.05, **p<0.01, ***p<0.001).*

NPs formed with 0.05% w/v solution of KC and the same concentration of P had lower PdI values for all of the formulations tested (Figure 5.1.6), which ranged from 0.210 to 0.460 (greater value was obtained for greater KC/P weight ratio).

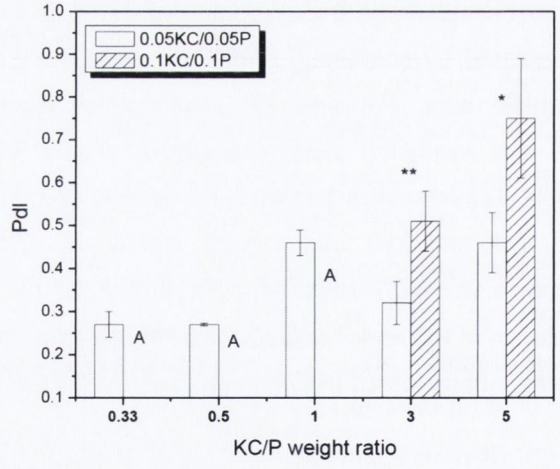

Fig. 5.1.6 *Comparison of polydispersity index values for NPs composed of two different concentrations of KC and P, (A – aggregates formed, statistical analysis: # - no significant difference, *p<0.05, **p<0.01, ***p<0.001).*

As shown in Figure 5.1.7 the concentration of KC/P had a significant impact on the surface charge of formed NPs. Lower concentration caused formation of NPs with greater ZP for both negatively and positively charged NPs, which could be due to the

weaker ionic interactions that between both polymers. Using KC and P solution at concentration of 0.1% w/v caused formation of aggregates.

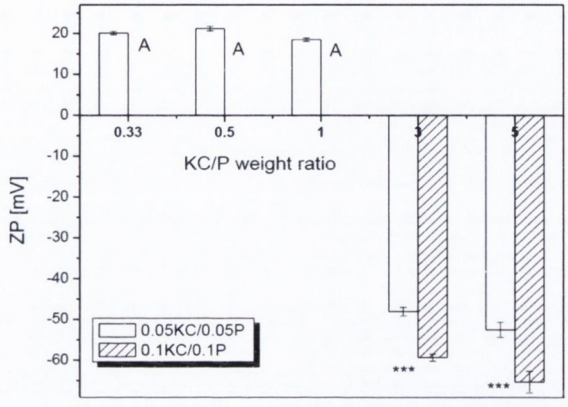

Fig. 5.1.7 *Comparison of zeta potential values for NPs composed of two different concentrations of KC and P, (A – aggregates formed, statistical analysis: # - no significant difference, *p<0.05, **p<0.01, ***p<0.001).*

Presented in this section data show that both: particle size (Figure 5.1.5) and PdI (Figure 5.1.6) of prepared NPs was improved, when concentration of KC and P was lowered to 0.5% w/v. However, it is important to note that previously presented insulin containing polysaccharide NPs showed a greater association efficiency of the drug when greater concentration of polymer was applied in their formulation (Sarmento et al., 2006 b, Gupta and Karar, 2011). NPs prepared from polymers at concentrations 0.1% w/v would be most desirable in terms of further drug loading. On the other hand, viscosity was higher at higher carrageenan concentration, which promoted the formation of agglomerates. At this point IC was showing the most promising interaction with P for nanocarrier formulation. Additionally it should be noted that amines can induce ionic gelation of IC (Yeo et al., 2001). Thus this most favourable interaction might be attributed to the amine moieties in the arginine – rich protamine.

5.2.4 Influence of formulation method on the properties of NPs

Up to this point, NPs were prepared by introducing an aliquot of carrageenan solution to the aliquot of P solution under magnetic stirring (method **1A**, Section 2.4.2.3). As KC/P formulations were proving to be the most problematic in terms of NPs formation, another formulation method was tested in order to check the impact of preparation method on the NPs formation and its properties.

In method **1B** an aliquot of polymer solution was introduced to the aliquot of P solution under magnetic stirring (Section 2.4.2.3). 0.05% w/v solution of KC and

0.05% w/v solution of P were used. NPs prepared by two different methods were compared. Figure 5.1.8 illustrates the comparison of the particle size of NPs composed of 0.05% w/v solution of KC and 0.05% w/v solution of P.

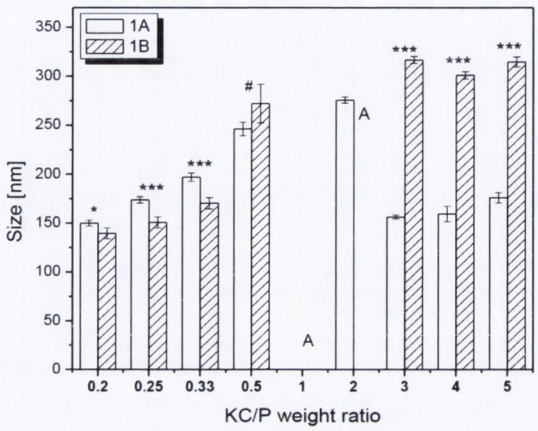

Fig. 5.1.8 *Comparison of particle size values for NPs composed of KC/P and formed by two different methods. (A - aggregates formed, statistical analysis: # - no significant difference, *p<0.05, **p<0.01, ***p<0.001).*
*(Method **1A**: an aliquot of P solution was added to the aliquot of KC solution under magnetic stirring, method **1B**: an aliquot of KC solution was introduced to the aliquot of P solution under magnetic stirring).*

Preparation method 1A (adding P solution to the stirred aliquot of KC solution) yielded NPs smaller in size and with lower PdI values in case of negatively charged NPs (Figure 5.1.8 and 5.1.9). Significant differences between the sizes of NPs were observed for all formulations tested, with exception of KC/P weight ratio of 0.5. However, positively charged NPs smaller in size and with lower PdI values were obtained with method 1B (adding an aliquot of polymer solution to the stirred aliquot of protamine solution). As an example, at the KC/P weight ratio of 0.33, NPs formed by method 1A had the particle size of 197 nm and PdI of 0.270 while for method 1B size of those NPs was 170 nm with PdI value of 0.220.

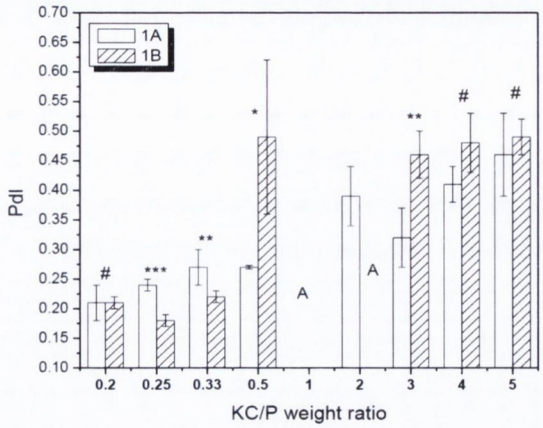

Fig. 5.1.9 *Comparison of polydisersity index values for NPs composed of KC/P and formed by two different methods. (A - aggregates formed, statistical analysis: # - no significant difference, *p<0.05, **p<0.01, ***p<0.001).*
*(Method **1A**: an aliquot of P solution was added to the aliquot of KC solution under magnetic stirring, method **1B**: an aliquot of KC solution was introduced to the aliquot of P solution under magnetic stirring).*

Considering the charge of NPs formed by two various methods (Figure 5.1.10) there were no significant differences observed for positively charged NPs, except for the KC/P weight ratio of 0.2. However, significantly different ZP values were observed for negatively charged NPs. Lower ZP was obtained when an aliquot of polymer solution was introduced to an aliquot of P solution under magnetic stirring (method 1B).

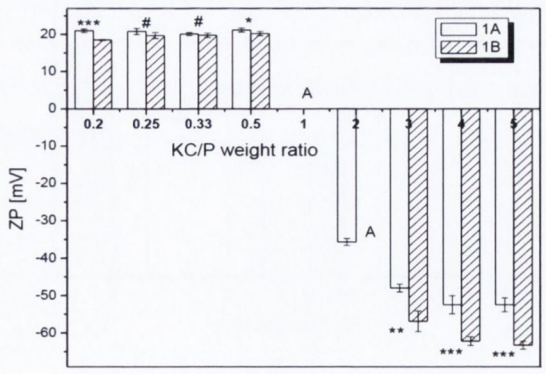

Fig. 5.1.10 *Comparison of zeta potential values for NPs composed of KC/P and formed by two different methods. (A - aggregates formed, statistical analysis: # - no significant difference, *p<0.05, **p<0.01, ***p<0.001).*
*(Method **1A**: an aliquot of P solution was added to the aliquot of KC solution under magnetic stirring, method **1B**: an aliquot of KC solution was introduced to the aliquot of P solution under magnetic stirring).*

Method 1A of NPs preparation involved adding an aliquot of positively charged P solution to an aliquot of negatively charged carrageenan solution and yielded NPs smaller in particle size in case of negatively charged NPs. Method 1B reversed this step and yielded NPs smaller in particle size and PdI for positively charged NPs. Thus the order of solution addition appears to have an impact on NP formation perhaps due to microenvironmental pH changes around negatively charged polymer chains and positively charged P residues (Qiu and Park, 2001).

As negatively charged NPs formulated by method 1A were smaller in particle size and had lower PdI values, this method was applied for all of the further formulations tested. As KC/P NPs prepared from polymer solutions at concentration of 0.1% w/v were not presenting favourable particle size and PdI, no further testing was performed with these solutions. The KC/P formulations were deemed not feasible for the formation of suitable nanocarriers for drug delivery.

As IC/P NPs were presenting he most favourable characteristics, the method of NPs preparation was examined by testing reverse sequence carrageenan/P addition. 0.1% w/v solution of IC and 0.1% w/v solution of P was used for NPs formation. Comparison of the particle size, PdI and ZP of NPs formed using method 1A and 1B was performed. Additionally statistical significance of these data was evaluated. Figure 5.1.11 compares the particle size and Figure 5.1.12 compared PdI values of NPs composed of 0.1% w/v solution of IC and 0.1% w/v solution of P.

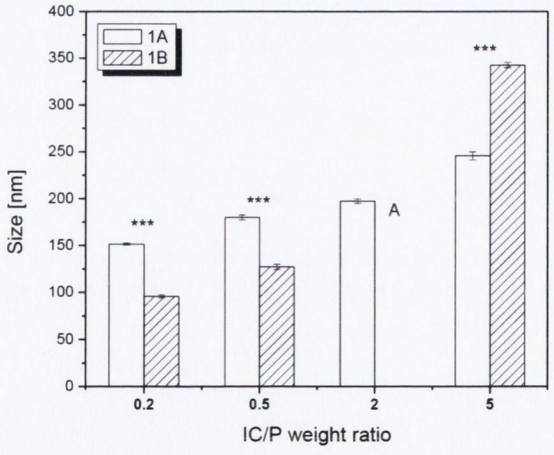

Fig. 5.1.11 *Comparison of particle size values for NPs composed of IC/P and formed by two different methods. (A - aggregates formed, statistical analysis: # - no significant difference, *p<0.05, **p<0.01, ***p<0.001).*
*(Method **1A**: an aliquot of P solution was added to the aliquot of IC solution under magnetic stirring, method **1B**: an aliquot of IC solution was introduced to the aliquot of P solution under magnetic stirring).*

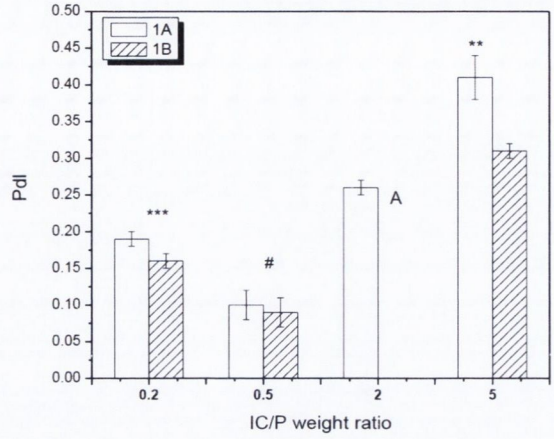

Fig. 5.1.12 *Comparison of polydispersity index values for NPs composed of IC/P and formed by two different methods. (A - aggregates formed, statistical analysis: # - no significant difference, *p<0.05, **p<0.01, ***p<0.001).*
*(Method **1A**: an aliquot of P solution was added to the aliquot of IC solution under magnetic stirring, method **1B**: an aliquot of IC solution was introduced to the aliquot of P solution under magnetic stirring).*

Similarly, as for KC/P formulations, the results confirmed that the particle size (Figure 5.1.11) and Pdl (Figure 5.1.12) of formed NPs were smaller for greater IC/P weight ratios (2 and 5) when method 1A was applied for NPs preparation (P solution added to the stirred aliquot of IC solution). Again when method 1B was employed in NPs preparation, the particle size was smaller and Pdl was lower for positively charged NPs. Significant differences in ZP of NPs prepared by the two various methods was observed only in case of negatively charged NPs (Figure 5.1.13). NPs with lower surface charge were obtained when polymer solution was added to the stirred aliquot of P solution. Positively charged NPs had similar charge for both methods tested (1A and 1B).

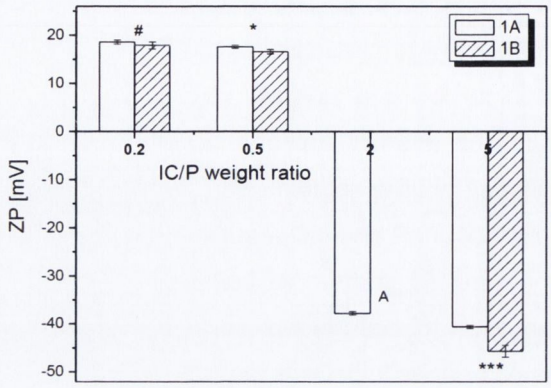

Fig. 5.1.13 *Comparison of zeta potential values for NPs composed of IC/P and formed by two different methods. (A - aggregates formed, statistical analysis: # - no significant difference, *p<0.05, **p<0.01, ***p<0.001).*
*(Method **1A**: an aliquot of P solution was added to the aliquot of IC solution under magnetic stirring, method **1B**: an aliquot of IC solution was introduced to the aliquot of P solution under magnetic stirring).*

Final conclusion of testing various methods of NPs preparation was that negatively charged NPs prepared by method 1A (adding P solution to the stirred aliquot of IC solution) had relatively small particle size and low PdI, while the order of solution mixing was less important in case of positively charged NPs. From this point NPs were prepared by method 1A, unless otherwise indicated.

5.2.5 Formation of NPs using protamine solution at pH 3 and iota carrageenan

To facilitate incorporation of insulin into prepared empty nanocarriers pH of one of the components has to be lowered (similar to the formation of alginic acid low viscosity (AAL)/protamine solution at pH 3 (P_pH3) NPs, Section 4.1.7). Acid instability is a reported property of carrageenans (Phillips and Williams, 2000). Thus, altering the pH of protamine solution to pH 3 appeared to be the most promising option. A range of NPs was formed with 0.1% w/v solution of IC and 0.1% w/v solution of P. Particle size, PdI and ZP of formed NPs was measured and tabulated (Table B.5, Appendix B). Furthermore, physicochemical properties of formed NPs (pH and viscosity) were evaluated and are presented in Table B.5 (Appendix B). Figure 5.1.14 presents the particle size and PdI index values for all of the IC/P_pH3 formulations tested.

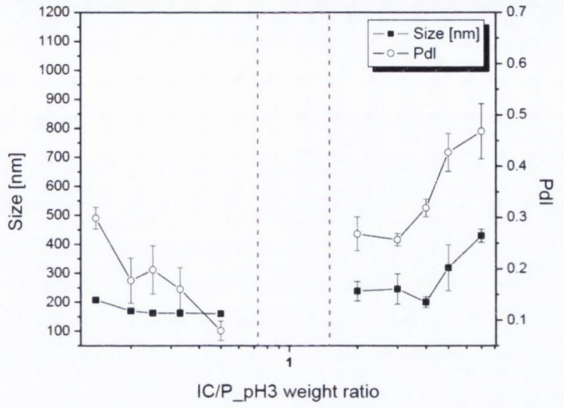

Fig. 5.1.14 *Particle size and polydisperity index values of NPs composed of IC and P (P_pH3). Preparation method **1A**: P solution at pH 3 added to an aliquot of IC solution, (---- - aggregates formed).*

NPs larger in size and with greater Pdl were obtained when more polymer was taken for NPs preparation. Particle size and Pdl of formed NPs increased with higher IC/P_pH3 weight ratio. Aggregates were formed when negatively charged residues of IC reacted completely with positively charged residues of P at pH 3 (a large increase in particle size and Pdl values). Smaller in size (lower than 200 nm) and with lower Pdl NPs were formed while more P than polymer was used for their preparation. Both: negatively and positively charged NPs were formed with ZP range of -43 mV – 22 mV, as shown in Figure 7.1.15.

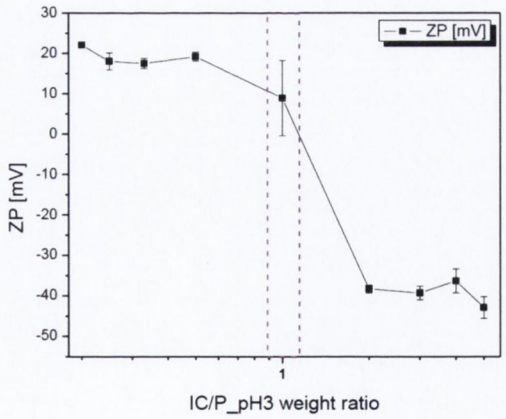

Fig. 5.1.15 *Zeta potential of NPs composed of IC and P (P_pH3). Preparation method **1A**: P solution at pH 3 added to an aliquot of IC solution, (---- - aggregates formed).*

To check the impact of pH of P solution on the NPs characteristics, NPs prepared with P solution adjusted to pH 3 and pH non-adjusted were compared. 0.1% w/v

solution of IC and 0.1% w/v solution of P (or P at pH 3) were used for NPs preparation. NPs were made according to method 1A: an aliquot of P solution at pH 3 was introduced into an aliquot of IC solution.

Figure 5.1.16 compares the particle size and Figure 5.1.17 compares PdI values for NPs prepared with P solution with pH adjusted to 3 and non-adjusted.

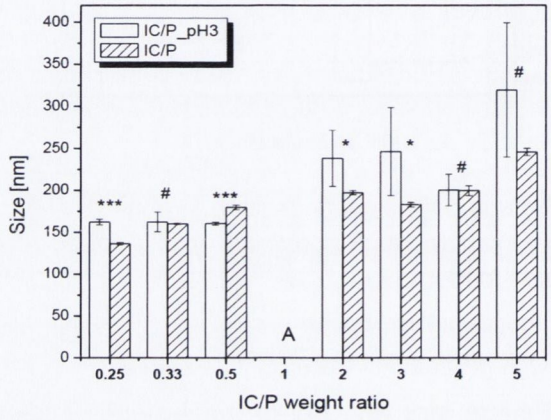

Fig. 5.1.16 *Comparison of particle size values for NPs composed of IC/P (pH of P solution non-adjusted) and IC/P_pH3 (pH of P solution adjusted to 3). (A - aggregates formed, statistical analysis: # - no significant difference, *p<0.05, **p<0.01, ***p<0.001).*

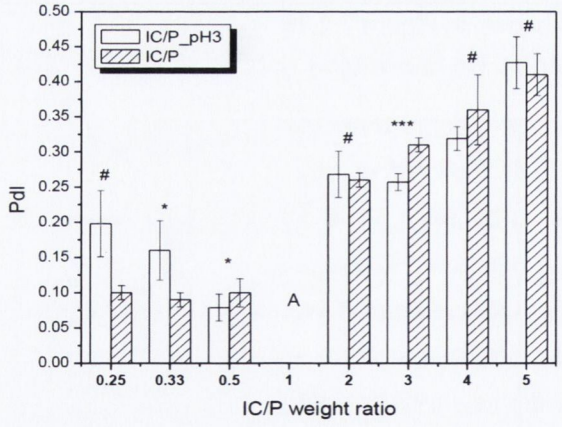

Fig. 5.1.17 *Comparison of polydispersity index values for NPs composed of IC/P (pH non-adjusted) and IC/P_pH3 (pH of P solution adjusted to 3). (A - aggregates formed, statistical analysis: # - no significant difference, *p<0.05, **p<0.01, ***p<0.001).*

The adjustment of P solution to pH 3 did not appear to have a considerable impact neither on the particle size of prepared NPs (Figure 5.1.16) nor on PdI index values (Figure 5.1.17). Significantly different values of particle size and PdI were noticed for

only a few of the formulations tested. Lowering pH of P solution did not impact on the final charge of NPs formed (Figure 5.1.18). Negatively and positively charged NPs were formed at the same IC/P and IC/P_pH3 weight ratios. Also aggregates were formed at the same weight ratio of IC/P or IC/P_pH3 equal to 1.

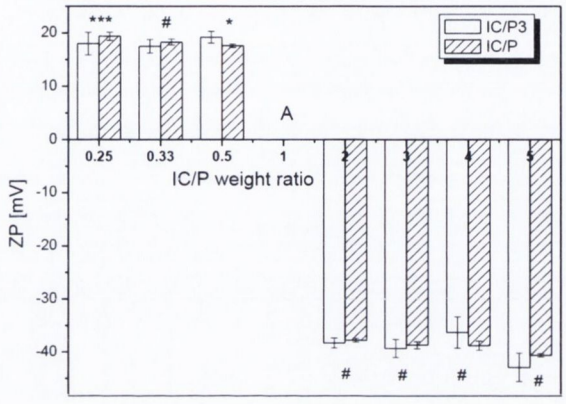

Fig. 5.1.18 *Comparison of zeta potential values for NPs composed of IC/P (pH non-adjusted) and IC/P_pH3 (pH of P solution adjusted to 3). (A - aggregates formed, statistical analysis: # - no significant difference, *p<0.05, **p<0.01, ***p<0.001).*

pH of P solution was also adjusted for LC/P formulations as the preliminary studies showed the ability of LC and P to form PEC at the nano-size range (Section 5.2.2). Particle size, PdI and ZP of nanocomplexes formed between LC in 0.1% w/v solution of and P in 0.1% w/v solution at pH 3 were measured and are summarised in Table B.6 (Appendix B). To select the best formulations for further drug loading particle size, PdI and ZP of NPs composed of LC/P_pH3 and IC/P_pH3 were compared. 0.1% w/v solutions of LC, IC and P_pH3 were used for NPs formation and method 1A was employed. Figure 5.1.19 compares the particle size and Figure 5.1.20 compares PdI for NPs composed of LC/P_pH3 and IC/P_pH3.

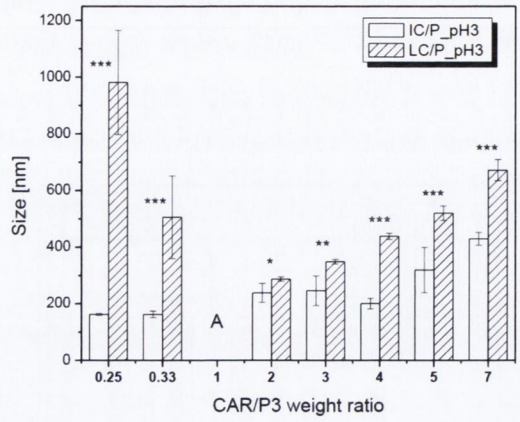

Fig. 5.1.19 *Comparison of particle size values for NPs composed of LC/P_pH3 and IC/P_pH3. (CAR – carrageenan, A - aggregates formed, statistical analysis: # - no significant difference, *p<0.05, **p<0.01, ***p<0.001).*

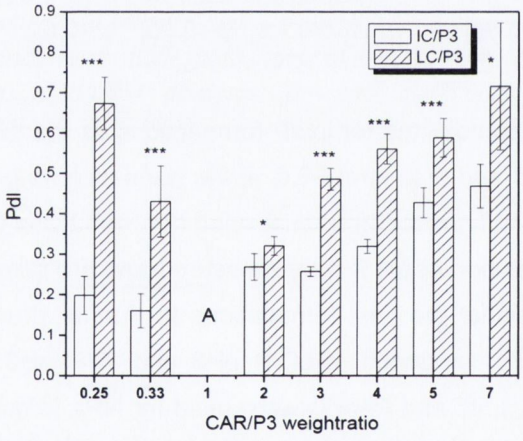

Fig. 5.1.20 *Comparison of polydispersity index values for NPs composed of LC/P_pH3 and IC/P_pH3. (CAR – carrageenan, A - aggregates formed, statistical analysis: # - no significant difference, *p<0.05, **p<0.01, ***p<0.001).*

Analysis of particle size (Figure 5.1.19) and PdI values (Figure 5.1.20) of NPs formed with two various polymers (LC and IC) and P solution at pH 3 showed that significantly smaller particles and with lower PdI NPs were obtained when IC was used as the anionic component. Aggregation of NPs occurred at the same polymer/P_pH3 weight ratio of 1. It was noted again that positively charged NPs for both types of carrageenans displayed better particle size distribution profiles. Figure 5.1.20 compares ZP values for NPs formed form two various types of polymers (IC and LC) and P solution at pH 3.

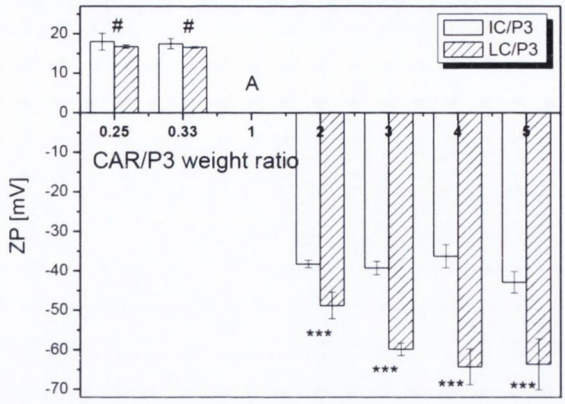

Fig. 5.1.21 *Comparison of zeta potential values for NPs composed of LC/P_pH3 and IC/P_pH3. (CAR – carrageenan, A - aggregates formed, statistical analysis: # - no significant difference, *p<0.05, **p<0.01, ***p<0.001).*

There was no significant difference for the ZP values of positively charged NPs, as in those formulations the charge was contributed mainly by P. In case of negatively charged NPs, significantly lower ZP values were obtained for NPs prepared with LC. As reported by Grehna et al. (2009), the difference between three types of carrageenans is the number of sulphate groups per unit. Because LC has three sulphate groups per two sugar units, while IC has two of them, LC forms NPs with lower final charge of NPs.

The comparison of NPs formed with three various types of carrageenan showed that NPs prepared using 0.1% w/v solution of IC and 0.1% w/v solution of P at pH 3 had the most favourable characteristics considering the particle size and homogeneity of formed NPs.

5.2.6 Influence of Ca^{2+} and Zn^{2+} cations on carrageenan/ protamine NPs formation

Calcium has been widely used to crosslink negatively charged polysaccharides to aid NP formation and to promote better size distribution and polydispersity of formed NPs (Liu et al., 2008). As reported, Ca^{2+} ions favour IC gel formation while K^{+} ions favour KC gel formation (Thrimawithana et al., 2010). Therefore addition of Ca^{2+} was tested for the improvement in IC crosslinking and formation of more compact NPs. NPs composed of IC and P (both as 0.1% w/v solutions and pH of P solution was adjusted to 3) were tested for further improvement, as those NPs indicated the most favourable characteristic considering their particle size and homogeneity (Section 5.2.5). At first, Ca^{2+} at concentration of 0.05 M was tested. However, only micron sized particles were formed after addition of Ca^{2+} ions to the IC/P_pH3 formulations.

To further check the impact of Ca^{2+} concentration, it was decreased to 0.01 M. This decrease in the ion concentration brought the particle size of formed PECs back into the nano – range, however polydispersity indices were greater compared to those of formulations without Ca^{2+}. To further optimise the formulation another ion, which could be used to promote better NP formation, was sought. As an insulin/protamine formulation containing Zn^{2+} ions (NPH) is in clinical use (Gualandi – Signoroni and Giorgi, 2001), $ZnCl_2$ was employed to test its effect on IC/P NP formation. The presence of Zn^{2+} ions at 0.01 M concentration presented NPs with the smallest particle size and the lowest PdI between all the ion solutions tested. However, particle size of NPs formed with divalent cation addition was still larger compared to formulations without ions. Figure 5.1.22 and Figure 5.1.23 compares the particle size and PdI for NPs composed of IC/P_pH3 without and with addition of cations.

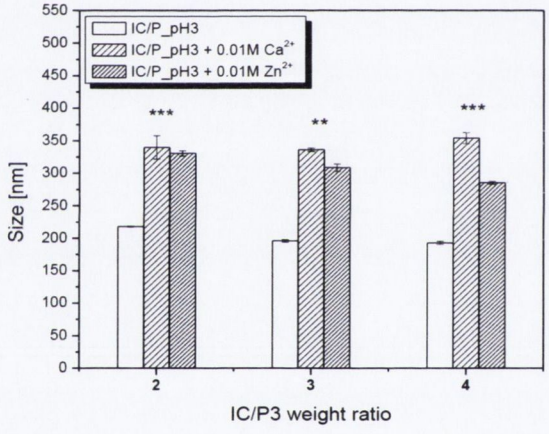

Fig. 5.1.22 *Comparison of particle size values for NPs composed of IC and P_pH3 without/ with addition of cations (statistical analysis: # - no significant difference, *p<0.05, **p<0.01, ***p<0.001).*

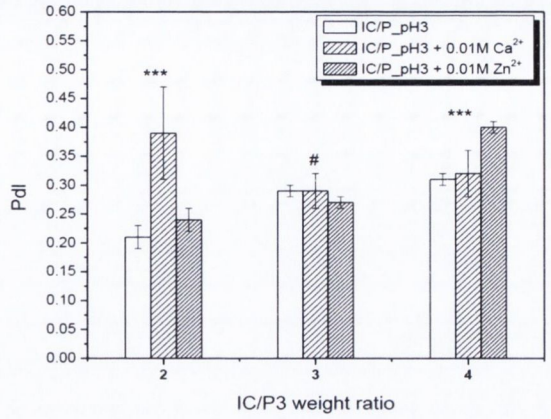

Fig. 5.1.23 *Comparison of polydispersity index values for NPs composed of IC and P_pH3 without/ with addition of cations (statistical analysis: # - no significant difference, *p<0.05, **p<0.01, ***p<0.001).*

Analysis of the particle size and Pdl of NPs formed with/without addition of cations showed that particles with smaller size and with lower Pdl were obtained without introduction of divalent cations (Figure 5.1.22 and Figure 5.1.23). As expected, additional cations present in formulations resulted in lowering ZP for all weight ratios tested due to reaction with the anionic sulphate groups of the polymer (Figure 5.1.24).

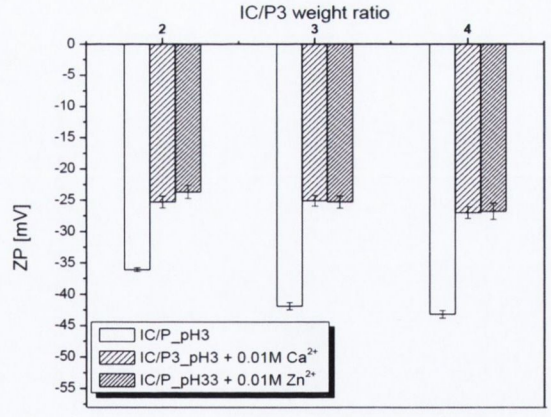

Fig. 5.1.24 *Comparison of zeta potential values for NPs composed of IC and P_pH3 without/ with addition of cations (statistical analysis: # - no significant difference, *p<0.05, **p<0.01, ***p<0.001).*

Analysis of formulation properties prepared using three various types of carrageenans (KC, LC and IC) indicated that IC formed NPs with the most favourable characteristics considering the particle size and Pdl. 0.1% w/v solutions of IC and P were used to prepare the NPs. It was noted that the method of NPs

preparation had a significant impact on their characteristics. Based on the performed tests, method 1A (introduction of an aliquot of P solution into an aliquot of IC solution under magnetic stirring) was chosen as the final method used for further tests. Lowering pH of P solution to 3 did not change the characteristics of formed NPs compared with those composed of P, where pH of the solution was unadjusted. Additional divalent cations had negative effects considering particle size and PdI of IC/P_pH3 NPs.

5.3 Physical stability of IC/P_pH3 NPs

Similarly to the studies performed for NPs composed of AAL/P_pH3 (Section 4.3 of this thesis) physical stability of the most favourable formulations of IC/P_pH3 NPs was investigated. Six types of IC/P_pH3 (at IC/P_pH3 weight ratio of 0.2, 0.3, 0.5 as positively charged and 2, 3, 4 as negatively charged NPs) were selected for further stability studies in buffers/solutions having various pH and ionic strength. Particle size, PdI and ZP were measured directly after NPs preparation, buffer addition and up to 3 days of storage at RT for each buffer/solution tested.

5.3.1 Stability of IC/P_pH3 NPs up to 72 h storage at RT

Stability of native dispersion of IC/P_pH3 NPs was tested first, up to 72 h of storage at RT. The particle size, PdI and ZP of prepared NPs was measured after preparation of NPs and every 24 h. Figure 5.2.1 presents the particle size of NPs upon storage at RT.

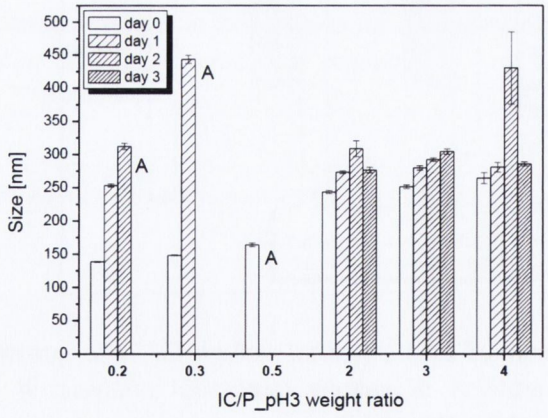

Fig 5.2.1 *Stability of NPs composed of IC and P_pH3 up to 72 h of storage at RT – particle size measurements, (A – aggregates formed).*

An increase in the particle size was noticed only for positively charged NPs (weight ratios of 0.2, 0.3 and 0.5), (Figure 5.2.1). Within those NPs IC/P_pH3 at weight ratio of 0.2 was the most stable formulation (formation of aggregates was noticed after 3

days of storage). IC/P_pH3 weight ratio of 0.5 was the most unstable formulation, as aggregates (micron sized particles) were formed after 24 h of storage. In case of negatively charged NPs (weight ratios of 2, 3 and 4) only a small increase in the particle size was observed upon storage. Similar changes were observed for PdI values of the NPs (Figure 5.2.2).

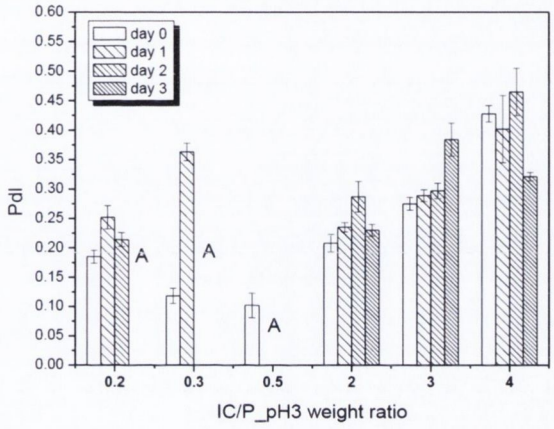

Fig 5.2.2 *Stability of NPs composed of IC and P_pH3 up to 72 h of storage at RT – polydispersity measurements, (A – aggregates formed).*

Analysis of PdI values confirmed good stability of negatively charged NPs, however it was noticed that an increase in the polymer content used for NPs preparation (greater IC/P_pH3 weight ratios) resulted in an increase in the PdI values of formed NPs (0.208 for IC/P_pH3 weight ratio of 2 and 0.428 for IC/P_pH3 weight ratio of 4). In case of positively charged NPs the greatest increase in PdI was observed for the 0.5 IC/P_pH3 weight ratio, which confirmed instability of this formulation already after 24 h of storage. NPs with the greatest P content were seen to be the most stable positively charged NPs.

As presented in Figure 5.2.3, ZP values of both negatively and positively charged IC/P_pH3 NPs remained relatively stable upon the storage at RT. The least stable formulation also had the lowest absolute ZP value (0.5 IC/P_pH3 NPs).

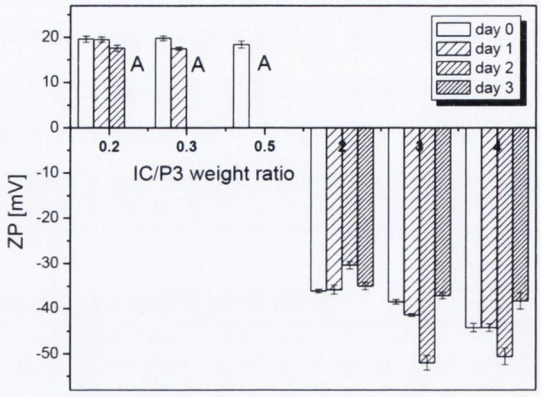

Fig 5.2.3 *Stability of NPs composed of IC and P_pH3 up to 72 h of storage at RT – zeta potential measurements, (A – aggregates formed).*

5.3.2 Stability of IC/P_pH3 NPs in 0.1 M and 0.01 M HCl

Stability studies in HCl solutions at concentrations of 0.1 M and 0.01 M (pH 2) was performed first. Measurements of particle size, PdI and ZP of NPs before/ after addition of HCl and on storage in the solutions were carried out. Figure 5.2.4 shows the changes in the particle size after addition of HCl.

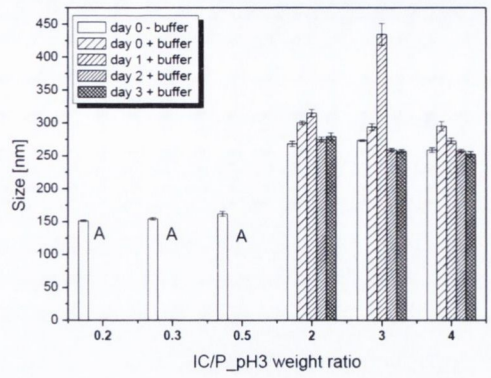

a)

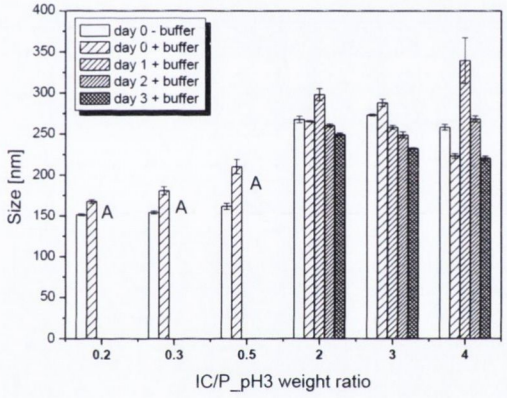

b)

Fig 5.2.4 *Stability of NPs composed of IC and P_pH3 in* ***a)*** *0.1 M HCl and* ***b)*** *0.01 M HCl – particle size measurements, (A – aggregates formed).*

Negatively charged NPs have shown similar behaviour in 0.1 M and 0.01 M HCl. Very good stability of these NPs was confirmed by their relatively stable particle size (Figure 5.2.4) and PdI values (Figure 5.2.5) after mixing with HCl and up to 3 days of storage. A different behaviour was noticed for positively charged NPs in acidic conditions. Aggregates were formed directly after mixing NPs with 0.1 M HCl. Diluting the solution of HCl to 0.01 M resulted in an improved stability of positively charged NPs, however aggregates were formed after 24 h of storage for all positively charged formulations.

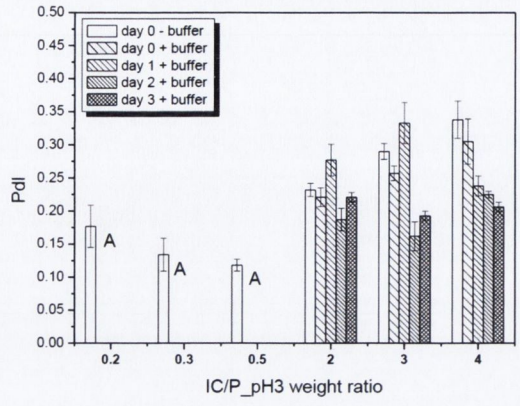

a)

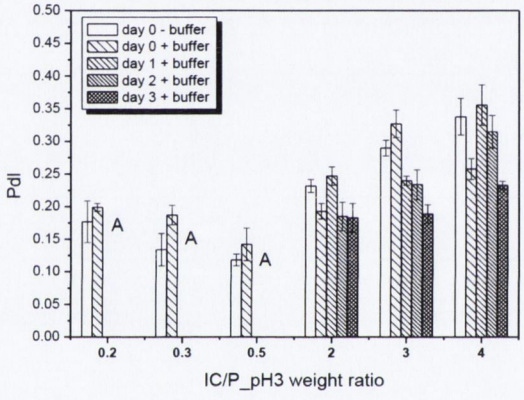

b)

Fig 5.2.5 *Stability of NPs composed of IC and P_pH3 in* ***a)*** *0.1 M HCl and* ***b)*** *0.01 M HCl – polydispersity measurements, (A – aggregates formed).*

Small changes in ZP of negatively charged NPs were noticed after mixing the dispersion with HCl at both concentrations (Figure 5.2.6), which confirmed good stability of these NPs at very low pH. Positively charged NPs formed aggregates directly after adding 0.1 M HCl. NPs in 0.01 M HCl solution did not change the charge for 0.3 and 0.5 IC/P_pH3 weight ratio formulations. An increase in the NPs charge was observed for IC/P_pH3 weight ratio of 0.2.

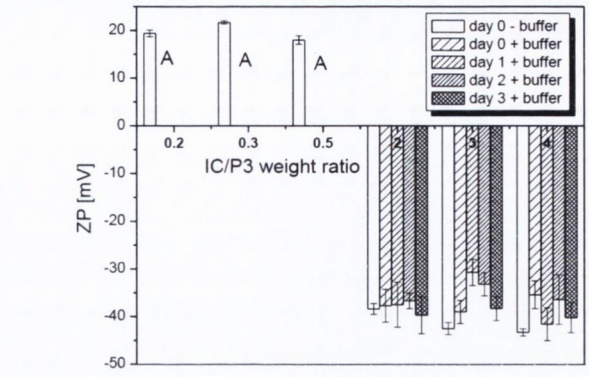

a)

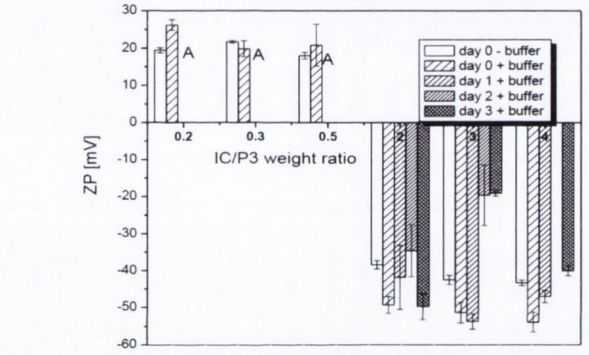

b)

Fig 5.2.6 *Stability of NPs composed of IC and P_pH3 in* ***a)*** *0.1 M HCl and* ***b)*** *0.01 M HCl – zeta potential measurements, (A – aggregates formed).*

Generally, the stability of IC/P_pH3 NPs in HCl solution was strongly dependent on the initial charge of NPs. The particle size, PdI and ZP of negatively charged formulations did not change upon addition of HCl and subsequent storage. As reported by Capron et al., who studied *in vitro* gastric stability of carrageenan, no hydrolysis of κ-carrageenan occurred in the most dramatic conditions (6 h, pH 1.2). Moreover, as reported, ι-carrageenan is always more resistant to the acidic condition compared to the κ-carrageenan (Capron et al., 1996). Positively charged NPs formed aggregates directly after addition of 0.1 M HCl solution or after 24 h in 0.01 M HCl. Weak interactions between positively charged P and IC (Stability study, Section 5.3.1) and introduction of negatively charged ions caused destabilisation of PEC and formation of aggregates. In general, negatively charged NPs showed better colloidal stability at low pH (HCl) comparing to the positively charged NPs.

5.3.3 Stability of IC/P_pH3 NPs in 0.1 M acetate buffer at pH 4.5

Stability of IC/P_pH3 NPs in 0.1 M acetate buffer at pH 4.5 was tested next, as pH of the stomach varies form 1.5 – 5. Particle size, PdI and ZP of NPs were measured after addition of the buffer and storage in acetate at pH 4.5.

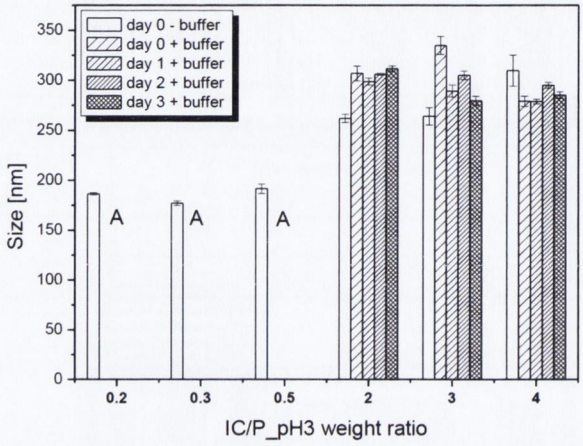

Fig 5.2.7 *Stability of NPs composed of IC and P_pH3 in 0.1 M acetate buffer pH 4.5 – particle size measurements, (A – aggregates formed).*

Figure 5.2.7 shows changes in the particle size of NPs after mixing and storage in the acetate buffer at pH 4.5. Stability of NPs, similar to the stability in HCl solutions, was dependent on the type of NP and its polymer/P weight ratio. Positively charged NPs formed aggregates immediately after adding the acetate buffer (rapid increase in the particle size and PdI, Figure 5.2.7 and 5.2.8). Very small changes in the particle size of negatively charged NPs were observed after addition of the buffer, suggesting very good stability of these NPs at pH 4.5. PdI values of these NPs decreased after adding the buffer (Figure 5.2.8).

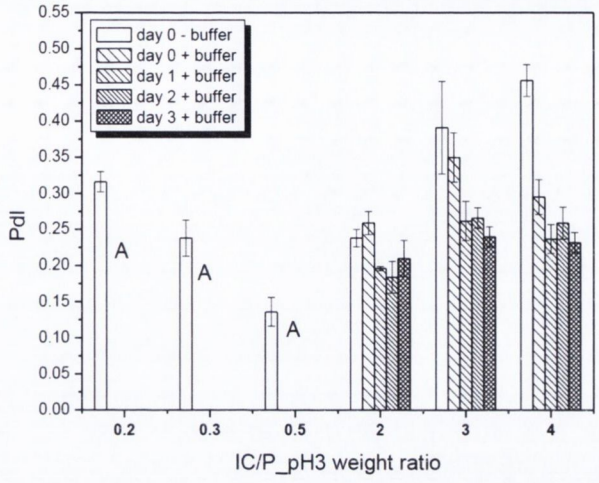

Fig 5.2.8 *Stability of NPs composed of IC and P_pH3 in 0.1 M acetate buffer pH 4.5 – polydispersity measurements, (A – aggregates formed).*

Addition of the acetate buffer caused a decrease in ZP values was noticed for all formulations of negatively charged NPs (Figure 5.2.9). The charge of these NPs remained stable upon further storage in the buffer. In case of positively charged NPs aggregation occurred directly after buffer addition.

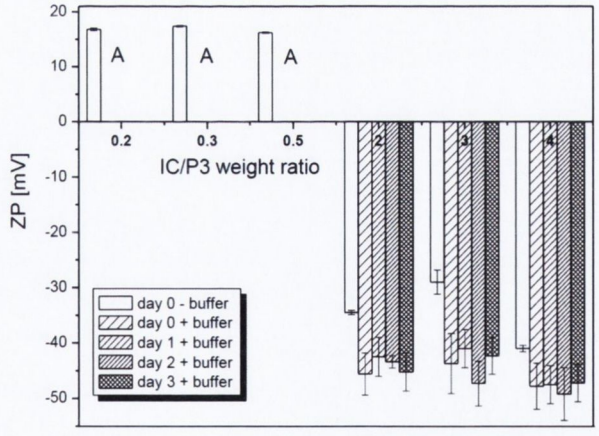

Fig 5.2.9 *Stability of NPs composed of IC and P_pH3 in 0.1 M acetate buffer pH 4.5 – zeta potential measurements, (A – aggregates formed).*

Generally, negatively charged NPs exhibited good stability in the acetate buffer at pH 4.5, while the positively charged NPs aggregated immediately after addition the buffer.

5.3.4 Stability of AAL/P_pH3 NPs in 0.1 M HEPES at pH 6.5

Particle size, PdI and ZP of NPs were measured after addition of the buffer and storage in HEPES at pH 6.5. Figure 5.2.10 illustrates changes in the particle size after addition of the buffer and during storage.

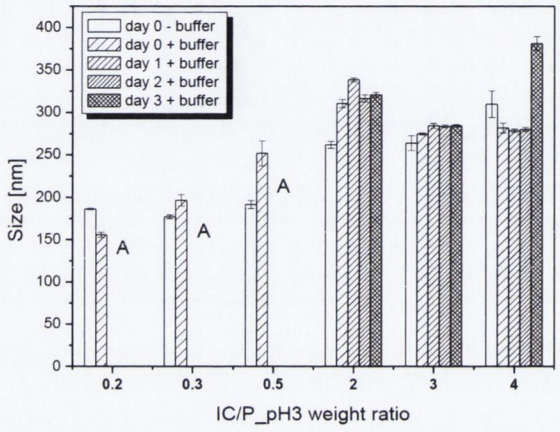

Fig 5.2.10 *Stability of NPs composed of IC and P_pH3 in 0.1 M HEPES buffer pH 6.5 – particle size measurements, (A – aggregates formed).*

Negatively charged NPs after addition of the buffer and subsequent storage were seen to be stable. PdI values for two of these NPs (IC/P_pH3 weight ratio of 3 and 4) decreased in this solution. Positively charged NPs were stable after addition of the buffer (there was no change in particle size (Figure 5.2.10), while PdI values decreased for two formulations (Figure 5.2.11)), however aggregation was visible after 24 h of storage.

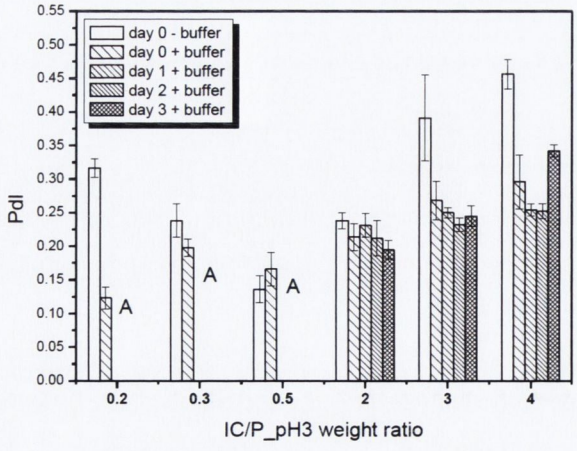

Fig 5.2.11 *Stability of NPs composed of IC and P_pH3 in 0.1 M HEPES buffer pH 6.5 – polydispersity measurements, (A – aggregates formed).*

A small increase in ZP values of positively charged NPs was observed after mixing with 0.1 M HEPES (reached value of 20 mV and above). In case of negatively charged NPs, ZP values initially decreased to finally increase to their initial values (Figure 5.2.12).

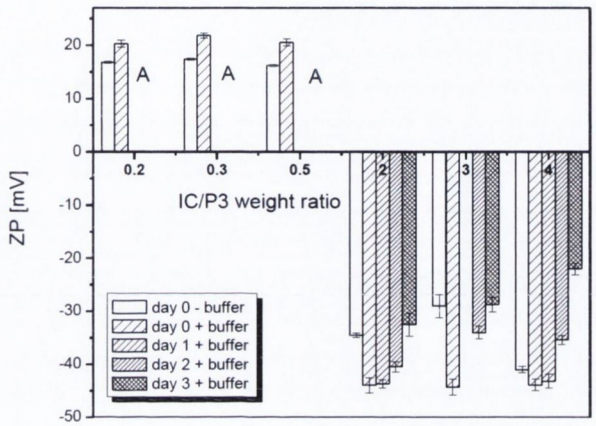

Fig 5.2.12 *Stability of NPs composed of IC and P_pH3 in 0.1 M HEPES buffer pH 6.5 – zeta potential measurements, (A – aggregates formed).*

Generally, negatively charged NPs showed good stability in the tested buffer (stable particle size). Positively charged NPs remained as discreet NPs after mixing with the HEPES buffer, however aggregation occurred after 24 h of storage.

5.3.5 Stability of IC/P_pH3 NPs in 0.1 M and 0.01 M PBS at pH 7.4

Stability of IC/P_pH3 NPs in phosphate buffer saline (PBS) at pH 7.4 was tested next. To evaluate the impact of ionic strength on the stability of NPs, two various concentrations of PBS were tested: 0.1 M and 0.01 M. Figure 5.2.13 shows changes in the particle size of NPs after mixing with the PBS solution and storage. The particle size of negatively charged NPs gradually increased after addition of PBS solution (0.1 M or 0.01 M), although it remained in the nano-range (476 nm – 547 nm after 3 days of storage in 0.1 M PBS and 360 nm – 565 nm, after 3 days of storage in 0.01 M PBS). Positively charged NPs formed aggregates directly after adding 0.01 M PBS, however, no immediate aggregation was observed after addition of 0.1 M PBS. In the latter case, aggregates were visible after 24 h of storage.

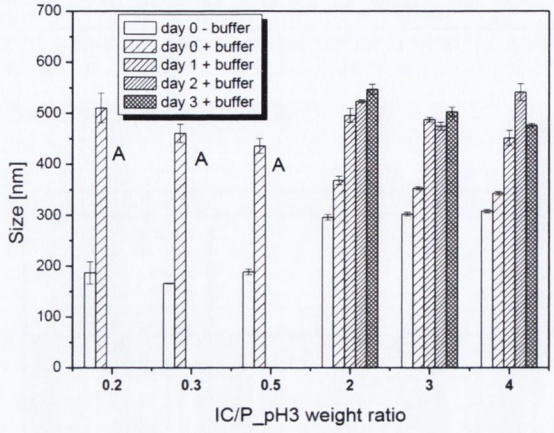

a)

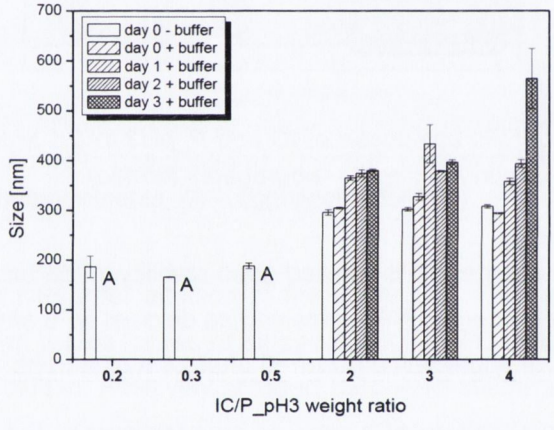

b)

Fig 5.2.13 *Stability of NPs composed of IC and P_pH3 in* ***a)*** *0.1 M PBS and* ***b)*** *0.01 M PBS pH 7.4 – particle size measurements, (A – aggregates formed).*

The changes in PdI values after addition of PBS solutions are shown in Figure 5.2.14. As illustrated, PdI of positively charged NPs increased rapidly as aggregates were formed. A small increase in the PdI values of negatively charged NPs was noticed, which shows good homogeneity of these NPs in PBS.

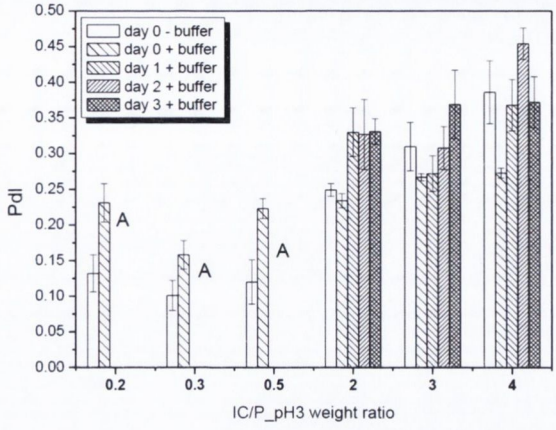

a)

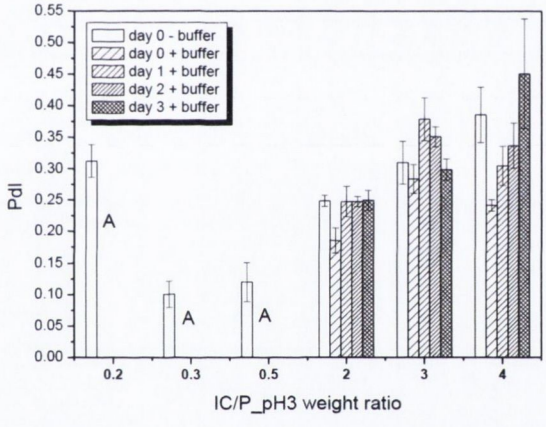

b)

Fig 5.2.14 *Stability of NPs composed of IC and P_pH3 in* ***a)*** *0.1 M PBS and* ***b)*** *0.01 M PBS pH 7.4 – polydispersity measurements, (A – aggregates formed).*

Figure 5.2.14 shows changes in ZP values of NPs after addition of PBS solutions. ZP of positively charged NPs switched to negative values after mixing with 0.1 M PBS (from 19.9 mV to -8.5 mV for IC/P_pH3 weight ratio of 0.5). Although, when less concentrated PBS was used (0.01 M), aggregation of positively charged NPs occurred. Neutralisation of the surface charge can explain the rapid formation of aggregates in 0.01 PBS, but not in 0.1 M PBS. Zeta potential of negatively charged NPs decreased after adding PBS and reached values of -18.5 mV – -20.7 mV for 0.1 M PBS and -28.8 mV – -32.9 mV for 0.01 M PBS. The charge of these NPs did not change upon storage in PBS.

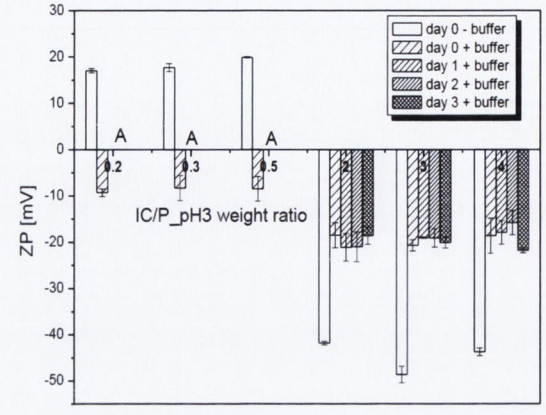

a)

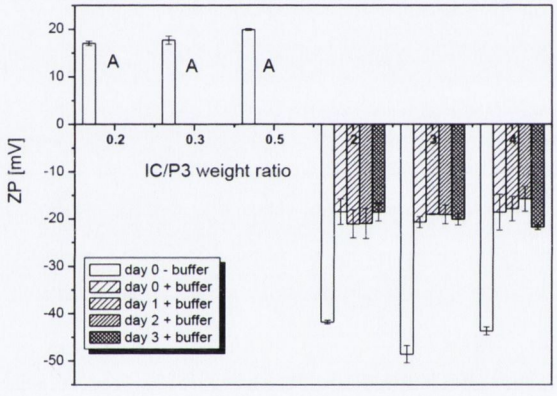

b)

Fig 5.2.15 *Stability of NPs composed of IC and P_pH3 in* ***a)*** *0.1 M PBS and* ***b)*** *0.01 M PBS pH 7.4 – zeta potential measurements, (A – aggregates formed).*

Generally, negatively charged NPs were more stable in PBS, comparing to the positively charged NPs (aggregates formed directly (for 0.01 M PBS) or after 24 h (for 0.1 M PBS)).

5.3.6 Stability of IC/P_pH3 NPs in 0.1 M and 0.01 M NaCl

To test the impact of ionic strength on the stability of NPs, two concentrations of NaCl were used: 0.1 M and 0.01 M. Figure 5.2.16 shows changes in the size of NPs after mixing with NaCl solution.

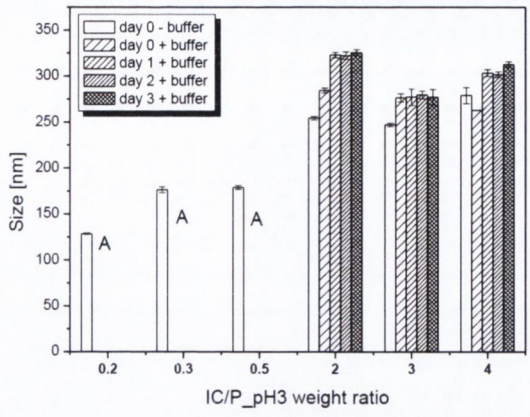

a)

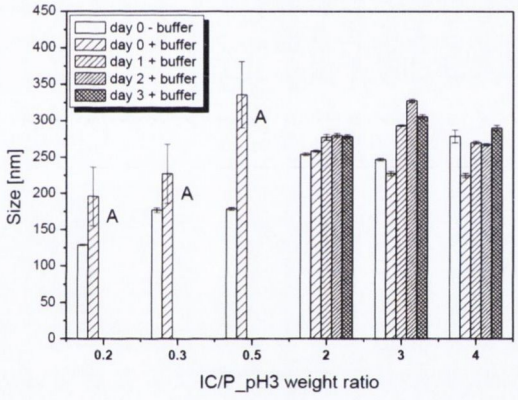

b)

Fig 5.2.16 *Stability of NPs composed of IC and P_pH3 in* ***a)*** *0.1 M NaCl and* ***b)*** *0.01 M NaCl – particle size measurements, (A – aggregates formed).*

Stability of NPs in NaCl (0.1 M an 0.01 M) strongly depended on the initial charge of NPs. As indicated in Figure 5.2.16 and 5.2.17, a rapid increase in the particle size and PdI values (aggregation) was observed after adding 0.1 M NaCl to the positively charged NPs, whereas aggregation of NPs was seen only after 24 h of storage when 0.01 M NaCl was employed (an increase in the particle size and PdI values). Negatively charged NPs were stable in both solutions of NaCl tested. Small changes in the particle size and PdI of these formulations were noticed after addition of NaCl solution and further storage (Figure 5.2.16 and Figure 5.2.17).

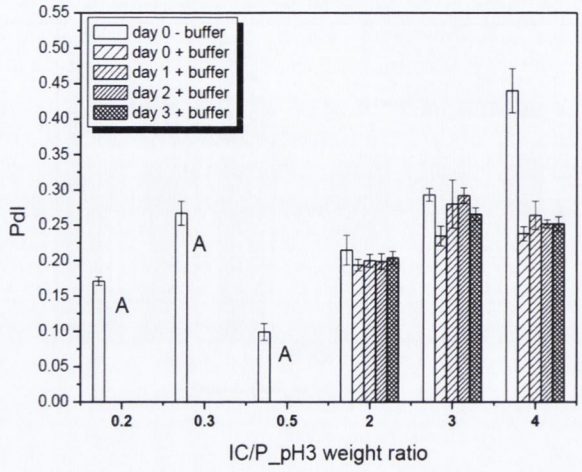

a)

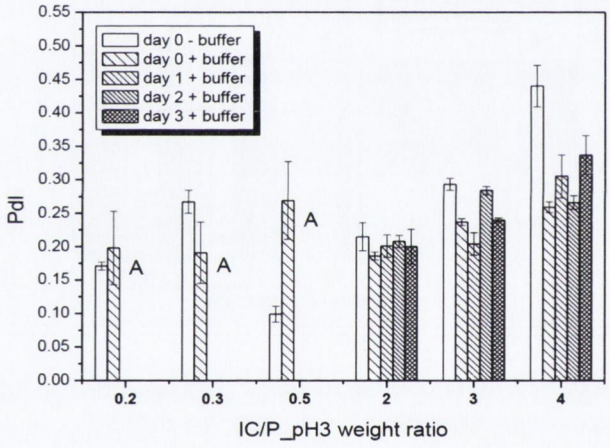

b)

Fig 5.2.17 *Stability of NPs composed of IC and P_pH3 in* ***a)*** *0.1 M NaCl and* ***b)*** *0.01 M NaCl – polydispersity measurements, (A – aggregates formed).*

An increase in the charge of NPs was noticed after addition of diluted NaCl (0.01 M), (Figure 5.2.18). ZP of negatively charged NPs did not change severely after addition of NaCl solutions. A small decrease in ZP values was observed for the formulation at IC/P_pH3 weight ratio of 2.

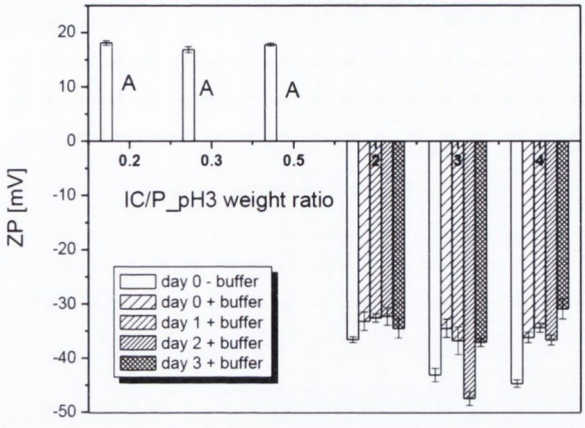

a)

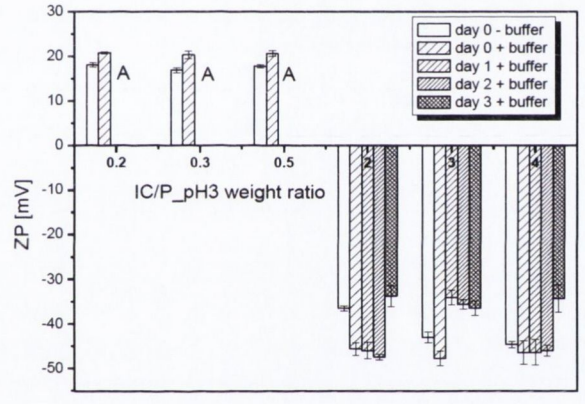

b)

Fig 5.2.18 *Stability of NPs composed of IC and P_pH3 in* ***a)*** *0.1 M NaCl and* ***b)*** *0.01 M NaCl – zeta potential measurements, (A – aggregates formed).*

The strength of NaCl solution had no impact on the stability of negatively charged NPs, as no considerable changes to the particle size, surafce charge and homogeneity were noted. Positively charged NPs were more stable in 0.01 M than in 0.1 M NaCl, however aggregates were formed after 24 h of storage. Introduction of additional electrolyte counterions from NaCl (Na^+ and Cl^-) can have an impact on the strength of interactions between the oppositely charged IC and P. Here, weakening in ionic interactions between the NP constituents due to the presence of NaCl resulted in the formation of aggregates.

5.3.7 Stability of IC/P_pH3 NPs in cell culture medium

Stability studies in cell culture medium were performed as further studies included experiments with Caco-2 cells. Stability of prepared NPs was tested in culture medium with/without addition of glucose, which was added to obtain the osmolarity

of normal saline solution. Table 5.2 summarises the changes in the NPs size, PdI and ZP after dilution in cell culture medium and adding glucose. The stability of NPs in the medium was depended on the initial charge of tested NPs. As presented in Table 5.2, both types of positively charged NPs formed aggregates after dilution in 0% MEM. There were no changes observed in the particle size and PdI values of negatively charged NPs after dilution in the 0% MEM and glucose addition. However, an increase in the charge of these NPs was noticed after dilution in the cell culture medium. Aggregation of positively charged NPs might be caused by a mixture of salts presented in 0% MEM. Introduction of additional ions caused weakening of ionic interactions between the positively charged protamine and polymer, as observed in buffers and other solutions above, and resulted in the formation of aggregates.

Table 5.2 *Stability of IC/P_pH3 NPs in 0% MEM and in 0% MEM with glucose.*

IC/P_pH3 weight ratio	NPs concentration in 0%MEM [mg/ml]	Size [nm]		PdI		ZP [mV]	
		in 0% MEM		**in 0% MEM**		**in 0% MEM**	
		after preparation - glucose	after preparation + glucose	after preparation - glucose	after preparation + glucose	after preparation - glucose	after preparation + glucose
4.	1.0	369±7	-	0.336±0.017	-	-49.2±0.7	-
	0.5	353±4	363±6	0.255±0.023	0.241±0.020	-35.7±1.1	-31.5±1.24
	0.4	n/d	394±6	0.311±0.017	0.295±0.023	-34.1±0.9	-32.1±0.94
	0.3	353±1	374±7	0.260±0.022	0.289±0.037	-31.2±1.7	-33.4±1.94
	0.2	354±12	-	0.301±0.012	-	-32.5±1.1	-
	0.1	342±4	-	0.235±0.011	-	-31.3±1.8	-
2.	1.0	343±3	-	0.292±0.007	-	-42.2±0.8	-
	0.5	352±3	406±5	0.241±0.016	0.271±0.018	-33.8±1.1	-32.5±0.86
	0.4	400±7	362±3	0.284±0.019	0.206±0.020	-32.8±0.8	-32.9±1.28
	0.3	368±5	382±5	0.244±0.009	0.267±0.011	-33.0±1.4	-30.1±0.85
	0.2	356±4	-	0.243±0.006	-	-31.0±1.1	-
	0.1	359±6	-	0.259±0.012	-	-31.3±1.4	-

A - aggregates formed, n/d – not determined

Table 5.2 *Stability of IC/P_pH3 NPs in 0% MEM and in 0% MEM with glucose.*

IC/P_pH3 weight ratio	NPs concentration in 0%MEM [mg/ml]	Size [nm]		PdI		ZP [mV]	
		in 0% MEM		**in 0% MEM**		**in 0% MEM**	
		after preparation - glucose	after preparation + glucose	after preparation - glucose	after preparation + glucose	after preparation - glucose	after preparation + glucose
0.5	1.0	206±6	-	0.112±0.006	-	15.7±0.3	-
	0.5	A	A	A	A	A	A
	0.4	A	A	A	A	A	A
	0.3	A	A	A	A	A	A
	0.2	A	-	A	-	A	-
	0.1	A	-	A	-	A	-
0.2	1.0	169±2	-	0.222±0.006	-	19.5±0.5	-
	0.5	A	A	A	A	A	A
	0.4	A	A	A	A	A	A
	0.3	A	A	A	A	A	A
	0.2	A	-	A	-	A	-
	0.1	A	-	A	-	A	-

A - aggregates formed, n/d – not determined

5.4 Conclusions

Carrageenans proved to be suitable polymers for novel nanoparticle formation via polyelectrolyte complexation with protamine sulfate. Type and concentration of carrageenans used was of particular importance, with particle size and PdI decreasing in the following order: KC>LC>IC. To determine carrageenan – protamine interactions viscosity of formed NP dispersions was measured. The reduced viscosity of the NP formulations in comparison to carrageenan solutions was suggestive of complex formation with protamine. The anionic character of IC combined with cationic groups of P appeared to possess the most desirable charge balance, since created the smallest in size and PdI and most stable NPs. KC did not show desirable interactions with P at all of the polymer/protamine weight ratios tested. KC/P formulations showed the poorest particle size distribution and extensive agglomerate formation.

An alteration of protamine solution to pH 3 and subsequent complexation with IC did not impact the particle size, PdI and ZP of NPs formed. This fact plays an important role, as described NPs were further used as suitable carriers for oral insulin delivery. The addition of calcium and zinc ions had a negative effect on nanoparticle formulation, especially considering their well-documented ability to induce iota carrageenan gel formation. Concentration of ions appeared to hold significant importance here, with lower ion concentration yielding better NPs characteristics. The undesirable effects of calcium ions on nanoparticle formation may be attributed to an excess of positive charge in formulation and crosslinking of the polymer. Therefore, the most favourable NP formulations were obtained without additional divalent cations.

The most promising formulations (with the smallest particle size and the lowest PdI) were chosen for colloidal stability testing. Stability of the tested NPs was strongly dependent on the initial surface charge of particles. Negatively charged IC/P_pH3 NPs were stable for up to 3 days when store as native dispersions (no major changes in the particle size, PdI and ZP values). The stability of positively charged NPs was dependent on the IC/P_pH3 weight ratio, with the poorest stability observed for NPs at IC/P_pH3 weight ratio of 0.5, as this formulation had the lowest initial ZP.

Good colloidal stability was seen for all negatively charged formulations (IC/P_pH3 weight ratios of 2, 3 and 4) in all solutions with different pH. This is mainly due to the properties of carrageenan, which is reported to be stable, even in harsh gastric conditions (Capron et al., 1996). There were no major changes in the particle size and PdI of those NPs in all buffers/solutions tested. In case of positively charged NPs, aggregates were formed either immediately or at most after 24 h of storage. It

was noticed that the formation of aggregates was reliant on the ionic strength of the introduced solution. It can be concluded that perhaps weaker ionic interactions between positively charged groups of P and negatively charged groups of IC were present in these NPs, as the positively charged formulations were unstable even when stored as native dispersions. Introduction of additional ions from buffers/solutions might have caused further destabilisation of the complex and formation of aggregates.

The ease of formulation and mild preparative conditions required for IC/P_pH3 NPs formation appear promising in terms of novel nanocarrier formation. In addition, the biocompatibility of carrageenans, their abundance in nature and their relative inexpensive, further indicate their feasibility as novel nanocarriers for drug delivery.

CHAPTER 6

PHYSICOCHEMICAL CHARACTERISATION, *IN VITRO* TOXICITY AND PEPTIDE TRANSPORT CHARACTERISTICS OF INSULIN LOADED NANOPARTICLES

6.1 Introduction

Development with subsequent extensive physicochemical characterisation of alginate/protamine and carrageenan/protamine nanocarierrs was described in Chapters 4 and 5, respectively.

It was shown that two differently charged (negatively and positively) types of nanoparticles (NPs) were formed by combining 0.1% w/v solution of alginic acid at low viscosity and 0.1% w/v solution of protamine at pH 3 (AAL/P_pH3 NPs) and 0.1% w/v solution of iota carrageenan and 0.1% w/v solution of protamine at pH 3 (IC/P_pH3 NPs) at various weight ratios. Stability studies were performed with the most promising formulations of described NPs (with the smallest particle size and the lowest PdI values). Colloidal stability of selected negatively charged formulations (AAL/P_pH3 weight ratios of 5, 2.5, 1.5 and IC/P_pH3 weight ratios of 4 and 2) and positively charged formulations (AAL/P_pH3 weight ratios of 0.5, 0.3, 0.2 and IC/P_pH3 weight ratios of 0.5 and 0.2) was examined in a range of media with various pH. It was shown that the stability of tested NPs was strongly dependent on the initial charge of NPs tested.

Based on the results presented in Chapters 4 and 5, a range of carriers was selected for further insulin loading (AAL/P_pH3 weight ratios of 5, 1.5, 0.5 and 0.2 and IC/P_pH3 weight ratios of 4, 2, 0.5 and 0.2). Selected NPs were characterised by the smallest particle size, narrow particle size distribution profiles (lowest polydispersity (PdI)) and various zeta potential (ZP) values (both: negatively and positively charged NPs were selected).

The goal of this part of work was to prepare insulin-loaded NPs based on the selected carriers as described above. Two insulin concentrations of 100 µg/ml and 500 µg/ml were studied. Formed NPs were characterised in terms of their physicochemical properties (particle size, PdI and ZP) and stability under storage. Association efficiency and *in vitro* release of insulin in media at various pH was further examined. *In vitro* toxicity and peptide transport through Caco-2 monolayers was tested to assess their suitability and potential as oral nanoparticulate drug delivery systems.

6.2 Formulation and *in vitro* characterisation of AAL/P_pH3 NPs loaded with insulin

6.2.1 Insulin association efficiency of AAL/P_pH3 NPs

To determine the amount of drug that can be loaded into the prepared carrier, insulin association efficiency was tested. Two amounts of insulin (100 and 500 µg/ml) were loaded and tested for their association efficiency (AE). Four types of AAL/P_pH3 NPs were studied for their ability to encapsulate/bind insulin. The amount of non-

associated insulin was separated by a combined ultrafiltration-centrifugation technique as described in Section 2.4.2.11. The physical characteristics of NPs before and after centrifugation were tested to investigate effects of the separation process on physical stability of NPs. The data is summarised in Table C.1 and Table C.2 (Appendix C).

Analysis of properties of AAL/P_pH3 NPs loaded with 100 µg/ml pre- and post-processing shows no major changes to the particle size, PdI and charge for AAL/P_pH3 NPs with weight ratios of 5 and 0.2. NPs with AAL/P_pH3 weight ratios of 1.5 and 0.5 were found to be unstable as a decrease in ZP was observed and the samples aggregated. Therefore these two types of NPs were excluded from further studies with the concentration of insulin of 500 µg/ml. Association efficiency (AE) and drug loading of the various AAL/P_pH3 NPs are summarised in Table 6.1.1.

Table 6.1.1 *Association efficiency and drug loading of NPs composed of AAL/P_pH3 loaded with 100 µg/ml and 500 µg/ml of insulin.*

AAL/P_pH3 weight ratio	NPs with 100 µg/ml of insulin	NPs with 500 µg/ml of insulin	NPs with 100 µg/ml of insulin	NPs with 500 µg/ml of insulin
	AE [%]		Drug loading [%]	
5	99.9±0.2	99.0±1.8	9.1±0.0	33.1±0.5
1.5	99.9	-	9.1	-
0.5	89.9	-	8.3	-
0.2	93.2±4.4	86.7±4.2	8.6±0.4	30.2±1.0

AE of prepared AAL/P_pH3 NPs was controlled by the polymer/protamine weight ratio. Excellent AE values were obtained for the AAL/P_pH3 weight ratio of 5 for both amounts of insulin loaded. Almost 100% of insulin was incorporated into this type of NPs. A lower amount of AAL and increasing amount of P in NP (0.2 AAL/P_pH3 weight ratio) resulted in smaller AE values. Only 93% of the initial amount of insulin was incorporated when 100 µg/ml peptide was used. Increasing the amount of insulin to 500 µg/ml decreased AE of this system to 87%. Similar observations were made for the drug loading. AAL/P_pH3 NPs loaded with 100 µg/ml of insulin had similar drug loading of approximately 9%, similar to alginate/chitosan NPs developed by Sarmento et al. (2007 b). Sarmento's NPs were formed by ionotropic pre-gelation of alginate followed by polyelectrolyte complexation to chitosan. AE of insulin in the study of Sarmento et al. was over 70% and furthermore insulin was released in a pH-dependent manner under stimulated gastrointestinal conditions. Drug loadings of approximately 30% and above were obtained when 500 µg/ml peptide was used.

6.2.2 Characterisation of AAL/P_pH3 NPs loaded with insulin

As mentioned in the previous section, NPs with AAL/P_pH3 weight ratios of 1.5 and 0.5 were found to be unstable, therefore physicochemical characterisation of only

two formulations (negatively charged at AAL/P_pH3 weight ratio of 5 and positively charged at AAL/P_pH3 weight ratio of 0.2) loaded with insulin was carried out next. Figure 6.1.1 illustrates comparison of the particle size for empty and insulin loaded NPs composed of AAL/P_pH3.

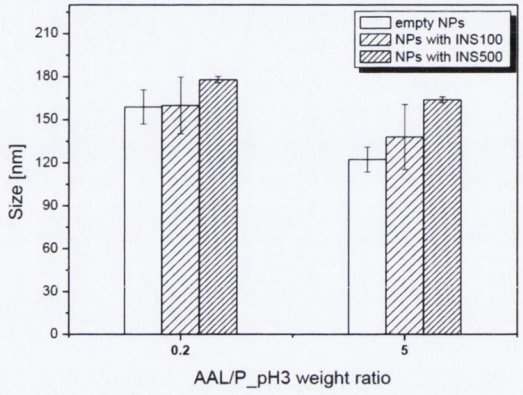

Fig. 6.1.1 *Comparison of particle size values for empty and insulin loaded AAL/P_pH3 NPs. (INS100 - NPs loaded with 100 µg/ml of insulin, INS500 - NPs loaded with 500 µg/ml of insulin).*

Loading NPs with insulin caused a small increase in the size of the formed NPs. It can be noticed that the size was increased with the amount of insulin loaded, but only for the NPs loaded with 500 µg/ml, for both types of NPs tested (negatively and positively charged). The mean size of negatively charged NPs (AAL/P_pH3 5 weight ratio) increased from 122 to 164 nm while that for the positively charged NPs (AAL/P_pH3 0.2 weight ratio) increased from 159 nm (empty NPs) to 178 nm.

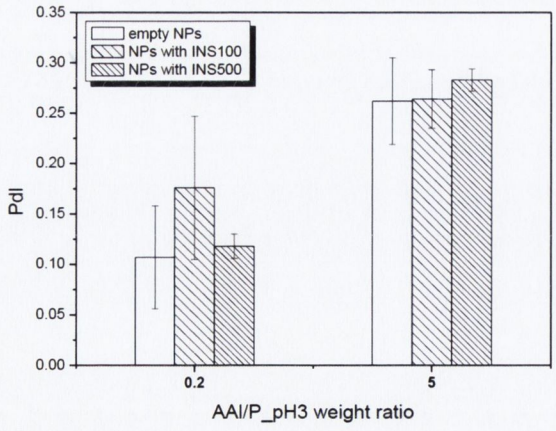

Fig. 6.1.2 *Comparison of polydispersity index values for empty and insulin loaded AAL/P_pH3 NPs. (INS100 - NPs loaded with 100 µg/ml of insulin, INS500 - NPs loaded with 500 µg/ml of insulin).*

No change in PdI values for both: negatively and positively charged NPs was observed (Figure 6.1.2). The mean values varied from 0.262 for empty NPs to 0.283 for NPs loaded with 500 µg/ml of insulin for negatively charged NPs and from 0.107 for empty NPs to 0.118 for NPs loaded with 500 µg/ml of insulin for positively charged NPs. Small fluctuations in the charge of prepared NPs (ZP measurements) were observed when insulin was incorporated (Figure 6.1.3).

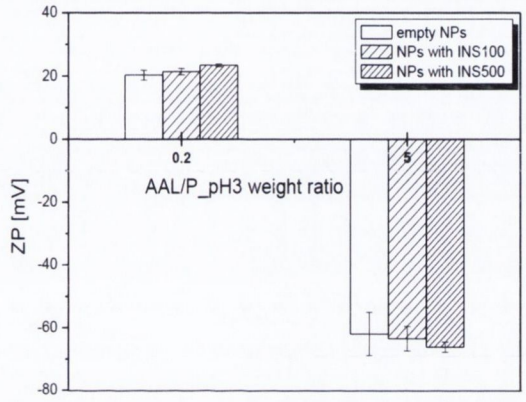

Fig. 6.1.3 *Comparison of zeta potential values for empty and insulin loaded AAL/P_pH3 NPs. (INS100 - NPs loaded with 100 µg/ml of insulin, INS500 - NPs loaded with 500 µg/ml of insulin).*

Incorporation of insulin had no impact on ZP values of negatively charged NPs. In case of positively charged NPs ZP increased from 20.3 mV for empty NPs to 23.4 mV ($p<0.001$) for NPs loaded with 500 µg/ml of insulin. The increase in ZP of positively charged NPs can be explained by the positive charge of insulin, which was dissolved in protamine solution at pH 3, below its isoelectric point (pI of insulin is 5.3).

6.2.3 Stability of AAL/P_pH3 NPs loaded with insulin

Physical stability of insulin-loaded AAL/P_pH3 NPs was examined up to 3 days of storage at room temperature (RT). Changes in the particle size of NPs loaded with insulin are presented in Figure 6.1.4.

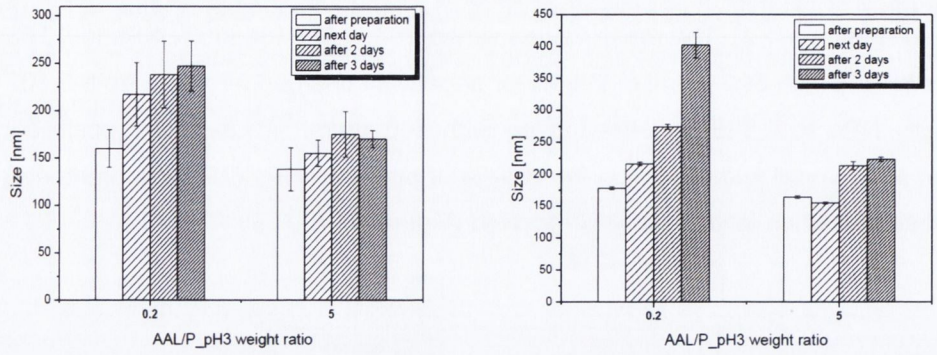

a) b)

Fig. 6.1.4 *Stability of AAL/P_pH3 NPs loaded with:* ***a)*** *100 µg/ml and* ***b)*** *500 µg/ml of insulin up to 72 h of starage at RT – particle size measurements.*

Generally, negatively charged NPs (AAL/P_pH3 weight ratio of 5) were seen to be more stable upon storage than positively charged NPs (AAL/P_pH3 weight ratio of 0.2), for both amounts of insulin loaded. The particle size of AAL/P_pH3 NPs (weight ratio of 5) loaded with 100 µg/ml of insulin increased from 138 to 170 nm upon 3 days of storage. In case NPs loaded with insulin 500 µg/ml the increase from 164 to 223 nm was observed. A larger increase in size was noticed for positively charged NPs. The size increased from 160 to 247 nm for NPs loaded with 100 µg/ml of insulin. In case of 500 µg/ml dose, a larger increase in size was noticed (from 178 nm to 402 nm) after 3 days of storage at RT).

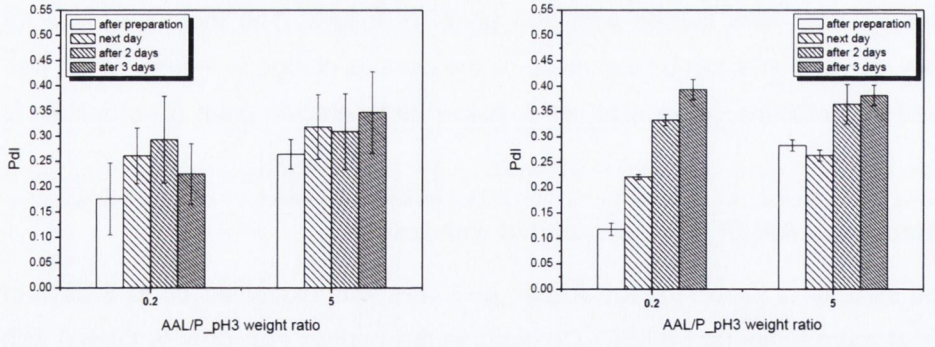

a) b)

Fig. 6.1.5 *Stability of AAL/P_pH3 NPs loaded with:* ***a)*** *100 µg/ml and* ***b)*** *500 µg/ml of insulin up to 72 h of starage at RT – polydispersity index measurements.*

No change in PdI values for AAL/P_pH3 NPs loaded with 100 µg/ml of was seen (Figure 6.1.5). In case of positively charged, 500 µg/ml-insulin containing NPs, PdI increased from 0.118 to 0.393 after 3 days of storage at RT. A smaller increase was observed for negatively charged NPs (from 0.283 to 0.381 after 3 days of storage).

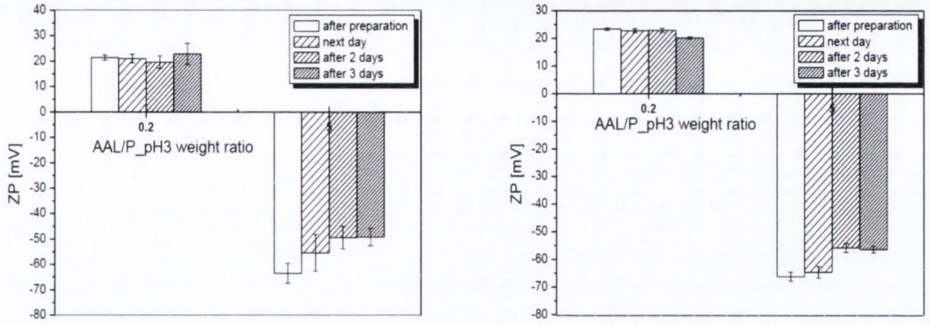

a) b)

Fig. 6.1.6 *Stability of AAL/P_pH3 NPs loaded with:* ***a)*** *100 µg/ml and* ***b)*** *500 µg/ml of insulin up to 72 h of starage at RT – zeta potential measurements.*

ZP of positively charged NPs remained stable for formulations with both amounts of insulin (100 and 500 µg/ml) loaded into AAL/P_pH3 NPs (Figure 6.1.6). In case of negatively charged NPs an increase in ZP was observed upon storage. It increased from -63.5 mV to -49.2 mV for NPs loaded with 100 µg/ml and from -66.2 to -56.4 mV for 500 µg/ml of insulin.

The stability study confirmed good characteristics of AAL/P_pH3 NPs loaded with 100 µg/ml and 500 µg/ml of insulin upon 3 days of storage at RT. Negatively charged NPs had better colloidal stability than positively charged NPs, however both types of AAL/P_pH3 NPs tested remained in the nanosize range over 3 days of storage.

6.2.4 Release of insulin from AAL/P_pH3

6.2.4.1 Release from AAL/P_pH3 NPs loaded with 100 µg/ml of insulin

Release studies in four media at various pH were performed: 0.01 M HCl (pH 2), 0.1 M acetate buffer (pH 4.5), 0.01 M PBS (pH 7.4) and FaSSIF (Fasted State Simulated Intestinal Fluid) to simulate pH and conditions present in the various parts of the GI tract. Release profiles from two types of NPs (negatively charged at AAL/P_pH3 weight ratio of 5 and positively charged at the AAL/P_pH3 weight ratio of 0.2) loaded with 100 µg/ml of insulin were investigated.

6.2.4.1.1 Release in HCl buffer (pH 2)

The properties of AAL/P_pH3 NPs (size, PdI and ZP) were studied before and after release in HCl (Table C.3, Appendix C). An increase in the particle size and PdI was observed after release in HCl for both types of NPs tested. The changes in ZP were dependent on the type of NPs. ZP of negatively charged NPs increased to a positive value (-62.6 mV to 12.9 mV), while there was a small increase in ZP of positively charged NPs (from 21.5 mV to 23.6 mV).

Insulin release profiles when HCl, pH 2, was used as the medium are presented in Figure 6.1.6. Nearly 100% of insulin released in the first minutes of studies from positively charged NPs, however only 45% of insulin was released within the first 10 minutes of the study from negatively charged NPs and the amount of released insulin slowly increased to reach 84% after 6 h of the study.

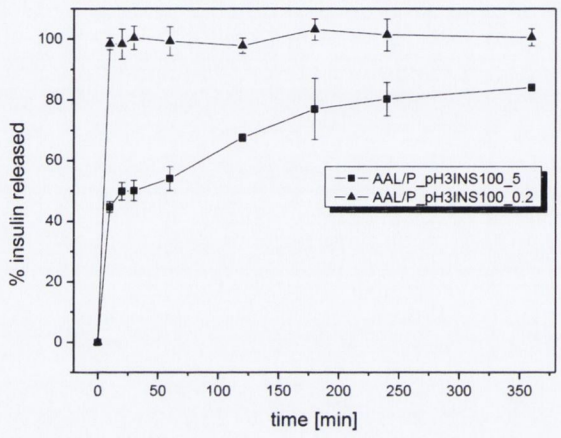

Fig. 6.1.6 *Insulin release profiles from AAL/P_pH3 NPs loaded with 100 µg/ml of insulin (AAL/P_pH3 INS100) in 0.01 M HCl, pH 2. Amount of released insulin was quantified by RP – HPLC.*
(AAL/P_pH3INS100_5 – NPs with AAL/P_pH3 weight ratio of 5 loaded with 100 µg/ml of insulin, AAL/P_pH3INS100_0.2 – NPs with AAL/P_pH3 weight ratio of 0.2 loaded with 100 µg/ml of insulin).

The data from the release studies were fitted to the first order equation (see Chapter 2, Section 2.4.2.12, Equation 2.3). The parameter estimates and related statistics are summarised in Table 6.1.2. It can be observed that the rate of insulin release and the amount of insulin released at infinity depends on the type of NPs and the values are significantly different for both formulations.

Table 6.1.2 *Model parameter estimates and their statistical significance for insulin release from AAL/P_pH3 NPs loaded with 100 µg/ml of insulin in HCl, pH 2, fitted to the first order model.*

AAL/P_pH3 weight ratio	k [min^{-1}]	p-value	W_∞ [µg/mg of NPs]	p-value
5	0.060±0.012	<0.001 (significantly different)	71±2.7	<0.001 (significantly different)
0.2	0.375±0.052		100±3.0	

6.2.4.1.2 Release in the acetate buffer (pH 4.5)

Changes in the properties of tested AAL/P_pH3 NPs before and release studies in 0.1 M acetate buffer at pH 4.5 were investigated (Table C.3, Appendix C). A small increase in particle size and PdI was observed for negatively charged NPs. ZP of these NPs increased from -67.6 to -37.6 mV. Aggregation occurred in case of positively charged NPs and the ZP values decreased from 21.5 to 12.5 mV. The release profiles of insulin in the acetate buffer at pH 4.5 are presented in Figure 6.1.7. More than 90% of insulin was released from the negatively charged NPs in the first 10 minutes of the study and this amount did not change until 6 hours of the experiment. A similar amount of insulin was released from positively charged NPs and 100% of loaded insulin was released from positively charged NPs after 6 hours.

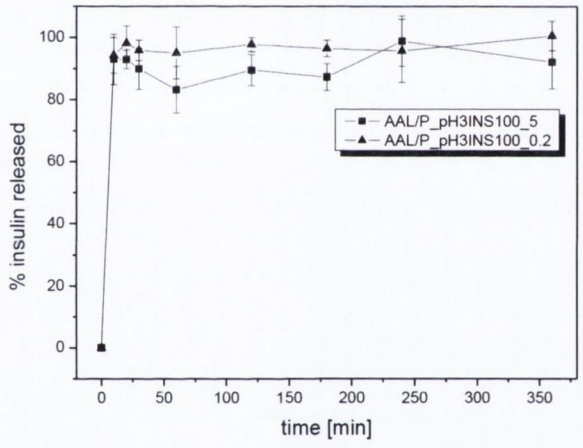

Fig. 6.1.7 *Insulin release profiles from AAL/P_pH3 NPs loaded with 100 µg/ml of insulin (AAL/P_pH3 INS100) in 0.1 M acetate buffer, pH 4.5. Amount of released insulin was quantified by RP – HPLC.*
(AAL/P_pH3INS100_5 – NPs with AAL/P_pH3 weight ratio of 5 loaded with 100 µg/ml of insulin, AAL/P_pH3INS100_0.2 – NPs with AAL/P_pH3 weight ratio of 0.2 loaded with 100 µg/ml of insulin).

Data obtained from the release studies were fitted to the first order equation (Table 6.1.3). The release rates and amounts of the peptide released at infinity were comparable.

Table 6.1.3 *Model parameter estimates and their statistical significance for insulin release from AAL/P_pH3 NPs loaded with 100 µg/ml of insulin in acetate buffer, pH 4.5, fitted to the first order model.*

AAL/P_pH3 weight ratio	k [min^{-1}]	p-value	W_∞ [µg/mg of NPs]	p-value
5	0.311±0.075	0.21 (not significantly different)	92±4.4	0.09 (not significantly different)
0.2	0.247±0.069		97±4.6	

6.2.4.1.3 Release in PBS (pH 7.4)

The properties of AAL/P_pH3 NPs were investigated before and after release studies in PBS (Table C.3, Appendix C). An increase in particle size and PdI occurred for negatively charged NPs with ZP increasing from -62.6 to 15.5 mV. Positively charged NPs formed aggregates in PBS, which was reflected in the increased particle size and PdI values. ZP decreased from 21.5 mV to -1.3 mV. The release profiles of insulin in PBS at pH 7.4 are presented in Figure 6.1.8. It can be seen that the profiles were very similar for both types of NPs. More than 90% of insulin was released in the first 10 minutes of the study with the amount of insulin released reaching 100% after 6 h of the study.

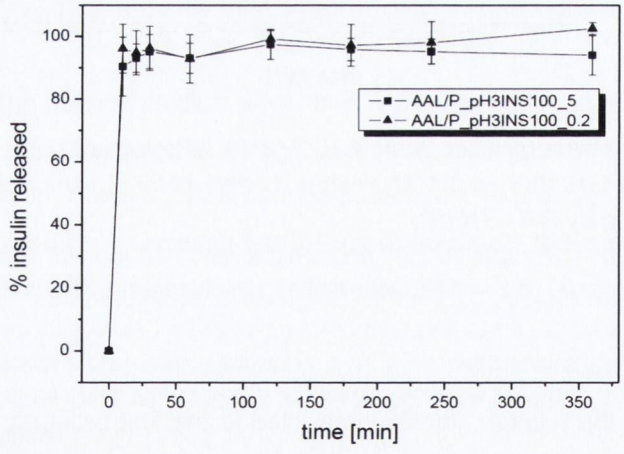

Fig. 6.1.8 *Insulin release profiles from AAL/P_pH3 NPs loaded with 100 µg/ml of insulin (AAL/P_pH3 INS100) in 0.01 M PBS, pH 7.4. Amount of released insulin was quantified by RP – HPLC.*
(AAL/P_pH3INS100_5 – NPs with AAL/P_pH3 weight ratio of 5 loaded with 100 µg/ml of insulin, AAL/P_pH3INS100_0.2 – NPs with AAL/P_pH3 weight ratio of 0.2 loaded with 100 µg/ml of insulin).

First order equation was used to fit the release data. The parameter estimates and related statistics are summarised in Table 6.1.4. There was no significant difference between the rates and amounts of the peptide released at infinity.

Table 6.1.4 *Model parameter estimates and their statistical significance for insulin release from AAL/P_pH3 NPs loaded with 100 µg/ml of insulin in PBS, pH 7.4, fitted to the first order model.*

AAL/P_pH3 weight ratio	k [min^{-1}]	p-value	W_∞ [µg/mg of NPs]	p-value
5	0.272±0.094	0.29 (not significantly different)	95±3.9	0.56 (not significantly different)
0.2	0.211±0.066		97±6.0	

6.2.4.1.4 Comparison of release profiles from AAL/P_pH3 NPs loaded with 100 µg/ml of insulin

The percentage of insulin released from AAL/P_pH3 NPs loaded with 100 µg/ml of insulin in various buffers was compared. Figures 6.1.9 a and 6.1.9 b illustrate the release profiles from the same type of NPs in various buffers. No modulation of insulin released depending on pH was observed for positively charged NPs. Approximately 100% of peptide was released in the first 10 minutes of the studies (Figure 6.1.9 b). Negatively charged NPs showed similar release profiles for the acetate buffer, pH 4.5 and PBS pH 7.4, while slower release in HCl, pH 2, was observed (Figure 6.1.9 a).

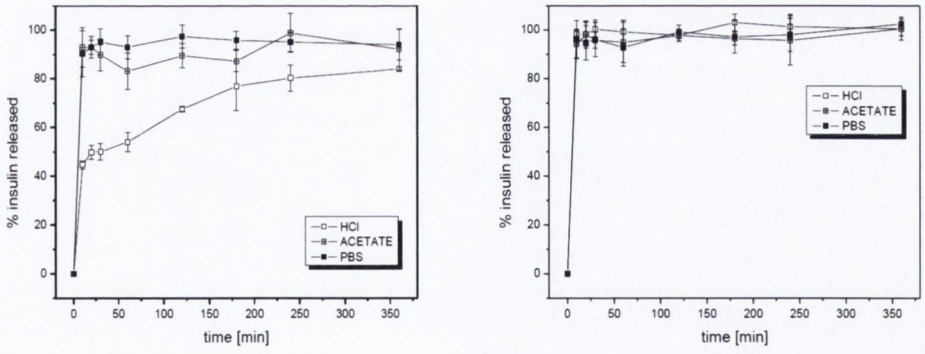

Fig. 6.1.9 *Insulin release profiles in HCl, acetate buffer and PBS from* ***a)*** *negatively charged AAL/P_pH3 NPs loaded with 100 µg/ml of insulin,* ***b)*** *positively charged AAL/P_pH3 NPs loaded with 100 µg/ml of insulin. Amount of released insulin was quantified by RP – HPLC.*

6.2.4.1.5 Release in FaSSIF

Simulating small intestinal conditions with biorelevant media such as fasted state simulated intestinal fluid (FaSSIF) has become standard practise in dissolution/release testing (Zoeller and Klein, 2007), therefore release experiments were also performed in this medium.

Particle size, PdI and ZP of the tested NPs were measure before and after release to FaSSIF (Table C.4, Appendix C). Interestingly, the size of negatively charged NPs decreased from 139 to 58 nm, which is close to the size of colloidal entities formed by medium constituents in pure FaSSIF (70 nm), suggesting dissolution/disintegration of NPs. A small increase in the particle size was observed for positively charged NPs. There was almost no change in PdI values for negatively charged NPs, while for positively NPs an increase was seen (from 0.113 to 0.289). Both types of NPs had similar ZP after release (-24.6 mV for negatively charged NPs and -28.1 mV for positively charged NPs). Insulin release profiles from AAL/P_pH3 NPs loaded with 100 µg/ml of insulin in FaSSIF are presented in Figure 6.1.10. Similar release profiles were obtained for both types of NPs tested, however there was a statistically significant difference in the amount released at 2 hours of the experiment. Approximately 100% insulin loaded liberated within first 10 minutes of the study.

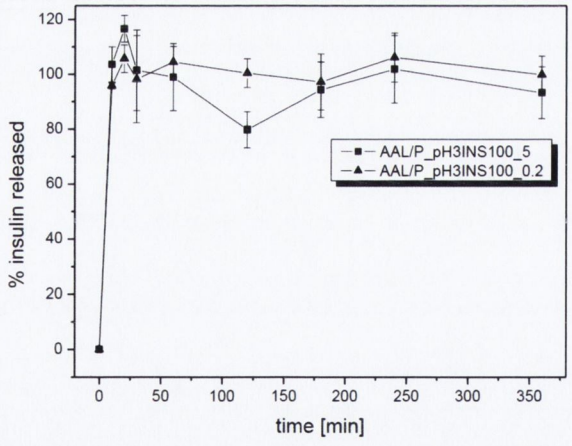

Fig. 6.1.10 *Insulin release profiles from AAL/P_pH3 NPs loaded with 100 µg/ml of insulin (AAL/P_pH3 INS100) in FaSSIF. Amount of released insulin was quantified by RP – HPLC.*
(AAL/P_pH3INS100_5 – NPs with AAL/P_pH3 weight ratio of 5 loaded with 100 µg/ml of insulin, AAL/P_pH3INS100_0.2 – NPs with AAL/P_pH3 weight ratio of 0.2 loaded with 100 µg/ml of insulin).

First order equation was used to fit data obtained from the release studies (data not shown) There was no significant difference between the amounts of insulin that was

released from the tested NPs in FaSSIF ($p>0.05$), however it was impossible to estimate the rate of insulin release due to large fluctuations in the amount of insulin released within the first 1 h of the study resulting in poor fit.

6.2.4.2 Release from AAL/P_pH3 NPs loaded with 500 µg/ml of insulin

AAL/P_pH3 NPs were loaded with a larger amount of insulin (500 µg/ml) and release properties in three various media: 0.01 M HCl (pH 2), 0.1 M acetate buffer (pH 4.5) and 0.01 M PBS (pH 7.4) were investigated.

6.2.4.2.1 Release in HCl buffer (pH 2)

Properties of NPs were before and after release studies were investigated (Table C.5, Appendix C). An increase in the particle size and PdI was measured for negatively charged NPs, but they still remained in the nano range. Charge of these NPs increased to 10.8 mV (from an initial value of -66.2 mV). In case of positively charged NPs ZP did not change but an increase in the particle size and PdI was observed (formation of microparticles). The release profiles in HCl (pH 2) are presented in Figure 6.1.11. There was a difference between the amounts of insulin released from the different types of NPs, but majority of peptide released in the first minutes of the studies. Approximately 76% of insulin was released from negatively charged NPs in the first 10 minutes of the study and this amount increased to 85% after 6 h. 100% insulin loaded was released in HCl from positively charged NPs within the first 10 minutes of the study.

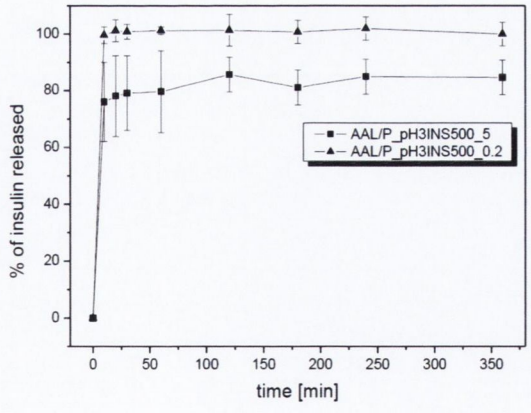

Fig. 6.1.11 *Insulin release profiles from AAL/P_pH3 NPs loaded with 500 µg/ml of insulin (AAL/P_pH3 INS500) in 0.01 M HCl, pH 2. Amount of released insulin was quantified by RP – HPLC.*
(AAL/P_pH3INS500_5 – NPs with AAL/P_pH3 weight ratio of 5 loaded with 500 µg/ml of insulin, AAL/P_pH3INS500_0.2 – NPs with AAL/P_pH3 weight ratio of 0.2 loaded with 500 µg/ml of insulin).

Fitting the release data to the first order equation resulted in obtaining the parameter estimates, which are presented in Table 6.1.5. It can be observed that the amount of insulin released from NPs was significantly different, however the rate of its release was similar.

Table 6.1.5 *Model parameter estimates and their statistical significance for insulin release from AAL/P_pH3 NPs loaded with 500 µg/ml of insulin in HCl, pH 2, fitted to the first order model.*

AAL/P_pH3 weight ratio	k [min^{-1}]	p-value	W_∞ [µg/mg of NPs]	p-value
5	0.317±0.019	0.07 (not significantly different)	425±22.8	<0.01 (significantly different)
0.2	0.419±0.072		496±11.6	

6.2.4.2.2 Release in the acetate buffer (pH 4.5)

Properties of NPs before and after release were studies (Table C.5, Appendix C). A small increase in particle size was observed for negatively charged NPs after release studies. PdI did not change but an increase in the ZP was observed (from -66.2 to -19.9 mV). Positively charged NPs formed aggregates during release studies in the acetate buffer, while ZP decreased to 12.3 mV from 23.4 mV. Release profiles in the acetate buffer are presented in Figure 6.1.12.

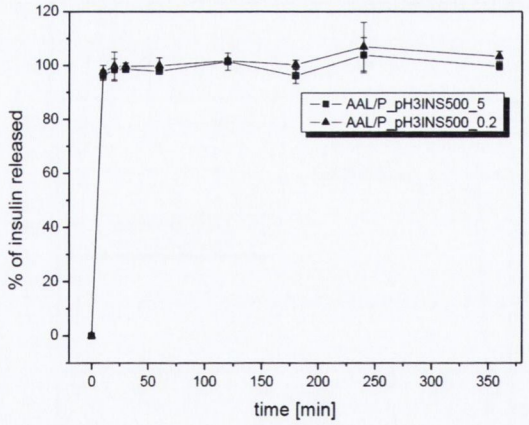

Fig. 6.1.12 *Insulin release profiles from AAL/P_pH3 NPs loaded with 500 µg/ml of insulin (AAL/P_pH3 INS500) in 0.1 M acetate buffer, pH 4.5. Amount of released insulin was quantified by RP – HPLC.*
(AAL/P_pH3INS500_5 – NPs with AAL/P_pH3 weight ratio of 5 loaded with 500 µg/ml of insulin, AAL/P_pH3INS500_0.2 – NPs with AAL/P_pH3 weight ratio of 0.2 loaded with 500 µg/ml of insulin).

There were no significant differences in release profiles between the two types of NPs tested. Data obtained from release studies was fitted to the first order equation

(Table 6.1.6). There were no significant differences between the amount of insulin released at infinity and the rates of release.

Table 6.1.6 *Model parameter estimates and their statistical significance for insulin release from AAL/P_pH3 NPs loaded with 500 µg/ml of insulin in acetate buffer, pH 4.5, fitted to the first order model.*

AAL/P_pH3 weight ratio	k [min^{-1}]	p-value	W_∞ [µg/mg of NPs]	p-value
5	0.365±0.062	0.58 (not significantly different)	497±7.5	0.16 (not significantly different)
0.2	0.337±0.074		508±11.5	

6.2.4.2.3 Release in PBS (pH 7.4)

Table C.5 (Appendix C) shows properties of NPs before and after the studies. Negatively charged NPs in PBS remained stable, with a small increase in the particle size but significantly increased ZP values from -66.2 to -17.1 mV. Positively charged NPs formed aggregates with a ZP value of -1.0 mV. Profiles of insulin release in PBS are presented in Figure 6.1.13.

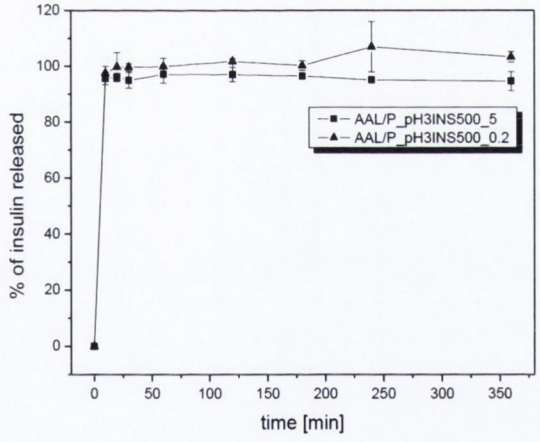

Fig. 6.1.13 *Insulin release profiles from AAL/P_pH3 NPs loaded with 500 µg/ml of insulin to 0.01 M PBS, pH 7.4. Amount of released insulin was quantified by RP – HPLC.*
(AAL/P_pH3INS500_5 – NPs with AAL/P_pH3 weight ratio of 5 loaded with 500 µg/ml of insulin, AAL/P_pH3INS500_0.2 – NPs with AAL/P_pH3 weight ratio of 0.2 loaded with 500 µg/ml of insulin).

Parameter estimates (first order equation) and related statistics are summarised in Table 6.1.7. There was a significant difference in the release rates and amounts of the peptide released at infinity observed when these two types of NPs were

compared. A smaller amount of insulin could be released from negatively charged NPs, but the rate of its release was faster.

Table 6.1.7 *Model parameter estimates and their statistical significance for insulin release from AAL/P_pH3 NPs loaded with 500 µg/ml of insulin in PBS, pH 7.4, fitted to the first order model.*

AAL/P_pH3 weight ratio	k [min^{-1}]	p-value	W_∞ [µg/mg of NPs]	p-value
5	0.454±0.030	<0.05 (significantly different)	480±7.3	<0.05 (significantly different)
0.2	0.349±0.040		490±2.9	

6.2.4.2.4 Comparison of release profiles from AAL/P_pH3 NPs loaded with 500 µg/ml of insulin

The amount of insulin released from AAL/P_pH3 NPs loaded with 500 µg/ml of insulin to the various buffers was compared. Release profiles for two different types of NPs into the buffers tested are summarised in Figure 6.1.14 a (negatively charged NPs) and Figure 6.1.14 b (positively charged NPs). No modulation of insulin released depending on pH was observed for positively charged NPs. Approximately 100% of peptide was released in the first 10 minutes of studies (Figure 6.1.14 b). Negatively charged NPs showed similar release profiles for the acetate buffer, pH 4.5 and PBS pH 7.4, while smaller amount of insulin was released in HCl, pH 2 (Figure 6.1.14 a).

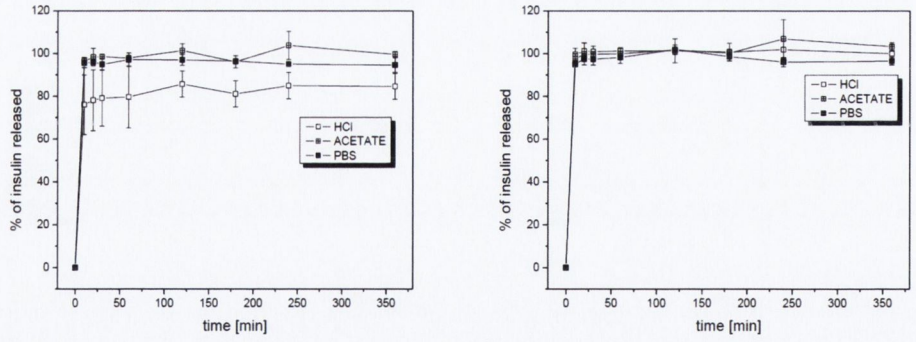

a) **b)**

Fig. 6.1.14 *Insulin release profiles in HCl, acetate buffer and PBS from* ***a)*** *negatively charged AAL/P_pH3 NPs loaded with 500 µg/ml of insulin,* ***b)*** *positively charged AAL/P_pH3 NPs loaded with 500 µg/ml of insulin. Amount of released insulin was quantified by RP – HPLC.*

6.2.4.3 Comparison of release profiles from AAL/P_pH3 NPs loaded with 100 and 500 µg/ml of insulin

To evaluate the influence of the amount of insulin loaded into AAL/P_pH3 NPs on the rate of insulin release in various buffers, the first order model parameters were estimated and compared (Table 6.1.8). Significant differences for negatively charged NPs were noted when HCl (pH 2) was used as the release medium and for positively charged NPs in PBS.

Table 6.1.8 *Model parameter estimates and their statistical significance for insulin release from AAL/P_pH3 NPs loaded with 100 µg/ml (INS100) and 500 µg/ml (INS500) of insulin obtained by fitting experimental data to the first order model. (Statistical analysis: # - no significant difference, *p<0.05, **p<0.01, ***p<0.001).*

AAL/P_pH3 weight ratio	Buffer	k [min^{-1}]		Statistical significance
		INS100	INS500	
5	HCl, pH 2	0.0604±0.0122	0.3166±0.0192	***
	Acetate, pH 4.5	0.3107±0.0753	0.3653±0.0620	#
	PBS, pH 7.4	0.2716±0.0942	0.4540±0.0301	#
0.2	HCl, pH 2	0.3752±0.0523	0.4194±0.0717	#
	Acetate, pH 4.5	0.2473±0.0687	0.3374±0.0739	#
	PBS, pH 7.4	0.2109±0.0657	0.3490±0.0403	**

The different release behaviour may be explained by the different composition and localisation of components in the NP. Approximately 100% of insulin was released from positively charged NPs in all media tested. Additionally, the rates of peptide release were very fast and there was no significant difference between media with various pH. The observed immediate release of insulin from positively charged NPs may be related to the release from nanoparticle surface, due to the weak interaction forces between the polyelectrolytes and the protein.

In case of negatively charged NPs, the release profiles can be explained by the properties of the alginate forming a pH responsive hydrogel. Gastric protection against insulin release can be attributed to its more effective retention by a tight alginate network at low pH (Sarmento et al., 2007 b). At higher pH (basic environment) alginate is eroded and the drug is released as a result of a diffusion and erosion of the matrix (Soni et al., 2010).

Different percentage and various rates of insulin released in HCl were observed when different amounts of insulin were loaded. More insulin was released when 500 µg/ml was loaded more likely due to liberation of insulin from nanoparticle surface.

6.2.5 Cytotoxicity of AAL/P_pH3 NPs

Cytotoxicity of prepared AAL/P_pH3 NPs were studied in the Caco-2 cell line. NP concentration dependent cell viability is presented in Figure 6.1.15.

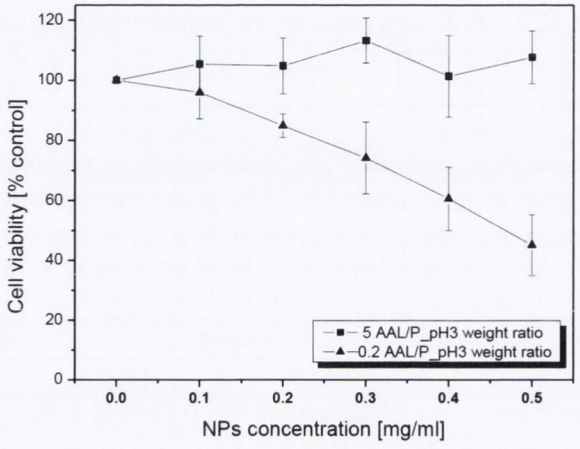

Fig. 6.1.15 *Viability of Caco-2 cells after 72 hours exposure to AAL/P_pH3 NPs in serum-free medium.*

Viability of Caco-2 cells was strongly dependent on the type of NPs used. Negatively charged NPs at all of the concentrations tested (0.1 – 0.5 mg/ml) did not have an impact on the cell viability after 72 h of incubation. Moreover, there was an increase (by 5-10%) in the cell viability. In case of positively charged NPs, containing more protamine than alginate, the viability of the cells was concentration dependent. A decrease (to 95%) in the amount of cells surviving was observed after incubation with 0.1 mg/ml NPs for 72 h. Cell viability reached 45% when NPs at a concentration of 0.5 mg/ml were applied. The toxic effects may be produced mainly by the free polycation (P) rather than by P bound to the polyanion in the NPs. As presented in Chapter 4 and 5 of this thesis (Section 4.3.7 for AAL/P_pH3 NPs and Section 5.3.7 for IC/P_pH3 NPs), the positively charged NPs aggregated in the cell culture medium, perhaps leading to release of free P. Umerska (2012) presented that the half maximal inhibitory concentration (IC_{50}) of P in Caco-2 was 0.24±0.01 mg/ml.

6.2.6 Transport of insulin from AAL/P_pH3 NPs through Caco-2 monolayers

Caco-2 monolayers were obtained by seeding the cells on Transwell plates (Section 2.4.2.16.1) and culturing them for at least 21 days to achieve proper tight junction formation. Transepithelial electrical resistance (TEER) measurements were performed during this period to assess the cell growth and tight junction formation. As reported, typically TEER values of > 300 Ohm·cm^2 indicate adequate monolayer integrity (van Breement and Li, 2005). Figure 6.1.16 shows an example of tight

junction formation reflected in TEER values as measured during the culture period of 21 days. It could be noticed that the cells grew faster in the first 15 days. After that period TEER values reached 300 Ohm·cm^2 and only a small increase was observed in the following days.

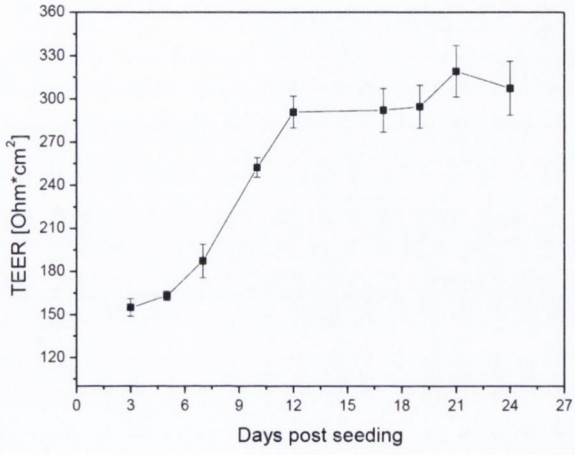

Fig. 6.1.16 *Integrity of Caco-2 tight cell junctions.*

To evaluate the transport of insulin loaded into AAL/P_pH3 NPs (loaded with 500 µg/ml), solution of insulin standard (500 µg/ml) was used as a reference. Additionally, transport of insulin dissolved in 0.1% w/v P solution was examined to see the influence of P on Caco-2 tight junctions opening. To control the tight junction integrity during the experiment, fluorescein leakage and TEER measurements were performed. As reported, fluorescein as a fluorescent dye, is widely used as a paracellular marker for monitoring the tight junction integrity during *in vitro* experiments performed on various permeability models, i.e. animal tissue and Caco-2 cell monolayers (Berginc et al., 2007). Examples of how AAL/P_pH3 NPs (negatively and positively charged) changed TEER values and fluorescein transport across the monolayer are presented in Figure 6.1.17 (Fig 6.1.17 a – changes in TEER value, Fig 6.1.17 b – fluorescein appearance in the acceptor compartment).

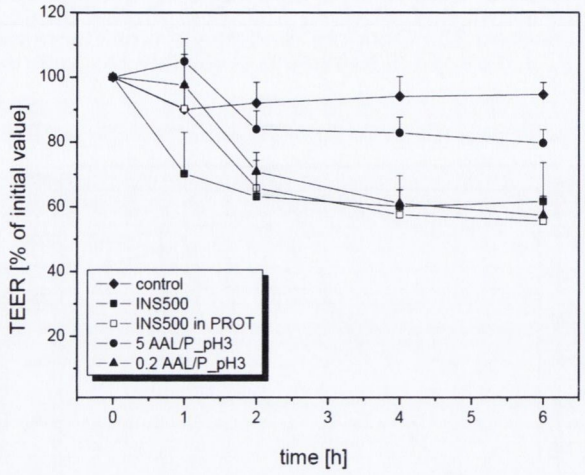

a)

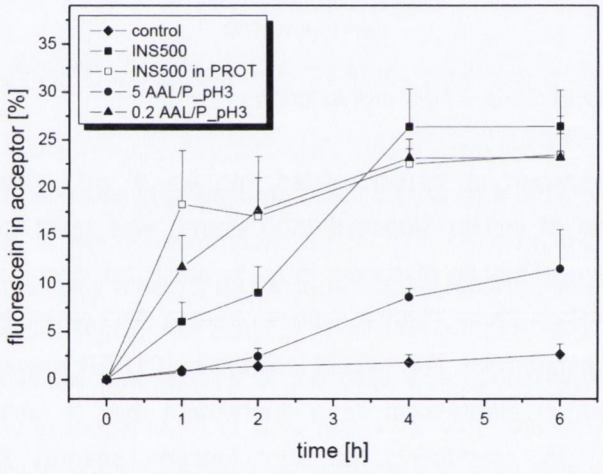

b)

Fig. 6.1.17 *Time course of TEER (**a**) and fluorescein appearance in acceptor (**b**) during transport studies across Caco-2 monolayers.*
(Control – monolayers with no sample tested, INS500 – insulin solution 500 µg/ml (reference), INS500 in PROT – insulin solution 500 µg/ml dissolved in 0.1% w/v protamine solution, 5 AAL/P_pH3 – NPs with AAL/P_pH3 weight ratio of 5, 0.2 AAL/P_pH3 – NPs with AAL/P_pH3 weight ratio of 0.2).

A decline in TEER values was observed for all types of samples tested. The fastest decrease was observed for the insulin solution (reference sample) and a decrease by 25% and 40% was observed after 1 and 6 h incubation, respectively. Comparable lessening in TEER values was observed for insulin dissolved in P solution and NPs with the AAL/P_pH3 weight ratio of 0.2. A different profile of changes in TEER values was observed for negatively charged AAL/P_pH3 NPs, containing more alginate than protamine. For this sample, initially an increase in TEER values by 10% was observed after the first hour of incubation. After next hour the values decreased to

90% of the starting value and remained stable at this value until the end of the study. A similar behaviour was observed for fluorescein appearance in the acceptor reservoir. In the first 2 hours of the study the percentage of fluorescein was similar to the control. It increased after 4 h of incubation and reached the final value of 10% for negatively charged AAL/P_pH3 NPs. A larger amount of fluorescein was transported when insulin reference sample was applied (30% after 6 hours). A comparable (to the reference) amount of fluorescein was noticed for insulin dissolved in P solution and for NPs with the AAL/P_pH3 weigh ratio of 0.2. A larger amount of fluorescein appeared in the acceptor in the first 2 hours of the study for insulin dissolved in P solution and for NPs with AAL/P_pH3 weight ratio of 0.2, comparing to the insulin standard. After 4 hours the values were similar (23% of fluorescein was present in the acceptor for AAL/P_pH3 NPs with the weight ratio of 0.2 and insulin standard in P solution, while 26% of fluorescein in acceptor appeared for insulin standard). The amount of insulin transported through Caco-2 monolayers from the various systems is presented in Figure 6.1.18.

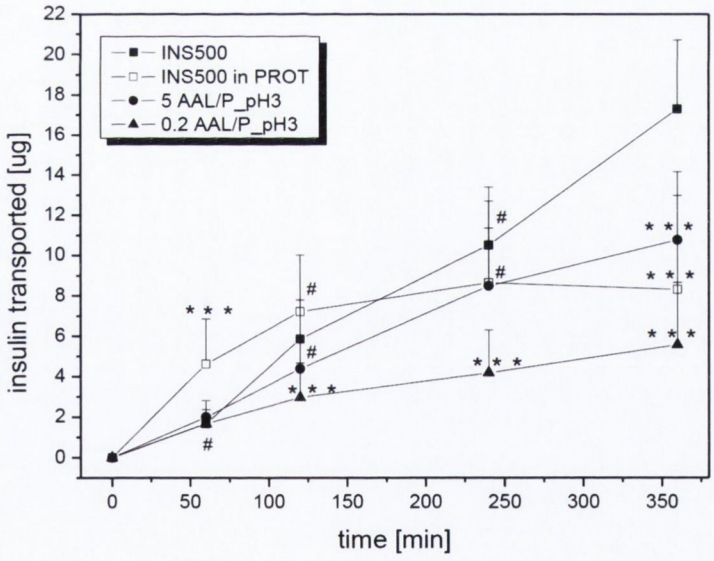

Fig. 6.1.18 *Transport of insulin from solutions and NPs through Caco-2 monolayers. (Statistical analysis: # - no statistical difference, *p<0.05, **p<0.01, ***p<0.001). Amount of transported insulin was quantified by RP – HPLC.*
(INS500 – insulin solution 500 µg/ml (reference), INS500 in PROT – insulin solution 500 µg/ml dissolved in 0.1% w/v protamine solution, 5 AAL/P_pH3 – NPs with AAL/P_pH3 weight ratio of 5, 0.2 AAL/P_pH3 – NPs with AAL/P_pH3 weight ratio of 0.2).

A significant difference in the amount of insulin transported ($p<0.001$) after 6 hours of the experiment was observed for AAL/P_pH3 NPs and insulin dissolved in P solution in comparison to the reference. More insulin was transported in the first

hour of study when it was dissolved in P solution ($p<0.001$), while the amount of the peptide that crossed the monolayer was comparable for the other systems. The lowest amount of insulin transported after 2, 4 and 6 hours was that from the 0.2 AAL/P_pH3 system, while no statistically significant difference was noticed for the 5.0 AAL/P_pH3 NPs and the reference at 2 and 4 hours.

To estimate the rate of insulin transport through Caco-2 monolayers, the apparent permeability coefficient (P_{app}) was calculated (Section 2.4.2.16.5, equation 2.4). The P_{app} values were compared to that of the insulin reference. The amount of insulin transported over 6 hours and the rate of the transport are presented in Table 6.1.9.

Table 6.1.9 *Amount of insulin transported from solutions and NPs at 6 hours of the experiment and P_{app} values across Caco-2 monolayers (Statistical analysis: *p<0.05, **p<0.01, ***p<0.001).*
(INS500 – insulin solution 500 µg/ml (reference), INS500 in PROT – insulin solution 500 µg/ml dissolved in 0.1% w/v protamine solution, 5 AAL/P_pH3 – NPs with AAL/P_pH3 weight ratio of 5, 0.2 AAL/P_pH3 – NPs with AAL/P_pH3 weight ratio of 0.2).

Sample	Insulin transported [µg]	P_{app} [$x10^{-6}$ $cm \cdot s^{-1}$]
INS500	17.28±3.43	2.24±0.48
INS500 in PROT	8.30±4.67 ***	1.42±0.48 **
5 AAL/P_pH3	10.76±3.38 ***	1.29±0.42 ***
0.2 AAL/P_pH3	5.57±3.08 ***	0.81±0.38 ***

The smallest amount of insulin was transported from 0.2 AAL/P_pH3 NPs. Additionally, the rate of the peptide transport was the slowest. A larger amount of insulin was transported from negatively charged NPs (5.0 AAL/P_pH3). For insulin dissolved in P solution the decrease in the transport rate and the amount of insulin transported was lower, comparing to the insulin reference. Detailed statistical analysis of the transport data in shown in Table 6.1.10.

Table 6.1.10 *Statistical analysis of the amount of insulin transported from solutions and NPs at 6 hours of the experiment and P_{app} values across Caco-2 monolayers (Statistical analysis: *p<0.05, **p<0.01, ***p<0.001).*
(INS500 – insulin solution 500 µg/ml (reference), INS500 in PROT – insulin solution 500 µg/ml dissolved in 0.1% w/v protamine solution, 5 AAL/P_pH3 – NPs with AAL/P_pH3 weight ratio of 5, 0.2 AAL/P_pH3 – NPs with AAL/P_pH3 weight ratio of 0.2).

P_{app}	INS500	INS500 in PROT	5.0 AAL/P_pH3	0.2 AAL/P_pH3
INS500	--------	**	***	***
INS500 in PROT	**	-----	#	*
5.0 AAL/P_pH3	***	#	----------	*
0.2 AAL/P_pH3	***	*	*	----------
Insulin transported [µg]	INS500	INS500 in PROT	5.0 AAL/P_pH3	0.2 AAL/P_pH3
INS500	----------	***	***	***
INS500 in PROT	***	--------	#	#
5.0 AAL/P_pH3	***	#	----------	*
0.2 AAL/P_pH3	***	#	*	----------

A significantly different amount of insulin was transported from both types of AAL/P_pH3 NPs and when insulin was dissolved in P solution, comparing to the insulin reference. Additionally, insulin incorporated into positively charged NPs (0.2 AAL/P_pH3) resulted in a lower amount of insulin transported, comparing to other samples tested. Similar results were obtained for the P_{app} values. The rate of the insulin transport significantly varied from the control for all of the samples tested ($p<0.001$). Also, different rates of insulin transport were observed for the two types of AAL/P_pH3 NPs ($p<0.05$).

Study performed by Déat-Lainé et al. tested microparticles prepared from whey protein and alginate microparticles for intestinal absorption of insulin (Déat-Lainé et al., 2013). The impact on insulin incorporation into whey protein, alginate and also into whey protein/alginate microparticles was studied. Interestingly, transport of insulin and its permeability coefficient was significantly superior to the control (free insulin dissolved in medium) when insulin was incorporated into whey protein, however transport was not modulated when insulin was incorporated into alginate microparticles. Obtained permeability results corresponded with TEER values. The authors suggested that different transport mechanisms were utilised for insulin transport, but this hypothesis was not further evaluated (Déat-Lainé et al., 2013).

6.3 Formulation and *in vitro* characterisation of IC/P_pH3 NPs loaded with insulin

6.3.1 Characterisation of IC/P_pH3 NPs loaded with insulin

Two types of negatively and two types of positively charged IC/P_pH3 carrier NPs were selected as outlined in Introduction to this chapter (Section 6.1). Two various doses of insulin: 100 and 500 µg/ml were then incorporated into the chosen IC/P_pH3 carriers. Loaded NPs were characterised according to their particle size, PdI and surface charge and compared with empty carriers Figure 6.2.1 compares the particle size of empty IC/P_pH3 NPs with those that were insulin loaded.

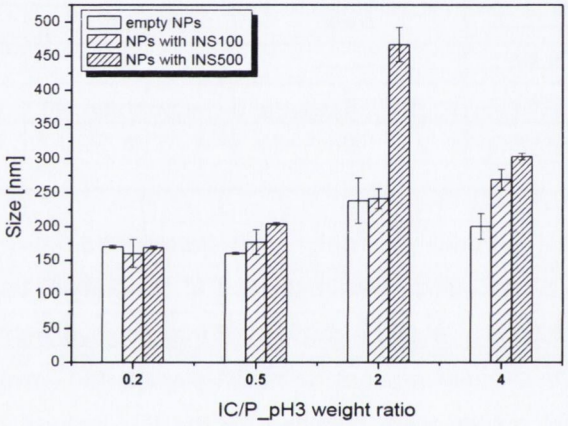

Fig. 6.2.1 *Comparison of particle size values for empty and insulin loaded IC/P_pH3 NPs. (INS100 - NPs loaded with 100 µg/ml of insulin, INS500 - NPs loaded with 500 µg/ml of insulin).*

Smaller in size NPs were obtained when more P was present in NPs (positively charged with IC/P_pH3 weight ratios of 0.2 and 0.5). Minor changes in the particle size were observed when insulin was incorporated into these types of NPs. For NPs with a greater amount of IC (negatively charged with IC/P_pH3 weight ratios of 2 and 4) the addition of insulin caused a considerable increase in the NP size. A larger increase in the particle size was noticed for the 2 IC/P_pH3 system. The mean particle size of empty NPs was 238 nm and it increased to 467 nm when loaded with 500 µg/ml of insulin. Similar changes were observed for PdI values (Figure 6.2.2). Smaller values were obtained for positively charged NPs with values approximately 0.150. For negatively charged NPs the greatest increase was observed for the 2 IC/P_pH3 system, where the PdI value changed from 0.268 to 0.425 when loaded with 500 µg/ml of insulin.

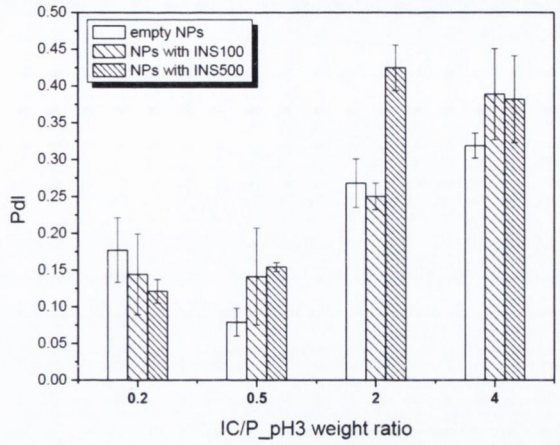

Fig. 6.2.2 *Comparison of polydispersity index values for empty and insulin loaded IC/P_pH3 NPs. (INS100 - NPs loaded with 100 µg/ml of insulin, INS500 - NPs loaded with 500 µg/ml of insulin).*

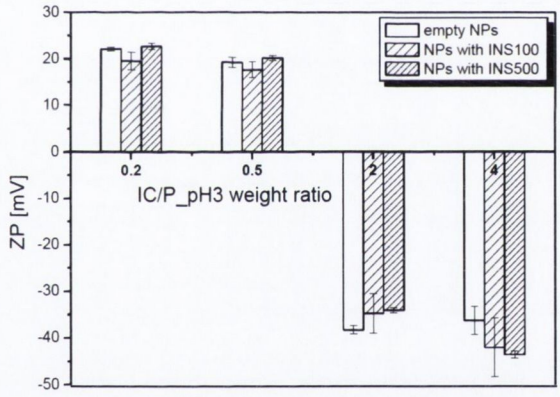

Fig. 6.2.3 *Comparison of zeta potential values for empty and insulin loaded IC/P_pH3 NPs. (INS100 - NPs loaded with 100 µg/ml of insulin, INS500 - NPs loaded with 500 µg/ml of insulin).*

ZP of positively charged NPs was app. 20 mV for the 0.5 IC/P_pH3 sample and 22 mV for the 0.2 IC/P_pH3 system for both empty and insulin loaded NPs (Figure 6.2.3). ZP decreased when insulin was loaded to the 4 IC/P_pH3 sample, while an increase in ZP was observed when the peptide was loaded to 2 IC/P_pH3 NP NPs.

6.3.2 Stability of IC/P_pH3 NPs loaded with insulin

Physical stability of IC/P_pH3 NPs loaded with insulin was examined up to three days of storage at RT. The size measurements of IC/P_pH3 NPs loaded with insulin and stored at RT are presented in Figure 6.2.4. No changes in the particle size were observed for negatively charged NPs loaded with 100 µg/ml of insulin, which had

app. 300 nm. The positively charged NPs, 0.2 IC/P_pH3, showed better stability than the 0.5 IC/P_pH3 system. A gradual increase in the particle size for the former was observed and this system reached the particle size of 358 nm after 3 days. Aggregation was observed for the 0.5 IC/P_pH3 sample on the next day after preparation.

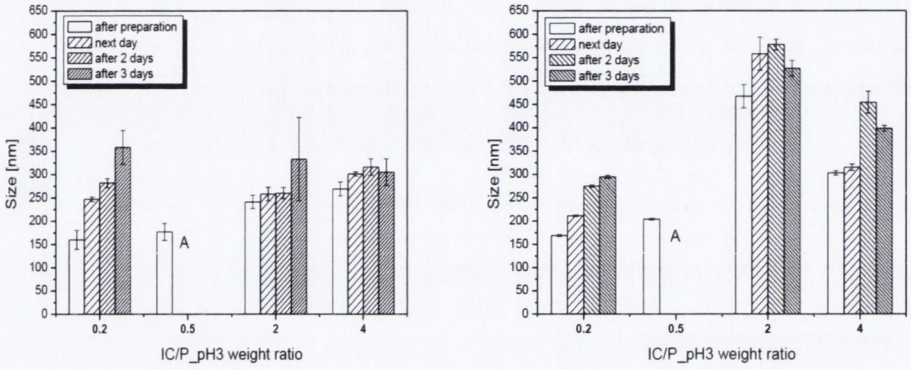

a) **b)**

Fig. 6.2.4 *Stability of IC/P_pH3 NPs loaded with:* ***a)*** *100 µg/ml and* ***b)*** *500 µg/ml of insulin up to 72 h of starage at RT – particle size measurements (A – aggregates formed).*

A gradual increase in the particle size was observed for the 0.2 IC/P_pH3 (500 µg/ml insulin) system. The NPs reached the particle size of 295 nm after three days of storage. Similarly to the sample with the lower insulin dose, aggregation occurred for the 0.5 IC/P_pH3 (500 µg/ml insulin) system. There was a slight increase in the particle size of negatively charged NPs loaded with 500 µg/ml insulin, but no aggregation was observed. The particle size exceeded 500 nm in the case of the 2 IC/P_pH3 sample, but both negatively charged formulations were seen to be stable upon storage.

PdI values for the samples are presented in Figure 6.2.5. Higher PdI values were obtained for one of the positively charged NPs (0.5 IC/P_pH3) for both amounts of insulin loaded, as aggregation occurred. In case of the 0.2 IC/P_pH3 system the PdI values increased slowly upon storage. There were no major changes observed for PdI values of negatively charged NPs on storage over 3 days.

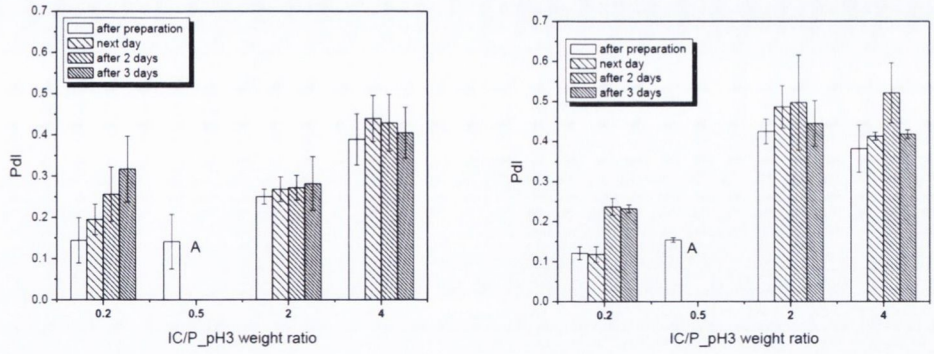

a) **b)**

Fig. 6.2.5 *Stability of IC/P_pH3 NPs loaded with:* ***a)*** *100 µg/ml and* ***b)*** *500 µg/ml of insulin up to 72 h of starage at RT – polydispersity measurements (A – aggregates formed).*

A small decrease in ZP values was observed for the 0.2 IC/P_pH3 (500 µg/ml of insulin) sample (Figure 6.2.6). Surface charge of negatively charged NPs remained stable upon storage for three days.

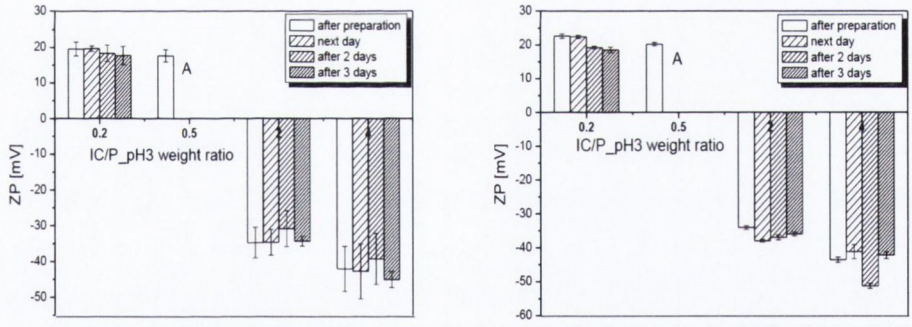

a) **b)**

Fig. 6.2.6 *Stability of IC/P_pH3 NPs loaded with:* ***a)*** *100 µg/ml and* ***b)*** *500 µg/ml of insulin up to 72 h of starage at RT – zeta potential measurements (A – aggregates formed).*

Stability studies performed on IC/P_pH3 NPs loaded with 100 and 500 µg/ml of insulin showed a difference in the physical (colloidal) stability depending of the composition of the NPs. Negatively charged NPs remained stable upon storage at RT for three days, with small increases in the particle size and PdI values. The 0.5 IC/P_pH3 sample (positively charged) aggregated on day 2 of storage, however another positively charged formulation, 0.2 IC/P_pH3 NPs, was seen to be stable.

6.3.3 Insulin association efficiency of IC/P_pH3 NPs composed

Based on the above initial studies and seeing that the 0.5 IC/P_pH3 system is physically unstable, three types of IC/P_pH3 NPs were further tested. NP properties (particle size, PdI and ZP) were measured after preparation and after centrifugation. Obtained data is summarised in Tables C.6 and C.7 (Appendix C). There were no changes in the particle size of tested IC/P_pH3 NPs, but there were small changes in the PdI values. ZP values remained stable for the samples loaded with 100 µg/ml, but they decreased for the positively charged IC/P_pH3 NPs loaded with 500 µg/ml and this decrease could be caused by protamine detachment from the surface of NPs.

AE values for IC/P_pH3 NPs loaded with 100 and 500 µg/ml insulin are presented in Table 6.2.1.

Table 6.2.1 *Association efficiency and drug loading of NPs composed of IC/P_pH3 loaded with 100 µg/ml and 500 µg/ml of insulin.*

IC/P_pH3 weight ratio	NPs with 100 µg/ml of insulin	NPs with 500 µg/ml of insulin	NPs with 100 µg/ml of insulin	NPs with 500 µg/ml of insulin
	AE [%]		Drug loading [%]	
4	99.0±0.6	100.0±0.0	9.1±0.1	33.3±0.0
2	99.0±0.4	100.0±0.7	9.1±0.0	33.3±0.0
0.2	53.9±17.4	20.4±3.4	5.1±1.6	9.3±1.4

The amount of insulin incorporated into IC/P_pH3 NPs was determined by the polymer:protamine weight ratio. Excellent AE of 99-100% was obtained for negatively charged IC/P_pH3 NPs for both amounts of insulin tested (100 and 500 µg/ml). A decrease in the amount of polymer and an increase in the amount of protamine (positively charged NPs) resulted in smaller AE values (54% for 0.2 IC/P_pH3, when 100 µg/ml of insulin was tested). A further increase in the amount of insulin loaded into positively charged IC/P_pH3 NPs resulted in smaller AE values, which were app. 20%. High drug loading was obtained for negatively charged NPs, as indicated by the high AE values, compared with the 0.2 IC/P_pH3 system. As previously reported, interactions between the protein and the polymer contributes to increased encapsulation efficiency (Boury et al., 1997). Lower AE values obtained for positively charged NPs might be the result of competitive interactions between polymer-protamine and polymer-insulin.

6.3.4 Release of insulin from IC/P_pH3

6.3.4.1 Release from IC/P_pH3 NPs loaded with 100 µg/ml of insulin

Release studies in the four media at various pH were performed: 0.01 M HCl (pH 2), 0.1 M acetate buffer (pH 4.5), 0.01 M PBS (pH 7.4) and FaSSIF (Fasted State

Simulated Intestinal Fluid) to simulate pH and conditions present in the various parts of the GI tract. Release profiles from two types of NPs (negatively charged at IC/P_pH3 weight ratio of 4 and 2), and positively charged (at the IC/P_pH3 weight ratio of 0.2) loaded with 100 µg/ml of insulin were investigated.

6.3.4.1.1 Release in HCl buffer (pH 2)

Properties of IC/P_pH3 NPs were investigated before and after release in HCl solution. Particle size, PdI and ZP values are presented in Table C.8 (Appendix C). An increase in the particle size and PdI was observed after release studies for all NP types, although the particle size remained in the nano range. ZP of all types of NPs increased and it was app. -30 mV for negatively charged NPs and 25 mV for the positively charged sample.

Insulin release profiles from the NPs are plotted in Figure 6.2.7. It could be observed that release of insulin depends strongly of the type of NPs used. App. 90% of insulin was released from the positively charged NPs within 10 minutes of the study and 100% was released after 6 hours of studies. Various amounts of insulin were released from negatively charged NPs. 13% of insulin was released in the first 10 minutes from 2 IC/P_pH3 NPs and the amount was raising to the final 30% released after 6 h of the study. NPs with a higher amount of polymer (4 IC/P_pH3) released 20% of insulin after 10 min. This amount increased to app. 50% after 6 h of the study.

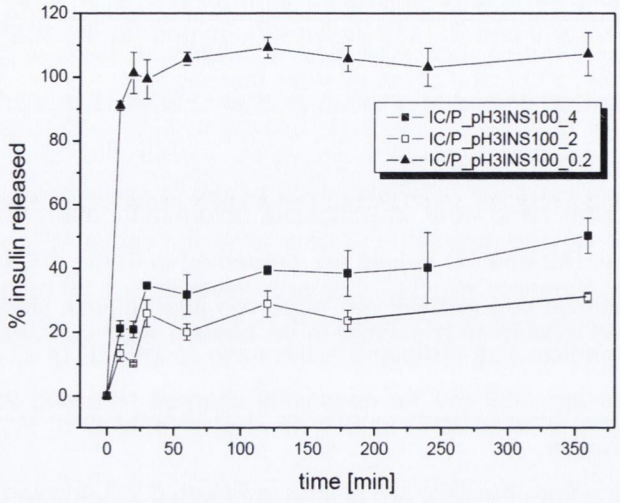

Fig. 6.2.7 *Insulin release profiles from IC/P_pH3 NPs loaded with 100 µg/ml of insulin in 0.01 M HCl, pH 2. Amount of released insulin was quantified by RP – HPLC.*
(IC/P_pH3INS100_4 – NPs at IC/P_pH3 weight ratio of 4 loaded with 100 µg/ml of insulin, IC/P_pH3INS100_2 – NPs at IC/P_pH3 weight ratio of 2 loaded with 100 µg/ml of insulin, IC/P_pH3INS100_0.2 – NPs at IC/P_pH3 weight ratio of 0.2 loaded with 100 µg/ml of insulin).

Release profiles from IC/P_pH3 NPs loaded with 100 µg/ml of insulin in 0.01 M HCl, pH 2. Model parameter estimates obtained after fitting the release data to the first order equation are shown in Table 6.2.3. There was a significant difference between the amount and the rate of insulin released between the different types of NPs. Smaller amounts of insulin and with greater rates can be released form negatively charged NPs (IC/P_pH3 weight ratios of 4 and 2), while all insulin loaded was released from positively charged NPs (IC/P_pH3 weight ratio of 0.2) after 6 h of experiment.

Table 6.2.2 *Model parameter estimates and their statistical significance for insulin release from IC/P_pH3 NPs loaded with 100 µg/ml of insulin in HCl, pH 2, fitted to the first order model.*

IC/P_pH3 weight ratio	k [min^{-1}]	p-value	W_∞ [µg/mg of NPs]	p-value
4	0.045±0.013	<0.001 (significantly different)	44±5.4	<0.001 (significantly different)
2	0.063±0.015		27±1.5	
0.2	0.022±0.036		105±5.4	

6.3.4.1.2 Release in the acetate buffer (pH 4.5)

Particle size, PdI and ZP of tested NPs were measured after their preparation and release in the acetate buffer (Table C.8, Appendix C). Negatively charged NPs remained relatively stable on release studies, however an increase in the particle size and minor changes in PdI values were observed. There were no changes in ZP of negatively charged NPs. Aggregation occurred in case of the positively charged system during release studies.

Data on release of insulin from the various NPs was plotted against the time of release and is shown in Figure 6.2.8.

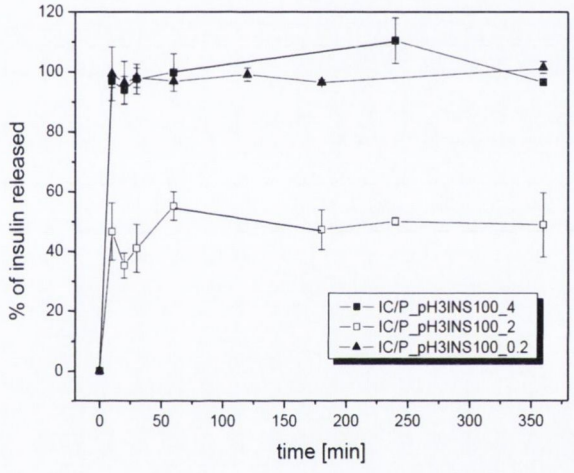

Fig. 6.2.8 *Insulin release profiles from IC/P_pH3 NPs loaded with 100 µg/ml of insulin in 0.1 M acetate, pH 4.5. Amount of released insulin was quantified by RP – HPLC.*
(IC/P_pH3INS100_4 – NPs with IC/P_pH3 weight ratio of 4 loaded with 100 µg/ml of insulin, IC/P_pH3INS100_2 – NPs with IC/P_pH3 weight ratio of 2 loaded with 100 µg/ml of insulin, IC/P_pH3INS100_0.2 – NPs with IC/P_pH3 weight ratio of 0.2 loaded with 100 µg/ml of insulin).

Similar release profiles were observed for the 4 and 0.2 IC/P_pH3 systems and almost all insulin loaded was released within first 10 minutes of the study. Different release profiles were noticed for the 2 IC/P_pH3 system, where only 30 – 40% of insulin was released from this type of NPs. Values of model parameter estimates obtained after fitting release data to the first order equation are presented in Table 6.2.3. There were no significant differences in the rate of insulin release from the different types of NPs, however the amount released at infinity was reliant on the type of NPs, as the 2 IC/P_pH3 system had much lower W_∞ values.

Table 6.2.3 *Model parameter estimates and their statistical significance for insulin release from IC/P_pH3 NPs loaded with 100 µg/ml of insulin in acetate buffer, pH 4.5, fitted to the first order model.*

IC/P_pH3 weight ratio	k [min^{-1}]	p-value	W_∞ [µg/mg of NPs]	p-value
4	0.361±0.111	0.35 (not significantly different)	100±3.2	<0.001 (significantly different)
2	0.211±0.142		52±3.4	
0.2	0.263±0.079		104±5.1	

6.3.4.1.3 Release in PBS buffer (pH 4.5)

Particle size, PdI and ZP values before and after release studies are shown in Table C.8 (Appendix C). An increase in the particle size was observed for negatively charged NPs and the positively charged system aggregated. Surprisingly, PdI decreased for the 4 IC/P_pH3 system suggesting dissolution, while for the 2 IC/P_pH3 sample a small increase in PdI was observed. Release profiles of insulin from IC/P_pH3 NPs in PBS are shown in Figure 6.2.9.

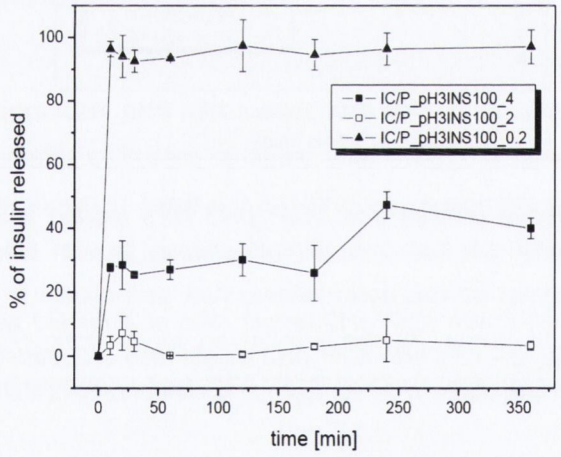

Fig. 6.2.9 *Insulin release profiles from IC/P_pH3 NPs loaded with 100 µg/ml of insulin in 0.01 M PBS, pH 4.5. Amount of released insulin was quantified by RP – HPLC.*
(IC/P_pH3INS100_4 – NPs with IC/P_pH3 weight ratio of 4 loaded with 100 µg/ml of insulin, IC/P_pH3INS100_2 – NPs with IC/P_pH3 weight ratio of 2 loaded with 100 µg/ml of insulin, IC/P_pH3INS100_0.2 – NPs with IC/P_pH3 weight ratio of 0.2 loaded with 100 µg/ml of insulin).

It was seen that 87 – 97% of insulin released from the positively charged system. A smaller amount of insulin was released from negatively charged NPs. App. 28 – 47% of insulin was released from the 4 IC/P_pH3 NPs, while only 3 – 8% insulin release was observed for the 2 IC/P_pH3 NPs. Model parameter estimates were obtained after fitting the release data to the first order equation (Table 6.2.4). There was a

significant difference between the amount and the rate of insulin released depending on the type of NPs used. The smallest amount and the smallest rate of release was measured for the 2 IC/P_pH3 formulation.

Table 6.2.4 *Model parameter estimates and their statistical significance for insulin release from IC/P_pH3 NPs loaded with 100 µg/ml of insulin (IC/P_pH3 INS100) in PBS, pH 7.4, fitted to the first order model.*

IC/P_pH3 weight ratio	k [min^{-1}]	p-value	W_∞ [µg/mg of NPs]	p-value
4	0.176±0.047	<0.05 (significantly different)	33±2.1	<0.001 (significantly different)
2	0.018±0.020		5±2.7	
0.2	0.235±0.115		96±3.1	

6.3.4.1.4 Comparison of release profiles from IC/P_pH3 NPs loaded with 100 µg/ml of insulin

Percentages of insulin released from IC/P_pH3 NPs loaded with 100 µg/ml of insulin were compared.

Release profiles from the same type of NPs in the various buffers are presented in Figure 6.2.10 (negatively charged NPs) and Figure 6.2.11 (positively charged NPs).

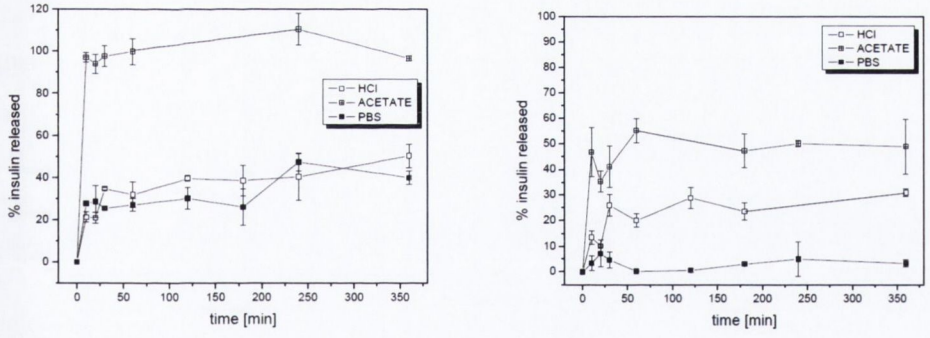

a) **b)**

Fig. 6.2.10 *Release profiles in HCl, acetate buffer and PBS from negatively charged NPs loaded with 100 µg/ml of insulin* ***a)*** *IC/P_pH3 weight ratio of 4,* ***b)*** *IC/P_pH3 weight ratio of 2. Amount of released insulin was quantified by RP – HPLC.*

Similar release profiles were observed for the 4 IC/P_pH3 NPs in HCl and PBS (20 – 50% of insulin release), however nearly 100% of the peptide release immediately in the acetate buffer. Different amounts of insulin were released from the 2 IC/P_pH3 NP formulation. The smallest peptide amount was measured when PBS was used, while the greatest peptide release was observed in the acetate buffer. Analysis of

release profiles from the positively charged NPs did not show major differences between the amounts of insulin released in different media (Figure 6.2.11).

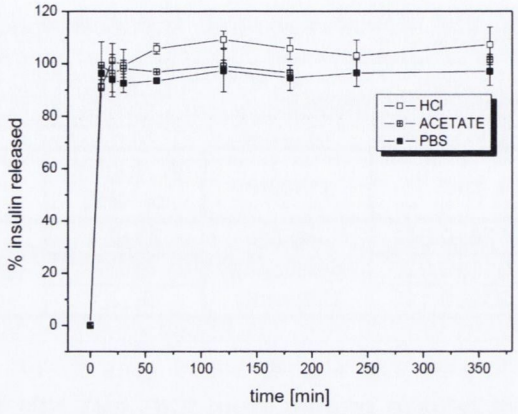

Fig. 6.2.11 *Release profiles in HCl, acetate buffer and PBS from positively charged NPs (IC/P_pH3 weight ratio of 0.2) loaded with 100 µg/ml of insulin. Amount of released insulin was quantified by RP – HPLC.*

6.3.4.1.5 Release in FaSSIF

Particle size, PdI and ZP of tested NPs were measured after their preparation and release in FaSSIF (Table C.9, Appendix C). The particle size of negatively charged NPs decreased to 55-60 nm suggesting dissolution of NPs as the size of these entities was similar to that of pure FaSSIF (70 nm). The particle size of positively charged NPs was observed to increase when measured after the release studies. PdI values decreased for negatively charged NPs and increased for positively charged NPs and were app. 0.25. ZP of all of the types of NPs tested was similar after release to FaSSIF and was -29.2 mV to -27.4 mV.

Insulin release profiles from IC/P_pH3 NPs loaded with 100 µg/ml of NPs in FaSSIF are presented in Figure 6.2.12.

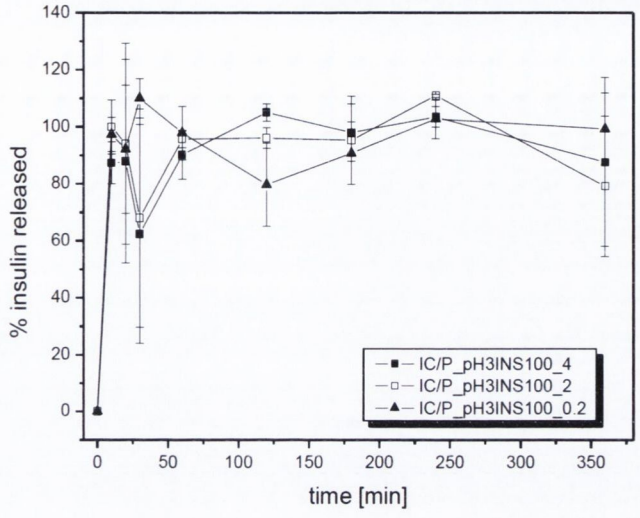

Fig. 6.2.12 *Insulin release profiles from IC/P_pH3 NPs loaded with 100 µg/ml of insulin in FaSSIF. Amount of released insulin was quantified by RP – HPLC. (IC/P_pH3INS100_4 – NPs with IC/P_pH3 weight ratio of 4 loaded with 100 µg/ml of insulin, IC/P_pH3INS100_2 – NPs with IC/P_pH3 weight ratio of 2 loaded with 100 µg/ml of insulin, IC/P_pH3INS100_0.2 – NPs with IC/P_pH3 weight ratio of 0.2 loaded with 100 µg/ml of insulin).*

Fluctuations in the amount if insulin released to FaSSIF could be observed for all of the types of NPs tested, reflected in large standard deviations for some of the time points. App. 100% of the insulin loaded was released after 6 hours of the studies. Fitting the data obtained to the first order equation allowed model parameter to be estimated (Table 6.2.5). There was no significant difference observed between the various types of NPs tested.

Table 6.2.5 *Model parameter estimates and their statistical significance for insulin release from IC/P_pH3 NPs loaded with 100 µg/ml of insulin in FaSSIF, fitted to the first order model.*

IC/P_pH3 weight ratio	k [min^{-1}]	p-value	W_∞ [µg/mg of NPs]	p-value
4	0.233±0.017	0.09 (not significantly different)	98±6.9	0.57 (not significantly different)
2	0.310±0.019		100±5.9	
0.2	0.395±0.113		96±8.3	

6.3.4.2 Release from IC/P_pH3 NPs loaded with 500 µg/ml of insulin

IC/P_pH3 NPs were loaded with a larger amount of insulin (500 µg/ml) and release profiles in three various media: 0.01 M HCl (pH 2), 0.1 M acetate buffer (pH 4.5) and 0.01 M PBS (pH 7.4) were investigated.

6.3.4.2.1 Release in HCl buffer (pH 2)

The properties of tested NPs were studied by measuring particle size, PdI and ZP before and after release studies (Table C.10, Appendix C). A small increase in size and PdI occurred for the 4 and 0.2 IC/P_pH3 systems. Aggregates were formed in the case of the 2 IC/P_pH3 formulation after release in HCl. Micron sized particles were formed and an increase of PdI was noticed for this type of NPs. All types of NPs had positive charge in HCl, which was the greatest for the 4 IC/P_pH3 system (31.5 mV).

Insulin release profiles from the different types of NPs in HCl (pH 2) are presented in Figure 8.2.13. The smallest amount of insulin was released from the 2 IC/P_pH3 NPs (60 - 70%). More than 80% was released from the 4 IC/P_pH3 formulation, while app. 100% of insulin released from the positively charged NPs.

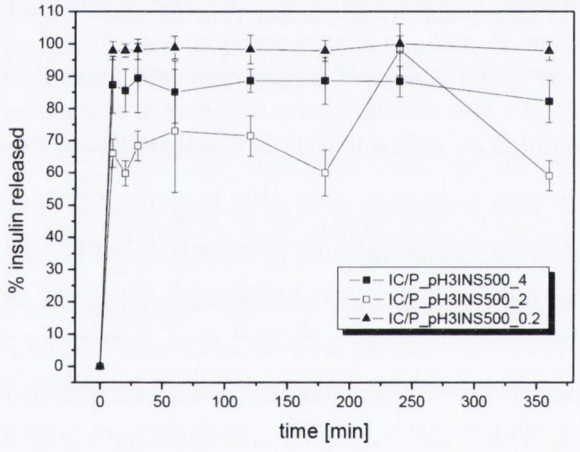

Fig. 6.2.13 *Insulin release profiles from IC/P_pH3 NPs loaded with 500 µg/ml of insulin in 0.01 M HCl, pH 2. Amount of released insulin was quantified by RP – HPLC.*
(IC/P_pH3INS500_4 – NPs with IC/P_pH3 weight ratio of 4 loaded with 500 µg/ml of insulin, IC/P_pH3INS500_2 – NPs with IC/P_pH3 weight ratio of 2 loaded with 500 µg/ml of insulin, IC/P_pH3INS500_0.2 – NPs with IC/P_pH3 weight ratio of 0.2 loaded with 500 µg/ml of insulin).

Model parameter estimates obtained after fitting release data to the first order equation are summarised in Table 6.2.6. There was no difference between the rates of insulin release from the different types of NPs tested, but the amount released at infinity varied. The 2 IC/P_pH3 sample released the smallest amount of insulin (335 µg/mg of NPs), while the greatest amount of insulin was released from the 0.2 IC/P_pH3 system.

Table 6.2.6 *Model parameter estimates and their statistical significance for insulin release from IC/P_pH3 NPs loaded with 500 µg/ml of insulin in HCl, pH 2, fitted to the first order model.*

IC/P_pH3 weight ratio	k [min^{-1}]	P value	W_∞ [µg/mg of NPs]	P value
4	0.276±0.063	0.26 (not significantly different)	434±34.2	<0.001 (significantly different)
2	0.311±0.116		335±26.1	
0.2	0.389±0.082		492±11.6	

6.3.4.2.2 Release in the acetate buffer (pH 4.5)

Properties of NPs (size, PdI and ZP) were measured after their preparation and after release studies (Table C.10, Appendix C). Small increases in the particle size and PdI occurred for negatively charged NPs but no aggregates were formed. ZP slightly decreased and was app. -46 mV. Positively charged NPs formed aggregates on release in the acetate buffer.

Release profiles in the acetate buffer at pH 4.5 are presented in Figure 6.2.14. Similar profiles were obtained for the 4 and 0.2 IC/P_pH3 NPs and 90% - 100% of insulin was quickly released in the acetate buffer. In the case of the 2 IC/P_pH3 formulation, fluctuations in the amount of insulin were observed with 64% - 96% of insulin released during 6 h of study.

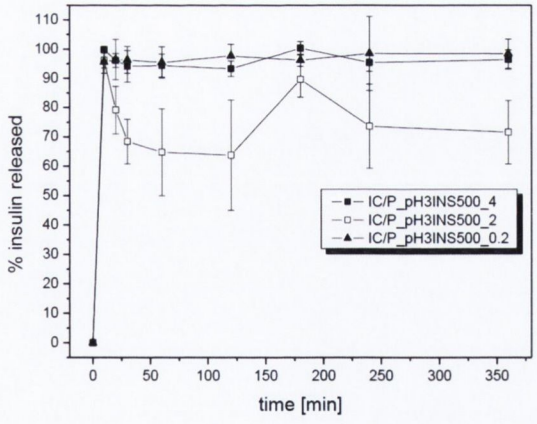

Fig. 6.2.14 *Insulin release profiles from IC/P_pH3 NPs loaded with 500 µg/ml of insulin in 0.1 M acetate, pH 4.5. Amount of released insulin was quantified by RP – HPLC.*
(IC/P_pH3INS500_4 – NPs with IC/P_pH3 weight ratio of 4 loaded with 500 µg/ml of insulin, IC/P_pH3INS500_2 – NPs with IC/P_pH3 weight ratio of 2 loaded with 500 µg/ml of insulin, IC/P_pH3INS500_0.2 – NPs with IC/P_pH3 weight ratio of 0.2 loaded with 500 µg/ml of insulin).

Model parameter estimates obtained after fitting release data to the first order equation are summarised in Table 6.2.7. Significant differences in the rate of insulin

released can be observed. A lower rate was obtained for the 2 IC/P_pH3 NPs, while similar k values were obtained for the other types of NPs tested. The lowest amount of insulin could be released from the 2 IC/P_pH3 system and the greatest from the positively charged NPs (0.2 IC/P_pH3).

Table 6.2.7 *Model parameter estimates and their statistical significance for insulin release from IC/P_pH3 NPs loaded with 500 µg/ml of insulin in acetate buffer, pH 4.5, fitted to the first order model.*

IC/P_pH3 weight ratio	k [min^{-1}]	p-value	W_∞ [µg/mg of NPs]	p-value
4	0.349±0.240	0.06 (not significantly different)	481±14.6	<0.05 (significantly different)
2	0.068±0.024		401±65.1	
0.2	0.304±0.048		486±26.3	

6.3.4.2.3 Release in PBS (pH 7.4)

The particle size, PdI and charge of NPs before and after release studies were measured and are summarised in Table C.10 (Appendix C). Only one type of NPs remained relatively stable on release studies (4 IC/P_pH3 NPs), however there was an increase in the particle size and PdI observed for 2 IC/P_pH3 weight ratio NPs while the ZP remained negative -30.7 mV. Micron sized particles were formed when the 2 IC/P_pH3 was subjected to release studies. Aggregation was seen for the positively charged NPs (IC/P_pH3 weight ratio of 0.2).

Release profiles from IC/P_pH3 NPs loaded with 500 µg/ml of insulin in PBS are presented in Figure 6.2.15. Similar profiles were obtained for the 4 and 0.2 IC/P_pH3 system with a quick release of app. 90% of insulin within first 10 minutes of the studies. Large fluctuations in the amount of insulin released were observed for the 2 IC/P_pH3 system (15 – 84% of insulin was released during 6 h of study).

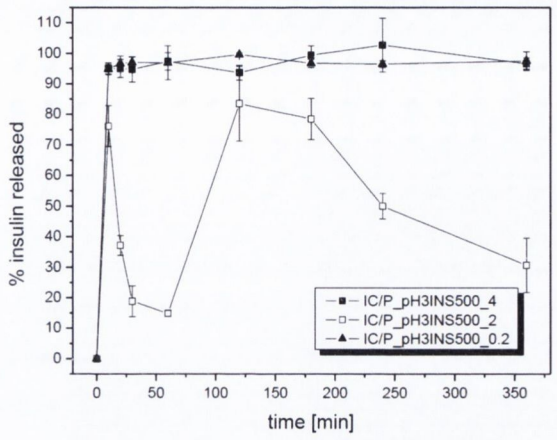

Fig. 6.2.15 *Insulin release profiles from IC/P_pH3 NPs loaded with 500 µg/ml of insulin in 0.01 M PBS, pH 7.4. Amount of released insulin was quantified by RP – HPLC.*
(IC/P_pH3INS500_4 – NPs with IC/P_pH3 weight ratio of 4 loaded with 500 µg/ml of insulin, IC/P_pH3INS500_2 – NPs with IC/P_pH3 weight ratio of 2 loaded with 500 µg/ml of insulin, IC/P_pH3INS500_0.5 – NPs with IC/P_pH3 weight ratio of 0.5 loaded with 500 µg/ml of insulin).

Model parameter estimates obtained after fitting release data to the first order equation are summarised in Table 6.2.8. There was a significant difference between the rate and the amount of insulin released from the different types of NPs, however this may have been caused by the unusually large variations in the amount of insulin released from the 2 IC/P_pH3 NP system. The fitted parameters should be treated with caution as poor fit quality was determined for this sample (R^2 = 0.374).

Table 6.2.8 *Model parameter estimates and their statistical significance for insulin release from IC/P_pH3 NPs loaded with 500 µg/ml of insulin in PBS, pH 7.4, fitted to the first order model.*

IC/P_pH3 weight ratio	k [min^{-1}]	p-value	W_∞ [µg/mg of NPs]	p-value
4	0.408±0.088	<0.001 (significantly different)	484±6.6	<0.001 (significantly different)
2	0.027±0.007		268±39.0	
0.2	0.346±0.038		486±8.8	

6.3.4.2.4 Comparison of release profiles from IC/P_pH3 NPs loaded with 500 µg/ml of insulin

Percentages of insulin released from IC/P_pH3 NPs loaded with 500 µg/ml of insulin in various media were compared To investigate the influence of environmental pH used for insulin release from NPs, the release profiles of negatively charged NPs are

presented in Figure 6.2.16, while those for the positively charged NPs are shown in Figure 6.2.17.

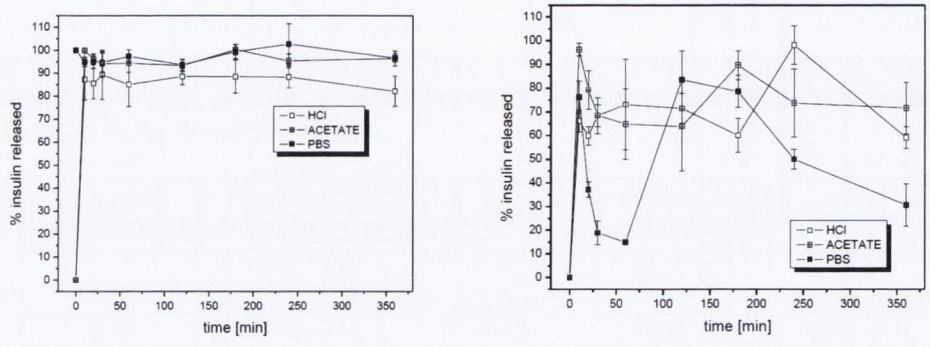

a) **b)**

Fig. 6.2.16 *Release profiles in HCl, acetate buffer and PBS from negatively charged NPs loaded with 500 µg/ml of insulin* ***a)*** *IC/P_pH3 weight ratio of 4,* ***b)*** *IC/P_pH3 weight ratio of 2. Amount of released insulin was quantified by RP – HPLC.*

Analysis of release profiles from the 4 IC/P_pH3 NPs shows a similar behaviour of these NPs in all of three media tested, although the smallest amount of insulin (80 – 90%) was released in HCl. Large fluctuations in the amount of insulin released were observed for the 2 IC/P_pH3 system for all of the buffers tested. Similar release profiles were observed for the positively charged NPs tested with 90-100% of insulin quickly released in all of the media tested.

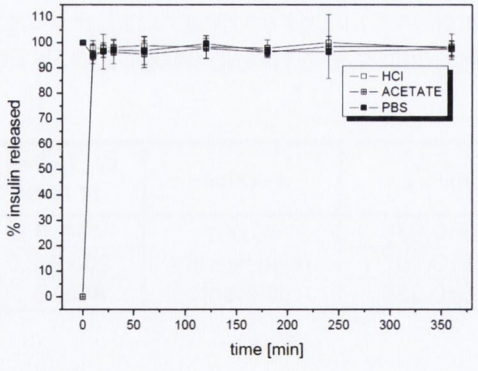

Fig. 6.2.17 *Release profiles in HCl, acetate buffer and PBS from positively charged NPs (IC/P_pH3 weight ratio of 0.2) loaded with 500 µg/ml of insulin. Amount of released insulin was quantified by RP – HPLC.*

Comparative studies were also performed to investigate the influence of the amount of insulin loaded into IC/P_pH3 NPs on the release rates of the peptide (Table 6.2.9). No differences in release rates for all NPs were observed when the acetate buffer

was used. On the other hand, the rate of release in HCl solution was always different when different amounts of the peptide were loaded in NPs and the insulin liberation was faster for the 500 μg/ml peptide loading. Significant differences in release rates were seen for the 4 IC/P_pH3 system in PBS, while similar rates were obtained for the other systems.

Table 6.2.9 *Model parameter estimates and their statistical significance for insulin release from IC/P_pH3 NPs loaded with 100 and 500 μg/ml of insulin fitted to the first order model.*
*(Statistical analysis: # - no significant difference, *p<0.05, **p<0.01, ***p<0.001).*

IC/P_pH3 weight ratio	Buffer	k [min^{-1}]		p-value
		INS100	INS500	
4	HCl, pH 2	0.045±0.013	0.276±0.063	**
	Acetate, pH 4.5	0.361±0.111	0.349±0.240	#
	PBS, pH 7.4	0.176±0.047	0.408±0.088	**
2	HCl, pH 2	0.063±0.015	0.311±0.240	*
	Acetate, pH 4.5	0.211±0.142	0.068±0.024	#
	PBS, pH 7.4	0.018±0.020	0.027±0.007	#
0.2	HCl, pH 2	0.217±0.036	0.389±0.082	*
	Acetate, pH 4.5	0.263±0.079	0.304±0.028	#
	PBS, pH 7.4	0.235±0.115	0.346±0.038	#

The carrageenan/protamine weight ratio was seen to have an significant impact on insulin release in the various media tested. Similarly to the alginate/protamine NPs, the most significant difference in release occurred between negatively and positively charged NPs. In general, positively charged NPs released nearly 100% of insulin loaded in the first 10 minutes of the study. There was no significant difference between the amount of insulin loaded and the pH of medium tested for this type of NPs. This complete and very fast peptide release could be explained by the uneven distribution of insulin throughout the particle. It suggested here that there may be a similar mechanism of release as in case of initial burst release, which as reported, occurs mainly due to heterogeneous drug distribution within the system. Proteins that are either loosely associated with the surface or embedded in the surface layer are responsible for the burst release (Sah et al., 1994, O'Hagan et al., 1994, Igartua et al., 1997, Rafati et al., 1997). Surface associated drugs are widely known to be main causes for initial burst release (Yeo and Park, 2004).

Different release profiles were obtained for the two types of negatively loaded NPs. Slow and sustained release of the peptide occurred in HCl and PBS for the 4 IC/P_pH3 system, while this type of release (slow and sustained) was observed in all media tested for the 2 IC/P_pH3 formulation. This type of release is interesting as it offers a great degree of modulation and it would suggest that insulin is encapsulated inside the NPs rather than on their surface. It can be assumed that stronger

interactions between the components are present in the 2 IC/P_pH3 sample as the amount of insulin released is smaller in comparison to the 4 IC/P_pH3 system. Incorporation of a larger amount of insulin (500 μg/ml) resulted in a higher percentage of insulin released in case of negatively charged NPs, which would suggest a different distribution of insulin within NPs with the high peptide content compared to the 100 μg/ml insulin–containing NPs. A larger amount of insulin would appear at or close to the NP surface due to NP matrix saturation. No difference in release properties was observed for the positively charged NPs, when various amounts of insulin were loaded. Similar data for release was reported by Li et al., where chitosan – carrageenan polyelectrolyte complex (PEC) was used to encapsulate bovine serum albumin (BSA) to study the potential of this PECs as a pH responsive oral delivery system (Li et al., 2013). The release kinetics of BSA loaded PEC particles were investigated in SGF (Simulated Gastric Fluid, pH 1.2) and SIF (Simulated Intestinal Fluid, pH 7.5). The initial burst release of BSA observed in SIF was much faster than that in SGF. Proposed by the authors mechanism suggests that in acidic SGF conditions chitosan and carrageenan were bound tightly and therefore, further release was limited because of the absence of swelling or disintegration of PEC. In SIF (pH 7.5), the ionic attraction between polymers became weaker, which led to significant swelling and disintegration of PEC, which allowed large amount of encapsulated BSA to be released (Li et al., 2013). Similar release profiles were obtained for negatively charged IC/P_pH3 NPs. Much lower amount of insulin was released to HCl buffer (pH 2), which would correspond to the SGF conditions in comparison to PBS (pH 7.4, SIF conditions). Therefore a similar release mechanism, as that reported by Li et al. (2013), may be applicable to insulin release from negatively charged IC/P_pH3 NPs.

6.3.5 Cytotoxicity of IC/P_pH3 NPs

Cytotoxicity of insulin-loaded IC/P_pH3 NPs was studied by incubation of NPs with various concentrations with Caco-2 cells.

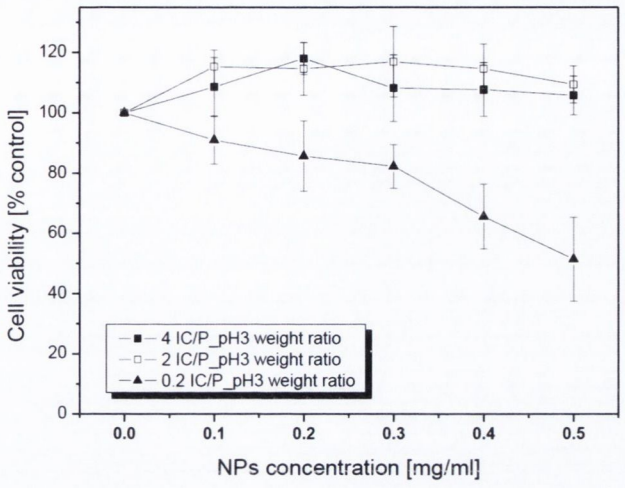

Fig. 6.2.18 *The viability of Caco-2 cells after 72 hours exposure to IC/P_pH3 NPs in serum-free medium.*

The viability of the cells was strongly dependent on the composition of NPs tested. Using the negatively charged NPs, containing more carrageenan than protamine, did not only show the cell damage, but also resulted in an increased proliferation (by up to 15%) comparing to the control. A decrease in the cell viability was observed when positively charged NPs were applied to the Caco-2 cells. 51% of cell viability was measured when positively charged NPs at concentration of 0.5 mg/ml were incubated with Caco-2 cells for 72 h.

6.3.6 Transport of insulin from ICP_pH3 NPs through Caco-2 monolayer

Transport of insulin loaded into IC/P_pH3 NPs was studied through Caco-2 monolayers prepared as described in (Section 2.4.2.16.1). To evaluate the effect of IC/P_pH3 NPs on the tight junctions integrity, TEER values and fluorescein appearance in the acceptor compartment were measured during the studies. Additionally, transport of insulin dissolved in protamine solution was tested. Insulin solution (500 µg/ml) was the reference. TEER and fluorescein measurements are presented in Figure 6.2.19.

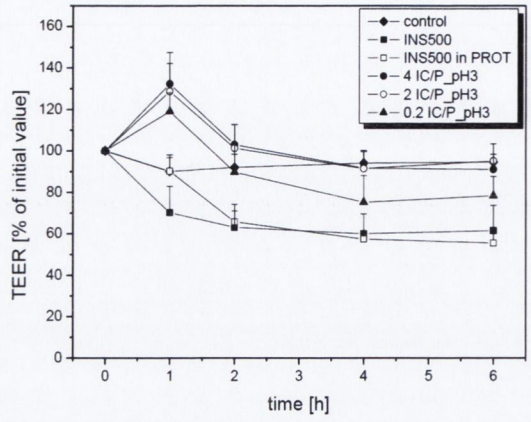

a)

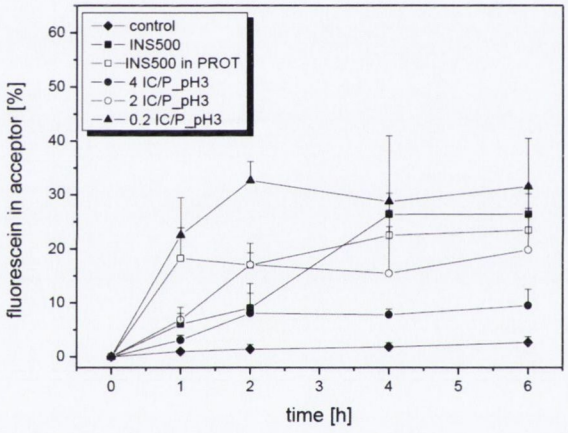

b)

Fig. 6.2.19 *Time course of TEER and fluorescein transport across Caco-2 monolayers under influence of insulin as a standard and IC/P_pH3 NPs.*
(Control – monolayers with no sample tested, INS500 – insulin solution 500 µg/ml (reference), INS500 in PROT – insulin solution 500 µg/ml dissolved in 0.1% w/v protamine solution, 4 IC//P_pH3 – NPs with IC/P_pH3 weight ratio of 4, 2 IC//P_pH3 – NPs with IC/P_pH3 weight ratio of 2, 0.2 IC//P_pH3 – NPs with IC/P_pH3 weight ratio of 0.2).

An increase in TEER values (by 20 – 30%) was observed after 1 h incubation with IC/P_pH3 NPs. In the next hour the TEER values were similar to the control. Further incubation with IC/P_pH3 NPs resulted in different TEER values achieved, which were dependent on the type of NPs. Negatively charged NPs (4 and 2 IC/P_pH3) had TEER values similar to the control, while in case of the positively charged NPs (0.2 IC/P_pH3 weight ratio) the values decreased to 80%. Lowest TEER values were obtained for the insulin standard and insulin dissolved in protamine solution (decrease to 60% of the initial value), although after 1 h of incubation a lower decrease in TEER was noted when insulin dissolved in P solution was used (Figure

6.2.19 a). A similar behaviour was observed for the fluorescence appearance in the acceptor compartment. The greatest and the fastest leakage of fluorescein was observed for the positively charged IC/P_pH3 NPs (0.2 weight ratio). Lower values (of app. 25%) were obtained for the insulin reference and insulin dissolved in P solution. Almost 10% of the starting amount of fluorescein was noticed for the 4 IC/P_pH3 system, while for the other NP type (2 IC/P_pH3) it reached 20% after 6 h of study.

The amount of insulin transported through Caco-2 monolayers from IC/P_pH3 NPs is presented in Figure 6.2.20.

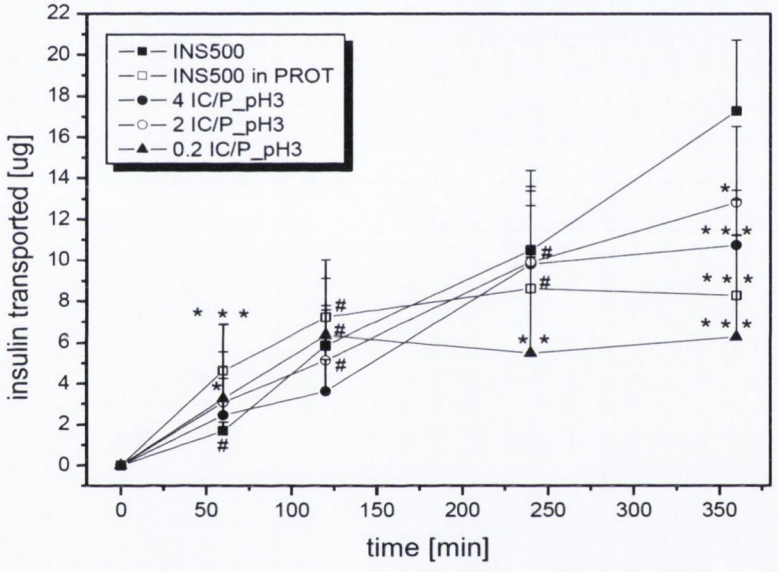

Fig. 6.2.20 *Transport of insulin from solutions and NPs through Caco-2 monolayers. (Statistical analysis: # - no statistical difference, *p<0.05, **p<0.01, ***p<0.001). Amount of transported insulin was quantified by RP – HPLC.*
(INS500 – insulin solution 500 µg/ml (reference), INS500 in PROT – insulin solution 500 µg/ml dissolved in 0.1% w/v protamine solution, 4 IC//P_pH3 – NPs with IC/P_pH3 weight ratio of 4, 2 IC//P_pH3 – NPs with IC/P_pH3 weight ratio of 2, 0.2 IC//P_pH3 – NPs with IC/P_pH3 weight ratio of 0.2).

Analysis of the transport profiles of insulin incorporated into IC/P_pH3 NPs and insulin dissolved in P solution showed significant differences in the final amount (after 6 hours) of insulin transported in comparison to the reference. Also, different rates of insulin transport were observed. A significantly greater amount of insulin was transported after 1 h of incubation with insulin dissolved in P solution and the 0.2 IC/P_pH3 system comparing to the reference. Further incubation resulted in an increase in the amount of insulin transported from the reference and from the negatively charged NPs, while the amount of insulin transported from the positively

charged NPs was significantly smaller. At the final point of the study (6 h), a difference in the amount of insulin transported was seen for all samples tested, comparing to the insulin reference. The rate of insulin transported through the Caco-2 monolayers was expressed by permeability coefficient (P_{app}). Amounts of insulin transported and the rate of their transport are summarised in Table 6.2.10.

Table 6.2.10 *Amount of insulin transported and its apparent permeability (P_{app}) across Caco-2 monolayers in the presence of insulin as a reference, insulin dissolved in protamine and IC/P_pH3 NPs. (Statistical analysis: *p<0.05, **p<0.01, ***p<0.001).*
(INS500 – insulin solution 500 µg/ml (reference), INS500 in PROT – insulin solution 500 µg/ml dissolved in 0.1% w/v protamine solution, 4 IC//P_pH3 – NPs with IC/P_pH3 weight ratio of 4, 2 IC//P_pH3 – NPs with IC/P_pH3 weight ratio of 2, 0.2 IC//P_pH3 – NPs with IC/P_pH3 weight ratio of 0.2).

Sample	Insulin transported [µg]	P_{app} [x10^{-6} cm·s^{-1}]
INS500	17.28±3.43	2.24±0.48
INS500 in PROT	8.30±4.67 ***	1.42±0.48 **
4 IC/P_pH3	10.75±2.69 ***	1.33±0.33 ***
2 IC/P_pH3	12.84±3.68 *	1.57±0.36 **
0.2 IC/P_pH3	6.28±4.97 ***	0.86±0.55 ***

Analysis of data presented in Table 6.2.13 showed a significant impact of protamine content in NPs on the amount and the rate of insulin transport. Smaller amounts of insulin and with smaller rate were transported from the positively charged NPs (0.2 IC/P_pH3). It could be noticed that significantly smaller amounts of insulin were transported from all of the samples tested in comparison to the reference. However, incorporating insulin into negatively charged NPs (4 and 2 IC/P_pH3 systems) resulted in a greater amount of insulin transported, comparing to positively charged NPs. Statistical analysis of all of the samples tested is summarised in Table 6.2.11.

Table 6.2.11 *Statistical analysis of amount of insulin transported and its permeability coefficient for insulin loaded into IC/P_pH3 NPS and insulin dissolved in protamine. (Statistical analysis: # - no statistical difference, *p<0.05, **p<0.01, ***p<0.001).*
(INS500 – insulin solution 500 µg/ml (reference), INS500 in PROT – insulin solution 500 µg/ml dissolved in 0.1% w/v protamine solution, 4 IC//P_pH3 – NPs with IC/P_pH3 weight ratio of 4, 2 IC//P_pH3 – NPs with IC/P_pH3 weight ratio of 2, 0.2 IC//P_pH3 – NPs with IC/P_pH3 weight ratio of 0.2).

P_{aap}	INS500	INS500 in PROT	4.IC/P_pH3	2 IC/P_pH3	0.2 IC/P_pH3
INS500	--------	**	***	**	***
INS500 in PROT	**	----------	#	#	#
4 IC/P_pH3	***	#	----------	#	#
2 IC/P_pH3	**	#	#	----------	*
0.2 IC/P_pH3	***	#	#	*	----------
Insulin transported [µg]	INS500	INS500 in PROT	4.IC/P_pH3	2 IC/P_pH3	0.2 IC/P_pH3
INS500	--------	***	***	*	***
INS500 in PROT	***	----------	#	*	#
4 IC/P_pH3	***	#	----------	#	#
2 IC/P_pH3	*	*	#	----------	#
0.2 IC/P_pH3	***	#	#	#	----------

In addition to the above conclusions, significant differences were observed in P_{app} values for all of the samples comparing to the reference sample. P_{aap} values for the 2 IC/P_pH3 NPs varied form the sample containing insulin dissolved in P solution.

6.4 Conclusions

Two various types of NPs (AAL/P_pH3 and IC/P_pH3) loaded with two amounts of insulin (100 and 500 µg/ml) were prepared and *in vitro* characterised for their potential as oral insulin delivery systems. Incorporation of insulin into NPs resulted in only small changes in the NPs characteristics (size, PdI and ZP). Small increase in the particle size and PdI of negatively charged NPs was observed, while the charge of positively charged NPs increased due to the incorporation insulin having positive charge. Colloidal stability of insulin-loaded NPs was investigated up to 3 days of storage at RT. Negatively charged AAL/P_pH3 NPs loaded with insulin had better stability than positively charged NPs, however both types of AAL/P_pH3 NPs had particles in the nanosize range after 3 days of storage. Also, better stability was noticed for negatively charged IC/P_pH3 NPs loaded with insulin, with the 0.5 IC/P_pH3 sample (positively charged) aggregating after 1 day of storage. However, another positively charged formulation investigated, 0.2 IC/P_pH3 NPs, was seen to be stable.

Very high AE was obtained for AAL/P_pH3 NPs (93 – 100% when 100 µg/ml of insulin was loaded and 87 – 99% when 500 µg/ml of insulin was loaded, with lower AE obtained for positively charged NPs. In case of IC/P_pH3 NPs the AE was dependent on the initial charge of NPs. Excellent association efficiency was obtained for negatively charged IC/P_pH3 NPs (99% for 100 µg/ml of insulin and 100% for 500 µg/ml of insulin loaded), however lower AE was obtained for positively charged IC/P_pH3 NPs (53% for 100 µg/ml of insulin and 20% for 500 µg/ml of insulin loaded). Thus, negatively charged NPs were better as drug delivery systems in terms of AE.

Different amounts and different rates of insulin were released (*in vitro*) from negatively and positively charged NPs in media with different pH. Approximately 100% of insulin was released from both types (AAL/P_pH3 and IC/P_pH3) of positively charged NPs. Slower and more sustained release of insulin in HCl from negatively charged AAL/P_pH3 NPs was seen. Different release profiles were obtained for negatively charged IC/P_pH3 (4 and 2 IC/P/_pH3 NPs). The major difference was the release to HCl at pH 2 (for NPs loaded with 100 µg/ml of insulin), where all app. 100% of insulin was released from NPs at 4 IC/P_pH3 weight ratio, while in case of 2 IC/P_pH3 weight ratio the final amount of insulin was 30% after 6 h of the study (Figure 8.2.10).

Cytotoxicity assay performed with the Caco-2 cell line confirmed the non-cytotoxic nature of negatively charged AAL/P_pH3 and IC/P_pH3 NPs. 45% of cells remained viable after 72 h incubation with positively charged AAL/P_pH3 NPs at concentration of 0.5 mg/ml NPs, while 52% of live cells were seen after incubation with positively charged IC/P_pH3 NPs at the same concentration as in case of AAL/P_pH3 NPs.

Transport of insulin incorporated into NPs and insulin dissolved in P solution through Caco-2 monolayers was investigated. Differences in the final amount of insulin transported after 6 h of the study in comparison to the reference (solution of insulin) were observed, consistent with the rank of P_{app} values. A significantly greater amount of insulin was transported from solution containing insulin dissolved in P and from positively charged NPs at 1 h of incubation. Further incubation resulted in greater amounts of peptide transported from negatively charged NPs and insulin reference.

CHAPTER 7

GENERAL DISCUSSION

Insulin is a polypeptide hormone that is commonly used in the treatment of diabetes, as it controls the amount of the glucose in the blood. Since the discovery of insulin various attempts have been made to overcome the injection-based therapy, which is the only route of its delivery to date. Most attempts failed to progress beyond the proof of concept stage mainly because of low bioavailability of insulin, variability in dose response and other factors that called into question the commercial viability of such formulations. Products for pulmonary (Exubera®, Pfizer) and buccal (only in Ecuador) delivery of insulin have been introduced to the market, but they did not last for long. One year after the product introduction, in October 2007, Pfizer announced that production of Exubera® would be discontinued, due to the poor sales.

Oral delivery is the most widely accepted means of drug administration as it is non-invasive, avoids injections and decreases the risk of infections. However, it is not feasible for direct delivery of protein and peptide drugs, due to the following obstacles (Shaji and Patole, 2008):

- acidic environment in the stomach that can lead to protein denaturation
- proteolytic enzymes in the stomach and intestine that can degrade the protein
- mucin barrier
- impermeability of the intestinal wall for macromolecules.

None of the numerous therapeutic proteins on the market are delivered orally at present. To overcome the barriers of poor bioavailability of insulin, several approaches have been explored: chemical modification (Asada et al., 1995), co-administration with absorption enhancers and/or enzyme inhibitors (Ziv et al., 1987) and incorporation into carriers, such as liposomes (Kisel et al., 2001), mixed micelles (Scott-Moncrieff et al., 1994), lipid based systems (Silva-Cunha et al., 1997), microspheres (Kim et al., 2005) and nanoparticles (Sarmento et al., 2006 a). Among the approaches used to overcome the barriers of poor bioavailability of insulin, a new class of penetration enhancers called cell penetrating peptides (CPPs) represents a new and innovative concept, which bypasses some problems of the drug bioavailability. CPPs show the ability to unlock intracellular and also intranuclear targets for the delivery of agents ranging from peptides and antibodies to drug loaded nanoparticles. CPPs are short peptide sequences that are able to transport molecules across cell membranes (Munyendo et al., 2012). The use of CPPs in drug delivery systems is summarised in Figure 7.1.

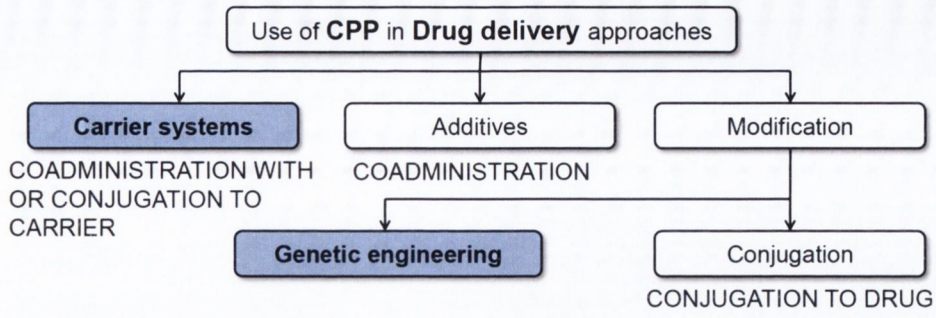

Fig. 7.1 *The use of CPPs in drug delivery.*

The studies presented in this thesis focused on preparation of a novel system that would be suitable for an oral insulin delivery by testing two different approaches: genetic modifications of insulin to enhance its transport through epithelial cell layer and loading insulin into nanocarriers to protect it against degradation (Figure 7.1).

Currently, insulin is produced by recombinant DNA technology, using *E. coli* or yeast as a host organism. To facilitate further modifications of the insulin gene, several plasmids with insulin were designed and prepared. The design of the plasmids was based on the combination of the simplicity of a bacterial expression system with benefits of the expression in yeast, which is achieved by directing the expressed protein with the signal peptide to the oxidation system of the bacterial periplasmic space. The advantages of these novel DNA constructs include low cost, convenience and speed of the method. Optimisation of expression conditions was further investigated by testing two different induction systems: IPTG and auto-induction, and also various temperatures. The impact of those factors on the solubility and the localisation of expressed protein was also examined. Final optimisation of the purification protocols was established. Prepared plasmids can be used for further genetic modifications such as fusions of insulin gene with cell penetrating peptides. An example of this type of fusion was reported by Rojas et al., where a twelve amino acid residue of a membrane translocating sequence (MTS) was fused to the C-terminus of glutathione S-transferase (GST). The resultant GST-MTS fusion proteins were efficiently imported into NIH 3T3 fibroblasts and other cells (Rojas et al., 1998).

The second approach that has been investigated in the present work was the incorporation of insulin into nanocarriers composed of natural polymers (alginic acid or carrageenan) and protamine as a cell penetrating peptide. Polymeric nanoparticles have attracted an increased attention, as they show the ability to entrap macromolecules, protect against degradation, and enhance transmucosal transport (de la Fuente et al., 2008). Especially natural polymers are of particular interest due to their nontoxic, biocompatible, biodegradable and hydrophilic nature

(Sonia and Sharma, 2012). A wide variety of techniques are available for the preparation of polymeric nanoparticles (Vauthier and Bouchemal, 2009). Among them, a polyelectrolyte complexation method (PEC) has received increasing attention, as nanoparticles formed by this method have several favourable characteristics for cellular uptake and colloidal stability, including suitable diameter and surface charge, spherical morphology and a low polydispersity index (PdI). Preparation of nanoparticles by this method avoids using harsh conditions, such as organic solvents and sonication. It can be carried out in aqueous conditions at ambient temperature, which do not adversely affect the stability and biological activity of bioactive agents (Hu et al., 2012).

It has been recently demonstrated that PEC formation is a potentially useful technique to fabricate protein drug delivery systems for oral administration (Shu et al., 2009). In the current work, the conditions for the formation of insulin-free NPs were determined initially and the manufacture process was optimised by testing the impact of process variables (e.g., the type of polymer used, solution viscosity, concentration, and ratio of the polymer solutions) on the properties of PECs. Colloidal stability of selected formulations was further tested in media at different pH. Insulin was then incorporated into characterised nanocarriers and the impact of the peptide on the physicochemical properties of the particles, such as: particle size, zeta potential, polydispersity index, as well as the association efficiency, drug loading and release was examined. Cytotoxicity of selected formulations in the Caco-2 cell line was performed. Finally, transport of insulin loaded into nanocarriers through Caco-2 monolayers was examined.

7.1 Preparation of a novel insulin plasmids

An early attempts to obtain recombinant human insulin by expression of proinsulin gene in *E. coli* faced several problems such as: low expression, difficulties with inclusion bodies solubility, short half-life, high proteolysis and non-efficient translation of coding sequences. Various strategies have been employed to overcome those problems, such as: secreting proinsulin and soluble cytoplasmic proinsulin (Winter et al., 2000; Mergulhao et al., 2004). A novel fusion protein system, which does not require *in vitro* refolding was introduced (Malik et al., 2007); although this periplasmic production system also has some disadvantages such as limited secretion (Chan et al., 1981; Francetic et al., 2000). Because of its advantages, the inclusion body strategy, having often high expression and low proteolysis, has become the default route for production of target proteins in *E. coli*. Several fusion partners such as: β-galactosidase, protein A, glutathione-S-transferase, the immunoglobulin binding Z-domain of protein A, His tagged sequences with a hexahistidine, H64A subtilisin or

factor Xa have been also tested for increasing expression levels and the stability of target protein and to facilitate the purification process (Shen, 1984; Murby et al., 1991; Kang and Yoon, 1994; Cho et al., 2001). Additionally, it was reported that fusion proteins can increase the solubility of the target protein, and this higher solubility can also induce higher refolding yield (Samuelsson et al., 1994; Tikhonov et al., 2001). Based on these reports, various DNA constructs, which allow expression of recombinant human proinsulin in bacterial cells, were designed and prepared. The novel design of expression plasmids was based on the intention to employ the oxidative system present in the periplasmic space of bacteria for introduction of the correct disulfide bridges. This has been achieved by a fusion of proinsulin gene with a periplasmic localisation signal peptide, which should ensure directing the proinsulin to the bacterial oxidation system and by simultaneous co-expression with DsbA protein.

The pET expression system is one of the most powerful systems developed for the expression of recombinant proteins in *E. coli* (Studier and Moffatt, 1986). The pET-22b vector (pHB1-3 constructs) has a very strong and stringent T7 lac promoter and additional signal peptide, which should facilitate secretion of proinsulin into periplasm. Many secretory proteins, produced in both prokaryotic and eukaryotic cells, are initially expressed in cytoplasm with amino-terminal extension (an extra 15-30 amino acids sequence called signal peptide). This signal (leader) peptide is responsible for routing the polypeptide through the membrane. After crossing the membrane the signal peptide is cleaved by distinct enzymes called signal peptidases (SPases) (Tuteja, 2005).

To increase the probability of biological activity by export to the periplasm, vector pET-39b was selected next (plasmid pMD2). Vector pET-39b encodes DsbA tag, which contains a signal sequence that directs the signal protein to the periplasm and catalyses the formation and isomerisation of disulfide bridges. In addition, pET-39b contains His tag sequence at N-terminal, which is useful during the purification step. As reported by Winter et al., fusion of proinsulin to C-terminus of the periplasmic disulfide oxidoreductase DsbA via trypsin cleavage site resulted in increased yields of proinsulin by intra- or intermolecular catalysis of disulfide bond formation (Winter et al., 2000). Another report indicates that an overexpression of either DsbA or DsbC can double the yield of periplasmic insulin-like growth factor (IGF)-I in *E. coli* (Joly et al., 1998). Similarly, a recombinant human immunodeficiency virus type 1 protease (HIV-1Pr) was overexpressed in *E. coli* as a fusion protein with bacterial periplasmic protein dithiol oxidase (DsbA) or glutathione S-transferase (GST), also containing a hexa-histidine tag sequence (Volontè et al., 2011). As reported previously, the yield of native proinsulin obtained from the DsbA-proinsulin was a 1000-fold higher

compared to the secretory expression yield described for isolated proinsulin (Chan et al., 1981). This suggests that DsbA is a very effective and powerful fusion partner considering high amounts of soluble and correctly disulfide bridged proinsulin.

pMD3 plasmid was designed for inclusion body purification. The proinsulin gene with shortened C-peptide was cloned into pET-19b vector, which contains His tag sequence and enterokinase cleavage site, which facilitates an easy digestion and purification of the plasmid. Ding et al. reported the construction of a pET19-based expression clone containing HTLV-1 (Human T-cell leukemia virus type 1) protease fused to a decahistidine-containing leader peptide. The recombinant protein was efficiently expressed in *E. coli*, and the fusion protein was easily purified by affinity chromatography (Ding et al., 1998). Lin et al. have determined the identity of *E. coli* fRMsr (free form of methionine-R-sulfoxide) through its purification from the MsrAB strain and proteomic analysis. The gene of interest was cloned into a modified pET19 expression vector containing an N-terminal His-tag and intervening enterokinase and PreScission (Amersham Pharmacia, Little Chalfont, U.K.) protease cleavage sites (Lin et al., 2007 b). Successfully prepared plasmids were further tested for expression and determination of cellular localisation in *E. coli*.

Optimisation of expression conditions for prepared plasmids was performed. *E. coli* as a host organism offers a rapid, high yield, and economical way to produce recombinant proteins. However, high-level production of functional eukaryotic proteins in *E. coli* is not a routine matter, and can be quite challenging, as various conditions are required to be optimised for different proteins (Sivashanmugam et al., 2009). Several factors needed to be optimised in the proinsulin production in *E. coli*, such as induction system: IPTG and auto-induction, various media (ZYP-5052, ZYM-5052) and temperatures have been explored.

It is well known that the temperature shift in fermentation is an effective way to induce the expression of a target protein (Strandberg and Enfors, 1991). A decrease in the culture temperature and using longer induction time markedly increased target protein expression (Weickert et al., 1997, Kagawa et al., 2003, Hidari et al., 2005, Hou et al., 2007 b). The impact of temperature shift for the expression of human growth hormone expression in fed-batch fermentation was reported (Tabandeh et al., 2005). Dependence of the culture medium and the post-induction temperature on the yield of the periplasmic protein expressed in *E. coli* was reported by Hernandez et al. A synthetic human interferon gamma (hIFN-c) gene was fused to SP1 and SP3, two Sec-dependent artificial signal peptides to transport the hIFN-c to the periplasm of *E. coli* BL21-SI (Hernandez et al., 2008).

The selection of an appropriate fusion tag plays a very important role, not only for protein expression, but even more for its purification. As an example, a study

performed by Cho et al. explored four types of fusion peptides: β-galactosidase (LacZ), maltose binding protein (MBP), glutathione-S-transferase (GST), and $(His)_6$-tagged sequence (HTS) for the production and purification of a single chain of human insulin precursor (Cho et al., 2001). The IPTG system was used for protein induction. Various chromatography techniques such as DEAE-Sephacel and Sephadex G-200 gel filtration chromatography, amylose affinity chromatography, glutathione-sepharose 4B affinity chromatography, and nickel chelating affinity chromatography system as a kind of immobilised metal ion affinity chromatography (IMAC) were employed for the purification of expressed proteins. Various recovery yields were obtained for the insulin precursor depending on the type of the fusion protein (Cho et al., 2001). In the present work, periplasmic fractions prepared from cultures grown in two different temperatures 30°C and 37°C were purified with Ni^{2+} column. In order to separate insulin from the DsbA protein, digestion with a specific protease was required. A similar strategy as that described in Novo Nordisk US Patent 7,396,903, presenting a process for preparing insulin compounds with ALP protease, was employed (Bogsnes et al., 2008).

The next step was purification of protein expressed in the form of IBs. pHB1 plasmid was chosen as it showed the best expression level comparing all prepared plasmids. A literature review was performed to design the protocol for purification of proinsulin from inclusion bodies. To increase the yield and recovery of the protein during the purification process, optimisation studies were performed. Optimisation of the refolding reaction by testing various refolding reagents was carried out, resulting in th significant improvement in the yield of refolding reaction. The protocol for purification of the IBs expressed by pHB1 plasmid was established, however final cleavage conditions need to be optimised.

Prepared plasmids can be used to perform further cloning with CPPs and test it for the permeability improvement. However first, the confirmation of proper disulfide bridges formation and biological activity of purified insulin should be carried out.

7.2 Carrier system for insulin approach

7.2.1 Preparation of polyelectrolyte complex nanoparticles

Polymeric nano- and micro-particles have been recently extensively studied as carriers for protein delivery. Among polymeric NPs, NPs composed of polyelectrolytes have attracted particular attention, mainly because of their water soluble character (Hartig et al., 2007). Polyelectrolyte complexes are formed when macromolecules of opposite charge interact (Philipp et al., 1989). The interaction usually involves a polymeric acid or its salt with polymeric base or its salt. Depending on several factors, the complexes can remain in solution, can form compact

precipitate or gel, or can separate to dilute phase and concentrated complex coacervate phase (Guballa, 2012). The main attractive force is electrostatic interactions, however other space oriented intermacromolecular interactions, such as hydrogen bonding and non-oriented factors, such as hydrophobic and/or charge-transfer and/or van der Waals interactions can also play a critical role (Nakajima, 1980, Bekturov and Bimendina, 1981, Tsuchida and Abe, 1982, Kabanov and Zezin 1984, Philipp et al., 1989). The formation and properties of formed polyelectrolyte complexes (PECs) are influenced by several factors, such as: nature, position of ionic groups, molecule size, charge density and concentration of macromolecules, proportion of opposite charges, physicochemical environment (e.g., ionic strength, pH, temperature etc.), but also the method of preparation, in particular order and rate of solutions mixing (Hara and Nakajima, 1978, Nakajima, 1980, Bekturov and Bimendina, 1981,Tsuchida and Abe, 1982, Kabanov and Zezin, 1984, Philipp et al., 1989, Kötz et al., 1996).

Complexation of polymer leads to a loss of translational and conformational entropy of the polymer chain, which needs to be balanced during the complexation. The largest lost in entropy is noted for the first bond formed between the two polymers, but is much smaller for subsequent bonds. The entalpic change however, is nearly constant due to the interaction of the monomeric units. The short range of the interactions (Van der Waals forces) makes a good sterical fit between the polymers if complexation occurs (Guballa, 2012).

The properties of PEC are mostly determined by the degree of the interaction between polymers, especially on their charge densities (Guballa, 2012). Usually, there is a narrow window of physicochemical conditions where the complexes are formed and stay in the form of colloidal dispersion (Lankalapalli and Kolapalli, 2009). The colloidal stability of formed PECs depends on the repulsion between similarly charged particles. Neutralisation of the charge causes formation of aggregates, therefore the charge of the system must be either strongly negative or strongly positive to be stable. NPs that were described in this thesis (composed of AA/P and IC/P) were formed using mild conditions of manufacture, by simply mixing aqueous solutions of polymers at room temperature. Samrento et al., reported polysasccharide based NPs that were loaded with insulin (Sarmento et al., 2006 c). Aqueous solutions of dextran sulphate and chitosan as oppositely charged polymers were used to form the PECs. Particles with a mean diameter of 500 nm and a ZP of approximately −15 mV were produced under optimal conditions of DS:chitosan mass ratio of 1.5:1 at pH 4.8 (Sarmento et al., 2006 c). A similar method was employed to prepare PECs of alginate and chitosan (Saether et al., 2008). PECs were formed in a one-stage process, where one polymer solution was slowly added in a dropwise

manner into the other solution. They were prepared using homogenisers with various speed and diameters. Variations in the properties of polymers and the preparation procedures were studied. It was noted that the net charge ratio between chitosan and alginate, and the molecular weights (MW) of both the alginate and chitosan samples were the most significant parameters that influenced the particle size, ZP and pH. The mixing order also influenced the size of formed PECs, without influencing its ZP and pH (Saether et al., 2008). Many studies focused on the use of chitosan and other polymers for PEC formation. Review published by Hammam summarised the use of chitosan based PECs as potential drug carriers (Hamman, 2010). An investigation was done on the potential of PEC formation between λ-, κ-, and ι-carrageenan and chitosan to form controlled release systems for glucose oxidase. As reported, the complex between chitosan and κ-carrageenan showed high encapsulation efficiencies for glucose oxidase, while having the lowest release rate. Moreover, prepared complex was able to protect the encapsulated glucose oxidase against degradation at pH 1.2 solution, in a chitosanase solution and in pepsin solution (Briones and Sato, 2010, Hamman, 2010). Also study published by Li et al., showed preparation of PECs by using κ-carrageenan and chitosan that could be used for protein drug delivery (BSA was encapsulated as a model protein drug) (Li et al., 2013).

Several factors have been reported for having an impact on the PEC formation. As example, PECs can be reinforced by additional non-covalent crosslinking of chitosan, which is possible with chondroitin sulphate, collagen, PAA, xylan and leads to the formation of semi-interpenetrating polymer networks. Addition of ions to the PEC causes formation of ionically cross-linked systems. Ca^{2+} can be added with alginate or pectin, Al^{3+} can react with carboxymethyl cellulose sodium salt and K^{+} with carrageenan. Chitosan can also be crosslinked ionically, for example by addition to the formation of PEC of e.g. chondroitin sulphate. As reported by Gåserod et al., in the presence of Ca^{2+} ions, chitosan binds about 100 times more to the alginate, while forming microcapsules (Gåserod et al., 1998). As an example, study reported by Sarmento et al., showed preparation of insulin loaded NPs by ionotropic pre-gelation of alginate with calcium chloride followed by complexation between alginate and chitosan. Individual and smaller in size NPs, around 800 nm, were obtained at pH 4.7 with an alginate:chitosan mass ratio of 6:1 (Sarmento et al., 2006 a).

7.2.2 Design of new polyelectrolyte complex-based nanocarriers

7.2.2.1 Polyelectrolyte components of investigated NPs

As mentioned previously, natural polymers show a promising potential for the PEC formation. Two negatively charged (alginian and carrageenan) and one positively

charged natural polyelectrolytes were used in present study as candidates for the formation of polyelectrolyte complex NPs. These NP components had different molecular weights and charge densities. The fundamental properties of the polyelectrolytes used in present study are summarised in Table 7.1.

Table 7.1 *Summary of the properties of the polymers used for the fabrication of polyelectrolyte complex nanoparticles.*

Polyelectrolyte	MW [kDa]	Strength of acidic/ basic groups	Charge density
ALGINIC ACID	147*	Carboxylic group – weak acid	~1*
CARRAGEENAN	~500**	Sulphate group – strong acid	0.96 (κ-car) **
			1.49 (ι-car) **
			2.09 (λ-car) **
PROTAMINE	5.1***	Guanidinium group – strong base	High ***

(* Bowey et al., 2013, ** Hugerth et al., 1997, *** Umerska, 2012).

A range of solutions of three types of alginates with various viscosity (low, medium and high viscosity), three types of carrageenans (λ, κ, and ι) and protamine were characterised for their properties (pH and viscosity). Solutions of each polymer at three various concentrations were prepared. As noted, the viscosity of polymers decreased when the solution concentration decreased (Table 4.1, Table 5.1), however the change in concentration did not affect the viscosity of protamine solutions. Solutions of alginic acid at low and medium viscosity were tested for NP formation with protamine. In case of carrageenan, all three types of polymer were tested for NP formation with protamine, however only iota carrageenan was able to form stable PEC. As reported, an increase in the concentration of polymer used often leads to the increase in the size of formed NPs (Carneiro-da-Cunha et al., 2011), although lowering the concentration of polymer decreases the surface area and final loading capability of prepared NPs. Solutions of polymers and protamine at concentration of 0.1% w/v were used as the most favourable for NPs formation.

7.2.2.2 Physicochemical characteristics of investigated NPs

Screening of several polymer/protamine weight ratios was performed to obtain NPs with the most favourable properties (small particle size, low polydispersity index and different ZP). Each formulation was characterised by the particle size, polydispersity index and zeta potential. Moreover, pH and viscosity of formed nanodispersions were measured. In case of alginates, two types of alginic acid, of low and medium viscosity, were tested at first. The results showed no significant difference between the properties of NPs formed by alginic acid at low (AAL) and medium (AAM) viscosity. Alginic acid with low viscosity (AAL) was selected as the optimum type of

alginates for subsequent studies. Additionally, variations in relation to methods of NPs preparation were investigated: the rate and the sequence of mixing both components. It was established that NPs with smaller particle size and PdI were obtained when protamine solution was added to the stirred aliquot of alginic acid solution, in a fast way.

To facilitate incorporation of insulin into prepared NPs, pH of protamine solution was lowered to 3 (P_pH3), as insulin was completely soluble in this environment (solubility of insulin is 10 mg/ml at pH 2-3, Fischel-Ghodsian et al., 1988). Size of the formed NPs ranged from 100 to 200 nm and had polydispersity values between 0.107 – 0.370, where smaller values corresponded to lower AAL/P_pH3 weight ratios. The zeta potential of formed NPs varied from -62 mV – 20 mV for AAL/P_pH3 NPs. Charge neutralisation occurred at the AAL/P_pH3 weight ratio of 1.

Several reports show the use of alginate in drug delivery, however in most of the cases this polymer is combined with chitosan (a polycation). A study reported by Bowey et al., investigated the preparation of alginate/chitosan microparticles by spray drying. Mean diameter of the product was 2.1±0.3 μm. Analysis of particles by confocal spectroscopy showed that the protein and polymer were concentrated at the surface of the larger particles, while more evenly distributed through smaller particles (Bowey et al., 2013). Another study reported by Bürger et al., showed preparation of chitosan alginate capsules as a delivery system for the delivery of insulin. Preparation of capsules was based on the dropwise addition of alginate dispersion, containing insulin, to the chitosan dispersion, resulting in the capsules with diameters of 2.5±0.2 mm (Bürger et al., 2008). The group of Sarmento investigated alginate-chitosan NPs with insulin, however they were prepared by a pre-gelation method. An increase in particle size from 764 to 2209 nm with decreasing chitosan to alginate mass ratio from 6:1 to 3.3:1 was seen (Sarmento et al., 2006 a). Similar to our study, NPs of alginate and chitosan were formed by addition of 0.1% w/v alginate solution (pH 6.5) under high shear conditions to 0.1% w/v chitosan solution (pH 4.0) (Saether et al., 2008). The size of obtained NPs was 500 nm and greater, reaching values of 2 μm. The charge ratio and the molecular weight were shown to be parameters that affected the particle size, ZP and pH of the mixture. At charge ratios close to one (neutral), the sizes of the largest particles were less reproducible. The smallest particles were obtained by adding one of the two polymer solutions into an excess amount of the other solution and by using forms of the component polymers with low molecular weights (Saether et al., 2008). Li et al., also explored alginate-chitosan NPs prepared by PEC method as a drug delivery system for nifedipine. Described by this group NPs had very small sizes of 20 – 50

nm and were prepared by ionic pre-gelation of alginate core followed by chitosan polyelectrolyte complexation (Li et al., 2008).

In case of carrageenan, all of three types of this polymer were tested for their ability to form PEC NPs with protamine, although only iota carrageenan (IC) was able to form particles in the nano range. The particle size of these NPs was 161 – 320 nm and their polydispersity indices 0.079 – 0.427, with smaller values obtained for lower IC/P_pH3 weight ratios. ZP of described NPs ranged from -43 mV to 19 mV. Aggregates were formed at IC/P_pH3 weight ratio equal to 1. Similarly as in case of alginates, the use of chitosan as a positively charged polymer was reported to form complexes with carrageenans. However, it was reported that the nature or type of carrageenan considerably influenced the characteristics of the gels that were formed with chitosan (Shumilina and Shchipunov, 2002). It was shown that the mechanical strength of PEC gels formed between chitosan and different carrageenans were in the order of λ>ι>κ carrageenan, although the latter two formed stronger gels mainly due to the formation of more cross-links as a result of their double helix secondary structures, these gels were also more brittle. Moreover, the gels obtained for ι- and κ-carrageenan were temperature sensitive, due to their helix-coil conformational transitions in their molecules (Shumilina and Shchipunov, 2002). An investigation was performed on the potential to form PECs between carrageenan and chitosan (Li et al., 2013). The PECs were prepared by a polyplex formation at a high ionic strength (using NaCl) of solutions method and bovine serum albumin (BSA) as a model protein was encapsulated to study the potential for pH responsive oral drug delivery system (Li et al., 2013). Another study was performed on the preparation and characterisation of insulin entrapped into lectin-functionalised carboxymethylated κ-carrageenan microparticles (Leong et al., 2011). The encapsulation of insulin was performed by an ionic gelation technique. The size of the formed PECs was more than 1 mm.

7.2.2.3 Stability studies of NPs

The selection of candidates for further studies was based on their particle size, polydispersity and charge (NPs with the smallest size and PdI, having various surface charge (ZP)). Six types of AAL/P_pH3 (5, 2.5, 1.5, 0.5, 0.3 and 0.2 AAL/P_pH3 weight ratio) and four types of IC/P_pH3 NPs (4, 2, 0.5 and 0.2 IC/P_pH3 weight ratio) were selected for further stability studies in media at various pH. The colloidal stability of NPs was strongly dependent on the type of NPs, their composition and ZP. Summary of stability of NPs in various media is presented in Table 7.2 for AAL/P_pH3 NPs and in Table 7.3 for IC/P_pH3 NPs.

Negatively charged NPs were generally more stable compared to the positively charged NPs. Negatively charged AAL/P_pH3 NPs were stable in most of the media.

Instability and formation of aggregates occurred at very low pH (in 0.1 M and 0.01 M HCl). The poor stability of negatively charged NPs at low pH could be explained by the properties of alginic acid. Similarly to ionically cross-linked hydrogels, PECs exhibits pH-sensitive swelling under acidic conditions (Berger et al., 2004). As the pH value changes the charge balance inside formed PECs and therefore the degree of interaction between the two polymers is modified and swelling occurs mainly because of dissociation of the complex. In an acidic medium, the polyacid (carboxylate, $-COO^-$ of alginate) is perhaps neutralised due to the free amine groups of protamine. Their mutual repulsion and the entry of water together with counterions neutralising these charges cause swelling (Sankalia et al., 2007). As reported in the study performed by Sankalia et al., at pH 2.0 the ionic interaction between chitosan and alginate was greatly reduced, and folding of alginate was observed with increased micropore size, which allowed the greater part of the dissolution medium to enter with counterions. However at pH 6.8 chitosan remained protonated and formed much stronger network with alginate with small micropore size that restricted the entry of larger counterions (Sankalia et al., 2007). Similar behaviour was observed in the present work, however an increase in pH of the tested medium caused instability of positively charged NPs, which formed aggregates directly after adding the buffer. Ionic interactions between positively charged groups of protamine and ionic groups present in the media often resulted in neutralisation of the charge and formation of aggregates. Similar behaviour was observed for all types of positively charged NPs (AAL/P_pH3 and IC/P_pH3). Negatively charged IC/P_pH3 NPs showed very good stability in all media tested (Table 9.3). Lowering pH did not have an impact on their stability as in case of AAL/P_pH3 NPs. Study performed by Capron et al., showed *in vitro* gastric stability of carrageenan (Capron et al., 1996). They compared two types of carrageenans: κ- and ι-, showing that ι-carrageenan was more stable under gastric conditions.

Table 7.2 *Stability of* ***AAL/P_pH3*** *NPS in different media.*

AAL/P_pH3 weight ratio	Stability in medium							
	-	0.1 M HCl	0.01 M HCl	0.1 ACET pH 4.5	0.1 M HEPES pH 6.5	0.01 M PBS	0.1 M NaCl	0.01 M NaCl
5	●^{1}●^{2}●^{3}●^{4}	●▲	▲	●●●●	●●●●	●●●●	●●●●	●●●●
2.5	●●●●	●▲	▲	●●●●	●●●●	●●●●	●●●●	●●●●
1.5	●●●●	●▲	▲	●●●●	●●●●	●●●●	●●●▲	●●●●
0.5	●▲	●▲	●●	▲	●▲	▲	▲	▲
0.3	●●●●	●▲	●●	▲	●▲	▲	▲	▲
0.2	●●●●	●▲	●●	▲	●▲	▲	▲	●▲

ACET – acetate buffer. Appearance key: ● – dispersion of NPs, ▲ – aggregates appeared.
Symbol position: stability of NPs in medium after: 1 – preparation, 2 – 1 day of storage, 3 – 2 days of storage, 4 – 3 days of storage.

Table 7.3 *Stability of* ***IC/P_pH3*** *NPS in different media.*

IC/P_pH3 weight ratio	Stability in medium								
	-	0.1 M HCl	0.01 M HCl	0.1 ACET pH 4.5	0.1 M HEPES pH 6.5	0.1 M PBS	0.01 M PBS	0.1 M NaCl	0.01 M NaCl
4	●^{1}●^{2}●^{3}●^{4}	●●●●	●●●●	●●●●	●●●●	●●●●	●●●●	●●●●	●●●●
3	●●●●	●●●●	●●●●	●●●●	●●●●	●●●●	●●●●	●●●●	●●●●
2	●●●●	●●●●	●●●●	●●●●	●●●●	●●●●	●●●●	●●●●	●●●●
0.5	●▲	▲	●▲	▲	●▲	●▲	▲	▲	●▲
0.3	●●▲	▲	●▲	▲	●▲	●▲	▲	▲	●▲
0.2	●●●▲	▲	●▲	▲	●▲	●▲	▲	▲	●▲

ACET – acetate buffer. Appearance key: ● – dispersion of NPs, ▲ – aggregates appeared.
Symbol position: stability of NPs in medium after: 1 – preparation, 2 – 1 day of storage, 3 – 2 days of storage, 4 – 3 days of storage.

7.2.2.4 Incorporation of insulin into developed NPs and *in vitro* characterisation of formed NPs

7.2.2.4.1 Association efficiency of insulin into investigated NPs

One of the features of a successful nanoparticulate system that could be used as a delivery tool is a high drug loading capacity, which would reduce the amount of the polymer carrier required for delivery of the drug in the body. Loading of the drug can be done by two methods: incorporating the drug at the time of nanoparticles production (incorporation method) or adsorbing/absorbing the drug after formation of nanoparticles by incubating the carrier with a concentrated drug solution (adsorption/absorption technique) (Moharaj and Chen, 2006). Loading the drug and its entrapment efficiency strongly depends on the solid-state drug solubility in the matrix material or polymer, which is related to the polymer composition, its molecular weight, the drug polymer interaction and the presence of drug functional groups (Govender et al., 1999, Govender et al., 2000, Panyam et al., 2004). As reported, the greatest loading efficiency can be achieved when it is loaded near its isoelectric point, as it has minimum solubility and maximum adsorption (Calvo et al., 1997).

Four formulations from both types of prepared NPs (AAL/P_pH3 and IC/P_pH3) were tested for insulin association. Insulin was associated at the stage of NPs preparation (incorporation method) by dissolving the peptide in protamine solution at pH 3. Insulin dissolved in a medium with pH below its isoelectric point (pI of insulin is 5.3) acquired positive charge, which further facilitated its interaction with negatively charged groups of polymer. Incorporation of insulin into NPs resulted in only small changes in the particle size, PdI and ZP of formed NPs (Figure 6.1.1-6.1.3 for AAL/P_pH3 NPs and Figure 6.2.1-6.2.3 for IC/P_pH3 NPs). Small increase in the particle size and PdI of negatively charged NPs was observed, while the charge of positively charged NPs increased.

There was a difference in the association efficiency (AE) of insulin for negatively and positively charged NPs. Almost 100% of AE was obtained for negatively charged NPs when the dose of insulin loaded was 100 µg/ml. Similar values were obtained when 500 µg/ml of insulin was incorporated into prepared NPs. Strong interactions between the negative groups of polymers (carboxyl of alginate and sulphate of carrageenan) and positively charged insulin dissolved in protamine solution at pH 3 facilitated its incorporation and resulted in excellent AEs. Smaller amount of insulin were associated with positively charged NPs, with greater AE obtained for AAL/P_pH3 NPs (almost 90% of insulin was associated when both peptide concentrations were used (100 and 500 µg/ml)). AEs for positively charged IC/P_pH3 NPs were 54% - 57% for 100 µg/ml of insulin loaded and 18% - 21% for 500 µg/ml of insulin loaded.

Alginate microparticles prepared by spray drying demonstrated the encapsulation efficiency of insulin of 38.2±9.5% (Bowey et al., 2013). Loading efficiency of 56.7% was reported for alginate-chitosan microspheres loaded with insulin, prepared by membrane emulsification technique in combination with ion (Ca^{2+}) and polymer (chitosan) solidification (Zhang et al., 2011). Study performed by Silva et al. demonstrated encapsulation of insulin into reinforced alginate microspheres prepared by internal gelation (Silva et al., 2006). The encapsulation efficiency of insulin into those microspheres varied from 14% to 100%, reaching a maximum value when cellulose sulphate and dextran sulphate were incorporated in the alginate matrix. Relatively high association efficiency of 85% was obtained for polysaccharide NPs composed of dextran sulphate and chitosan (Sarmento et al., 2006 c). Encapsulation of insulin into lectin-functionalised carboxymethylated κ-carrageenan microparticles prepared by ionic gelation technique was 94.2±2.6% (Leong et al., 2011). Wu et al., reported investigations into water soluble chitosan microparticles loaded with insulin, prepared by PEC method (Wu et al., 2011). It was shown that water-soluble chitosan/insulin/tripolyphosphate (TPP) mass ratio played an important role in microparticles formation. The association efficiency of those particles was 48.28±0.90% (Wu et al., 2011). Therefore, in this thesis an important improvement has been made in terms of achievement of very high insulin loading in NPs approaching 100%.

7.2.2.4.2 *In vitro* release of insulin in media at various pH

The release profile of the drug is another very important consideration that must be tested for drug polymer formulations, as it will influence the proposed application and sustained drug delivery. There are several factors that have an impact on the release profile of the drug, which are: solubility of the drug, desorption of the surface bound/adsorbed drug, drug diffusion through the polymer matrix, NP matrix erosion/degradation and combination of erosion diffusion process (Kumari et al., 2010). The kinetics of the drug release depends upon the size of NPs and association efficiency of the drug. Larger particles have a smaller initial burst release than smaller particles, as rapid initial release is mainly attributed to weakly bound or adsorbed drug on the surface (Hans and Lowman, 2002, Mohapatro et al., 2008).

In vitro release of insulin from NPs loaded with 100 and 500 μg/ml of insulin in media at various pH was tested in this work. Release profiles and kinetics of insulin release are presented in details in Chapter 6 of this thesis. Table 7.4 summarises percentage of insulin released from all types of NPs studied, divided into negatively and positively charged, as the NPs charge and composition was one of the factors that had an impact on the final amount of insulin released. The rates of insulin release are summarised in Table 7.5.

Similar release profiles were obtained for all formulations of positively charged NPs, with 90 – 100% of initial quick release in all media tested. As insulin was first dissolved in the protamine solution and then added to the polymer solution, it may be hypothesised that the peptide is mostly localised on the surface of NPs. However in case of negatively charged NPs, different release profiles were obtained depending on pH of the medium and the amount of insulin loaded into NPs. As presented in Table 7.4 the amount of insulin released from NPs loaded with 500 µg/ml was much greater compared to the lower dose, even if association efficiency was similar. It is hypothesised here that different distribution of insulin within NPs with the high peptide content compared to the 100 µg/ml insulin–containing NPs can be responsible for such behaviour. A larger amount of insulin would appear at or close to the NP surface due to NP matrix saturation.

Another factor that had an impact on the amount of released insulin was pH of the release medium. As reported, both polymers are not stable as solutions at low pH and form gels in this environment, which stops entrapped insulin from being released. Slower and more sustained release from these types of NPs was obtained. To further explore the localisation of insulin and other NP components fluorescent labelling of the polymer and insulin is suggested as a future work. Zhang et al. evaluated release of insulin from alginate-chitosan microparticles prepared by membrane emulsification techniques. As reported, only 5% of insulin was released from microspheres after 2 hours of incubation in simulated intestinal fluid (pH 1.2), while after transferring to the simulated intestinal fluid (pH 6.8), 32% of the initial amount of insulin was released (Zhang et al., 2011). Insulin release behaviour from dextran sulphate (DS)/chitosan NPs in different aqueous pH buffers was evaluated by Sarmento et al. As reported by this research group, no significant amount of insulin (4%) was released from NPs placed at pH 1.2, 4.5 and 5.2, while at pH 6.8 insulin release resented sustained release profile with 40% of insulin being released within the first 15 minutes following a lower release rate. As explained by these researchers, at pH lower than pI of insulin (5.3), (Brange, 1987) insulin presents an overall positive charge that is able to interact with the polyanionic charge of NPs provided they are negatively charged. At this pH range, the strong electrostatic interactions between insulin and negatively charged polymer (in this case DS) may retain insulin in the DS/chitosan network. Additionally, described NPs appear to preserve their physical integrity, which contributed to the smaller amount of insulin released. However, 70% of insulin was released from characterised NPs at pH 6.8 after 24 h of study. As explained, the initial stage of insulin release at pH 6.8 is attributed to the insulin located at the surface on the NPs and the remainder of the unreleased insulin is probably entrapped within the NPs. This study suggests that *in*

vitro release behaviour of insulin from DS/chitosan NPs was according to a dissociation mechanism (Sarmento et al., 2006 c). The same research group investigated the effect of DS:chitosan mass ratio on the cumulative release of insulin at pH 6.8. Obtained results showed that the increase in the DS:chitosan mass ratio form 1:1 to 2:1 decreased the insulin cumulative release, suggesting the main role of negatively charged polymer, in this case DS, on the insulin entrapment and as well on the sustained effect of insulin release (Sarmento et al., 2006 c). PECs particles composed of κ-carrageenan and chitosan were investigated as a system for drug delivery (Li et al., 2013). BSA was loaded into formed PECs as a model protein and its release was tested in both SGF (pH 1.2) and SIF (pH 7.5). As reported, the prepared PECs showed sensitivity to pH changes. A typical controlled release of BSA from the PEC (180 μg of BSA from 3 mg of PEC) was obtained in SIF, which was due to the significant swelling and disintegration of PEC, but a little amount of BSA was released in the SIF, confirming acidic stability of prepared PECs (Li et al., 2013). Gan and Wang proposed the following protein release mechanisms: (a) desorption of the protein molecules from the surface of particles, (b) diffusion through the swollen PEC, and (c) disintegration of the PEC (Gan and Wang, 2004). In our case the release of the protein was mainly dependent on the NP composition. Fast and practically complete insulin release was observed from positively charged NPs, perhaps as a result of protein desorption from the surface of NPs and additional disintegration of PEC in ionic media. However, in case of negatively charged NPs, smaller amount of released insulin was due to its diffusion through swollen PEC.

Table 7.4 *Release of insulin from NPs to buffers at various pH.*

Polymer/protamine weight ratio		HCl pH 2.0		Acetate buffer pH 4.5		PBS pH 7.4		FaSSIF
		100 µg/ml	500 µg/ml	100 µg/ml	500 µg/ml	100 µg/ml	500 µg/ml	100 µg/ml
Negatively charged NPs	5 AAL/P_pH3	45%[1] – 84%[2]	76% – 85%	93% – 92%	96% – 100%	90% – 94%	96% – 95%	103% – 88%
	4 IC/P_pH3	21% – 50%	87%– 82%	97% – 97%	100% – 96%	28% – 40%	95% – 97%	87% – 88%
	2 IC/P_pH3	13% – 31%	66% – 55%	47% – 49%	96% – 72%	3% – 3%	76% – 31%	100% – 79%
Positively charged NPs	0.2 AAL/P_pH3	98% – 101%	100% – 100%	94% – 101%	98% – 102%	96% – 103%	95% – 96%	96% – 100%
	0.2 IC/P_pH3	91% – 107%	98% – 98%	99% – 102%	96% – 98%	96% – 97%	95% – 98%	97% – 99%

Appearance key: 1 – % of insulin released after 10 min, 2 – % of insulin released after 6 h of study.

Table 7.5 *The rate of insulin release (k^{-1})) from NPs to buffers at various pH, obtained by fitting the experimental data to the first order equation.*

Polymer/protamine weight ratio		HCl pH 2.0		Acetate buffer pH 4.5		PBS pH 7.4		FaSSIF
		100 µg/ml	500 µg/ml	100 µg/ml	500 µg/ml	100 µg/ml	500 µg/ml	100 µg/ml
Negatively charged NPs	5 AAL/P_pH3	0.060±0.012	0.317±0.019	0.311±0.075	0.365±0.062	0.272±0.094	0.454±0.030	0.034±0.015
	4 IC/P_pH3	0.045±0.013	0.276±0.063	0.361±0.111	0.349±0.240	0.176±0.047	0.408±0.088	0.233±0.017
	2 IC/P_pH3	0.063±0.015	0.311±0.116	0.211±0.142	0.068±0.024	0.018±0.020	0.027±0.007	0.310±0.019
Positively charged NPs	0.2 AAL/P_pH3	0.375±0.052	0.419±0.072	0.247±0.069	0.337±0.074	0.211±0.066	0.349±0.040	0.361±0.068
	0.2 IC/P_pH3	0.022±0.036	0.389±0.082	0.263±0.079	0.304±0.048	0.235±0.115	0.346±0.038	0.395±0.113

7.2.2.4.3 Cytotoxicity of NPs and transport of insulin *in vitro*

Viability of Caco-2 cells was strongly dependent on the type of NPs used. Both types of negatively charged NPs (AAL/P_pH3 and IC/P_pH3) did not have an impact on the cell proliferation after 72 h of incubation with NPs at concentration of 0.1 - 0.5 mg/ml. Moreover, a small increase (5-15%) in the cell viability was observed. In case of positively charged NPs, which contained more protamine than polymer, cell viability was concentration depended. 45 – 95% of cells remained viable after 72 h of incubation with positively charged AAL/P_pH3 NPs at concentrations of 0.5 – 0.1 mg/ml. In case of positively charged IC/P_pH3 NPs at concentrations of 0.5 – 0.1 mg/ml, 51 – 91% remained viable after 72 h of incubation. The toxic effect might be explained by the presence of free polycation, rather than polycation bound to the polymer. As described previously, positively charged NPs formed aggregates in the culture medium, which may have caused release of free P contributing to the its toxic effect. Umerska (2012) investigated the toxic effect of free P showing that IC_{50} of protamine was 0.24±0.01 mg/ml. Since, in the current work, only a narrow range of NP concentrations was tested, it was difficult to calculate accurate IC_{50} values for these samples. An estimated approximate value of IC_{50} for positively charged NPs is around 0.4 mg/ml, which is a two-times greater compared to the value for free P. Interactions of P with negatively charged polymer (AAL or IC) might lower the toxic effect of P.

In vitro transport of insulin dissolved in different solutions and loaded into developed NPs through Caco-2 monolayers was investigated. It was observed that the presence of protamine in the formulation had an impact on the initial transport rate, as greater amounts of insulin were transported within first hour of the study from two formulations: insulin dissolved in protamine solution and positively charged NPs (AAL/P_pH3 and IC/P_pH3 NPs containing more protamine than polymer) in comparison to insulin solution used as a standard. As reported, protamine has the ability to open tight junctions and facilitate drug transport (Reynolds, 2005, Vishnevskaia et al., 2013), which might suggest the greater amount of insulin transported. It was observed that a larger amount of fluorescein (used as a paracellular transport marker) appeared in the acceptor in the first 2 hours of the study for insulin dissolved in protamine solution and for positively charged NPs, consistent with the mechanism of opening tight junctions. Comparable amounts of insulin were transported from negatively charged NPs and insulin standard within the first hour of the study. The quantity of the peptide transported from negatively charged NPs at 6 hours of the experiment was however smaller comparing to the reference (insulin solution) but greater than for the sample containing insulin dissolved in P solution and for positively charged NPs. To further investigate the

mechanism of insulin transport through Caco-2 monolayer, fluorescent labelling of tested NPs components and insulin should be considered as future work.

Developed and described in this thesis nanoparticles show promising characteristics and can be considered as potential carriers for oral insulin delivery. Advantages of the developed system can be summarised as follows:

- Nanoparticle components: natural polyelectrolytes – biocompatible, biodegradable, non-toxic, safe to use (already used in the food/pharma industry), cheap and readily available
- Simplicity of preparation by polyelectrolyte complexation, using aqueous solutions of constituents without any organic solvents and other additives
- Non-toxic behaviour in biological *in vitro* tests
- Very high loading efficiency
- Polymer/protamine weigh ratio and pH of release medium modulated release (*in vitro*) of insulin

7.3 Main findings

- Five plasmids with insulin were designed and successfully prepared
- Induction of protein expression by IPTG and auto-induction system was investigated
- Prepared plasmids were able to express protein in various forms
- The highest expression yield was obtained for pHB1, however the protein was expressed in the form of inclusion bodies
- Fusion with DsbA increased the yield of protein expressed in the periplasm
- The temperature played an important role in the protein expression with the optimum between 22 - 28°C
- Optimisation of purification protocol for expressed protein was investigated
- Improvement in the yield of refolding reaction was obtained by testing different reagents
- Prepared plasmids can be further used for fusion with cell penetrating peptides
- Polyelectrolyte complex NPs were successfully formed between both types of alginates tested (AAL, AAM) and P, and also between three types of carrageenans (IC, LC, KC) and P
- NPs composed of alginic acid at low viscosity/protamine and iota-carrageenan/protamine were the smallest and most homogenous NPs formed
- The formation and properties of NPs were dependent on many variables, such as: the type of polyelectrolyte tested, the mass mixing ratio, the concentrations of polymer used and the method of NP preparation

- Properties of NPs made of protamine solution at pH 3 did not differ from those prepared using protamine solution at native pH (pH 5.8)
- Both, negatively and positively charged NPs were formed for both polymers (AAL and IC) tested
- Colloidal stability of NPs in media at various pH strongly dependent on their zeta potential
- Negatively charged NPs were stable in most of the media (lower stability was noticed at low pH), while positively charged NPs formed aggregates in all of the media tested
- Negatively charged NPs were non-cytotoxic, while positively charged NPs containing more protamine were cytotoxic at concentration of 0.2 mg/ml
- Association efficiency (AE) depended on the composition of NPs and almost 100% AE values obtained for negatively charged NPs
- Release of insulin from NPs in media at various pH was strongly dependent on the NP composition and pH of the medium, with complete and fast release (within the first 10 minutes of study) from positively charged NPs
- Release of insulin from negatively charged NPs was dependent on the type of NPs and environmental pH with the smallest quantity of the peptide released from NPs at IC/P_pH3 weight ratio of 2
- Amount and the rate of insulin transported through Caco-2 monolayers was dependent on the type of NPs and solution in which the peptide was dissolved
- Greater amounts of insulin were transported in the first hour of the study from insulin dissolved in 0.1% w/v solution of protamine and from positively charged NPs

7.4 Future work:

- Use an auto-induction system and lower temperatures for expression of protein in the periplasm from pMD2 plasmid
- Further optimisation of purification protocol for pMD2 plasmid
- Confirmation of native structure of purified insulin
- Selection of appropriate cell penetrating peptide and its cloning its sequence into selected plasmid
- Expression and purification insulin fused with CPP
- Fluorescent labelling of polymers (alginate, carrageenan) and insulin (FITC-insulin) to test their interactions and the mechanism of insulin transport through Caco-2 cells
- Proteolytic cleavage with enzymes: pepsin, trypsin and carboxipeptidase B

- *In vivo* animal studies on oral administration of insulin from NPs (peptide biodistribution, pharmacodynamics and pharmacokinetics)
- FTIR studies on molecular interactions between the polyelectrolytes and insulin
- Morphology studies (e.g. TEM, SEM and AFM) of NPs
- Evaluation of mucoadhesive properties of NPs

CHAPTER 8

REFERENCES

Abhinav, K., Lal, P.J., Amit, J., Vishwabhan, S., Review on niosomes as novel drug delivery system, 2011; International Journal of Pharmacy, 2(5): 61-65

Access Science, Insulin, http://www.accessscience.com/overflow.aspx?SearchInputText=Biosynthesis&ContentTypeSelect=10, accessed on 10/07/2013

Agulhon, P., Robitzer, M., David, L., Quignard, F., Structural Regime Identification in Ionotropic Alginate Gels: Influence of the Cation Nature and Alginate Structure, 2012; Biomacromolecules, 13: 215−220

Ahmad, A., Othman, I., Zaini, A., Chowdhury, E.H., Oral nano-insulin therapy: current progress on nanoparticle-based devices for intestinal epithelium-targeted insulin delivery, 2012; Journal of Nanomedicine & Nanotechnology, S4:007

Akiyama, Y., Kamitani, S., Kusukawa, N., Ito, K., *In vitro* catalysis of oxidative folding of disulfide-bonded proteins by the *Escherichia coli* dsbA (ppfA) gene product, 1992; The Journal of. Biological Chemistry, 31: 22440–22445

Al-Tabakha, M.M., Arida, A.I., Recent challenges in insulin delivery systems: A review, 2008; Indian Journal of Pharmaceutical Sciences, 70(3): 278-286

Alberti, K.G.M.M., Zimmet, P., Defronzo, R.A., Keen, H., Insulin therapy, International Textbook of Diabetes Mellitus (2nded), 1997; John Wiley & Sons, New York, 899–928

Alberti, K.G.M.M., Zimmet, P.Z., Definition, diagnosis and classification of diabetes mellitus its complications. Part 1: Diagnosis and Classification of Diabetes Mallitus Provisional Report of a WHO Consultation, 1998; Diabetic Medicine, 15: 539–553

Allan, F.N., Diabetes before and after insulin, 1972; Medical History, 16(3): 266-273

Andriamanantoanina, H., Rinaudo, M., Relationship between the molecular structure of alginates and their gelation in acidic conditions, 2010; Polymer International, 59: 1531–1541

Asada, H., Douen, T., Mizokoshi, Y., Fujita, T., Murakami, M., Yamamoto, A., Muranishi, S., Stability of acyl derivatives of insulin in the small intestine: Relative importance of insulin association characteristics in aqueous solution, 1994; Pharmaceutical Research, 11(8): 1115-1120

Asada, H., Douen, T., Mizokoshi, Y., Fujita, T., Murakami, M., Yamamoto, A., Muranishi, S., Absorption characteristics of chemically modified insulin derivatives with various fatty acids in the small and large intestine, 1995; Journal of Pharmaceutical Sciences, 84: 682-687

Augst, A.D., Kong, H.J., Mooney, D.J., Alginate hydrogels as biomaterials, 2006; Macromolecular Bioscience, 6(8): 623-633

Avadi, M.R., Sadeghi, A.M.M., Dounighi, N.M., Dinarvand, R., Atyabi, F., Rafiee-Tehrani, M., *Ex Vivo* Evaluation of Insulin Nanoparticles Using Chitosan and Arabic Gum, 2011; International Scholarly Research Network Pharmaceuticals, 1-6

Bai, J.P., Chang, L.L., Transepithelial transport of insulin: I. insulin degradation by insulin-degrading enzyme in small intestinal epithelium, 1995; Pharmaceutical Research, 12(8): 1171-1175

Bai, J.P., Chang, L.L., Effects of enzyme inhibitors and insulin concentration on transepithelial transport of insulin in rats, 1996; The Journal of Pharmacy and Pharmacology, 48(10): 1078-1082

Beals, J.M., De Filippis, M.R., Kovach, P.M., Insulin. In: Crommelin D.J.A, Sindelar R.D., Meibohm B (eds.). Pharmaceutical Biotechnology: Fundamentals and Applications, 3rd edition, 2008; Informa Healthcare: New York, 265–80

Bekturov, E.A., Bimendina, L.A., Interpolymer complexes, 1981; Advances in Polymer Science, 41: 99–147

Belzer, C., de Vos, W.M., Microbes inside--from diversity to function: the case of Akkermansia, 2012; Multidisciplinary Journal of Microbial Ecology, 6(8): 1449-1458

Berger, J., Reist, M., Mayer, J.M., Felt, O., Gurny, R., Structure and interactions in chitosan hydrogels formed by complexation or aggregation for biomedical applications, 2004; European Journal of Pharmaceutics and Biopharmaceutics, 57: 35–52

Berginc, K., Zakelj, S., Levstik, L., Ursic, D., Kristl, A., Fluorescein transport properties across artifcial lipid membranes Caco-2 cell monolayers and rat jejunum, 2007; European Journal of Pharmaceutics and Biopharmaceutics, 66: 281–285

Berkmen M., Boyd, D., Beckwith J., Disulfide bond formation in the periplasm, In: Ehrmann M, editor. The periplasm., 2007; Washington, DC: ASM Press., 122-140

Berth, G., Vukovic, J., Lechner, M.D., Physicochemical characterisation of carrageenans- a critical reinvestigation, 2008; Journal of Applied Polymer Science, 110: 3508-3524

Bessette, P.H., Cotto, J.J., Gilbert, H.F., Georgiou, G., *In vivo* and *in vitro* function of the *Escherichia coli* periplasmic cysteine oxidoreductase DsbG, 1999; The Journal of Biological Chemistry, 274: 7784–7792

Bhatnagar, S., Srivastava, D., Jayadev, M.S.K., Dubey, A.K., Molecular variants and derivatives of insulin for improved glycemic control in diabetes, 2006; Progress in Biophysics and Molecular Biology, 91: 199–228

Bies, C., Lehr, C., Woodley, J.F., Lectin-mediated drug targeting: History and Applications, 2004; Advanced Drug Delivery Reviews, 56(4): 425-435

Blattner, F.R., Plunkett, G., Bloch, C.A., Perna, N.T., Burland, V., Riley, M., Collado-Vides, J., Glasner, J.D., Rode, C.K., Mayhew, G.F., Gregor, J., Davis, N.W., Kirkpatrick, H.A., Goeden, M.A., Rose, D.J., Mau, B., Shao, Y., The complete genome sequence of *Escherichia coli* K-12, 1997; Sciences, 2777(5331):1453-1462

Bogsnes, A., Christensen, I., Balschmidt, P., Process for preparing insulin compounds. Novo Nordisk, 2008; US 7396903

Boury, F., Marchais, H., Proust, J. E., Benoit, J.P., Bovine serum albumin release from poly(alpha-hydroxy acid) microspheres: effects of polymer molecular weight and surface properties, 1997; Journal of Controlled Release, 45: 75-86

Boutsikaris, G.Ch., Establishing a Novel Laboratory Scale Expression System for Recombinant Human Insulin in Bacteria, MSc Thesis TCD, 2009;

Bowey, K., Swift, B.E., Flynn, L.E., Neufeld, R.J., Characterisation of biologically active insulin-loaded alginate microparticles prepared by spray drying, 2013; Drug Development and Industrial Pharmacy, 39(3): 457-465

Braddock, M., Chambers, A., Wilson, W., Esnouf, M.P., Adams, S.E., Kingsman, A.J., Kingsman, S.M., HIV1 TAT "activates" presynthesised RNA in the nucleus, 1989; Cell, 58: 269-279

Brader, M., Dunn, M. F., Insulin Hexamers: New Conformations and Applications, 1991; Trends in Biochemical Sciences, 16: 341 -345

Brange, J., Galenics of Insulin: The Physicochemical and Pharmaceutical Aspects of Insulin, Insulin Preparations, 1987; Springer-Verlag

Bretzel, R., Jahr, H., Eckhard, M., Martin, I., Winter, D., Brendel, M., Islet cell transplantation today, 2007; Langenbeck's Archives of Surgery, 392(3): 239-253

Briones, A.V., Sato, T., Encapsulation of glucose oxidase (GOD) in polyelectrolyte complexes of chitosan-carrageenan, 2010; Reactive and Functional Polymers, 70: 19–27

British Pharmacopoeia, 2012; London: HMSO

Bürger, C., Maffezzolli, S., Clasen, P., Lucinda-Silva, R.M., Rodrigues, C.A., Chitosan-alginate capsules as oral delivery system for insulin: studies *in vitro* and *in vivo*, 2008; Rev. Journal of Basic and Applied Sciences, 29(3): 239-244

Calvo, P., Remunan-Lopez, C., Vila-Jato, J.L., Alonso, M.J., Novel hydrophilic chitosan-polyethylene oxide nanoprticles as protein carriers, 1997; Journal of Applied Polymer Science, 63: 125-132

Campo, V.L., Kawano, D.F., Braz da Silva J.R.D., Carvalho, I., Carrageenans: biological properties, chemical modifications and structural analysis - a review, 2009; Carbohydrate Polymers, 77: 167-180

Capron, I., Yvon, M., Muller, G., *In-vitro* gastric stability of carrageenan, 1996; Food Hydrocolloids, 10(2): 239-244

Carino, G.P., Mathiowitz, E., Oral insulin delivery, 1999; Advanced Drug Delivery Reviews, 35: 249-257

Carneiro-da-Cunha, M.G., Cerqueira, M.A., Souza, B.W.S., Teixeira, J.A., Vicente, A.A., Influence of concentration, ionic strength and pH on zeta potential and mean hydrodynamic diameter of edible polysaccharide solutions envisaged for multinanolayered films production, 2011; Carbohydrate Polymers, 85: 522–528

Carrier, R.L., Miller, L.A., Ahmed, I., The utility of cyclodextrins for enhancing oral bioavailability, 2007; Journal of Controlled Release, 123(2): 78-99

Carter, P., Kelly, R.F., Rodrigues, M.L., Rodrigues M.L., Snedecor, B., Covarrubias, M., Velligan, M.D., Wong, W.L.T., Rowland, A.M., Kotts, C.E., Carver, M.E., Yang, M., Bourell, J.H., Shepard, H.M., Henner, D., High level *Escherichia coli* expression and production of a bivalent humanised antibody fragment, 1992; Biotechnology, 10: 163-167

Castellanos-Serra, L.R., Hardy, E., Ubieta, R., Vispo, N.S., Fernandez, C., Besada, V., Falcon, V., Gonzales, M., Santos, A., Perez, G., Silva, A., Herrera, L., Expression and folding of an interleukin-2-proinsulin fusion protein and its conversion into insulin by a single step enzymatic removal of the C-peptide and the N-terminal fused sequence, 1996; Federation of European Biochemical Societies Letters, 378: 171–176

Chalasani, K.B., Russell-Jones, G.J., Yandrapu, S.K., Diwan, P.V., Jain, S.K., A novel vitamin B12-nanosphere conjugate carrier system for peroral delivery of insulin, 2007; Journal of Controlled Release, 117(3): 421-429

Chan, S.J., Weiss, J., Konrad, M., White, T., Bahl, C., Yu, S.D., Marks, D., Steiner, D.F., Biosynthesis and periplasmic segregation of human proinsulin in *Escherichia coli*, 1981; Proceedings of the National Academy of Sciences USA, 78: 5401–5405

Chance, R., Glazer, N., Wishner, K., Insulin Lispro (Humalog), 1999; Biopharmaceuticals, an Industrial Perspective, 149-171

Chang, M., Chou, J.C., Chen, C.P., Liu, B.R., Lee, H.J., Noncovalent protein transduction in plant cells by macropinocytosis, 2007; New Phytol., 174: 46-56

Chang, S-G., Kim, D-Y., Choi, K-D., Shin, J-M., Shin, H-Ch., Human insulin production from novel mini-proinsulin which has high receptor-binding activity, 1998; Biochemical Journal, 329: 631-635

Chen, C., Snedecor, B., Nishihara, J.C., Joly, J.C., McFarland, N., Andersen, D.C., Battersby, J.E., Champion, K.M., High-level accumulation of a recombinant antibody fragment in the periplasm of *Escherichia coli* requires a triple-mutant (degP prc spr) host strain, 2004; Biotechnology and Bioengineering, 85: 463-474

Chen, M.C., Sonaje, K.J., Sung, H.W., A review of the prospects for polymeric nanoparticle platforms in oral insulin delivery, 2011; Biomaterials, 32(36): 9826-9838

Chen, Y.J., Liu, B.R., Dai, Y.H., Lee, C.Y., Chan, M.H., Chen, H.H., Chiang, H.J., Lee, H.J., A gene delivery system for insect cells mediated by arginine-rich cell-penetrating peptides, 2012; Gene, 493: 201-210

Chien, Y.W., Human Insulin: Basic Sciences to Therapeutic Use, 1996; Drug development and Industrial Pharmacy, 22(8): 753-789

Cho, C.W., Park, S.H., Nam, D.H., Production and purification of single chain human insulin precursors with various fusion peptides, 2001; Biotechnology and Bioprocess Engineering, 6: 144–149

Choi, J.H., Lee, S.Y., Secretory and extracellular production of recombinant proteins using *Escherichia coli*, 2004; Applied Microbiology and Biotechnology, 64: 625-635

Choi, Y.S., Lee, J.Y., Suh, J.S., Kwon, Y.M., Lee, S.J., Chung, J.K., Lee, D.S., Yang, V.C., Chung, C.P., Park, Y.J., The systemic delivery of siRNAs by a cell penetrating peptide, low molecular weight protamine, 2010; Biomaterials, 31(6): 1429-43

Chugh, A., Eudes, F., Cellular uptake of cell-penetrating peptides pVEC and transportan in plants, 2008; Journal of Peptide Science, 14: 477-481

Clark, de Bernandez, E., Protein Refolding for Industrial Processes, 2001; Current Opinion in Biotechnology, 12: 202-207

Clement, S., Dandona, P., Still, J.G., Kosutic, G., Oral modified insulin (HIM2) in patients with type 1 diabetes mellitus: Results from a phase I/II clinical trial. Metabolism, 2004; 53(1): 54-58

Collins-Racie, L.A., McColgan, J.M., Grant, K.L., Di Blasio Smith, E.A., McCoy, J.M., LaVallie, E.M., Production of recombinant bovine enterokinase catalytic subunit in *Escherichia coli* using the novel secretory fusion partner DsbA, 1995; Biotechnology (NY), 13: 982–987

Coppi, G., Iannuccelli, V., Leo, E., Bernabei, M.T., Cameroni, R., Protein immobilisation in crosslinked alginate microparticles, 2002; Journal of Microencapsulation, 19(1): 37-44

Corrigan, D.O., Healy, A.M., Corrigan, O.I., Preparation and release of salbutamol from chitosan and chitosan co-spray dried compacts and multiparticulates, 2006; Journal of Pharmaceutics and Biopharmaceutics, 62: 295-305

Cousens, L.S., Shuster, J.R., Gallegos, C., Ku, L., Stempien, M.M., Urdea, M.S., Sanchez Pescador, R., Taylor, A., Tekamp-Olson, P., High level expression of proinsulin in the yeast *Saccharomyces cerevisiae*, 1987; Gene, 61: 265–275

Cui, F.D., Tao, A.J., Cun, D.M., Zhang, L.Q., Shi, K., Preparation of Insulin Loaded PLGA-Hp55 Nanoparticles for Oral Delivery, 2007; Journal of Pharmaceutical Sciences, 96(2): 421-427

Damgé, C., Reis., C.P., Maincent, P., Nanoparticle strategies for the oral delivery of insulin, 2008; Expert Opinion on Drug Delivery, 5(1): 45 – 68

Damgé, C., Socha, M., Ubrich, N., Maincent, P., Poly(e-Caprolactone)/Eudragit Nanoparticles for Oral Delivery of Aspart-Insulin in the Treatment of Diabetes, 2010; Journal of Pharmaceutical Sciences, 99(2): 879-889

Daneman, D., Type 1 diabetes, 2006; The Lancet, 367(9513): 847-858

Dave, N., Hazra, P., Khedkar, A., Manjunath, H.S., Iyer, H., Suryanarayanan, S., Process and purification for manufacture of a modified insulin intended for oral delivery, 2008; Journal of Chromatography. A, 1177(2): 282-286

De Grully, C., Development of an auto-induction system in *E.coli* for high level expression of modified human insulin for oral delivery, Research project, TCD, 2012;

De la Fuente, M., Seijo, B., Alonso, M.J., Novel hyaluronan-based nanocarriers for transmucosal delivery of macromolecules, 2008; Macromolecular Bioscience, 8: 441-450

De Marco, A., Strategies for successful recombinant expression of disulfide bonds-dependent proteins in *Escherichia coli*, 2009; Microbial Cell Factories, 8: 26

Déat-Lainé, E., Hoffart, V., Garrait, G., Beyssac, E., Whey protein and alginate hydrogel microparticles for insulin intestinal absorption: Evaluation of permeability enhancement properties on Caco-2 cells, 2013; International Journal of Pharmaceutics, 453(2): 336-342

Degim, Z., Ünal, N., Eşsiz, D., Abbasoglu, U., The effect of various liposome formulations on insulin penetration across Caco-2 cell monolayer, 2004; Life Sciences, 75(23): 2819-2827

Delie, F., Blanco-Prieto, M., Polymeric particulates to improve oral bioavailability of peptide drugs, 2005; Molecules, 10: 65–80

Derman, A,I., Beckwith, J., *Escherichia coli* alkaline phosphatase fails to acquire disulfide bonds when retained in the cytoplasm, 1991; Journal of Bacteriology, 173: 7719-7722

Derossi, D., Joliot, A.H., Chassaing, G., Prochiantz, A., The third helix of the 331 Antennapedia homeodomain translocates through biological membranes, 1994; The Journal of Biological Chemistry, 269: 10444–10450

Desai, K.G., Park, H.J., Preparation of cross-linked chitosan microspheres by spray drying: Effect of cross-linking agent on the properties of spray dried microspheres, 2005; Journal of Microencapsulation, 22(4): 377-395

Desai, N.R., Shrank, W.H., Fischer, M.A., Avorn, J., Liberman, J.N., Schneeweiss, S., Pakes, J., Brennan, T.A., Choudhry, N.K., Patterns of medication initiation in newly diagnosed diabetes mellitus: quality and cost implications, 2012; The American Journal of Medicine, 125(3): 302-308

Deshayes, S., Morris, M.C., Divita, G., Heitz, F., Cell-penetrating peptides: tools for intracellular delivery of therapeutics, 2005; Cellular and Molecular Life Sciences, 62: 1839–1849

Devi, N., Maji, T.K., Microencapsulation of isoniazid in genipin-crosslinked gelatin-A-κ-carrageenan polyelectrolyte complex, 2010; Drug Development and Industrial Pharmacy, 36(1): 56-63

Diabetes treatment: World Drug Market: 2012-2013

Dietz, G.P., Bahr, M., Synthesis of cell-penetrating peptides and their application in neurobiology, 2007; Methods in Molecular Biology, 399: 181-198

Ding, Y.S., Owen, S.M., Lal, R.B., Ikeda, R.A., Efficient Expression and Rapid Purification of Human T-Cell Leukemia Virus Type 1 Protease, 1998; Journal of Virology, 72(4): 3383-3386

Dingermann, T., Recombinant therapeutic proteins: Production platforms and challenges, 2008; Biotechnology Journal, 3: 90-97

Draget, K.I., Smidsrod, O., Skjak-Braek, G., Alginates form algae, 2005; Polysaccharides and Polyamides in the Food Industry. Properties, Production, and Patents

Dumitriu, S., Chornet, E., Inclusion and release of proteins from polysaccharide-based polyion complexes, 1998; Advanced Drug Delivery Reviews, 31: 223-246

Eaimtrakarn, S., Rama Prasad, Y.V., Ohno, T., Konishi, T., Yoshikawa, Y., Shibata, N., Takada, K., Absorption enhancing effect oflabrasol on the intestinal absorption of insulin in rats, 2002; Journal of Drug Targeting, 10(3): 255-260

El-Andaloussi, S., Holm, T., Langel, U., Cell-penetrating peptides: mechanisms and applications, 2005; Current Pharmaceutical Design, 11: 3597-3611

European Medicines Agency, Assessment report for Protamine containing medicinal Products, 2012; Review under Article 5(3) of Regulation (EC) No 726/2004

Ezhevsky, S.A., Nagahara, H., Vocero-Akbani, A.M., Gius, D.R., Wei, M.C., Dowdy, S.F., Hypo-phosphorylation of the retinoblastoma protein (pRb) by cyclin D:Cdk4/6 complexes results in active pRb, 1997; Proceedings of the National Academy of Sciences USA, 94: 10699-10704

Fischer, B., Sumner, I., Goodenough, P., Isolation, renaturation, and formation of disulfide bonds of eukaryotic proteins expressed in *Escherichia coli* as inclusion bodies, 1993; Biotechnology and Bioengineering, 41: 3-13

Fishel-Ghodsian, F., Brown, L., Mathiowitz, E., Brandenburg, D., Langer, R., Enzymatically controlled drug delivery, 1988; Proceedings of the National Academy of Sciences USA, 85(7): 2403–2406

Francetic, O., Belin, D., Badaut, C., Pugsley, A.P., Expression of the endogenous type II secretion pathway in *Escherichia coli* leads to chitinase secretion, 2000; European Molecular Biology Organisation Journal, 19: 6697–6703

Gacesa, P., Alginates, 1988; Carbohydrate Polymers, 8(3): 161-182

Gan., Q., Wang, T., Chitosan nanoparticle as protein delivery carrier-systematic examination of fabrication conditions for efficient loading and release, 2007; Colloids and Surfaces B, 59(1): 24–34

Gåserød, O., Smidsrød, O., Skjåk-Braek, G., Microcapsules of alginate-chitosan-I. A quantative study of the interaction between alginate and chitosan, 1998; Biomaterials, 19(20): 1815-1825

George, M., Abraham, T.E., Polyionic hydrocolloids for the intestinal delivery of protein drugs: Alginate and chitosan — a review, 2006; Journal of Controlled Release, 114(1): 1-14

Georgiou, G., Valax, P., Isolating inclusion bodies from bacteria, 1999; Methods in Enzymology, 309: 48-58

Gonçalves, C., Pereira, P., Gama, F.M., Self-assembled hydrogel nanoparticles for drug delivery applications, 2010; Materials, 3: 1420-1460

Govender, T., Stolnik, S., Garnett, M.C., Illum, L., Davis, S.S., PLGA nanoparticles prepared by nanoprecipitation: drug loading and release studies of a water soluble drug, 1999; Journal of Controlled Release, 57: 171-185

Govender, T., Riley, T., Ehtezazi, T., Garnett, M.C., Stolnik, S., Illum, L., Davis, S.S., Defining the drug incorporation properties of PLA-PEG nanoparticles, 2000; International Journal of Pharmaceutics, 199: 95-110

Grabovac, V., Foger, F., Bernkop-Schnurch, A., Design and in vivo evaluation of a patch delivery system for insulin based on thiolated polymers, 2008; International Journal of Pharmaceutics, 248(1-2): 169-174

Grenha, A., Gomes, M.E., Rodrigues, M., Santo, V.E., Mano, J.F., Neves, N.M., Reis, R.L., Development of new chitosan/carrageenan nanoparticles for drug delivery applications, 2009; Journal of Biomedical Materials Research Part A, 1265 – 1272

Gualandi-Signorini, A.M., Giorgi, G., Insulin formulations – a review, 2001; European Review for Medical and Pharmacological Sciences, 5: 73-83

Guballa, S.K., Polyelectrolyte complex: A pharmaceutical review, 2012; International Journal of Pharma and Bio Sciences, 2(3): 399-407

Gupta, J., Felner, E.I., Prausnitz, M.R., Minimally Invasive Insulin Delivery in Subjects with Type 1 Diabetes Using Hollow Microneedles, 2009; Diabetes Technology and Therapeutics, 11(6): 329–337

Gupta, V.K., Karar, P.K., Optimisation of process variables for the preparation of chitosan-alginate nanoparticles, 2011; International Journal of Pharmacy and Pharmaceutical Sciences, 3(2): 1-3

Guyton, A.C., Digestion and absorption in the gastrointestinal tract; gastrointestinal disorders, in: Human Physiology and Mechanisms of Disease, 1992; 5th ed., Saunders, W.B., Philadelphia, 500–509

Halder, A., Maiti, S., Sa, B., Entrapment effciency and release characteristics of polyethyleneimine-treated or - untreated calcium alginate beads loaded with propranolol–resin complex, 2005; International Journal of Pharmaceutics, 302: 84–94

Hamidi, M., Azadi, A., Rafiel, P., Hydrogel nanoparticles in drug delivery, 2008; Advanced Drug Delivery Reviews, 60: 1638-1649

Hamman, J.H., Chitosan Based Polyelectrolyte Complexes as Potential Carrier Materials in Drug Delivery Systems, 2010; Mar. Drugs, 8: 1305-1322

Hans, M.L., Lowman, A.M.,: Biodegradable nanoparticles for drug delivery and targeting, 2002; Current Opinion in Solid State and Materials Science, 6(4): 319-327

Hara, M. Nakajima, A., Formation of the polyelectrolyte complex of heparin with aminoacetalised poly(vinyl alcohol), 1978; Polymer Journal, 10: 37–44

Hartig, S.M., Greene, R.R., Das Gupta, J., Carlesso, G., Dikov, M.M., Prokop, A., Davidson, J.M., Multifunctional nanoparticulate polyelectrolyte complexes, 2007; Pharmaceutical Research, 24(12): 2353-2369

Harrison's Principle of Internal Medicine 17 Ed., Insulin Biosynthesis, Secretion, and Action, 2008;

He, N.N., David, A.E., Zhang, J., Park, Y.S., Wang, J.X., Huang, Y.Z., Wang, J.K., Yang, V.C., Low molecular weight protamine/insulin formulation with potential to attenuate protamine masqueraded insulin allergy, 2011; Macromolecular Research, 19: 1224-1226

Heebøll-Nielsen, A., Choe, W.S., Middelberg, A.P.J., Thomas, O.R.T., Efficient inclusion body processing using chemical extraction and high gradient magnetic fishing, 2003; Biotechnology Progress, 19: 887-898

Heinemann, L., The Failure of Exubera: Are We Beating a Dead Horse?, 2008; Journal of Diabetes Science and Technology, 2(3): 518-529

Heinemann, L., Jacques, Y., Oral Insulin and Buccal Insulin: A Critical Reappraisal, 2009; Journal of Diabetes Science and Technology, 3(3): 568–584

Heinemann, L., New ways of insulin delivery, 2010; Int J Clin Pract, 64(166): 29-40

Heitz, F., Morris, M.C., Divita, G., Twenty years of cell-penetrating peptides: from molecular mechanisms to therapeutics, Themed Section: Vector Designand Drug Delivery, 2009; British Journal of Pharmacology, 157: 195–206

Heller, S., Kozlovski, P., Kurtzhals, P., Insulin's 85th anniversary – An enduring medical miracle, 2007; Diabetes Research and Clinical Practise, 78: 149-158

Henkin, R.I., Intranasal insulin: from nose to brain, 2010; Nutrition, 26: 624-633

Henriques, S.T., Costa, J., Castanho, M.A., Translocation of beta-galactosidase mediated by the cell-penetrating peptide pep-1 into lipid vesicles and human HeLa cells is driven by membrane electrostatic potential, 2005; Biochemistry, 44: 10189-10198

Hernandez, V.E.B., Paz Maldonado, L.M.T., Rivero, E.M., Barba de la Rosa, A.P., Jimenez-Bremont, J.F., Acevedo, L.G.O., De Leon Rodrıguez, A., Periplasmic expression and recovery of human interferon gamma in *Escherichia coli*, 2008; Protein Expression and Purification, 59: 169–174

Hidari, K.I., Horie, N., Murata, T., Miyamoto, D., Suzuki, T., Usui, T., Suzuki, Y., Purification and characterisation of a soluble recombinant human ST6Gal I functionality expressed in *Escherichia coli*, 2005; Glycoconjugate Journal, 22: 1–11

Holme, H.K., Lindmo, K., Kristiansen, A., Smidsrød, O., Thermal depolymerisation of alginate in the solid state, 2003; Carbohydrate Polymers, 54: 431-438

Holme, H.K., Davidsen, L., Kristiansen, A. Smidsrød, O., Kinetics and mechanisms of depolymerisation of alginate and chitosan in aqueous solution, 2008; Carbohydrate Polymers, 73(4): 656-664

Hosny, E.A., Al-Shora, H.I., Elmazar, M.M., Oral delivery of insulin from enteric-coated capsules containing sodium salicylate: effect on relative hypoglycemia of diabetic beagle dogs, 2002; International Journal of Pharmaceutics, 237(1-2): 71-76

Hou, Y.W., Chan, M.H., Hsu, H.R., Liu, B.R., Chen, C.P., Chen, H.H., Lee, H.J., Transdermal delivery of proteins mediated by non-covalently associated arginine-rich intracellular delivery peptides, 2007 a; Experimental Dermatology, 16: 999-1006

Hou, J., Yan, R., Ding, D., Yang, L., Wang, C., Wu, Z., Yu, X., Li, W., Li, M., Oral administration of a fusion protein containing eight GLP-1 analogues produced in *Escherichia coli* BL21(DE3) in streptozotocin-induced diabetic rats, 2007 b; Biotechnology Letters, 29: 1439-1446

Houamed, K., Fu, J., Roe, M.W., Philipson, L.H., Diabetes Mellitus: A Fundamental and Clinical Text, 3rd Edition, 4 Electrophysiology of the Pancreatic β-Cell, 2004; Lippincott Williams & Wilkins

Hu, J.W., Liu, B.R., Wu, C.Y., Lu, S.W., Lee, H.J., Protein transport in human cells mediated by covalently and noncovalently conjugated arginine-rich intracellular delivery peptides, 2009; Peptides, 30: 1669-1678

Hu, Y., Yang, T., Hu, X., Novel polysaccharide-based nanoparticle carriers prepared by polyelectrolyte complexation for protein delivery, 2012; Polymer Bulletin, 68: 1183-1199

Hubatsch, I., Ragnarsson, E.G.E., Artursson, A., Determination of drug permeability and prediction of drug absorption in Caco-2 monolayers, 2007; Nature Protocols, 2(9): 2111-2119

Hugerth, A., Caram-Lelham, N., Sundelöf, L-O., The effect of charge density and conformation on the polyelectrolyte complex formation between carrageenan and chitosan, 1997; Carbohydrate Polymers, 34(3): 149-156

Hwang, S.H., Maitani, Y., Takayama, K., Nagai, T., High Entrapment of Insulin and Bovine Serum Albumin into Neutral and Positively-Charged Liposomes by Remote Loading Method, 2000; Chemical and Pharmaceutical Bulletin, 48(3): 325-329

Igartua, M., Hernandez, R.M., Esquisabel, A., Gascon, A.R., Calvo, M.B., Pedraz, J.L., Influence of formulation variables on the *in vitro* release of albumin from biodegradable microparticulate systems, 1997; Journal of Microencapsulation, 14: 349-356

International Diabetes Federation. IDF Diabetes Atlas, 6th edn. Brussels, Belgium: International Diabetes Federation, 2013. http://www.idf.org/diabetesatlas, accessed on 19/07/2013

Irons, B., New pharmacotherapies for type 2 diabetes, 2013; Pharmacotherapy Self-Assessment Program, Cardiology/ Endocrinology, 5-25

Issa, M.M., Koping-Hoggard, M., Tommeraas, K., Varum, K.M., Christensen, B.E., Strand, S.P., Artursson, P., Targeted gene delivery with trisaccharide-substituted chitosan oligomers *in vitro* and after lung administration *in vivo*, 2006; Journal of Controlled Release,115(1), 103-112

Janaswamy, S., Chandrasekaran, R., Effect of calcium ions on the organisation of iota-carrageenan helices: an X-ray investigation, 2002; Carbohydrate Research, 337: 523-535

Jelvehgari, M., Zakeri-Milani, P., Siahi-Shadbad, M.R., Loveymi, B.D., Nokhodchi, A., Azari, Z., Valizadeh, H., Development of pH-sensitive Insulin Nanoparticles using Eudragit L100-55 and Chitosan with Different Molecular Weights, 2010; American Association of Pharmaceutical Sciences PharmSciTech., 11(3): 1237–1242

Jin, K., Thomas, O.R.T., Dunnill, P., Monitoring recombinant inclusion body recovery in an industrial disk stack centrifuge, 1994; Biotechnology and Bioengineering, 43: 455-460

Johansen, C., Gill, T., Gram, L., Antibacterial Effect of Protamine Assayed by Impedimetry, 1995; Journal of Applied Bacteriology., 78(3): 297-303

Joly, J.C., Leung, W.S., Swartz, J.R., Overexpression of *Escherichia coli* oxidoreductases increases recombinant insulin-like growth factor-I accumulation, 1998; Proceedings of the National Academy of Sciences USA, 95: 2773-2777

Jonasson, P., Nilsson, J., Samuelsson, E., Moks, T., Stahl, S., Uhlen, M., Single-step trypsin cleavage of a fusion protein to obtain human insulin and its C-peptide, 1996; Europen Journal of Biochemistry, 236: 656–661

Kabanov, V.A., Zezin, A.B., Soluble interpolymeric complexes as a new class of synthetic polyelectrolytes, 1984; Pure and Applied Chemistry, 56: 343–35

Kagawa, N., Cao, Q., Kusano, K., Expression of human aromatase (CYP19) in *Escherichia coli* by N-terminal replacement and induction of cold stress response, 2003; Steroids, 68: 205–209

Kaiser, R., Metzka, L., Enhancement of Cyanogen Bromide Cleavage Yields for Methionyl-Serine and Methionyl-Threonine Peptide Bonds, 1999; Analytical Biochemistry, 266(1): 1 -8

Kamei, N., Morishita, M., Eda, Y., Ida, N., Nishio, R., Takayama, K., Usefulness of cell penetrating peptides to improve intestinal insulin absorption, 2008; Journal of Controlled Release, 132(1): 21-25

Kang, Y., Yoon, J.W., Development of a high-expression vector (pYK10-9) of human proinsulin gene, 1991; Biotechnology Letters, 13: 755–760

Kang, Y., Yoon, J.W., Effect of modification of connecting peptide of proinsulin on its export, 1994; Journal of Biotechnology, 36: 45–54

Kavimandana, N.J., Peppas, N.A., Confocal microscopic analysis of transport mechanisms of insulin across the cell monolayer 2008, International Journal of Pharmaceutics, 354: 143-148

Kelly, D., Development of an optimised method for proinsulin refolding, 2011; Senior Sophister Project, TCD;

Kemmler, W., Peterson, J.D., Steiner, D.F., Studies on the conversion of proinsulin to insulin. I. Conversion in vitro with trypsin and carboxypeptidase, 1971; B. The Journal of Biological Chemistry, 246: 6786–6791

Khafagy, el-S., Morishita, M., Onuki, Y., Takayama, K., Current challenges in non-invasive insulin delivery systems: A comparative review, 2007; Advanced Drug Delivery Reviews, 59(15): 1521-1546

Khafagy, el-S., Morishita, M., Isowa, K., Imai, J., Takayama, K., Effect of cell penetrating peptides on the nasal absorption of insulin, 2009; Journal of Controlled Release, 133(2): 103-108

Kim, B-Y., Jeonga, J., Parkb, K., Kim, J-D., Bioadhesive interaction and hypoglycemic effect of insulin-loaded lectin–microparticle conjugates in oral insulin delivery system, 2005; Journal of Controlled Release, 102: 525–538

Kisel, M.A., Kulik, L.N., Tsybovsky, I.S., Vlasov, A.P., Kholodova, E.A., Zabarovskaya, Z.V., Liposomes with phosphatidylethanol as a carrier for oral delivery of insulin: studies in the rat, 2001; International Journal of Pharmaceutics, 216: 105-114

Kötz, J., Köpke, H., Schmidt-Naake, G., Vogl, O., Polyanion-polycation complex formation as a function of the position of the functional groups, 1996; Polymer, 37(13): 2775–2781

Kroeff, E.P., Owens, R.A., Campbell, E.L., Johnson, R.D., Marks, H.I., Production scale purification of biosynthetic human insulin by reversed-phase high-performance liquid chromatography, 1989; Journal of Chromatography, 461: 45–61

Kumari, A., Yadav, S.K., Yadav, S.C., Biodegradable polymeric nanoparticles based drug delivery systems, 2010; Colloids and Surfaces B: Biointerfaces, 75(1):1-18

Ladisch, M.R., Kohlmann, K.L., Recombinant Human Insulin, 1992; Biotechnology Progress, 8: 469-478

Laird, M.W., Cope, K., Atkinson, R., Donahoa, M., Johnson, K., Melick, M., Keratinocyte growth factor-2 production in an ompT-deficient *Escherichia coli* K-12 mutant, 2004; Biotechnology Progress, 20: 44-50

Lankalapalli, S., Kolapalli, V.R.M., Polyelectrolyte Complexes: A review of their Applicability in Drug Delivery Technology, 2009; Indian Journal of Pharmaceutical Sciences, 71(5): 481-487

Lars-Nieba, L., Honegger, A., Krebber, C., Pluckthun, A., Disrupting the hydrophobic patches at the antibody variable/constant domain interface: improved *in vivo* folding and physical characterisation of an engineered scFv fragment, 1997; Protein Engineering, 10(4):435-444

Le Roith, D., Taylor, S.I., Olefsky, J.M., Diabetes Mellitus. A fundamental and clinical text, 2004; Lippincott Williams & Wilkins

Leary, A.C., Dowling, M., Cussen, K., O'Brien, J., Stote, R.M., Pharmacokinetics and Pharmacodynamics of Intranasal Insulin Spray (Nasulin™) Administered to Healthy Male Volunteers, 2008; Journal of Diabetes Science and Technology, 2(6): 1054–1060

Lee, K.Q., Mooney, D.J., Alginate: Properties and biomedical applications, 2012; Progress in Polymer Science, 37: 106-126

Leobandung, W., Ichikawa, H., Fukumori, Y., Peppas, N.A., Preparation of stable insulin-loaded nanospheres of poly(ethylene glycol) macromers and N-isopropyl acrylamide, 2002; Journal of Controlled Release, 80(1-3): 357-363

Leong, K.H., Chung, L.Y., Noordin, M.I., Onuki, Y., Morishita, M., Takayama, K., Lectin-functionalised carboxymethylated kappa-carrageenan microparticles for oral insulin delivery, 2011; Carbohydrate Polymers, 86: 555-565

Li, C., Hein, S., Wang, K., Chitosan-Carrageenan Polyelectrolyte Complex for the Delivery of Protein Drugs, 2013; International Scholarly Research Network Biomaterials, 1-6

Li, P., Dai, Y-N., Wei, Q., Chitosan-Alginate Nanoparticles as a Novel Drug Delivery System for Nifedipine, 2008; International Journal of Biomedical Science, 4(3): 221-228

Li, Y., Shao, Z., Mitra, A.K., Dissociation of insulin oligomers by bile salt micelles and its effect on alpha-chymotrypsin-mediated proteolytic degradation, 1992; Pharmaceutical Research, 9(7): 864-869

Liang, J.F., Yang, V.C., Insulin-cell penetrating peptide hybrids with improved intestinal absorption efficiency, 2005; Biochemical and Biophysical Research Communications, 335(3): 734-738

Liao, Y.D., Jeng, J.C., Wang, C.F., Wang, S.C., Chang, S.T., Removal of N-terminal methionine from recombinant proteins by engineered *E. coli* methionine aminopeptidase, 2004; Protein Science, 13(7): 1802-1810

Lin, Y.H., Mi, F.L., Chen, C.T., Chang, W.C., Peng, S.F., Liang, H.F., Sung, H.W., Preparation and Characterisation of Nanoparticles Shelled with Chitosan for Oral Insulin Delivery, 2007 a; Biomacromolecules, 8(1): 146-152

Lin, Z., Johnson, LC., Weissbach, H., Brot, N., Lively, M.O., Lowther, W.T., Free methionine-(R)-sulfoxide reductase from *Escherichia coli* reveals a new GAF domain function, 2007 b; Proceedings of National Academy of Sciences, 104(23): 9597-9602

Liu, B.R., Huang, Y.W., Winiarz, J.G., Chiang, H.J., Lee, H.J., Intracellular delivery of quantum dots mediated by a histidine- and arginine-rich HR9 cell-penetrating peptide through the direct membrane translocation mechanism, 2011; Biomaterials, 32: 3520-3537

Liu, J., Zhao, Y., Guo, Q., Wang, Z., Wang, H., Yang, Y., Huang, Y., TAT-modified nanosilver for combating multidrug-resistant cancer, 2012; Biomaterials, 33: 6155-6161

Liu, Z., Jiao, Y., Wang, Y., Zhou, Ch., Zhang, Z., Polysaccharides-based nanoparticles as drug delivery systems, 2008; Advanced Drug Delivery Reviews, 60(15): 1650-1662

Lo, S.L., Wang, S., Intracellular Protein Delivery Systems Formed by Noncovalent Bonding Interactions between Amphipathic Peptide Carriers and Protein Cargos, 2010; Macromolecular Rapid Communications, 31: 1134-1141

Lodge, J., Lund, P., Minchin, S., Production of Proteins from Cloned Genes, Gene Cloning, Principles and Applications 1st edition, Chapter 9, 2006;

Lodish, H., Berk, A., Zipursky, S.L., et al., Molecular Cell Biology. 4th edition, 2000; New York: Freeman, W.H.,

Lu, S.W., Hu, J.W., Liu, B.R., Lee, C.Y., Li, J.F., Chou, J.C., Lee, H.J., Arginine-rich intracellular delivery peptides synchronously deliver covalently and noncovalently linked proteins into plant cells, 2010; Journal of Agricultural and Food Chemistry, 58: 2288-2294

Ma, E-L., Ma, H., Liu, Z., Zheng, Ch-X., Duan, M-X., *In vitro* and *in vivo* evaluation of a novel oral insulin formulation, 2006; Chinese Pharmacological Society, 27(10): 1382-1388

Mahkam, M., Bioadhesive alginate copolymers as platforms for oral delivery of insulin, 2009; Nature and Science, 7(6): 61-69

Malik, A., Jenzsch, M., Lübbert, A., Rudolph, R., Söhling, B., Periplasmic production of native human proinsulin as a fusion to *E. coli* ecotin, 2007; Protein Expression and Purification, 55: 100–111

Mano, M., Teodosio, C., Paiva, A., Simoes, S., Pedroso de Lima, M.C., On the mechanisms of the internalisation of S4(13)-PV cell-penetrating peptide, 2005; Biochemical Journal, 390: 603-612

Martin, M.E., Rice, K.G., Peptide-guided gene delivery, 2007; American Association of Pharmaceutical Sciences Journal., 9: 18-29

Maurizi, M.R., Proteases and protein degradation in *Escherichia coli*, 1992; Experientia, 48(2): 178 – 201

Mayfield, J.A., White, R.D., Insulin therapy for type 2 diabetes: Rescue, augmentation, and replacement of beta-cell function, 2004; American Family Physician, 70(3): 489-500

Meade, A.J., Meloni, B.P., Mastaglia, F.L., Knuckey, N.W., The application of cell penetrating peptides for the delivery of neuroprotective peptides/proteins in experimental cerebral ischaemia studies, 2009; Journal of Experimental Stroke and Translational Medicine, 2(1): 22-40

Meade, B.R., Dowdy, S.F., Exogenous siRNA delivery using peptide transduction domains/cell penetrating peptides, 2007; Advanced Drug Delivery Reviews, 59: 134-140

Mekras, C.I., Inhibition of Pepsin by Polyions and C.D. Studies, 1989; International Journal of Biological Macromolecules, 11(4): 207-212

Mergulhao, F.J., Taipa, M.A., Cabral, J.M., Monteiro, G.A., Evaluation of bottle-necks in proinsulin secretion by *Escherichia coli*, 2004; Journal of Biotechnology, 109: 31–43

Min, Ch-K., Son, Y-J., Kim, Ch-K., Park, S-J., Lee, J-W., Increased expression, folding and enzyme reaction rate of recombinant human insulin by selecting appropriate leader peptide, 2011; Journal of Biotechnology, 151: 350-356

Mesiha, M.S., Ponnapula, S.,Plakogiannis, F., Oral absorption of insulin encapsulated in artificial chyles of bile salts, palmitic acid and alpha-tocopherol dispersions, 2002; International Journal of Pharmaceutics, 249(1-2): 1-5

Mesiha, M.S., Sidhom, M.B., Fasipe, B., Oral and subcutaneous absorption of insulin poly(isobutylcyanoacrylate) nanoparticles, 2005; International Journal of Pharmaceutics, 228(2): 289-293

Mitri, J., Pittas, A.G., Inhaled insulin – what went wrong, 2009; Nature Reviews Endocrinology, 5: 24-25

Missiakas, D., Raina, S., Protein Folding in Bacterial Periplasm, 1997; Journal of Bacteriology, 179(8): 2465-2471

Mizrahy, S., Peer, D., Polysaccharides as building blocks for nanotherapeutics, 2012; Chemical Society Reviews, 7(41): 2623-2340

Mohanraj, V.J., Chen, Y., Nanoparticles - A Review, 2006; Tropical Journal of Pharmaceutical Research, 5 (1): 561-573

Morishita, M., Morishita, I., Takayama, K., Machida, Y., Nagai, T., Site-dependent effect of aprotinin, sodium caprate, Na_2EDTA and sodium glycocholate on intestinal absorption of insulin, 1993; Biological & Pharmaceutical Bulletin, 16(1): 68-72

Morishita, M., Kamei, N., Ehara, J., Isowa, K., Takayama, K., A novel approach using functional peptides for efficient intestinal absorption of insulin, 2007; Journal of Controlled Release, 118(2): 177-184

Moroder, L., Buchner, J., Disulfide-bond Formation and Isomerisation in Prokaryotes, 2009; Oxidative Folding of Peptides and Proteins,

Morris, M.C., Depollier, J., Mery, J., Heitz, F., Divita, G., A peptide carrier for the delivery of biologically active proteins into mammalian cells, 2001; Nature Biotechnology, 19: 1173-1176

Munyendo, W.L.L., Lv, H., Benza-Ingoula, H., Baraza, L.D., Zhou, J., Cell Penetrating Peptides in the Delivery of Biopharmaceuticals, 2012; Biomolecules, 2: 187-202

Murby, M., Cedergren, L., Nilsson, J., Nygren, P.A., Hammarberg, B., Nilsson, B., Enfors, S.O., Uhlén, M., Stabilisation of recombinant proteins from proteolytic degradation in *Escherichia coli* using a dual affnity fusion strategy, 1991; Biotechnology and Applied Biochemistry,14: 336–346

Murriel, C.L., Dowdy, S.F., Influence of protein transduction domains on intracellular delivery of macromolecules, 2006; Expert Opinion on Drug Delivery, 3(6): 739–46

Nagahara, H., Vocero-Akbani, A.M., Snyder, E.L., Ho, A., Latham, D.G., Lissy, N.A., Becker-Hapak, M., Ezhevsky, S.A., Dowdy, S.F., Transduction of full-length TAT fusion proteins into mammalian cells: TAT-p27(Kip1) induces cell migration, 1998; Nature Medicine, 4: 1449-1452

Nakajima, J., Formation of polyelectrolyte complexes, 1980; Journal of Macromolecular Science Part B, 17: 715–721

Nesher, R., Cerasi, E., Modeling Phasic Insulin Release. Immediate and Time-Dependent Effects of Glucose, ADA, 2002; Diabetes, 51(1): S53-S59

Niedzielski, M.F., Hopewell, R., Ismail, Z., Estable, M.C., MCEF is localised to the nucleus by protein sequences encoded within three distinct exons, where it represses HIV-1 Tat-transactivation of LTR-directed transcription, 2007; International Journal of Biological Science, 3: 225-236

Nilsson, J., Jonasson, P., Samuelsson, E., Stahl, S., Uhlen, M., Integrated production of human insulin and its C-peptide, 1996; Journal of Biotechnology, 48: 241-250

O'Hagan, D.T., Jeffery, H., Davis, S.S., The preparation and characterisation of PLGA microspheres: III. Microparticle/ polymer degradation rates and the *in vitro* release of a model protein, 1994; International Journal of Pharmaceutics, 103: 37-45

Owens, D.R., New horizons - alternative routes for insulin therapy, 2002; Nature Reviews Drug Discovery, 1(7): 529-540

Owens, D.R., Zinman, B., Bolli, G., Alternative routes of insulin delivery, 2003; Diabetic medicine, 20: 886-898

Palmer, I., Wingfield, P.T., Preparation and Extraction of Insoluble (Inclusion-Body) Proteins from *Escherichia coli*, 2004; Current Protocols in Protein Science, Unit: 6.3

Panyam, J., Williams, D., Dash, A., Leslie-Pelecky, D., Labhasetwar, V., Solid-state solubility influences encapsulation and release of hydrophobic drugs from PLGA/PLA nanoparticles, 2004; Journal of Pharmaceutical Sciences, 93: 1804-14

Pardakhty, A., Moazeni, E., Varshosaz, J., Hajhashemi, V., Rouholamini, N.A., Pharmacokinetic study of niosome-loaded insulin in diabetic rats, 2011; DARU Journal of Pharmaceutical Sciences, 19(6): 404-411

Park, K., Kwon, I.Ch., Park, K., Oral protein delivery: Current status and future prospect, 2011; Reactive and Functional Polymers, 71: 280–287

Patel, L.N., Zaro, J.L., Shen, W.C., Cell penetrating peptides: intracellular pathways and pharmaceutical perspectives, 2007; Pharmaceutical Research, 24(11): 1977–1992

Patel, L.N., Wang, J., Kim, K-J., Borok, Z., Crandall, E., Shen, W-Ch., Conjugation with Cationic Cell-Penetrating Peptide Increases Pulmonary Absorption of Insulin, 2009; Molecular Pharmaceutics, 6(2): 492–503

Pauletti, G., Gangwar, S., Knipp, G.T., Nerurkar, M.M., Okuma, F.W., Tamura, K., Siahaan, T.J., Borchardt, R.T., Structural requirements for intestinal absorption of peptide drugs, 1996; Journal of Controlled Release, 41: 3–17

Pavli, M., Vrečer, F., Baumgartner, S., Matrix tablets based on carrageenans with dual controlled release of doxazosin mesylate, 2010; International Journal of Pharmaceutics, 400(1-2): 15-23

Pavli, M., Baumgartner, S., Kos, P., Kogej, K., Doxazosin-carrageenan interactions: A novel approach for studying drug-polymer interactions and relation to controlled drug release, 2011; International Journal of Pharmaceutics, 421(1): 110-119

Peniche, C., Argüelles-Monal, W., Peniche, H., Acosta, N., Chitosan: An attractive biocompatible polymer for microencapsulation, 2003; Macromolecular Bioscience, 3(10): 511-520

Petrides, D., Sapidou, E., Calandranis, J., Computer-aided process analysis and economic evaluation for biosynthetic human insulin production - A case study, 1995; Biotechnology and Bioengineering, 48(5): 529-541

Philipp, B., Dautzenberg, H., Linow, K.J., Koetz, J., Dawydoff, W., Polyelectrolyte complexes. Recent developments and open problems, 1989; Progress in Polymer Science, 14: 91–172

Phillips, G.O., Williams, P.A., (Ed.), Handbook of hydrocolloids. Cambridge, Woodhead Publishing Limited, 2000;

Pinheiro, A.C., Bourbon, A.I., Medeiros, B., Da Silva, L.H.M., Da Silva M.C.H., Carneiro-da-cunha, M.G., Coimbra, M.A., Vincente, A.A., Interactions between κ-carrageenan and chitosan in nanolayered coatings – structural and transport properties, 2012; Carbohydrate Polymers, 87: 1081-1090

Pulks, E., Temperature impact on insulin expression in *E.coli* bacteria, 2012, Master thesis, TCD;

Qiu, Y., Park, K., Environment-sensitive hydrogels for drug delivery, 2001; Advanced Drug Delivery Reviews, 53: 321–339

Radwan, M.A., Aboul-Enein, H.Y., The effect of absorption enhancers on the initial degradation kinetics of insulin by alpha-chymotrypsin, 2001; International Journal of Pharmaceutics, 217(1-2): 111-120

Rafati, H., Coombes, A.G.A., Adler, J., Holland, J., Davis, S.S., Protein-loaded PLGA microparticles for oral administration: formulation, structural and release characteristics, 1997; Jornal of Controlled Release, 43: 89-102

Raina, S., Missiakas, D., Making and breaking disulfide bonds, 1997; Annual Review of Microbiology, 51: 179–202

Raj, N.K.K., Sharma, C.P., Oral insulin - a perspective, 2003; Journal of Biomaterials Applications, 17(3):183-196

Ramadas, M., Paul, W., Dileep, K.J., Anitha, Y., Sharma, C.P., Lipoinsulin encapsulated alginate–chitosan capsules: intestinal delivery in diabetic rats, 2000; Journal of Microencapsulation, 17: 405–411

Rao, J.P., Geckeler, K.E., Polymer nanoparticles: preparation techniques and size control parameters, 2011; Progress in Polymer Science, 36(6): 887 – 913

Reis, C.P., Neufeld, R.J., Vilela, S., Ribeiro, A.J., Veiga, F., Review and current status of emulsion/dispersion technology using an internal gelation process for the design of alginate particles, 2006; Journal of Microencapsulation, 23(3): 245-257

Reis, C.P., Ribeiro, A.J., Neufeld, R.J., Veiga, F., Alginate Microparticles as Novel Carriers for Oral Insulin Delivery, 2007; Biotechnology and Bioengineering, 96(5): 977-989

Reynolds, F., Weissleder, R., Josephson, L., Protamine as an efficient membrane-translocating peptide, 2005; Bioconjugate Chemistry, 16: 1240-1245

Rinaudo, M., Review: main properties and current applications of some polysaccharides as biomaterials, 2008; Polymer International, 57: 397-430

Rojas, M., Donahue, J.P., Tan, Z., Lin, Y-Z., Genetic engineering of proteins with cell membrane permeability, 1998; Nature Biotechnology, 16: 370-375

Rosenfeld, L., Insulin: Discovery and Controversy, 2002; Clinical Chemistry, 48(12): 2270-2288

Rudolph, R., Lilie, H., *In vitro* folding of inclusion body proteins, 1996; The Journal of the Federation of American Societies for Experimental Biology, 10: 49-56

Sadrzadeh, N., Glembourtt, M.J., Stevenson, C.L., Peptide drug delivery strategies for the treatment of diabetes, 2007; Journal of Pharmaceutical Sciences, 96(8): 1925-1954

Saether, H.V., Holme, H.K., Maurstad, G., Smidsrod, O., Stokke, B.T., Polyelectrolyte complex formation using alginate and chitosan, 2008; Carbohydrate Polymers, 74: 813-821

Sah, H., Toddywala, R., Chien, Y.W., The influence of biodegradable microcapsule formulations on the controlled release of a protein, 1994; Journal of Controlled Release, 30: 201-211

Sajeesh, S., Bouchemal, K., Marsaud, V., Vauthier, C., Sharma, C.P., Cyclodextrin complexed insulin encapsulated hydrogel microparticles, An oral delivery system for insulin, 2010; Journal of Controlled Release, 147(3): 377-384

Sakai, M., Imai, T., Ohtake, H., Azuma, H., Otagiri, M., Effects of absorption enhancers on the transport of model compounds in caco-2 cell monolayers: Assessment by confocal laser scanning microscopy, 1997; Journal of Pharmaceutical Sciences, 86(7): 779-785

Sambrook, J., Russell, D.W., Molecular Cloning: A Laboratory Manual, 2001; Cold Spring Harbour Laboratory Press, Cold Spring Harbour, New York

Samuelsson, E., Moks, T., Nilsson, B., Uhlén, M., Enhanced *in vitro* refolding of insulin-like growth factor I using a solubilising fusion partner, 1994; Biochemistry, 33: 4207–4211

Sankalia, M.G., Mashru, R.C., Sankalia, J.M., Sutariya, V.B., Reversed chitosan–alginate polyelectrolyte complex for stability improvement of alpha-amylase: Optimisation and physicochemical characterisation, 2007; European Journal of Pharmaceutics and Biopharmaceutics, 65: 215–232

Sarmento, B., Ferreira, D., Veiga, F., Ribeiro, A., Characterisation of insulin-loaded alginate nanoparticles produced by ionotropic pre-gelation through DSC and FTIR studies, 2006 a; Carbohydrate Polymers, 66 : 1–7

Sarmento, B., Ribeiro, A., Veiga, F., Ferreira, D., Development and characterisation of new insulin containing polysaccharide nanoparticles, 2006 b; Colloids and Surfaces B: Biointerfaces, 53: 193-202

Sarmento, B., Martins, S., Rebeiro, A., Veiga, F., Neufeld, R., Ferreira, D., Development and comparison of different nanoparticulate polyelectrolyte complexes as insulin carriers, 2006 c; International Journal of Peptide Research and Therapeutics, 12: 131-138

Sarmento, B., Bibeiro, A., Veiga, F., Ferreira, D., Neufeld, R., Oral Bioavailability of Insulin Contained in Polysaccharide Nanoparticles, 2007 a; Biomacromolecules, 8(10): 3054-3060

Sarmento, B., Ribeiro, A., Veiga, F., Sampaio, P., Neufeld, R., Ferreira, D., Alginate/chitosan nanoparticles are effective for oral insulin delivery, 2007 b; Pharmaceutical Research, 24 (12): 2198-2206

Schmidt, M., Babu, K.R., Khanna, N., Marten, S., Rinas, U., Temperature-induced production of recombinant human insulin in high-cell density cultures of recombinant *Escherichia coli*, 1999; Journal of Biotechnology, 68: 71 – 83

Schultz, T., Liu, J., Capasso, P., de Marco, A., The solubility of recombinant proteins expressed in *Escherichia coli* is increased by otsA and otsB co-transformation, 2007; Biochemical and Biophysical Research Communications, 355:234–239

Schumann, W., Ferreira, L.C.S., Production of recombinant proteins in *Escherichia coli*, 2004; Genetics and Molecular Biology, 27: 442-453

Scott-Moncrieff, J.C., Shao, Z., Mitra, A.K., Enhancement of intestinal insulin absorption by bile salt-fatty acid mixed micelles in dogs, 1994; Journal of Pharmaceutical Sciences, 83(10): 1465-1469

Sebbage, V., Cell-penetrating peptides and their therapeutic applications, 2009; Bioscience Horizons, 2(1): 64-72

Shaji, J., Patole, V., Protein and Peptide Drug Delivery: Oral Approaches, 2008; Indian Journal of Pharmaceutical Sciences, 70(3): 269–277

Shao, Z., Li, Y., Chermak, T., Mitra, A. K., Cyclodextrins as mucosal absorption promoters of insulin. II. effects of beta-cyclodextrin derivatives on alphachymotryptic degradation and enteral absorption of insulin in rats, 1994; Pharmaceutical Research, 11(8): 1174-1179

Shapiro, A.M., Ricordi, C., Hering, B.J., Auchincloss, H., Lindblad, R., Robertson, R.P., et al., International trial of the edmonton protocol for islet transplantation, 2006; The New England Journal of Medicine, 355(13): 1318-1330

Shen, S.H., Multiple joined genes prevent product degradation in *Escherichia coli*, 1984; Proceedings of the National Academy of Science USA., 81: 4627–4631

Shu, S., Zhang, X., Teng, D., Wang, Z., Li, C., Polyelectrolyte nanoparticles based on water-soluble chitosan-poly(L-aspartic acid)-polyethylene glycol for controlled protein release, 2009; Carbohydrate Research, 344(10): 1197–1204

Shumilina, E.V., Shchipunov, Y.A., Chitosan-carrageenan gels, 2002; Colloid Journal, 64: 372–378

Sie, P., Cremens, B., Dupouy, D., Caranobe, C., Dol, F., Boneu, B., Neutralisation of Dermatan Sulfate *in Vitro* and *in Vivo* by Protamine Sulfate and Polybrene, 1989; Thrombosis Research, 54(1): 63-74

Silva, C.M., Ribeiro, A.J., Ferreira, D., Veiga, F., Insulin encapsulation in reinforced alginate microspheres prepared by internal gelation, 2006; European Journal of Pharmaceutical Sciences, 29: 148-159

Silva-Cunha, A., Chéron, J., Puisieux, F., Seiller, M., W/O/W multiple emulsions of insulin containing a protease inhibitor and an absorption enhancer: preparation, characterisation and determination of stability towards proteases *in vitro*, 1997; International Journal of Pharmaceutics, 158: 79-89

Sindhu, A., Bharath, S., Furtado, S., Deveswaran, R., Basavaraj, B.V., Development of and advances in insulin delivery, 2011; South African Pharmaceutical Journal, 78(6): 32–37

Sinding, C., Making the unit of insulin: Standards, clinical work, and industry, 1920-1925, 2002; Bulletin of the History of Medicine, 76(2): 231-270

Singh, S.M., Panda, A.K., Solubilisation and refolding of bacterial inclusion body proteins, 2005; J Biosci Bioeng, 99(4): 303-310

Sinha, V.R., Kumria, R., Polysaccharides in colon-specific drug delivery, 2001; International Journal of Pharmaceutics, 224: 19–38

Sivashanmugam, A., Murray, V., Cui, Ch., Zhang, Y., Wang, J., Li, Q., Practical protocols for production of very high yields of recombinant proteins using *Escherichia coli*, 2009; Protein Science, 18(5): 936–948

Snyder, E.L., Dowdy, S.F., Cell Penetrating Peptides in Drug Delivery, 2004; Pharmaceutical Research, 21(3): 389 – 393

Son, Y-J., Park, K-H., Lee, S-Y., Oh, S-J., Kim, Ch-K., Choi, B-T., Park, Y-Ch., Seo, J-Ch., Effects of temperature shift strategies on human preproinsulin production in the fed-batch fermentation of recombinant *Escherichia coli*, 2007; Biotechnology and Bioprocess Engineering, 12(5): 556-561

Sonaje, K., Chen, Y.J., Chen, H.L., Wey, S.P., Juang, J.H., Nguyen, H.N., Hsu, C.W., Lin, K.J., Sung, H.W., Enteric-coated capsules filled with freeze-dried chitosan/poly(gamma-glutamic acid) nanoparticles for oral insulin delivery, 2010; Biomaterials, 31(12): 3384-3394

Soni, M.L., Kumar, M., Namdeo, K.P., Sodium alginate microspheres for extending drug release: formulation and *in vitro* evaluation, 2010; International Journal of Drug Delivery, 2: 64-68

Sonia, T.A., Sharma, Ch.P., An overview of natural polymers for oral insulin delivery, 2012; Drug Discovery Today, 17(13/14): 784-792

Soppimath, K.S., Aminabhavi, T.M., Kulkarni, A.R., Rudzinski, W.E., Biodegradable polymeric nanoparticles as drug delivery devices, 2001; Journal of Controlled Release, 70(1-2): 1-20

Splith, K., Neundorf, I., Antimicrobial peptides with cell-penetrating peptide properties and vice versa, 2011; European Biophysics Journal, 40: 387-397

Strandberg, L., Enfors, S.O., Batch and fed batch cultivations for the temperature induced production of a recombinant protein in *Escherichia coli*, 1991; Biotechnology Letters, 13: 609-614

Studier, F.W., Moffatt, B.A., Use of bacteriophage T7 RNA polymerase to direct selective high-level expression of cloned genes, 1986; Journal of Molecular Biology,189(1):113-30

Studier, F.W., Protein production by auto-induction in high-density shaking cultures, 2005; Protein Expression and Purification, 41: 207-234

Subramani, K., Pathak, S., Hosseinkhani, H., Recent trends in diabetes treatment using nanotechnology, 2012; Digest Journal of Nanomaterials and Biostructures, 7(1): 85-95

Sung, W.L., Yao, F.L., Zahab, D.M., Narang, S.A., Short synthetic oligodeoxyribonucleotide leader sequences enhance accumulation of human proinsulin synthesised in *Escherichia coli*, 1986; Proceedings of the National Academy of Science USA, 83: 561–565

Suzuki, K., Ando, T., Studies on protamines XVI. The complete amino acid sequence of clupeine, 1972; The Journal of Biochemistry, 72: 1419–1432

Tabandeh, F., Shojaosadati, S.A., Yakhchali, B., Khodabandeh, M., Sanati, M.H., Evaluation of heat induction strategy for recombinant human growth hormone expression in fed-batch fermentation, 2005; Iranian Journal of Biotechnology, 3(1): 24 -30

Talmadge, K., Brosius, J., Gilbert, W., An internal signal sequence directs secretion and processing of proinsulin in bacteria, 1981; Nature, 294: 176–178

Tang, J., Hu, M., Production of human proinsulin in *E.coli* in a non-fusion form, 1993; Biotechnology Letters, 15: 661–666

Taylor, G., Hoare, M., Gray, D.R., Marston, F.A.O., Size and density of protein inclusion bodies, 1986; Biotechnology, 4: 553-557

Temsamani, J., Vidal, P., The use of cell-penetrating peptides for drug delivery, 2004; Drug Discoveries & Therapeutics, 9(23): 1012 - 1019

Thrimawithana, T.R., Young, S., Dunstan, D.E., Alany, R.G., Texture and rheological characterisation of kappa and iota carrageenan in the presence of counter ions, 2010; Carbohydrate Polymers, 82(1): 69-77

Thrimawithana, T.R., Young, S.A., Bunt, C.R., Geen, C.R., Alany, R.G., *In-vitro* and *in-vivo* evaluation of carrageenan/methylcellulose polymeric systems for transscleral delivery of macromolecules, 2011; European Journal of Pharmaceutical Sciences, 44(3): 399-409

Tikhonov, R.V., Pechenov, S.E., Belacheu, I.A., Yakimov, S.A., Klyushnichenko, V.E., Boldireva, E.F., Korobko, V.G., Tunes, H., Thiemann, J.E., Vilela, L., Wulfson, A.N., Recombinant human insulin VIII. Isolation of fusion protein-S-sulfonate, biotechnological precursor of human insulin, from the biomass of transformed *Escherichia coli* cells, 2001; Protein Expression and Purification, 21: 176–182

Tiyaboonchai, W., Woiszwillo, J., Sims, R.C., Middaugh, C.R., Insulin containing polyethylenimine-dextran sulphate nanoparticles, 2003; International Journal of Pharmaceutics, 225(1-2): 139-151

Tofteng, A.P., Jensen, K.J., Schäffer, I., Hoeg-Jensen, T., Total Synthesis of des B30 Insulin Analogues by Biomimetic Folding of Single-Chain Precursors, 2008; European Journal of Chemical Biology, 9: 2989-2996

Tønnesen, H.H., Karlsen, J., Alginate in Drug Delivery Systems, 2002; Drug Development and Industrial Pharmacy, 28(6): 621–630

Torchilin, V.P., Tatp-mediated intracellular delivery of pharmaceutical nanocarriers, 2007; Biochemical Society Transactions, 35: 816-820

Torchilin, V.P., Cell penetrating peptide-modified pharmaceutical nanocarriers for intracellular drug and gene delivery, 2008; Biopolymers, 90: 604-610

Trotta, M., Cavalli, R., Carlotti, M.E., Battaglia, L., Debernardi, F., Solid lipid micro-particles carrying insulin formed by solvent-in-water emulsion-diffusion technique, 2005; International Journal of Pharmaceutics, 288(2): 281-288

Tsuchida, E., Abe, K., Interactions between macromolecules in solution and intermacromolecular complexes, 1982; Advances in Polymer Science, 45: 1-119

Tsumoto, K., Ejima, D., Kumagai, I., Arakawac, T., Practical considerations in refolding proteins from inclusion bodies, 2002; Academic Press: Protein Expression and Purification, 28(1): 1-8

Tuteja, R., Type I signal peptidase: An overview, 2005; Archives of Biochemistry and Biophysics, 441: 107-111

Umerska, A.M., Formulation and characterisation of polyelectrolyte complex nanoparticles for the delivery of salmon calcitonin, 2012; PhD thesis, TCD;

Umerska, A., Paluch, K.J., Inkielewicz-Stepniak, I., Santos-Martinez, M.J., Corrigan, O.I., Medina, C., Tajber, L., Exploring the assembly process and properties of novel crosslinker-free hyaluronate-based polyelectrolyte complex nanocarriers, 2012; International Journal of Pharmaceutics, 436(1-2): 75-87

Van Breement, R.B., Li, Y., Caco-2 cell permeability assays to measure drug absorption, 2005; Expert Opinion on Drug Metabolism & Toxicology, 1(2): 175-85

Vallejo, L.F., Rinas, U., Strategies for the recovery of active proteins through refolding of bacterial inclusion body proteins, 2004; Microbial Cell Factories, 3:1-12

Vauthier, Ch., Bouchemal, K., Methods for the Preparation and Manufacture of Polymeric Nanoparticles, 2009; Pharmaceutical Research, 26(5): 1025-1058

Ventura, S., Villaverde, A., Protein quality in bacterial inclusion bodies, 2006; Trends in Biotechnology, 24(4): 179-185

Vishnevskaia, O.N., Burdin, D.V., Gorshkov, A.N., Grefner, N.M., Markov, A.G., Influence of protamine on expression of tight junction proteins in Caco-2, 2013; Russian Journal of Physiology, 99(1): 81-91

Vives, E., Brodin, P., Lebleu, B., A truncated HIV-1 Tat protein basic domain rapidly translocates through the plasma membrane and accumulates in the cell nucleus, 1997; The Journal of Biological Chemisty, 272: 16010-16017

Vives, E., Present and future of cell-penetrating peptide mediated delivery systems: "is the Trojan horse too wild to go only to Troy?", 2005; Journal of Controlled Release, 109: 77-85

Volontè, V., Piubelli, L., Pollegioni, L., Optimising HIV-1 protease production in *Escherichia coli* as a fusion protein, 2011; Microbial Cell Factories, 10: 53

Wadia, J.S., Dowdy, S.F., Transmembrane delivery of protein and peptide drugs by TAT-mediated transduction in the treatment of cancer, 2005; Advanced Drug Delivery Reviews, 57: 579-596

Walsh G., Therapeutic insulins and their large-scale manufacture, 2005; Applied Microbiology and Biotechnology, 67: 151-159

Walsh, G., Pharmaceutical Biotechnology. Concepts and Applications, 2007; Wiley & Sons, Ltd

Walther, C., Meyer, K., Rennert, R., Neundorf, I., Quantum dot-carrier peptide conjugates suitable for imaging and delivery applications, 2008; Bioconjugate Chemistyr, 19: 2346-2356

Wee, S., Gombotz, W.R., Protein release from alginate matrices, 2012; Advanced Drug Delivery Reviews, 31(3): 267-285

Weickert , M.J., Pagratis, M., Curry, S.R., Blackmore, R., Stabilisation of apoglobin by low temperature increases yield of soluble recombinant haemoglobin in *Escherichia coli*, 1997; Applied and Environmental Microbiology, 63: 4313 – 4320

White, J.R., Campbell, R.K., Inhaled Insulin: An Overview, 2001; Clinical Diabetes, 19(1): 13-16

Whitehead, K., Shen, Z., Mitragotri, S., Oral delivery of macromolecules using intestinal patches: applications for insulin delivery, 2004; Journal of Controlled Release, 98(1): 37-45

Whitehead, K., Karr, N., Mitragotri, S., Safe and Effective Permeation Enhancers for Oral Drug Delivery, 2008; Pharmaceutical Research, 25(8): 1782-1788

Winter, J., Lilie, H., Rudolph, R., Renaturation of human proinsulin-a study on refolding and conversion to insulin, 2002; Analytical Biochemistry, 310(2): 148-155

Winter, J., Neubauer, P., Glockshuber, R., Rudolph, R., Increase production of human proinsulin in the periplasmic space of Escherichia coli by fusion to DsbA, 2000; Journal of Biotechnology, 84: 175-185

Wong, T.W., Chitosan and Its Use in Design of Insulin Delivery System, 2009; Recent Patents on Drug Delivery and Formulation, 3: 8-25

Wu, Z.H., Ping, Q.N., Wei, Y., Lai, J.M., Hypoglycemic efficacy of chitosan-coated insulin liposomes after oral administration in mice, 2004; Chinese Pharmacological Society, 25(7): 966-972

Wu, S., Tao, Y., Zhang, H., Su, Z., Preparation and Characterisation of Water-Soluble Chitosan Microparticles Loaded with Insulin Using the Polyelectrolyte Complexation Method, 2011; Journal of Nanomaterials, 6 pages

Wunderlich, M., Glockshuber, R., *In vivo* control of redox potential during protein folding catalysed by bacterial protein disulfide-isomerase (DsbA), 1993; The Journal of Biological Chemistry, 268: 24547–24550

Xia, C.Q., Wang, J., Shen, W.C., Hypoglycemic effect of insulin-transferrin conjugate in streptozotocin-induced diabetic rats, 2000; The Journal of Pharmacology and Experimental Therapeutics, 295(2): 594-600

Xia, H., Gao, X., Gu, G., Liu, Z., Zeng, N., Hu, Q., Song, Q., Yao, L., Pang, Z., Jiang, X., Chen, J., Chen, H., Low molecular weight protamine – functionalised nanoparticles for drug delivery to the brain after intranasal administration, 2011; Biomaterials, 32: 9888 – 9898

Xiong, X.Y., Li, Y.P., Li, Z.L., Zhou, C.L., Tam, K.C., Liu, Z.Y., Zie, G.X., Vesicles from Pluronic/poly(lactic acid) block copolymers as new carriers for oral insulin delivery, 2007; Journal of Controlled Release, 120(1-2): 11-17

Xu, X., Fu, Y., Hu, H., Duan, Y., Zhang, Z., Quantitative determination of insulin entrapment efficiency in triblock copolymeric nanoparticles by high-performance liquid chromatography, 2006, Journal of Pharmaceutical and Biomedical Analysis, 41: 266-273

Yamagata, T., Morishita, M., Kavimandan, M.J., Nakamura, K., Fukuoka, Y., Takayama, K., Peppas, N.A., Characterisation of insulin protection properties of complexation hydrogels in gastric and intestinal enzyme fluids, 2006; Journal of Controlled Release, 112(3): 343-349

Yamamoto, A., Taniguchi, T., Rikyuu, K., Tsuji, T., Fujita, T., Murakami, M., Muranishi, S., Effects of various protease inhibitors on the intestinal absorption and degradation of insulin in rats, 1994; Pharmaceutical Research, 11(10): 1496-1500

Yan, L., Wang, H.Y., Jiang, Y.F., Wang, Z., Liu, J.H., Yang, Y.X., Huang, S.W., Huang, Y.Z., Cell-penetrating Peptide-modified PLGA Nanoparticles for Enhanced Nose-to-brain Macromolecular Delivery, 2013; Macromolecular Research, 21(4): 435-441

Yang, Y.X., Jiang, Y.F., Wang, Z., Liu, J.H., Yan, L., Ye, J.X., Huang, Y.Z., Skin-permeable quaternary nanoparticles with layer-by-layer structure enabling improved gene delivery, 2012; Journal of Materials Chemistry, 22: 10029-10034

Yeo, Y., Baek, N., Park, K., Microencapsulation methods for delivery of protein drugs, 2001; Biotechnology and Bioprocess Engineering, 6(4): 213 – 230

Yeo, Y., Park, K., Control of Encapsulation Efficiency and Initial Burst in Polymeric Microparticle Systems, 2004; Archives of Pharmacal Research, 27(1): 1-12

Zalfen, A.M., Nizet, D., Jerome, C., Jerome, R., Frankenne, F., Foidart, J.M., Maquet, V., Lecomte, F., Hubert, P., Evrard, B., Controlled release of drugs from multi-component biomaterials, 2008; Acta Biomaterialia, 4(6): 1788-1796

Zapun, A., Creighton, T.E., Effects of DsbA on the disufide folding of bovine pancreatic trypsin inhibitor an a-lactalbumin, 1994; Biochemistry, 33: 5202–5211

Zhang, N., Li, J., Jiang, W., Ren, Ch., Li, J., Xin, J., Li, K., Effective protection and controlled release of insulin by cationic β-cyclodextrin polymers from alginate/chitosan nanoparticles, 2010; Pharmaceutical Nanotechnology, 393: 212-218

Zhang, N., Ping, Q.N., Huang, G.H., Xu, W.F., Investigation of lectin-modified insulin liposomes as carriers for oral administration, 2005; International Journal of Pharmaceutics, 294(1-2): 247-259

Zhang, Y., Wei, W., Lv, P., Wang, L., Maa, G., Preparation and evaluation of alginate-chitosan microspheres for oral delivery of insulin, 2011; European Journal of Pharmaceutics and Biopharmaceutics, 77: 11–19

Ziv, E., Lior, O., Kidron, M., Absorption of protein via the intestinal wall. A quantitative model, 1987; Biochemical Pharmacology, 36: 1035-1039

Zorko, M., Langel, U., Cell-penetrating peptides: mechanism and kinetics of cargo delivery, 2005; Adv. Drug Deliv. Rev., 57: 529-545

Zoeller T., Klein S., Simplified Biorelevant Media for Screening Dissolution Performance of Poorly Soluble Drugs, 2007; Dissolution Technologies, 8-13

Zündorf, I., Dingermann, T., From cattle, swine, and horse insulin to human insulin: the biotechnology and genetic technology of insulin production, 2001; Pharmazie in. Unserer Zeit, 30(1): 27-32

APPENDICES

APPENDIX A Characterisation of alginate/ protamine carriers

Table A.1 *Particle size, polydispersity (PdI), zeta potential (ZP), pH and viscosity of NPs composed of alginic acid low viscosity (AAL) and protamine (P). 0.1% w/v solutions of both components were used.*

AAL/P weight ratio	Particle size [nm]	PdI	ZP [mV]	pH	Viscosity [mPa·s]
	After preparation				
15	167±1	0.306±0.026	-67.2±7.4	6.46	2.20±0.16
12	160±9	0.301±0.042	-71.7±3.7	6.38	2.07±0.08
10	191±5	0.242±0.018	-66.6±7.9	6.44	2.04±0.05
8	141±1	0.258±0.008	-66.7±4.4	6.44	2.11±0.13
7.5	152±4	0.294±0.040	-50.4±3.0	6.46	2.02±0.19
6	127±1	0.268±0.019	-62.6±4.5	6.43	1.89±0.14
5	134±2	0.270±0.008	-62.2±4.5	6.46	1.80±0.14
4.5	122±13	0.255±0.020	-65.7±4.3	6.28	1.72±0.12
3	110±8	0.224±0.013	-60.8±2.5	6.33	1.57±0.11
2.5	106±10	0.212±0.015	-56.8±4.8	6.30	1.44±0.13
2	128±28	0.188±0.014	-59.1±4.0	6.26	1.32±0.11
1.5	116±19	0.162±0.017	-55.8±2.6	6.24	1.17±0.12
1	162±12	0.123±0.019	-52.5±1.4	6.11	1.03±0.15
0.95	163±2	0.125±0.020	-51.6±0.7	6.25	0.81±0.02
0.91	168±2	0.120±0.026	-51.5±2.7	6.12	0.74±0.08
0.87	332±1	0.368±0.017	-36.7±0.7	6.02	0.78±0.04
0.83	A	A	A	5.99 A	0.80±0.08 A
0.80	A	A	A	5.94 A	0.82±0.02 A
0.77	A	A	A	5.77 A	0.77±0.05 A
0.74	A	A	A	5.71 A	0.82±0.02 A
0.71	A	A	A	5.71 A	0.85±0.06 A
0.69	A	A	A	5.67 A	0.80±0.03 A
0.67	A	A	A	5.70 A	0.98±0.10 A
0.50	A	A	A	5.69 A	0.93±0.08 A
0.40	212±34	0.146±0.038	17.8±1.0	5.74	0.94±0.12
0.33	180±25	0.115±0.036	18.0±0.7	5.85	0.95±0.11
0.22	191±23	0.150±0.022	18.6±0.6	5.84	0.99±0.10
0.20	145±1	0.111±0.019	17.6±0.3	5.91	0.85±0.05
0.17	150±1	0.193±0.003	16.4±0.5	5.92	0.92±0.03
0.13	139±1	0.096±0.018	17.8±0.5	5.81	0.86±0.04
0.125	140±1	0.077±0.009	18.7±0.3	5.78	0.95±0.04
0.100	135±1	0.142±0.006	16.7±1.3	5.56	1.00±0.01
0.083	125±1	0.111±0.010	18.5±0.5	5.54	0.87±0.03
0.067	134±2	0.180±0.013	18.4±0.5	5.60	0.94±0.03

A - aggregates formed

Table A.2 *Particle size, polydispersity (PdI), zeta potential (ZP), pH and viscosity of NPs composed of alginic acid low viscosity (AAL) and protamine (P). 0.1% w/v solutions of both components were used. pH of P solution was adjusted to 2 (P_pH2). Preparation method* ***1A****: an aliquot of P solution was added to the aliquot of AAL solution under magnetic stirring.*

AAL/P_pH2 weight ratio	Particle size [nm]	PdI	ZP [mV]	pH	Viscosity [mPa·s]
	After preparation				
15	283±12	0.253±0.020	-59.3±4.1	4.64	1.69±0.16
12	259±3	0.244±0.012	-61.2±4.0	4.58	1.62±0.16
10	265±2	0.248±0.011	-61.7±3.5	4.43	1.55±0.21
8	256±5	0.274±0.008	-54.0±0.6	4.19	1.43±0.12
7.5	253±4	0.284±0.021	-53.5±1.7	4.13	1.31±0.08
6	231±11	0.219±0.026	-44.4±1.0	3.82	1.22±0.09
5	228±6	0.228±0.031	-36.5±1.8	3.60	1.07±0.15
4.5	248±2	0.222±0.014	-42.3±5.6	3.55	1.02±0.11
3	235±12	0.205±0.037	-36.8±3.2	3.12	0.83±0.08
2.5	A	A	A	2.96 A	0.87±0.06 A
2	A	A	A	n/d	n/d
1.5	A	A	A	n/d	n/d
1	A	A	A	n/d	n/d
0.67	A	A	A	n/d	n/d
0.5	A	A	A	n/d	n/d
0.4	A	A	A	n/d	n/d
0.33	A	A	A	n/d	n/d
0.22	A	A	A	n/d	n/d
0.2	A	A	A	n/d	n/d
0.17	A	A	A	n/d	n/d
0.13	A	A	A	n/d	n/d
0.125	A	A	A	n/d	n/d
0.100	A	A	A	n/d	n/d
0.830	A	A	A	n/d	n/d
0.067	A	A	A	n/d	n/d

A - aggregates formed, n/d - not determined

Table A.3 *Particle size, polydispersity (PdI), zeta potential (ZP), pH and viscosity of NPs composed of alginic acid low viscosity (AAL) and protamine (P). 0.1% w/v solutions of both components were used. pH of P solution was adjusted to 2 (P_pH2). Preparation method* ***1B****. An aliquot of AAL solution was introduced to the aliquot of P solution under magnetic stirring.*

AAL/P_pH2 weight ratio	Particle size [nm]	PdI	ZP [mV]	pH	Viscosity [mPa·s]
	After preparation				
15	330±5	0.287±0.004	-68.1±1.2	4.83	1.40±0.06
12	321±9	0.308±0.049	-65.9±1.1	4.59	1.21±0.02
10	364±5	0.342±0.037	-44.5±1.3	4.50	1.19±0.10
8	444±7	0.290±0.008	-57.7±1.1	4.25	1.09±0.08
7.5	365±6	0.291±0.028	-59.7±1.6	4.18	1.05±0.14
6	432±8	0.288±0.021	-54.3±1.1	3.86	0.95±0.06
5	423±10	0.227±0.016	-51.4±0.9	3.66	1.11±0.08
4.5	A	A	A	3.52 A	1.06±0.03 A
3	A	A	A	n/d	n/d
2.5	A	A	A	n/d	n/d
2	A	A	A	n/d	n/d
1.5	A	A	A	n/d	n/d
1	A	A	A	n/d	n/d
0.67	A	A	A	n/d	n/d
0.50	A	A	A	n/d	n/d
0.40	A	A	A	n/d	n/d
0.33	A	A	A	n/d	n/d
0.22	A	A	A	n/d	n/d
0.20	A	A	A	n/d	n/d
0.17	A	A	A	n/d	n/d
0.13	A	A	A	n/d	n/d
0.125	A	A	A	n/d	n/d
0.100	A	A	A	n/d	n/d

A - aggregates formed, n/d - not determined

Table A.4 *Particle size, polydispersity (PdI), zeta potential (ZP), pH and viscosity of NPs composed of alginic acid low viscosity (AAL) and protamine P. 0.1% w/v solutions of both components were used. pH of P solution was adjusted to 3 (P_pH3). Preparation method* ***1A****: an aliquot of P solution was added to the aliquot of AAL solution under magnetic stirring.*

AAL/P_pH3 weight ratio	Particle size [nm]	PdI	ZP [mV]	pH	Viscosity [mPa·s]
	After preparation				
15	151±0	0.321±0.077	-57.9±11	5.96	2.08±0.07
12	175±16	0.374±0.049	-63.3±3.3	5.89	2.15±0.07
10	167±10	0.377±0.033	-57.0±11.0	5.90	2.12±0.16
8	141±6	0.369±0.064	-65.4±6.2	5.80	2.09±0.25
7.5	146±19	0.402±0.027	-57.5±21.5	5.73	1.80±0.17
6	133±19	0.370±0.029	-48.9±12.8	5.65	1.53±0.06
5	122±9	0.262±0.043	-62.0±6.9	5.64	1.53±0.15
4.5	114±7	0.255±0.043	-54.8±1.8	5.54	1.43±0.08
3	145±9	0.286±0.075	-48.7±5.5	5.38	1.29±0.08
2.5	123±3	0.263±0.065	-52.6±3.5	5.23	1.12±0.08
2	103±2	0.223±0.031	-56.0±2.6	5.02	1.08±0.08
1.5	132±1	0.163±0.023	-51.2±4.0	4.74	0.86±0.09
1	A	A	A	3.82 A	0.80±0.11 A
0.67	254±7	0.168±0.059	16.9±0.9	3.49	0.74±0.13
0.50	181±10	0.200±0.159	18.4±0.8	3.43	0.79±0.12
0.40	177±7	0.120±0.024	18.7±1.0	3.42	0.78±0.13
0.33	168±5	0.119±0.013	19.7±0.8	3.38	0.77±0.10
0.22	160±4	0.124±0.018	20.3±0.8	3.34	0.78±0.14
0.20	159±12	0.107±0.051	20.3±1.6	3.29	0.78±0.12
0.167	154±5	0.115±0.033	19.0±1.6	3.30	0.79±0.08
0.133	145±4	0.196±0.049	20.4±1.2	3.27	0.78±0.07
0.125	144±8	0.162±0.019	20.0±1.5	3.28	0.84±0.16
0.100	153±14	0.221±0.029	20.5±0.9	3.26	0.77±0.15

A - aggregates formed

Table A.5 *Particle size, polydispersity (PdI), zeta potential (ZP), pH and viscosity of NPs composed of alginic acid low viscosity (AAL) and protamine P. 0.1% w/v solutions of both components were used. pH of P solution was adjusted to 3 (P_pH3). Preparation method* ***1B****: an aliquot of AAL solution was introduced to the aliquot of P solution under magnetic stirring.*

AAL/P_pH3 weight ratio	Particle size [nm]	PdI	ZP [mV]	pH	Viscosity [mPa·s]
	After preparation				
6	273±2	0.316±0.027	-45.5±1.5	5.68	1.89±0.15
5	271±2	0.271±0.014	-47.4±3.0	5.55	1.77±0.07
4	207±1	0.208±0.006	-48.1±1.9	5.48	1.71±0.08
3	205±1	0.202±0.015	-47.3±1.4	5.31	1.42±0.04
2.5	208±2	0.191±0.013	-53.7±0.7	5.22	1.28±0.04
2	196±4	0.181±0.020	-56.4±0.8	5.02	1.18±0.04
1.5	180±1	0.165±0.008	-45.2±0.7	4.77	0.98±0.04
1	A	A	A	3.77 A	0.91±0.05 A
0.67	183±2	0.105±0.023	18.3±0.4	3.48	0.94±0.05
0.50	148±2	0.132±0.013	17.7±0.5	3.38	0.83±0.04
0.40	140±2	0.126±0.021	19.2±0.3	3.34	0.96±0.07
0.33	138±1	0.122±0.009	17.6±0.6	3.31	0.93±0.04
0.25	112±2	0.145±0.013	18.3±0.6	3.29	0.88±0.02
0.20	146±4	0.281±0.014	20.3±0.5	3.23	0.86±0.06
0.167	109±1	0.211±0.006	19.0±0.3	3.29	0.93±0.06

A - aggregates formed

Table A.6 *Particle size, polydispersity (PdI), zeta potential (ZP), pH and viscosity of NPs composed of alginic acid medium viscosity (AAM) and protamine (P). 0.1% w/v solutions of both components were used. Preparation method* ***1A****: an aliquot of P solution was added to the aliquot of AAM solution under magnetic stirring.*

AAM/P weight ratio	Particle size [nm]	PdI	ZP [mV]	pH	Viscosity [mPa·s]
	After preparation				
15	241±13	0.412±0.015	n/d	6.69	3.86±0.22
12	343±10	0.418±0.030	n/d	6.66	3.73±0.05
10	200±2	0.414±0.005	-72.8±1.1	6.65	3.47±0.11
8	213±1	0.442±0.004	n/d	6.61	3.02±0.18
7.5	183±1	0.412±0.008	-60.7±1.2	6.67	3.11±0.24
6	179±2	0.425±0.010	n/d	6.58	2.69±0.05
5	211±3	0.461±0.020	-52.3±9.0	6.66	2.52±0.09
4.5	279±30	0.303±0.003	-72.0±1.5	6.60	2.54±0.20
3	258±6	0.285±0.011	-67.4±1.6	6.54	2.10±0.12
2.5	234±14	0.293±0.017	-65.6±1.0	6.51	1.88±0.15
2	213±27	0.258±0.010	-65.1±2.1	6.46	1.62±0.15
1.5	213±18	0.230±0.010	-59.7±1.7	6.46	1.29±0.14
1	218±25	0.150±0.018	-47.6±3.7	6.35	0.91±0.09
0.95	176±2	0.119±0.017	-48.7±1.2	6.37	0.77±0.03
0.91	184±2	0.107±0.014	-47.3±0.3	6.37	0.76±0.02
0.87	A	A	A	6.31 A	0.75±0.01 A
0.83	A	A	A	6.24 A	0.78±0.02 A
0.80	A	A	A	6.26 A	0.77±0.01 A
0.77	A	A	A	6.22 A	0.80±0.03 A
0.74	236±4	0.171±0.035	16.0±0.5	6.26	0.80±0.03
0.71	230±5	0.132±0.014	17.0±0.3	6.25	0.79±0.03
0.69	368±8	0.318±0.015	18.1±0.7	6.28	0.80±0.01
0.67	228±9	0.209±0.032	18.4±0.4	6.00	0.88±0.08
0.50	207±10	0.183±0.020	19.1±0.5	6.02	0.90±0.10
0.40	229±22	0.135±0.024	19.1±0.3	6.04	0.89±0.09
0.33	194±8	0.131±0.028	18.3±0.5	6.08	0.75±0.06
0.22	187±16	0.119±0.026	19.3±1.0	6.03	0.84±0.09
0.20	148±1	0.149±0.014	18.8±0.6	6.14	0.78±0.01
0.17	142±2	0.110±0.020	19.8±0.4	6.13	0.83±0.02
0.13	140±2	0.172±0.014	19.6±0.8	6.09	0.83±0.01
0.125	135±2	0.134±0.007	20.6±0.4	6.11	0.86±0.02
0.100	161±4	0.254±0.004	19.2±1.0	6.01	0.94±0.05
0.083	148±1	0.241±0.002	n/d	6.01	0.90±0.03
0.067	129±2	0.193±0.018	n/d	6.01	0.90±0.05

A - aggregates formed, n/d - not determined

Table A.7 *Particle size, polydispersity (PdI), zeta potential (ZP), pH and viscosity of NPs composed of alginic acid medium viscosity (AAM) and protamine (P). 0.1% w/v solutions of both components were used. Preparation method* ***1B****: an aliquot of AAM solution was introduced to the aliquot of P solution under magnetic stirring.*

AAM/P weight ratio	Particle size [nm]	PdI	ZP [mV]	pH	Viscosity [mPa·s]
	After preparation				
5	275±2	0.286±0.009	-70.5±1.4	6.42	3.08±0.27
3	260±5	0.339±0.053	-60.0±0.9	6.31	2.57±0.09
1.5	214±2	0.262±0.012	-61.2±0.7	5.78	1.46±0.02
1	181±2	0.138±0.042	-49.3±0.6	6.17	0.96±0.13
0.67	171±1	0.076±0.043	16.1±0.4	6.07	0.93±0.03
0.33	125±0	0.107±0.028	17.8±0.5	6.05	0.85±0.02
0.20	135±1	0.193±0.025	19.8±0.5	6.08	0.90±0.02

Table A.8 *Particle size, polydispersity (PdI), zeta potential (ZP), pH and viscosity of NPs composed of alginic acid medium viscosity (AAM) and protamine P. 0.1% w/v solutions of both components were used. pH of P solution was adjusted to 3 (P_pH3). Preparation method* ***1A****: an aliquot of P solution was added to the aliquot of AAM solution under magnetic stirring.*

AAM/P_pH3 weight ratio	Particle size [nm]	PdI	ZP [mV]	pH	Viscosity [mPa·s]
	After preparation				
15	236±20	0.455±0.026	-77.3±4.5	5.82	3.17±0.32
12	229±14	0.445±0.024	-78.5±1.4	5.67	3.27±0.21
10	203±19	0.408±0.049	-72.0±7.3	5.66	2.95±0.15
8	224±11	0.420±0.044	-71.7±4.5	5.53	3.03±0.25
7	159±3	0.377±0.059	-68.1±1.5	5.45	2.78±0.18
6	174±14	0.353±0.043	-69.9±3.6	5.36	2.58±0.15
5	178±10	0.365±0.063	-67.2±3.2	5.21	2.34±0.22
4	153±2	0.310±0.057	-65.5±3.9	5.06	2.14±0.30
3	138±7	0.275±0.016	-60.0±4.8	4.82	1.77±0.24
2.5	129±8	0.237±0.015	-57.0±4.1	4.62	1.44±0.26
2	128±11	0.216±0.027	-51.4±1.4	4.60	1.28±0.19
1.5	137±12	0.135±0.023	-44.3±7.2	4.18	0.94±0.14
1	A	A	A	3.46 A	0.89±0.05 A
0.67	184±2	0.112±0.048	19.4±1.2	3.29	0.88±0.03
0.50	170±3	0.090±0.018	21.9±0.6	3.21	0.84±0.07
0.40	162±2	0.081±0.018	21.4±0.8	3.16	0.87±0.04
0.33	155±6	0.085±0.028	22.3±1.1	3.14	0.89±0.02
0.25	146±1	0.094±0.011	21.2±0.2	3.09	0.86±0.08
0.20	149±4	0.080±0.018	24.4±1.1	3.08	0.87±0.08
0.167	148±1	0.089±0.021	24.6±0.5	2.98	0.94±0.02
0.143	137±0	0.091±0.014	22.5±0.8	3.04	0.86±0.11
0.125	139±1	0.061±0.025	23.8±1.1	2.97	0.78±0.04
0.100	130±4	0.100±0.018	23.0±2.1	3.06	0.83±0.09
0.083	127±1	0.094±0.006	20.8±0.4	3.01	0.77±0.04

A - aggregates formed

Table A.9 *Particle size, polydispersity (PdI), zeta potential (ZP), pH and viscosity of NPs composed of alginic acid medium viscosity (AAM) and protamine P. 0.1% w/v solutions of both components were used. pH of P solution was adjusted to 3 (P_pH3). Preparation method* ***1B****: an aliquot of AAM solution was introduced to the aliquot of P solution under magnetic stirring.*

AAM/P_pH3 weight ratio	Particle size [nm]	PdI	ZP [mV]	pH	Viscosity [mPa·s]
	After preparation				
6	270±5	0.270±0.010	-68.0±1.1	5.58	2.80±0.20
5	254±2	0.277±0.005	-68.1±2.0	5.49	2.54±0.08
4	254±1	0.273±0.026	-69.2±1.7	5.39	2.00±0.22
3	225±1	0.240±0.015	-63.1±1.1	5.23	1.90±0.17
2.5	218±2	0.231±0.008	-56.9±1.9	5.09	1.65±0.09
2	200±2	0.207±0.007	-55.7±1.2	4.88	1.35±0.11
1.5	179±1	0.140±0.015	-43.9±1.1	4.52	1.00±0.05
1	A	A	A	3.59 A	0.91±0.04 A
0.67	147±1	0.065±0.026	18.0±0.5	3.36	0.86±0.07
0.50	121±2	0.065±0.010	19.1±0.7	3.29	0.85±0.04
0.40	123±2	0.066±0.007	20.7±0.2	3.24	0.83±0.01
0.33	112±1	0.045±0.018	19.6±1.1	3.19	0.81±0.01
0.25	100±1	0.057±0.016	18.9±0.6	3.19	0.83±0.03
0.20	99±1	0.112±0.013	20.8±0.8	3.18	0.86±0.04
0.17	89±2	0.077±0.018	16.3±1.1	3.20	0.85±0.02

A - aggregates formed

APPENDIX B Characterisation of carrageenan/ protamine carriers

Table B.1 *Particle size, polydispersity (PdI), zeta potential (ZP), pH and viscosity of NPs composed of κ - carrageenan (KC) and protamine (P). 0.1% w/v solutions of both components were used.*

KC/P weight ratio	Particle size [nm]	PdI	ZP [mV]	pH	Viscosity [mPa·s]
	After preparation				
5	385±20	0.750±0.140	-65.3±2.7	6.62	2.54±0.07
3	337±8	0.510±0.070	-59.3±0.9	6.62	1.44±0.10
2.5	376±21	0.470±0.060	-51.9±1.0	6.51	0.82±0.06
1.0	A	A	A	6.37 A	0.70±0.06 A
0.50	A	A	A	6.22 A	0.77±0.02 A
0.33	A	A	A	6.19 A	0.76±0.02 A

A - aggregates formed

Table B.2 *Particle size, polydispersity (PdI), zeta potential (ZP), pH and viscosity of NPs composed* of λ - carrageenan (LC) and protamine *(P). 0.1% w/v solutions of both components were used.*

LC/P weight ratio	Particle size [nm]	PdI	ZP [mV]	pH	Viscosity [mPa·s]
	After preparation				
5	264±2	0.490±0.010	-59.4±33	6.71	2.26±0.10
3	263±8	0.390±0.020	-61.4±1.8	6.82	1.42±0.04
1	A	A	A	6.77 A	0.95±0.09 A
0.50	251±18	0.290±0.020	16.3±0.5	6.45	0.69±0.02
0.33	237±14	0.270±0.010	18.9±0.6	6.41	0.71±0.04
0.20	241±6	0.270±0.010	19.0±0.8	6.32	0.61±0.01

A - aggregates formed

Table B.3 *Particle size, polydispersity (PdI), zeta potential (ZP), pH and viscosity of NPs composed of ι - carrageenan (IC) and protamine (P). 0.1% w/v solutions of both components were used.*

IC/P weight ratio	Particle size [nm]	PdI	ZP [mV]	pH	Viscosity [mPa·s]
	After preparation				
5	246±4	0.410±0.030	-40.6±0.3	7.00	1.98±0.03
4	200±6	0.360±0.050	-38.8±0.9	n/d	n/d
3	183±3	0.310±0.010	-38.7±0.7	6.15	1.69±0.05
2	197±2	0.260±0.010	-37.8±0.4	6.23	1.22±0.02
1	A	A	A	6.09 A	0.96±0.08 A
0.50	180±3	0.100±0.020	17.6±0.3	6.01	1.02±0.00
0.33	160±1	0.090±0.010	18.3±0.6	6.05	1.05±0.02
0.25	136±1	0.100±0.010	19.4±0.8	n/d	n/d
0.20	151±1	0.190±0.010	18.6±0.4	n/d	n/d

A - aggregates formed, n/d – not determined

Table B.4 *Particle size, polydispersity (PdI), zeta potential (ZP), pH and viscosity of NPs composed of κ - carrageenan (KC) and protamine (P).* ***0.05% w/v*** *solutions of both components were used.*

KC/P weight ratio	Particle size [nm]	PdI	ZP [mV]	pH	Viscosity [mPa·s]
	After preparation				
5	176±5.	0.460±0.070	-52.5±1.9	6.74	1.79
4	160±8	0.410±0.030	-52.5±2.4	6.62	1.96
3	156±2	0.320±0.050	-48.0±1.1	6.50	1.66
2	276±3	0.390±0.050	-35.7±0.9	6.34	1.08
1	438±14	0.460±0.030	18.5±0.4	6.23	1.10
0.50	246±7	0.270±0.003	21.2±0.6	6.12	1.59
0.33	197±4	0.270±0.030	20.1±0.4	5.99	1.25
0.25	174±3	0.240±0.010	20.8±0.8	6.06	1.09
0.20	150±3	0.210±0.030	21.0±0.5	6.14	1.04

Table B.5 *Particle size, polydispersity (PdI), zeta potential (ZP), pH and viscosity of NPs composed of ι - carrageenan (IC) and protamine P. 0.1% w/v solutions of both components were used. pH of P solution was adjusted to 3 (P_pH3).*

IC/P_pH3 weight ratio	Particle size [nm]	PdI	ZP [mV]	pH	Viscosity [mPa·s]
	After preparation				
7	430±23	0.468±0.0.54	n/d	n/d	n/d
5	319±80	0.427±0.037	-42.9±2.7	6.35	1.94
4	201±19	0.319±0.017	-36.3±3.0	4.08	1.76
3	246±52	0.257±0.012	-39.3±1.7	3.88	1.57
2	238±33	0.268±0.033	-38.3±0.9	3.78	1.21
1	A	A	A	3.44 A	1.14 A
0.50	161±2	0.079±0.019	19.2±1.1	3.25	1.02
0.33	162±12	0.160±0.042	17.5±1.3	3.26	1.02
0.25	162±3	0.198±0.047	18.0±2.1	3.16	1.04
0.20	170±2	0.177±0.044	22.1±0.5	n/d	n/d
0.14	208±1	0.299±0.021	n/d	n/d	n/d

A - aggregates formed, n/d – not determined

Table B.6 *Particle size, polydispersity (PdI), zeta potential (ZP), pH and viscosity of NPs composed of λ -* carrageenan (LC) *and protamine P. 0.1% w/v solutions of both components were used. pH of P solution was adjusted to 3 (P_pH3).*

LC/P_pH3 weight ratio	Particle size [nm]	PdI	ZP [mV]	pH	Viscosity [mPa·s]
	After preparation				
7	672±37	0.715±0.157	-72.4±4.7	n/d	n/d
5	520±25	0.588±0.048	-63.7±6.4	6.19	4.91
4	438±11	0.560±0.037	-64.3±4.5	5.43	4.36
3	349±8	0.485±0.027	-59.9±1.6	4.66	3.38
2	287±7	0.320±0.023	-48.8±3.4	4.23	2.32
1	A	A	A	3.58 A	1.12 A
0.33	506±146	0.430±0.088	16.6±0.2	3.24	0.77
0.25	981±184	0.673±0.065	16.8±0.4	3.20	0.95

A - aggregates formed, n/d – not determined

APPENDIX C *In vitro* characterisation of AAL/P_pH3 and IC/P_pH3 NPs loaded with insulin

Table C.1 *Characterisation of AAL/P_pH3 NPs loaded with **100 µg/ml** of insulin after preparation and reconstitution following filtration/centrifugation.*

AAL/P_pH3 weight ratio	Particle size [nm]		PdI		ZP [mV]	
	after preparation	after reconstitution	after preparation	after reconstitution	after preparation	after reconstitution
5	145±17	170±34	0.274±0.056	0.262±0.032	-64.7±3.4	-60.3±5.4
1.5	140±1	156±1	0.149±0.016	0.198±0.011	-37.3±1.9	-53.7±0.4
0.5	228±5	185±3	0.206±0.017	0.174±0.022	19.2±0.3	11.3±0.7
0.2	160±15	141±12	0.144±0.061	0.112±0.067	20.9±1.1	20.8±1.3

Table C.2 *Characterisation of AAL/P_pH3 NPs loaded with **500 µg/ml** of insulin after preparation and reconstitution following filtration/centrifugation.*

AAL/P_pH3 weight ratio	Particle size [nm]		PdI		ZP [mV]	
	after preparation	after reconstitution	after preparation	after reconstitution	after preparation	after reconstitution
5	236±31	252±39	0.365±0.080	0.421±0.104	-62.7±3.9	-60.7±8.3
0.2	173±15	169±24	0.202±0.025	0.182±0.042	21.8±1.0	15.5±3.1

Table C.3 *Characterisation of AAL/P_pH3 NPs loaded with* ***100 µg/ml*** *of insulin after release to the following media: 0.01 M HCl, 0.1 M acetate buffer, 0.01 M PBS.*

AAL/P_pH3 weight ratio	Particle size [nm]			
	after preparation	After release studies		
		to 0.01M HCl	to 0.1M acetate	to 0.01M PBS
5	131±8	310±55	322±26	343±67
0.2	136±11	520±42	A	A
AAL/P_pH3 weight ratio	PdI			
	after preparation	After release studies		
		to 0.01M HCl	to 0.1M acetate	to 0.01M PBS
5	0.244±0.014	0.488±0.117	0.333±0.050	0.274±0.038
0.2	0.199±0.066	0.442±0.033	A	A
AAL/P_pH3 weight ratio	ZP [mV]			
	after preparation	After release studies		
		to 0.01M HCl	to 0.1M acetate	to 0.01M PBS
5	-62.6±2.7	12.9±5.3	-37.6±4.5	-15.5±2.3
0.2	21.5±0.7	23.6±1.1	A	A

A - aggregates formed

Table C.4 *Characterisation of AAL/P_pH3 NPs loaded with* ***100 µg/ml*** *of insulin after release to FaSSIF.*

AAL/P_pH3 weight ratio	Particle size [nm]		PdI		ZP [mV]	
	after preparation	after release to FaSSIF	after preparation	after release to FaSSIF	after preparation	after release to FaSSIF
5	139±24	58±5	0.266±0.022	0.233±0.039	-61.6±4.2	-24.6±2.4
0.2	168±12	204±9	0.113±0.035	0.289±0.052	21.7±1.0	-28.4±1.6
Pure FaSSIF	70±12	-	0.201±0.037	-	-10.9±4.4	-

Table C.5 *Characterisation of AAL/P_pH3 NPs loaded with* ***500 µg/ml*** *of insulin after release to the following media: 0.01 M HCl, 0.1 M acetate buffer, 0.01 M PBS.*

AAL/P_pH3 weight ratio	Particle size [nm]			
	after preparation	After release studies		
		to 0.01 M HCl	to 0.1 M acetate	to 0.01 M PBS
5	164±2	479±66	327±6	310±24
0.2	178±2	A	A	A
AAL/P_pH3 weight ratio	PdI			
	after preparation	After release studies		
		to 0.01 M HCl	to 0.1 M acetate	to 0.01 M PBS
5	0.283±0.011	0.421±0.058	0.244±0.023	0.299±0.013
0.2	0.118±0.012	A	A	A
AAL/P_pH3 weight ratio	ZP [mV]			
	after preparation	After release studies		
		to 0.01 M HCl	to 0.1 M acetate	to 0.01 M PBS
5	-66.2±1.6	10.8±0.5	-19.9±3.3	-17.1±3.6
0.2	23.4±0.5	A	A	A

A - aggregates formed

Table C.6 *Characterisation of IC/P_pH3 NPs loaded with **100 µg/ml** of insulin after preparation and reconstitution following filtration/centrifugation.*

IC/P_pH3 weight ratio	Particle size [nm]		PdI		ZP [mV]	
	After preparation	After reconstitution	After preparation	After reconstitution	After preparation	After reconstitution
4	357±79	379±56	0.383±0.057	0.449±0.074	-41.4±2.7	-43.1±2.7
2	306±67	341±58	0.250±0.018	0.316±0.065	-33.2±3.3	-32.5±2.5
0.2	158±16	169±41	0.142±0.033	0.222±0.055	18.0±1.6	19.3±4.2

Table C.7 *Characterisation of IC/P_pH3 NPs loaded with **500 µg/ml** of insulin after preparation and reconstitution following filtration/centrifugation.*

IC/P_pH3 weight ratio	Particle size [nm]		PdI		ZP [mV]	
	After preparation	After reconstitution	After preparation	After reconstitution	After preparation	After reconstitution
4	465±99	481±27	0.620±0.083	0.494±0.100	-45.5±2.7	-43.0±4.7
2	403±67	339±59	0.457±0.098	0.369±0.060	-38.9±3.1	-35.3±8.9
0.2	182±13	192±79	0.169±0.258	0.258±0.115	20.0±1.8	12.4±2.2

Table C.8 *Characterisation of IC/P_pH3 NPs loaded with* ***100 µg/ml*** *of insulin after release to the following media: 0.01 M HCl, 0.1 M acetate buffer, 0.01 M PBS.*

IC/P_pH3 weight ratio	Particle size [nm]			
	after preparation	After release studies		
		to 0.01 M HCl	to 0.1 M acetate	to 0.01 M PBS
4	390±9	708±30	615±19	785±24
2	332±3	433±15	603±7	607±5
0.2	173±2	304±11	A	A
IC/P_pH3 weight ratio	PdI			
	after preparation	After release studies		
		to 0.01 M HCl	to 0.1 M acetate	to 0.01 M PBS
4	0.409±0.064	0.485±0.120	0.185±0.056	0.086±0.068
2	0.269±0.018	0.241±0.019	0.258±0.015	0.337±0.016
0.2	0.209±0.011	0.110±0.056	A	A
IC/P_pH3 weight ratio	ZP [mV]			
	after preparation	After release studies		
		to 0.01 M HCl	to 0.1 M acetate	to 0.01 M PBS
4	-46.6±0.2	-28.0±4.9	-44.4±3.3	-29.6±2.2
2	-38.8±0.3	-30.3±4.8	-47.6±2.7	-32.2±1.2
0.2	19.9±0.7	25.1±1.2	A	A

A - aggregates formed

Table C.9 *Characterisation of IC/P_pH3 NPs loaded with **100 µg/ml** of insulin after release to FaSSIF.*

IC/P_pH3 weight ratio	Particle size [nm]		PdI		ZP [mV]	
	After preparation	After release to FaSSIF	After preparation	After release to FaSSIF	After preparation	After release to FaSSIF
4	285±32	55±3	0.391±0.064	0.203±0.038	-44.4±4.0	-27.5±1.5
2	255±27	60±3	0.256±0.014	0.292±0.080	-35.7±2.7	-29.2±1.7
0.2	165±16	206±22	0.130±0.061	0.252±0.086	20.2±1.3	-28.3±1.5
Pure FaSSIF	70±12	-	0.201±0.037	-	-10.9±4.4	-

Table C.10 *Characterisation of IC/P_pH3 NPs loaded with* ***500 µg/ml*** *of insulin after release to the following media: 0.01 M HCl, 0.1 M acetate buffer, 0.01 M PBS.*

IC/P_pH3 weight ratio	Particle size [nm]			
	After preparation	After release studies		
		to 0.01 M HCl	to 0.1 M acetate	to 0.01 M PBS
4	303±5	321±53	338±9	627±20
2	467±25	A	673±15	1275±168
0.2	169±2	223±8	A	A
IC/P_pH3 weight ratio	PdI			
	After preparation	After release studies		
		to 0.01 M HCl	to 0.1 M acetate	to 0.01 M PBS
4	0.382±0.059	0.437±0.020	0.302±0.026	0.362±0.038
2	0.425±0.031	A	0.445±0.046	0.692±0.124
0.2	0.121±0.016	0.251±0.011	A	A
IC/P_pH3 weight ratio	ZP [mV]			
	After preparation	After release studies		
		to 0.01 M HCl	to 0.1 M acetate	to 0.01 M PBS
4	-43.6±0.8	31.5±2.3	-45.4±3.3	-30.7±1.4
2	-34.1±0.5	A	-47.0±0.7	-33.4±1.8
0.2	22.6±0.7	15.5±12.1	A	A

A - aggregates formed

ABSTRACT "Engineering a novel insulin delivery system"
Maria Dul, School of Pharmacy and Pharmaceutical Sciences TCD

The studies in this thesis investigated preparation of a novel system that would be suitable for an oral delivery of insulin. Two various approaches: genetic modification of insulin gene to establish a simple system of insulin production and formulation of polyelectrolyte complex nanoparticles as potential carriers for the delivery of insulin were examined.
To facilitate further modifications of insulin gene, several plasmids with insulin were designed and prepared. The design of the plasmids was based on the combination of the simplicity of a bacterial expression system with benefits of the expression in yeast, which is achieved by directing the expressed protein with the signal peptide to the oxidation system of the bacterial periplasmic space. Five plasmids with insulin were successfully prepared (pHB1, pHB2, pHB3, pMD2, pMD3) and all of them expressed insulin, however its amount and form was different. Optimisation of expression conditions was further investigated by testing two induction systems: isopropyl β-D-1-thiogalactopyranoside (IPTG) and auto-induction and also various temperatures. The impact of those factors on the solubility and localisation of expressed protein was also examined. Expression of the protein was controlled by measuring the optical density of the culture at 600 nm. Samples prepared for expression, solubility and periplasmic localisation test were tested with SDS-PAGE and Western blot techniques. Two plasmids: pMD2 (protein expressed in the periplasm) and pHB1 (the greatest amount of protein expressed in the insoluble form) were selected for further purification process. Final optimisation of the purification protocols was established for selected plasmids. It involved affinity chromatography (Ni column for purification of His tagged proteins) and Achromobacter lyticus protease (ALP) cleavage for purification of periplasmic fraction of protein expressed by plasmid pMD2. A more complex purification process had to be applied for purification of insoluble form of protein expressed by pHB1 plasmid, as the protein had to be isolated, washed, cleaved, purified and finally renaturated. Moreover, optimisation of the refolding reaction was performed using four various redox conditions: glutathione/glutathione disulfide, β-mercaptoethanol, dithiothreitol and cysteine/cystine, as this reaction was one of the steps that resulted in final low yield of the purification process. The amount of the protein was quantified by BioRad Protein Assay. Additionally samples were analysed with SDS-PAGE and Western blot technique. Prepared plasmids can be used for further genetic modifications as preparing fusions of insulin gene with cell penetrating peptides.
The second approach that has been investigated in the present work development and incorporation of insulin into nanocarriers composed of natural polymers (alginic acid and carrageenan) and protamine as a cell penetrating peptide. Polyelectrolyte complexation was used to manufacture NPs. At first, the conditions for the formation of insulin-free nanoparticles (NPs) were determined and the manufacture process was optimised by testing the impact of process variables (e.g. the type of polymer used: solution viscosity, concentration and mixing ratio of the polymers) on the properties of NPs. The particle size and size distribution (PdI) were analysed using dynamic light scattering and zeta potential (ZP) was measured with the use of laser Doppler velocimetry. Physical stability of selected formulations was tested upon storage at room temperature and in liquid media at various pH. The impact of the loaded peptide on the physicochemical properties of NPs such as: particle size, ZP, PdI as well as peptide association efficiency (AE), drug loading and *in vitro* insulin release was examined. Cytotoxicity of selected formulations in the Caco-2 cell line was performed. Finally, *in vitro* transport of insulin loaded into prepared nanocarriers through Caco-2 monolayers was examined. Simple, organic solvent and surfactant-free production method by mixing aqueous solutions of polyelectrolytes at room temperature was successfully employed to fabricate novel, cross-linker-free and non-sedimenting NPs. It was possible to obtain NPs with good physical properties (i.e. small and homogenously dispersed) for all of both types of polymers tested. Both, negatively and positively charged NPs, were formed by changing the polymer/protamine weight ratio. Physical stability of NPs upon storage at room temperature and in buffers at various pH was strongly dependent on the initial charge of NPs with better stability of negatively charged NPs in most cases. Two amounts of insulin were loaded into NPs: 100 and 500 µg/ml. Almost 100% AEs were obtained for negatively charged NPs for both doses of insulin loaded. Smaller amounts of insulin were associated with positively charged NPs, with greater AE obtained with alginate-based NPs. Similar *in vitro* release profiles were obtained all formulations of positively charged NPs, with 90 – 100% of insulin released in first 10 minutes in all of the buffers tested. Release from negatively charged NPs was depended on the formulation, amount of insulin loaded and pH of the buffer. Negatively charged NPs were non-toxic, while 45% - 51% Caco-2 cells (0.5 mg/ml NPs) remained viable after 72 h of incubation with positively charged NPs. The amount and kinetics of insulin transported through Caco-2 monolayers was dependent on the composition of formulation tested.